

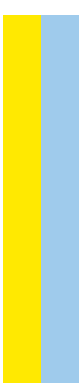
DOUTORAMENTO
CIÊNCIAS BIOMÉDICAS

Targeting depression at the cellular level: The role of the modulation of glucocorticoids and oxidative stress in serotonergic drugs efficacy

Ana Salomé Correia

D

2024



Ana Salomé Correia. Targeting depression at the cellular level: The role of the modulation of glucocorticoids and oxidative stress in serotonergic drugs efficacy



Targeting depression at the cellular level: The role of the modulation of glucocorticoids and oxidative stress in serotonergic drugs efficacy

Ana Salomé dos Santos Correia



ANA SALOMÉ DOS SANTOS CORREIA

**TARGETING DEPRESSION AT THE CELLULAR LEVEL: THE
ROLE OF THE MODULATION OF GLUCOCORTICIDS AND
OXIDATIVE STRESS IN SEROTONERGIC DRUGS EFFICACY**

Tese de candidatura ao grau de Doutor em Ciências Biomédicas, Programa Doutoral da Universidade do Porto (Instituto de Ciências Biomédicas Abel Salazar).

Orientador: Nuno Vale

Categoria: Professor Associado Convidado

Afiliação: Faculdade de Medicina da Universidade do Porto

Coorientador: Ana Sebastião

Categoria: Professora Catedrática

Afiliação: Faculdade de Medicina da Universidade de Lisboa

Coorientador: Armando Cardoso

Categoria: Professor Auxiliar

Afiliação: Faculdade de Medicina da Universidade do Porto

U. PORTO



U. PORTO



U

LISBOA
UNIVERSIDADE
DE LISBOA



FACULDADE DE
MEDICINA
LISBOA

Financial Support

This research was supported by a PhD Grant (SFRH/BD/146093/2019) from the Fundação para a Ciência e Tecnologia (FCT), República de Portugal, Ciência, Educação e Inovação, Pessoas 2030, Portugal 2030, and the European Union programs.



EDUCAÇÃO, CIÊNCIA E INOVAÇÃO



Declaração de Honra

Declaro que a presente tese é de minha autoria e não foi utilizada previamente noutro curso ou unidade curricular, desta ou de outra instituição. As referências a outros autores (afirmações, ideias, pensamentos) respeitam escrupulosamente as regras da atribuição, e encontram-se devidamente indicadas no texto e nas referências bibliográficas, de acordo com as normas de referência. Tenho consciência de que a prática de plágio e auto-plágio constitui um ilícito académico.

Ana Correia

Agradecimentos

Um doutoramento é uma montanha-russa de emoções, são 4 anos da vida em que a dedicação tem de ser imensa, numa batalha constante contra a incerteza e insegurança. Foram anos muito felizes, mas também recheados de medo.

Ao longo de qualquer jornada da nossa vida, o mais importante é termos as nossas pessoas connosco, aquelas que sabemos que estão sempre presentes para nos segurar a mão sempre que precisamos. A presença dessas pessoas é o que torna qualquer missão aparentemente impossível, em possível.

Assim, quero começar por agradecer às pessoas mais importantes nesta jornada: os meus pais. A estas duas pessoas, há tanto para agradecer. Sem eles, não seria a pessoa que sou hoje e, com toda a certeza, sei que posso contar sempre com eles em todos os momentos da minha vida – sejam eles bons ou maus - tal como pude contar durante todos os altos e baixos desta jornada.

Aos meus avós, por sempre acreditarem e por todo o orgulho sempre demonstrado em mim, mesmo quando eu própria não o conseguia sentir.

Ao Gonçalo, por me fazer rir mesmo quando a vontade era exatamente oposta.

Aos meus amigos, por estarem sempre cá, incondicionalmente. Em especial ao Rui, por toda a motivação transmitida e por me fazer acreditar que o futuro após este caminho pode ser risonho.

Às minhas amigas Mariana, Filipa e Cristiana, por todas as partilhas durante este caminho que percorremos juntas.

Às minhas colegas e amigas Diana e Sara, por tanto me ensinarem e por toda a amizade e partilha.

Ao Luís, por tanto me ouvir a apoiar.

Por fim, obrigada também ao meu orientador, assim como a todos os excelentes profissionais que tive o privilégio de conhecer ao longo destes anos, desde aqueles que me transmitiram valiosos ensinamentos no INSA, até os colegas do i3S e do IMM. Com todos eles, adquiri um conhecimento inestimável.

O meu doutoramento não teria sido possível sem estas pessoas. Venham novos capítulos!

List of Publications

In developing this thesis, Ana Salomé Correia has integrated various published articles, as outlined in the list below.

Correia, A.S.*; Cardoso, A.; Vale, N. Highlighting Immune System and Stress in Major Depressive Disorder, Parkinson's, and Alzheimer's Diseases, with a Connection with Serotonin. *Int. J. Mol. Sci.* **2021**, *22*, 8525.

Correia, A.S.*; Vale, N. Antidepressants in Alzheimer's Disease: A Focus on the Role of Mirtazapine. *Pharmaceuticals* **2021**, *14*, 930.

Correia, A.S.*; Fraga, S.; Teixeira, J.P.; Vale, N. Cell Model of Depression: Reduction of Cell Stress with Mirtazapine. *Int. J. Mol. Sci.* **2022**, *23*, 4942.

Correia, A.S.*; Vale, N. Tryptophan Metabolism in Depression: A Narrative Review with a Focus on Serotonin and Kynurenine Pathways. *Int. J. Mol. Sci.* **2022**, *23*, 8493.

Correia, A.S.*; Cardoso, A.; Vale, N. Significant Differences in the Reversal of Cellular Stress Induced by Hydrogen Peroxide and Corticosterone by the Application of Mirtazapine or L-Tryptophan. *Int. J. Transl. Med.* **2022**, *2*, 482-505.

Correia, A.S.*; Silva, I.; Oliveira, J.C.; Reguengo, H.; Vale, N. Serotonin Type 3 Receptor Is Potentially Involved in Cellular Stress Induced by Hydrogen Peroxide. *Life* **2022**, *12*, 1645.

Correia, A.S.*; Cardoso, A.; Vale, N. Oxidative Stress in Depression: The Link with the Stress Response, Neuroinflammation, Serotonin, Neurogenesis and Synaptic Plasticity. *Antioxidants* **2023**, *12*, 470.

Correia, A.S.*; Silva, I.; Reguengo, H.; Oliveira, J.C.; Vasques-Nóvoa, F.; Cardoso, A.; Vale, N. The Effect of the Stress Induced by Hydrogen Peroxide and Corticosterone on Tryptophan Metabolism, Using Human Neuroblastoma Cell Line (SH-SY5Y). *Int. J. Mol. Sci.* **2023**, *24*, 4389.

Correia, A.S.*; Marques, L.; Cardoso, A.; Vale, N. Exploring the Role of Drug Repurposing in Bridging the Hypoxia-Depression Connection. *Membranes*. **2023**, *13*, 800.

Correia, A.S.*; Cardoso, A.; Vale, N. BDNF Unveiled: Exploring Its Role in Major Depression Disorder Serotonergic Imbalance and Associated Stress Conditions. *Pharmaceuticals* **2023**, *15*, 2081.

Correia, A.S.*; Torrado, M.; Coelho, T.; Carvalho, E.; Inteiro-Oliveira, S.; Diógenes, M.J.; Pêgo, A.P.; Santos, S.; Sebastião, A.; Vale, N. BDNF Modulation in Response to Oxidative Stress and Corticosterone: Role of Scopolamine and Mirtazapine. Submitted in *Life Sciences*, January **2024**.

*Ana Salomé Correia (Correia, A.S.), as the first author, was the primary contributor to all aspects of these publications. This included the conception and design, execution of the experiments, data analysis and interpretation, as well as the writing, discussion, and editing of the articles.

Table of Contents

I. Introduction.....	1
1. The Contextual Landscape of Major Depressive Disorder.....	3
2. Exploring the Role of Oxidative Stress, Tryptophan Metabolism, Brain-Derived Neurotrophic Factor, and Hypothalamic–Pituitary–Adrenal Axis Dysfunction in Major Depressive Disorder	6
2.1. Oxidative Stress Dysregulation: An Overlook	6
2.1.1. Oxidative Stress As A Key Contributor to Major Depressive Disorder Pathogenesis.....	8
2.2. A Closer Look On Hypothalamic–Pituitary–Adrenal Axis In The Control of Stress Response	10
2.2.1. Unraveling the Hypothalamic–Pituitary–Adrenal Axis Dysregulation in Major Depressive Disorder	12
2.3. An Overlook on Tryptophan Metabolism.....	15
2.3.1. Tryptophan Metabolism as A Player in the Development of Major Depressive Disorder.....	17
2.3.2 Exploring Serotonin's Role in Major Depressive Disorder.....	20
2.4 The Multifaceted Roles of Brain-Derived Neurotrophic Factor.....	25
2.4.1. Exploring Brain-Derived Neurotrophic Factor in Major Depressive Disorder	28
3. Intersecting Pathways in Major Depressive Disorder: Oxidative Stress, Tryptophan Metabolism, Brain-Derived Neurotrophic Factor, and Hypothalamic–Pituitary–Adrenal Axis Dysfunction	30
3.1. Exploring the Connection Between Oxidative Stress and Major Depressive Disorder's Associated Stress Response	30
3.2. The Interplay Between Oxidative Stress and Serotonin in Major Depressive Disorder.....	32
3.3. Oxidative Stress's Impact on Synaptic Plasticity and Neurogenesis in Major Depressive Disorder	34
3.4. Tryptophan Metabolism Players and Depression's Associated Chronic Stress.....	36
3.5. Linking Tryptophan Metabolism with Brain-Derived Neurotrophic Factor Expression in Major Depressive Disorder.....	38
3.6. Bridging Brain-Derived Neurotrophic Factor with Hypothalamic–Pituitary–Adrenal Axis Dysregulation in Major Depressive Disorder.....	42
4. Pharmacological Interventions in the Management of Major Depressive Disorder ..	43
4.1. An Overlook of Pharmacotherapy for Major Depressive Disorder.....	43
4.2. Antidepressant Breakthroughs: Advancements in Pharmacotherapy for Depression.....	44

4.4. Mirtazapine: A Classic Antidepressant's Ongoing Relevance	51
II. Aim	54
III. Materials and Methods	56
1. Materials	57
2. SH-SY5Y and HT-22 Cell Culture	59
3. Morphological Analysis of SH-SY5Y and HT-22 cells	60
4. Cellular Viability Assays	60
5. Alkaline Comet Assay	60
6. 2',7'-Dichlorofluorescein Diacetate Assay	61
7. High-Performance Liquid Chromatography Analysis	61
8. Hypoxia Induction of Cells.....	62
10. Acute Hippocampal Slices Preparation	62
11. Embryonic Mice Neuronal Cortical and Hippocampal Cell Culture.....	63
12. Immunofluorescence Analysis.....	63
13. Western Blot Analysis	64
14. Statistical Analysis	64
IV. Results	67
1. Investigating the Effects of Mirtazapine and Cellular Stressors on Cellular Viability	69
1.1. Effect of Mirtazapine on SH-SY5Y and HT-22 Cellular Viability	69
1.2. Effect of Hydrogen Peroxide, Hydrocortisone and Corticosterone on SH-SY5Y and HT-22 Cellular Viability.....	72
2. Exploring the Effects of Mirtazapine and L-Tryptophan on the Damage Induced by Stressors in Neuronal Cell Lines.....	81
2.1. Effect of the Combination of Mirtazapine with Hydrogen Peroxide on SH-SY5Y and HT-22 Cellular Viability.....	81
2.2. Effect of the Combination of Mirtazapine with Corticosterone on SH-SY5Y and HT-22 Cellular Viability	84
2.3. Effect L-Tryptophan on SH-SY5Y and HT-22 Cellular Viability	86
2.4. Effect of the Combination of L-Tryptophan with Hydrogen Peroxide on SH-SY5Y and HT-22 Cellular Viability.....	87
2.5. Effect of the Combination of L-Tryptophan with Corticosterone on SH-SY5Y and HT-22 Cellular Viability	89
2.6. Effect of the Combination of Mirtazapine with Hydrogen Peroxide and Corticosterone on SH-SY5Y and HT-22 Reactive Oxygen Species Production.....	92
2.7. Effect of the Combination of L-Tryptophan with Hydrogen Peroxide and Corticosterone on SH-SY5Y and HT-22 Reactive Oxygen Species Production.....	95
3. Assessing the DNA Integrity of SH-SY5Y Cells Following Exposure to Stress-Inducing Agents and Mirtazapine	99

3.1. Effect of Hydrocortisone, Hydrogen Peroxide, Mirtazapine, and the Combination of Mirtazapine with Hydrogen Peroxide on DNA integrity.....	100
4. Investigating Drugs that Modulate Serotonin Type 3 Receptors in Hydrogen Peroxide and Corticosterone-Induced Cellular Stress	102
4.1. Presence of Serotonin Type 3 Receptors in SH-SY5Y cells and HT-22 cells.....	103
4.2. Effect of Scopolamine and Lamotrigine on SH-SY5Y and HT-22 Cell Viability ...	103
4.3. Effect of Mirtazapine, Scopolamine and Lamotrigine in Combination with Hydrogen Peroxide and Corticosterone on SH-SY5Y and HT-22 Cell Viability	107
4.4. Effect of Mirtazapine, Scopolamine and Lamotrigine in Combination with Hydrogen Peroxide and Corticosterone on Extracellular Serotonin Levels	110
5. Exploring the Impact of Hydrogen Peroxide and Corticosterone-Induced Stress on Tryptophan Metabolism in SH-SY5Y Cells	112
5.1. Effect of L-TRP, 5-HTP, 5-HT, 5-HIAA and Their Combinations with H ₂ O ₂ or Corticosterone on SH-SY5Y Cell Viability and Extracellular L-TRP, 5-HTP, 5-HT, 5-HIAA Concentration	113
5.2. Effect of H ₂ O ₂ and Corticosterone on Extracellular 5-HT Concentration	118
6. Neurotrophic Responses in Different Neuronal Models: BDNF Levels After Mirtazapine, Scopolamine, and Cellular Stress Exposure	119
6.1. BDNF Levels After Mirtazapine, Scopolamine, and Cellular Stress Exposure in Acute Hippocampal Slices	119
6.2. BDNF and phosphorylated TrkB Levels After Mirtazapine, Scopolamine, and Cellular Stress Exposure in Neuronal Hippocampal Cell Culture	122
6.3. BDNF Levels After Mirtazapine, Scopolamine, and Cellular Stress Exposure in Neuronal Cortical Cell Culture.....	131
7. Exploring the Role of Drug Repurposing in Bridging the Hypoxia–Depression Connection	133
7.1. The Effect of the Hypoxia Incubator Chamber on SH-SY5Y Cellular Viability and Morphology.....	134
7.2. The Effect of Chemically Induced Hypoxia with Cobalt Chloride on SH-SY5Y Cellular Viability and Morphology	138
7.3. The Effect of Echinomycin and the Combination of Echinomycin with Cobalt Chloride on SH-SY5Y Cellular Viability and Morphology	139
7.4. The Effect of Echinomycin and Cobalt Chloride on SH-SY5Y Cellular Viability and Morphology After Drug Application	141
8. Supplementary Results	145
8.1. Assessing the Impact of 24-Hour Exposure to Mirtazapine and Its Combination with Hydrogen Peroxide on the Viability of SH-SY5Y Cells	145
8.2. Effect of Serotonin Exposure on SH-SY5Y and HT-22 Cellular Viability	146
8.3. Effect of the Combination of Serotonin with Hydrogen Peroxide and Corticosterone on SH-SY5Y and HT-22 Cellular Viability	148

8.4. Effect of Quetiapine, Ketamine, Dextromethorphan, Celecoxib and TCB-2 in Combination with Hydrogen Peroxide and Corticosterone on SH-SY5Y Cell Viability.....	152
V. Discussion	157
VI. Concluding Remarks and Future Perspectives	183
VII. References	186

Abstract

Major depressive disorder is a significant challenge in global healthcare, characterized by its complexity and involvement of various biological systems. The disorder is associated with dysregulation in the hypothalamus-pituitary-adrenal axis, that leads to increased cortisol levels. Additionally, patients often exhibit elevated oxidative stress, chronic inflammation, neurotransmitter imbalances (especially in serotonin, dopamine, and noradrenaline), and decreased levels of brain-derived neurotrophic factor (BDNF). While these findings provide valuable insights into the pathophysiology of major depressive disorder, it is important to note that there is still much more to understand regarding these key features. Current treatments often face resistance and need for personalized approaches, and the probability of relapse is high, highlighting the urgent need for research into new therapeutic methods.

Animal studies have played a role in advancing our understanding of depression by providing insights into both the physiological and behavioral aspects of this disorder. However, it is important to consider that these studies present challenges and ethical considerations. To address these concerns, cellular models offer an alternative that bridges the gap between animal research and clinical applications, while minimizing harm to animals. By using different research approaches, including the use of cellular models, it is possible to make significant progress in the field of depression research and ultimately improve the lives of individuals affected by this condition.

This thesis centered on the investigation of tryptophan, mirtazapine (an established antidepressant drug connected with the serotonin signaling system) and other drugs with potential to be repurposed for depression therapy (with a particular focus on scopolamine). Using established cell lines (SH-SY5Y human neuroblastoma and HT-22 mouse hippocampal), primary cell cultures (from the hippocampus and cortex of mouse) and hippocampal slices from rat, the primary goal was to assess the effectiveness of the compounds in modulating the consequences of high glucocorticoid exposure and oxidative stress. The achievement of these goals was made possible using cellular viability techniques, along with the evaluation of reactive oxygen species levels, DNA damage, and extracellular serotonin levels. Furthermore, this research investigated the complex connection between tryptophan/serotonin metabolic pathway and cellular stress, and explored the influence of some of the investigated compounds on BDNF and its activated receptor, phosphorylated full length tropomyosin receptor kinase B. Additionally, an exploratory study to explore the potential role of hypoxia stimuli in the response to different drugs with antidepressant potential, using chemical and physical induction of hypoxia to cells was conducted.

In summary, the several results presented in this work demonstrated that the chosen compounds effectively mitigated the oxidative stress induced damage to cells, but not corticosterone induced stress, protecting cells possibly by acting on serotonin related pathways. Additionally, these results revealed that different methods of inducing stress produce distinct responses in the extracellular concentration of tryptophan metabolites, highlighting that serotonin may be particularly sensitive to environmental modulation. Moreover, the experiments on BDNF demonstrated complex and context-dependent responses. These findings support the need to consider diverse cellular contexts when evaluating neuronal responses to treatments. Particularly, while mirtazapine and scopolamine overall increased BDNF levels when combined with stressors in primary hippocampal and cortical cultures, the opposite occurred in hippocampal slices. In the hypoxia studies, all the drugs tested demonstrated an increase in cell viability when exposed to chemical hypoxia, in contrast to cells that were only subjected to chemical hypoxia without drug exposure, indicating a potential beneficial connection between the hypoxia response and the drugs tested, known for their antidepressant effects. It is also important to highlight that by investigating the potential of repurposed drugs and a conventional antidepressant with well-documented side effects that can only be modulated with extensive studies, this research contributes to a deeper understanding of depression while optimizing resource utilization.

Resumo

A perturbação depressiva major representa um desafio significativo na saúde global, sendo caracterizada pela sua complexidade e envolvimento de vários sistemas biológicos. Esta doença está associada à desregulação do eixo hipotálamo-hipófise-adrenal, sendo este responsável pelo aumento dos níveis de cortisol frequentemente observados em indivíduos com esta doença. Pacientes com depressão apresentam também, tipicamente, níveis elevados de stress oxidativo, inflamação crónica, desequilíbrios a nível de neurotransmissores (especialmente a serotonina, dopamina e noradrenalina) e níveis reduzidos do factor neurotrófico derivado do cérebro (BDNF). No entanto, embora ofereçam conhecimento valioso sobre a desta doença, é importante reconhecer que ainda há muito a investigar sobre estas características. Os tratamentos atuais enfrentam frequentemente resistência e necessitam de abordagens personalizadas, sendo que a probabilidade de recaída é elevada, destacando a necessidade urgente de investigação em novos métodos terapêuticos.

Estudos com animais têm sido um pilar na investigação desta doença, oferecendo informação sobre os aspetos fisiológicos e comportamentais deste distúrbio, mas, embora estes estudos tenham desempenhado um papel significativo no avanço do conhecimento sobre a depressão, vêm acompanhados de desafios e preocupações éticas. Assim, modelos celulares oferecem uma alternativa promissora, podendo em alguns casos preencher a lacuna entre a investigação animal e as aplicações clínicas, minimizando os danos aos animais e economizando recursos.

Esta tese centrou-se na investigação do triptofano, mirtazapina (um fármaco antidepressivo estabelecido clinicamente, associado ao sistema de sinalização da serotonina) e outros fármacos com potencial para serem reaproveitados na terapia desta doença (com um foco particular na escopolamina). Através do uso de linhas celulares estabelecidas (neuroblastoma humano e hipocampo de ratinho) e do uso de culturas primárias de células de hipocampo/córtex de ratinho, bem como fatias de hipocampo de rato, o objetivo principal foi avaliar a eficácia dos compostos em estudo em mitigar as consequências da exposição a níveis elevados de glucocorticoides e stress oxidativo. Para isso, utilizou-se técnicas de avaliação de viabilidade celular, avaliação de níveis de espécies reativas de oxigénio, danos no ADN e níveis de serotonina extracelular. Além disso, esta investigação explorou a interação complexa entre as vias metabólicas de triptofano/serotonina e stress celular, bem como a influência de alguns compostos em estudo no BDNF e o seu receptor ativado, receptor da tropomiosina quinase B fosforilado com o comprimento total (full length). Ainda, foi conduzido um estudo sobre

o possível papel dos estímulos de hipóxia na resposta a diferentes fármacos com potencial antidepressivo, utilizando indução química e física de hipóxia a nível celular.

Em suma, os vários resultados apresentados nesta tese destacaram que os compostos escolhidos mitigaram eficazmente os danos induzidos pelo stress oxidativo às células, mas não o stress induzido pela corticosterona, possivelmente protegendo as células por via de atuação em vias relacionadas à serotonina. Ainda, estes resultados realçaram que diferentes métodos de indução de stress produzem respostas distintas na concentração extracelular de metabolitos de triptofano, destacando que a serotonina parece ser particularmente sensível a modulação. Além disso, as experiências focadas no BDNF revelaram respostas complexas e dependentes do contexto neuronal em que são estudadas. De facto, enquanto a mirtazapina e a escopolamina, no geral, aumentaram os níveis de BDNF quando combinadas com agentes indutores de stress em culturas primárias de hipocampo e córtex, o oposto ocorreu em fatias de hipocampo. Nos estudos de hipóxia, todos os fármacos testados exibiram um aumento substancial na viabilidade celular quando expostos à hipóxia química, em contraste com células que foram submetidas apenas à hipóxia química, indicando assim uma possível conexão benéfica entre a resposta à hipóxia e os fármacos, conhecidos por possuírem efeitos antidepressivos. Também é importante destacar que ao investigar fármacos com potencial a serem reaproveitados, bem como um antidepressivo convencional com efeitos secundários bem documentados que só podem ser modulados com estudos extensos, esta investigação contribui para um entendimento mais profundo deste doença altamente complexa, otimizando a utilização de recursos.

List of Figures

Figure 1. Depression is a multifaceted condition characterized by different underlying factors. These include dysfunction in the HPA axis, imbalanced levels of neurotransmitters like 5-HT, NA and DA, fluctuations in neurotrophic factors such as BDNF, shrinkage of certain brain regions like the hippocampus, high levels of inflammation and oxidative stress, and reduced levels of neurogenesis.

Figure 2. Prooxidant factors such as toxins and pollutants promote high levels of ROS production that are kept at low levels by the antioxidant defenses. However, when ROS production overwhelms antioxidant defenses, harmful effects such as membrane disruption, protein and DNA damage occur, disrupting the normal cell signaling mechanisms and culminating in diseases such as cancer or neurological diseases.

Figure 3. High levels of ROS promote and are promoted by the stress response, neuroinflammation, and imbalances in neurotransmitter-related pathways and neurogenesis/synaptic plasticity processes. All these features underlie the pathophysiology of depression, being critical in disease development and progression.

Figure 4. Summary of the two major metabolic pathways of the amino acid TRP: 5-HT and Kyn pathways.

Figure 5. The TRP metabolism is important in several processes connected with depression, particularly neuroinflammation, stress response, gut microbiota dysregulation, and BDNF activity.

Figure 6. Molecular structure of the neurotransmitters 5-HT, NA and DA.

Figure 7. Simplified scheme of BDNF and 5-HT interaction in depression. In depression, there exists a complex interplay between BDNF and 5-HT. BDNF interacts with the TrkB receptor, thereby exerting its influence on serotonergic signaling pathways. Conversely, these pathways also impact BDNF signaling. Disruptions within these pathways, indicated by red dashed arrows, are observed in MDD. Consequently, these disruptions contribute to structural changes in the brain, impaired neuroplasticity, compromised synaptic regulation, and reduced levels of both serotonin and BDNF. These cumulative effects ultimately promote or contribute to the development of depressive symptoms.

Figure 8. Summary of the mechanism of action of mirtazapine. This drug is an antagonist of 5-HT_{2A}, 5-HT_{2C}, 5-HT₃, H₁, and α ₂ receptors, resulting in antidepressant and sedative effects.

Figure 9. Representative images (total magnification 100x) of SH-SY5Y and HT-22 cells morphology after exposure to different concentrations of mirtazapine. Cells were incubated with (A, G) vehicle (0.1% DMSO), (B, H) mirtazapine 0.01 μ M, (C, I) mirtazapine 0.1 μ M, (D, J) mirtazapine 1 μ M, (E, K) mirtazapine 10 μ M, and (F, L) mirtazapine 20 μ M. Scale bar: 50 μ m.

Figure 10. Effect of increasing concentrations of mirtazapine on the viability of SH-SY5Y and HT-22 cells, obtained by (A, C) MTT and (B, D) NR assays. The results are expressed as the percentage of vehicle and represent the mean \pm SEM of three independent experiments. Statistically significant # $p < 0.05$ vs. vehicle.

Figure 11. Representative images (100 \times total magnification) of SH-SY5Y and HT-22 cells after incubation of increasing concentrations of H₂O₂. Cells were treated with (A, B) vehicle, (0.1% H₂O), (C, I) H₂O₂ 50 μ M, (D, J) H₂O₂ 100 μ M, (E, K) H₂O₂ 150 μ M, (F, L) H₂O₂ 200 μ M, (G, M) H₂O₂ 250 μ M, (H, N) H₂O₂ 300 μ M. Scale bar: 50 μ m.

Figure 12. Effect of increasing concentrations of H₂O₂ on the viability of SH-SY5Y and HT-22 cells, obtained by (A, C) MTT and (B, D) NR assays. The results are expressed as the percentage of vehicle and represent the mean \pm SEM of three-six independent experiments. Statistically significant # $p < 0.05$, ## $p < 0.01$, ### $p < 0.001$, #### $p < 0.0001$ vs. vehicle.

Figure 13. Concentration-response curves for increasing concentrations of H₂O₂ on the viability of SH-SY5Y cells and HT-22 cells, obtained by (A, C) MTT and (B, D) NR assays. The results are expressed as the percentage of each respective vehicle and represent the mean \pm SEM of three-six independent experiments.

Figure 14. Representative images (100 \times total magnification) of SH-SY5Y and HT-22 cells after incubation of increasing concentrations of hydrocortisone. Cells were treated with (A, G) vehicle (0.1% DMSO), (B, H) hydrocortisone 100 μ M, (C, I) hydrocortisone 200 μ M, (D, J) hydrocortisone 300 μ M, (E, K) hydrocortisone 400 μ M, (F, L) hydrocortisone 500 μ M. Scale bar: 50 μ m.

Figure 15. Effect of increasing concentrations of hydrocortisone on the viability of SH-SY5Y and HT-22 cells, obtained by (A, C) MTT and (B, D) NR assays. The results are expressed as the percentage of vehicle and represent the mean \pm SEM of three independent experiments. Statistically significant # $p < 0.05$, ## $p < 0.01$ vs. vehicle.

Figure 16. Representative images (100 \times total magnification) of SH-SY5Y and HT-22 cells after incubation of increasing concentrations of corticosterone. Cells were treated with (A, G) vehicle (0.1% DMSO), (B, H) corticosterone 100 μ M, (C, I) corticosterone 200

μM , (D, J) corticosterone 300 μM , (E, K) corticosterone 400 μM , (F, L) corticosterone 500 μM . Scale bar: 50 μm .

Figure 17. Effect of increasing concentrations of corticosterone on the viability of SH-SY5Y and HT-22 cells, obtained by (A, C) MTT and (B, D) NR assays. The results are expressed as the percentage of vehicle and represent the mean \pm SEM of three-six independent experiments. Statistically significant # $p < 0.05$, ## $p < 0.01$, ### $p < 0.001$, #### $p < 0.0001$ vs. vehicle.

Figure 18. Concentration-response curves for increasing concentrations of corticosterone on the viability of SH-SY5Y cells and HT-22 cells, obtained by (A, C) MTT and (B, D) NR assays. The results are expressed as the percentage of each respective vehicle and represent the mean \pm SEM of three-six independent experiments.

Figure 19. Representative images (total magnification 100x) of SH-SY5Y and HT-22 cells morphology after exposure to H_2O_2 and to the combination of mirtazapine with H_2O_2 . Cells were incubated with (A,B) vehicle (0.1% DMSO), (C, I) H_2O_2 132 μM and 105 μM , respectively, (D, J) H_2O_2 132 μM + mirtazapine 0.01 μM and H_2O_2 105 μM + mirtazapine 0.01 μM , respectively, (E, K) H_2O_2 132 μM + mirtazapine 0.1 μM and H_2O_2 105 μM + mirtazapine 0.1 μM , respectively, (F, L) H_2O_2 132 μM + mirtazapine 1 μM and H_2O_2 105 μM + mirtazapine 1 μM , respectively, (G, M) H_2O_2 132 μM + mirtazapine 10 μM and H_2O_2 105 μM + mirtazapine 10 μM , respectively, (H, N) H_2O_2 132 μM + mirtazapine 20 μM and H_2O_2 105 μM + mirtazapine 20 μM , respectively. Scale bars: 50 μm and 179.3 μm .

Figure 20. Effect of increasing concentrations of mirtazapine, in combination with H_2O_2 , on the viability of (A) SH-SY5Y cells and (B) HT-22 cells, obtained by the MTT assay. The results are expressed as the percentage of vehicle and represent the mean \pm SEM of three independent experiments. Statistically significant # $p < 0.05$ and #### $p < 0.0001$ vs. vehicle, ** $p < 0.01$ and *** $p < 0.001$ vs. H_2O_2 132 μM , * $p < 0.05$ vs. H_2O_2 105 μM .

Figure 21. Representative images (total magnification 100x) of SH-SY5Y and HT-22 cells morphology after exposure to corticosterone and to the combination of mirtazapine with corticosterone. Cells were incubated with (A,B) vehicle (0.1% DMSO), (C, I) corticosterone 322 μM and 35 μM , respectively, (D, J) corticosterone 322 μM + mirtazapine 0.01 μM and corticosterone 35 μM + mirtazapine 0.01 μM , respectively, (E, K) corticosterone 322 μM + mirtazapine 0.1 μM and corticosterone 35 μM + mirtazapine 0.1 μM , respectively, (F, L) corticosterone 322 μM + mirtazapine 1 μM and corticosterone 35 μM + mirtazapine 1 μM , respectively, (G, M) corticosterone 322 μM +

mirtazapine 10 μM and corticosterone 35 μM + mirtazapine 10 μM , respectively, (H, N) corticosterone 322 μM + mirtazapine 20 μM and corticosterone 35 μM + mirtazapine 20 μM , respectively. Scale bars: 50 μm and 179.3 μm .

Figure 22. Effect of increasing concentrations of mirtazapine, in combination with corticosterone, on the viability of (A) SH-SY5Y cells and (B) HT-22 cells, obtained by the MTT assay. The results are expressed as the percentage of vehicle and represent the mean \pm SEM of three independent experiments. Statistically significant # $p < 0.05$ and ##### $p < 0.0001$ vs. vehicle, **** $p < 0.0001$ vs. corticosterone 322 μM .

Figure 23. Representative images (100 \times total magnification) of SH-SY5Y and HT-22 cells after incubation of increasing concentrations of L-TRP. Cells were treated with (A, I) vehicle (1% H_2O), (B, J) L-TRP 0.1 nM, (C, K) L-TRP 1 nM, (D, L) L-TRP 10 nM, (E, M) L-TRP 100 nM, (F, N) L-TRP 1 μM , (G, O) L-TRP 10 μM , (H, P) L-TRP 100 μM . Scale bars: 50 μm and 179.3 μm .

Figure 24. Effect of the incubation of 0.1 nM-100 μM of L-TRP on the viability of (A) SH-SY5Y cells and (B) HT-22 cells, determined by MTT methodology. The results represent the mean \pm SEM of three independent experiments, expressed as the percentage of the vehicle (100%).

Figure 25. Representative images (100 \times total magnification) of SH-SY5Y and HT-22 cells after incubation of H_2O_2 in combination with L-TRP. Cells were treated with (A,B) vehicle (1% H_2O), (C, K) H_2O_2 132 μM and 105 μM , respectively, (D, L) L-TRP 0.1 nM + H_2O_2 132 μM and L-TRP 0.1 nM + H_2O_2 105 μM , respectively, (E, M) L-TRP 1 nM + H_2O_2 132 μM and L-TRP 1 nM + H_2O_2 105 μM , respectively, (F, N) L-TRP 10 nM + H_2O_2 132 μM and L-TRP 10 nM + H_2O_2 105 μM , respectively, (G, O) L-TRP 100 nM + H_2O_2 132 μM and L-TRP 100 nM + H_2O_2 105 μM , respectively, (H, P) L-TRP 1 μM + H_2O_2 132 μM and L-TRP 1 μM + H_2O_2 105 μM , respectively, (I, Q) L-TRP 10 μM + H_2O_2 132 μM and L-TRP 10 μM + H_2O_2 105 μM , respectively, (J, R) L-TRP 100 μM + H_2O_2 132 μM and L-TRP 100 μM + H_2O_2 105 μM , respectively. Scale bar: 179.3 μm .

Figure 26. Effect of the incubation of (A) 132 μM of H_2O_2 and (B) 105 μM of H_2O_2 , in combination with 0.1 nM–100 μM of L-TRP, determined by MTT methodology. The results represent the mean \pm SEM of three independent experiments, expressed as the percentage of the vehicle (100%). Statistically significant ##### $p < 0.0001$ vs. vehicle, ** $p < 0.01$, *** $p < 0.001$, **** $p < 0.0001$ vs. H_2O_2 132 μM .

Figure 27. Representative images (100 × total magnification) of SH-SY5Y and HT-22 cells after incubation of corticosterone in combination with L-TRP. Cells were treated with (A,B) vehicle (0.1% DMSO / 1% H₂O), (C, K) corticosterone 322 μM and 35 μM, respectively, (D, L) L-TRP 0.1 nM + corticosterone 322 μM and L-TRP 0.1 nM + corticosterone 35 μM, respectively, (E, M) L-TRP 1 nM + corticosterone 322 μM and L-TRP 1 nM + corticosterone 35 μM, respectively, (F, N) L-TRP 10 nM + corticosterone 322 μM and L-TRP 10 nM + corticosterone 35 μM, respectively, (G, O) L-TRP 100 nM + corticosterone 322 μM and L-TRP 100 nM + corticosterone 35 μM, respectively, (H, P) L-TRP 1 μM + corticosterone 322 μM and L-TRP 1 μM + corticosterone 35 μM, respectively, (I, Q) L-TRP 10 μM + corticosterone 322 μM and L-TRP 10 μM + corticosterone 35 μM, respectively, (J, R) L-TRP 100 μM + corticosterone 322 μM and L-TRP 100 μM + corticosterone 35 μM, respectively. Scale bar: 179.3 μm.

Figure 28. Effect of the incubation of (A) 322 μM of corticosterone and (B) 35 μM of corticosterone in combination with 0.1 nM–100 μM of L-TRP, determined by MTT methodology. The results represent the mean ± SEM of three independent experiments, expressed as the percentage of the vehicle (100%). Statistically significant ##### $p < 0.0001$ vs. vehicle, ** $p < 0.01$, *** $p < 0.001$, **** $p < 0.0001$ vs. corticosterone 322 μM.

Figure 29. Effect on ROS production of 1h, 3h, 6h, 24h, and 48h-incubation of (A) 132 μM of H₂O₂, 0.01 μM/20 μM of mirtazapine and 132 μM of H₂O₂ + 0.01 μM/20 μM of mirtazapine (SH-SY5Y cells) and (B) 105 μM of H₂O₂, 0.01 μM/20 μM of mirtazapine and 105 μM of H₂O₂ + 0.01 μM/20 μM of mirtazapine (HT-22 cells), determined by DCFDA assay. The results are expressed as the percentage of each vehicle (100%) for each period (two-six independent experiments). Statistically significant # $p < 0.05$, ### $p < 0.001$, and ##### $p < 0.0001$ vs. vehicle, for each time point, and * $p < 0.05$, ** $p < 0.01$, and **** $p < 0.0001$ vs. H₂O₂ 132 μM (SH-SY5Y cells) and H₂O₂ 105 μM (HT-22 cells).

Figure 30. Effect on ROS production of 1h, 3h, 6h, 24h, and 48h-incubation of (A) 322 μM of corticosterone, 0.01 μM/20 μM of mirtazapine and 322 μM of corticosterone + 0.01 μM/20 μM of mirtazapine (SH-SY5Y cells) and (B) 35 μM of corticosterone, 0.01 μM/20 μM of mirtazapine and 35 μM of corticosterone + 0.01 μM/20 μM of mirtazapine (HT-22 cells), determined by DCFDA assay. The results are expressed as the percentage of each vehicle (100%) for each period (two-six independent experiments).

Figure 31. Effect on ROS production of 1h, 3h, 6h, 24h, and 4 h-incubation of (A) 132 μM of H₂O₂, 0.01 μM/100 μM of L-TRP and 132 μM of H₂O₂ + 0.1 nM/100 μM of L-TRP (SH-SY5Y cells) and (B) 105 μM of H₂O₂, 0.1 nM/100 μM of L-TRP and 105 μM of H₂O₂

+ 0.1 nM/100 μ M of L-TRP (HT-22 cells), determined by DCFDA assay. The results are expressed as the percentage of each vehicle (100%) for each period (two-six independent experiments). Statistically significant # $p < 0.05$, ## $p < 0.01$, ### $p < 0.001$, and #### $p < 0.0001$ vs. vehicle, for each time point, and * $p < 0.05$, ** $p < 0.01$ vs. H_2O_2 132 μ M.

Figure 32. Effect on ROS production of 1h, 3h, 6h, 24h, and 48 h-incubation of (A) 322 μ M of corticosterone, 0.1 nM/100 μ M of L-TRP and 322 μ M of corticosterone + 0.1 nM/100 μ M of L-TRP (SH-SY5Y cells) and (B) 35 μ M of corticosterone, 0.1 nM/100 μ M of L-TRP and 35 μ M of corticosterone + 0.1 μ M/100 μ M of L-TRP (HT-22 cells), determined by DCFDA assay. The results are expressed as the percentage of each vehicle (100%) for each period (two-six independent experiments).

Figure 33. Schematic illustration of the main findings of this work. In sum, our main findings evidence that both mirtazapine and L-TRP can counteract the harmful effects caused by H_2O_2 but not by corticosterone, revealing that these agents may have an important protective role in oxidative stress.

Figure 34. In this study, to explore an in vitro model of depression in SH-SY5Y cells, two stress inducers (H_2O_2 and glucocorticoids, namely hydrocortisone) were used, and the mirtazapine effectiveness against the induced oxidative stress was tested.

Figure 35. Effect of (A) hydrocortisone, and (B) H_2O_2 , mirtazapine and the combination of mirtazapine with H_2O_2 on the DNA integrity of SH-SY5Y cells, assessed by the by alkaline comet assay. The results are expressed as the percentage of the tail intensity and represent the mean \pm SEM of three independent experiments. Statistically significant # $p < 0.05$ and #### $p < 0.0001$ vs. vehicle, and ** $p < 0.01$ and **** $p < 0.0001$ vs. H_2O_2 (single agent, in the concentration exposed in each combination with mirtazapine).

Figure 36. Representative images (total magnification 200x) of SH-SY5Y cells after application of increasing concentrations of hydrocortisone, H_2O_2 , mirtazapine, and the combination of mirtazapine with hydrogen peroxide. These cells were stained with SYBR Gold, as described in the materials and methods section. Cells were treated with (A) vehicle (0.1% H_2O), (B) vehicle (0.1% DMSO), (C) MMS 0.5 mM (positive control), (D) hydrocortisone 50 μ M, (E) hydrocortisone 100 μ M, (F) hydrocortisone 150 μ M, (G) H_2O_2 10 μ M, (H) H_2O_2 66 μ M, (I) H_2O_2 132 μ M, (J) H_2O_2 200 μ M, (K) mirtazapine 0.01 μ M (L) mirtazapine 20 μ M, (M) H_2O_2 132 μ M + mirtazapine 0.01 μ M, (N) H_2O_2 132 μ M + mirtazapine 20 μ M, and (O) H_2O_2 200 μ M + mirtazapine 20 μ M. Scale bar: 50 μ m.

Figure 37. Representative images (400× total magnification) of (A) SH-SY5Y cells and (B) HT-22 cells after immunostaining with DAPI (stains nuclei, blue) and primary antibody rabbit polyclonal anti-5-HT3AR/ donkey anti-rabbit 488 secondary antibody (green), as previously described in the materials and methods section. Scale bar: 100 µm.

Figure 38. Representative images (100 × total magnification) of SH-SY5Y and HT-22 cells after incubation of (A,B) vehicle (0.1% DMSO), (C, M) scopolamine 0.01 µM, (D, N) scopolamine 0.1 µM, (E, O) scopolamine 1 µM, (F, P) scopolamine 10 µM, (G, Q) scopolamine 20 µM, (H, R) lamotrigine 0.01 µM, (I, S) lamotrigine 0.1 µM, (J, T) lamotrigine 1 µM, (K, U) lamotrigine 10 µM, (L, V) lamotrigine 20 µM. Scale bar: 50 µm.

Figure 39. Effect of increasing concentrations of scopolamine on the viability of SH-SY5Y and HT-22 cells, obtained by (A, C) MTT and (B, D) NR assays. The results are expressed as the percentage of vehicle and represent the mean ± SEM of three independent experiments.

Figure 40. Effect of increasing concentrations of lamotrigine on the viability of SH-SY5Y and HT-22 cells, obtained by (A, C) MTT and (B, D) NR assays. The results are expressed as the percentage of vehicle and represent the mean ± SEM of three independent experiments.

Figure 41. Representative images (100 × total magnification) of SH-SY5Y and HT-22 cells after incubation of H₂O₂ and corticosterone in combination with mirtazapine, scopolamine, and lamotrigine. Cells were treated with (A,I) vehicle (0.1% H₂O/ 0.1% DMSO), (B,J) H₂O₂ 132 µM (for SH-SY5Y cells) and H₂O₂ 105 µM (for HT-22 cells) + mirtazapine 20 µM, (C, K) H₂O₂ 132 µM (for SH-SY5Y cells) and H₂O₂ 105 µM (for HT-22 cells) + scopolamine 20 µM, (D, L) H₂O₂ 132 µM (for SH-SY5Y cells) and H₂O₂ 105 µM (for HT-22 cells) + lamotrigine 20 µM, (E, M) vehicle (0.1% DMSO), (F, N) corticosterone 322 µM (for SH-SY5Y cells) and corticosterone 35 µM (for HT-22 cells) + mirtazapine 20 µM, (G, O) corticosterone 322 µM (for SH-SY5Y cells) and corticosterone 35 µM (for HT-22 cells) + scopolamine 20 µM, (H, P) corticosterone 322 µM (for SH-SY5Y cells) and corticosterone 35 µM (for HT-22 cells) + lamotrigine 20 µM. Scale bar: 50 µm and 179.3 µm.

Figure 42. Effect of the incubation of (A) 132 µM of H₂O₂ and (C) 105 µM of H₂O₂, in combination with 20 µM of mirtazapine, scopolamine and lamotrigine, (B) 322 µM of corticosterone and (D) 35 µM of corticosterone, in combination with 20 µM of mirtazapine,

scopolamine and lamotrigine, determined by MTT methodology. The results represent the mean \pm SEM of three-six independent experiments, expressed as the percentage of the vehicle (100%). Statistically significant # $p < 0.05$, ## $p < 0.01$, ### $p < 0.001$, ##### $p < 0.0001$ vs. vehicle, and * $p < 0.05$, ** $p < 0.01$ vs. H₂O₂ 132 μ M, H₂O₂ 105 μ M, corticosterone 322 μ M, or corticosterone 35 μ M.

Figure 43. Concentrations of 5-HT (nM) in the extracellular medium of mirtazapine, scopolamine, and lamotrigine-treated SH-SY5Y and HT-22 cells, determined by ECD-HPLC. Results are derived from the analysis of the extracellular medium across a minimum of three separate and independently conducted experiments.

Figure 44. Concentrations of 5-HT (nM) in the extracellular medium of SH-SY5Y and HT-22 cells, treated with corticosterone, H₂O₂, and their combinations with mirtazapine, scopolamine, and lamotrigine determined by ECD-HPLC. Results are derived from the analysis of the extracellular medium across a minimum of three separate and independently conducted experiments.

Figure 45. Summary of 5-HT's branch of L-L-TRP biotransformation. This amino acid is (a) metabolized into 5-HTP, that is (b) converted into 5-HT, and finally (c) metabolized into 5-HIAA.

Figure 46. Representative images (100 \times total magnification) of SH-SY5Y exposed to (A) L-TRP 500 μ M, (B) L-TRP 500 μ M + H₂O₂ 300 μ M, and (C) L-TRP 500 μ M + corticosterone 500 μ M, (D) 5-HTP 500 μ M, (E) 5-HTP 500 μ M + H₂O₂ 300 μ M, and (F) 5-HTP 500 μ M + corticosterone 500 μ M, (G) 5-HT 500 μ M, (H) 5-HT 500 μ M + H₂O₂ 300 μ M, and (I) 5-HT 500 μ M + corticosterone 500 μ M, (J) 5-HIAA 500 μ M, (K) 5-HIAA 500 μ M + H₂O₂ 300 μ M, and (L) 5-HIAA 500 μ M + corticosterone 500 μ M. Scale bar: 50 μ m.

Figure 47. Effect of the incubation of 500 μ M of (A) L-TRP, (B) 5-HTP, (C) 5-HT, (D) 5-HIAA, 500 μ M of each metabolite in combination with 300 μ M of H₂O₂, and 500 μ M of each metabolite in combination with 500 μ M of corticosterone on the SH-SY5Y cellular viability, determined by MTT assay. The results represent the mean \pm SEM of three independent experiments, expressed as the percentage of the vehicle (100%). Statistically significant # $p < 0.05$, ### $p < 0.001$, ##### $p < 0.0001$ vs. vehicle, and ** $p < 0.01$, *** $p < 0.001$, **** $p < 0.0001$ vs. L-TRP 500 μ M, 5-HTP 500 μ M, 5-HT 500 μ M and 5-HIAA 500 μ M.

Figure 48. Variation of concentration (μ M) of (A) L-TRP, (B) 5-HTP, (C) 5-HT and (D) 5-HIAA in the extracellular medium of SH-SY5Y cells, in which the baseline represents (A) L-TRP, (B) 5-HTP, (C) 5-HT and (D) 5-HIAA 500 μ M. These cells were treated with H₂O₂

and corticosterone combined with these metabolites and analyzed by HPLC. Results are derived from the analysis of the extracellular medium across a minimum of three separate and independently conducted experiments.

Figure 49. Concentrations of 5-HT (nM) in the extracellular medium of SH-SY5Y cells treated with (A) H₂O₂ 50–300 μM and (B) corticosterone 100–500 μM, determined by HPLC (electrochemical method). The results represent the analysis of the supernatant collected from the three independent experiments.

Figure 50. Western blot analysis of BDNF monomer levels in acute hippocampal slices treated for 6h with mirtazapine 20 μM combined with (A) corticosterone 35 μM and (C) H₂O₂ 105 μM, and scopolamine 20 μM combined with (B) corticosterone 35 μM and (D) H₂O₂ 105 μM, after incubation with anti-BDNF primary antibody, previously detailed in the materials and methods section. Representative blot represented in (E). CORT: corticosterone; MIRT: mirtazapine; SCO: scopolamine. For clearer understanding and analysis, the results obtained for H₂O₂, mirtazapine, scopolamine, and corticosterone (for the same timepoint) are repeated in separate graphs. Statistically significant * p<0.05 and ** p < 0.01 vs. the aggressor (H₂O₂ 105 μM or corticosterone 35 μM), and # p<0.05 vs. vehicle.

Figure 51. Western blot analysis of BDNF dimer levels in acute hippocampal slices treated for 6h with mirtazapine 20 μM combined with (A) corticosterone 35 μM and (C) H₂O₂ 105 μM, and scopolamine 20 μM combined with (B) corticosterone 35 μM and (D) H₂O₂ 105 μM, after incubation with anti-BDNF primary antibody, previously detailed in the materials and methods section. Representative blot represented in (E). CORT: corticosterone; MIRT: mirtazapine; SCO: scopolamine. For clearer understanding and analysis, the results obtained for H₂O₂, mirtazapine, scopolamine, and corticosterone (for the same timepoint) are repeated in separate graphs. Statistically significant # p<0.05 and ## p < 0.01 vs. vehicle.

Figure 52. Representative images (200× total magnification) of neuronal hippocampal cell culture incubated for 6h (left) or 24h (right) with (A) vehicle (0.1% DMSO), (B) corticosterone 35 μM, (C) H₂O₂ 105 μM, (D) mirtazapine 10 nM, (E) mirtazapine 20 μM, (F) scopolamine 10 nM, (G) scopolamine 20 μM, (H) corticosterone 35 μM + mirtazapine 10 nM, (I) corticosterone 35 μM + mirtazapine 20 μM, (J) corticosterone 35 μM + scopolamine 10 nM, (K) corticosterone 35 μM + scopolamine 20 μM, (L) H₂O₂ 105 μM + mirtazapine 10 nM, (M) H₂O₂ 105 μM + mirtazapine 20 μM, (N) H₂O₂ 105 μM + scopolamine 10 nM, (O) H₂O₂ 105 μM + scopolamine 20 μM, after immunostaining with

Hoechst 33342 (blue), Alexa Fluor™ 647 Phalloidin (red), anti-BDNF (conjugated with Alexa Fluor™ 488, green) and anti- pTrkB (conjugated with Alexa Fluor™ 568, orange) primary antibodies. CORT: corticosterone; MIRT: mirtazapine; SCO: scopolamine. Scale bar (present in the first image): 50 µm.

Figure 53. Fluorescence intensity of BDNF expressed in neuronal hippocampal cell culture incubated for 6h (A, B) or 24h (C,D) with mirtazapine 10 nM or 20 µM combined with (A, C) corticosterone 35 µM and (B, D) H₂O₂ 105 µM, after immunostaining, as previously detailed in the materials and methods section. For clearer understanding and analysis, the results obtained for H₂O₂, mirtazapine, scopolamine, and corticosterone (for the same timepoint) are repeated in separate graphs. Statistically significant ### p<0.001 and ##### p < 0.0001 vs. vehicle, *** p<0.001 and **** p < 0.0001 vs. the aggressor (H₂O₂ 105 µM or corticosterone 35 µM).

Figure 54. Fluorescence intensity of BDNF expressed in neuronal hippocampal cell culture incubated for 6h (A, B) or 24h (C,D) with scopolamine 10 nM or 20 µM combined with (A, C) corticosterone 35 µM and (B, D) H₂O₂ 105 µM, after immunostaining, as previously detailed in the materials and methods section. For clearer understanding and analysis, the results obtained for H₂O₂, mirtazapine, scopolamine, and corticosterone (for the same timepoint) are repeated in separate graphs. Statistically significant ## p<0.01, ### p<0.001 and ##### p < 0.0001 vs. vehicle, ** p<0.01, *** p<0.001 and **** p < 0.0001 vs. the aggressor (H₂O₂ 105 µM or corticosterone 35 µM).

Figure 55. Fluorescence intensity of pTrkB in neuronal hippocampal cell culture incubated for 6h (A, B) or 24h (C,D) with mirtazapine 10 nM or 20 µM combined with (A, C) corticosterone 35 µM and (B, D) H₂O₂ 105 µM, after immunostaining, as previously detailed in the materials and methods section. For clearer understanding and analysis, the results obtained for H₂O₂, mirtazapine, scopolamine, and corticosterone (for the same timepoint) are repeated in separate graphs. Statistically significant ## p<0.01, ### p<0.001 and ##### p < 0.0001 vs. vehicle, **** p < 0.0001 vs. the aggressor (H₂O₂ 105 µM).

Figure 56. Fluorescence intensity of pTrkB in neuronal hippocampal cell culture incubated for 6h (A, B) or 24h (C,D) with scopolamine 10 nM or 20 µM combined with (A, C) corticosterone 35 µM and (B, D) H₂O₂ 105 µM, after immunostaining, as previously detailed in the materials and methods section. For clearer understanding and analysis, the results obtained for H₂O₂, mirtazapine, scopolamine, and corticosterone (for the same timepoint) are repeated in separate graphs. Statistically significant ##### p < 0.0001

vs. vehicle, ** $p < 0.01$, *** $p < 0.001$, and **** $p < 0.0001$ vs. the aggressor (H_2O_2 105 μM or corticosterone 35 μM).

Figure 57. Western blot analysis of BDNF levels in neuronal cortical cells treated for 6h (A,B,E,F) or 24h (C,D,G,H), with mirtazapine 10 nM or 20 μM combined with (A, C) corticosterone 35 μM and (B, D) H_2O_2 105 μM , and scopolamine 10 nM or 20 μM combined with (E,G) corticosterone 35 μM and (F, H) H_2O_2 105 μM , after incubation with anti-BDNF primary antibody, previously detailed in the materials and methods section. Representative blots are presented in image I. The Ponceau lanes are representative of the bands used as the loading control for normalization. CORT: corticosterone; MIRT: mirtazapine; SCO: scopolamine. For clearer understanding and analysis, the results obtained for H_2O_2 , mirtazapine, scopolamine, and corticosterone (for the same timepoint) are repeated in separate graphs. Statistically significant ## $p < 0.01$ vs. vehicle, and ** $p < 0.01$ vs. the aggressor (H_2O_2 105 μM).

Figure 58. (A) Comparative effect of induced hypoxia (with the hypoxia incubator) vs. normoxia on SH-SY5Y cell lines, 48h. The results represent the mean \pm SEM of three independent experiments, and representative images (100 \times total magnification) of SH-SY5Y cells under (B) hypoxia and (C) normoxia. Scale bar: 50 μm .

Figure 59. Representative images (100 \times total magnification) of SH-SY5Y cells under hypoxia conditions, induced by the hypoxia incubator chamber. Cells were treated with (A) mirtazapine 10 nM, (B) mirtazapine 20 μM , (C) TCB-2 10 nM, (D) TCB-2 20 μM , (E) dextromethorphan 10 nM, (F) dextromethorphan 20 μM , (G) ketamine 10 nM, (H) ketamine 20 μM , (I) quetiapine 10 nM (J) quetiapine 20 μM , (K) scopolamine 10 nM, (L) scopolamine 20 μM , (M) celecoxib 10 nM, (N) celecoxib 20 μM , (O) lamotrigine 10 nM, and (P) lamotrigine 20 μM . Scale bar: 50 μm .

Figure 60. Effect of the incubation of 10 nM and 20 μM of (A) mirtazapine, (B) TCB-2, (C) dextromethorphan, (D) ketamine, (E) quetiapine, (F) scopolamine, (G) celecoxib, and (H) lamotrigine on the viability of SH-SY5Y cells, under hypoxia conditions induced by the hypoxia incubator chamber, determined by MTT assay. The results represent the mean \pm SEM of three independent experiments, expressed as the percentage of the hypoxia vehicle (100%). Statistically significant ## $p < 0.01$ and ### $p < 0.001$ vs. vehicle.

Figure 61. Effect of the incubation of 10 nM and 20 μM of mirtazapine, TCB-2, dextromethorphan, ketamine, quetiapine, scopolamine, celecoxib, and lamotrigine on the viability of SH-SY5Y cells, determined by MTT assay. The results represent the mean

± SEM of three independent experiments, expressed as the percentage of the normoxic vehicle (100%). Statistically significant # $p < 0.05$ vs. vehicle.

Figure 62. Representative images (100 × total magnification) of SH-SY5Y cells after exposure to (A) 0.1% H₂O (vehicle), (B) CoCl₂ 0.1 mM, (C) CoCl₂ 0.25 mM, (D) CoCl₂ 0.5 mM, and (E) CoCl₂ 1 mM. Scale bar: 50 μm.

Figure 63. Effect of the incubation of 0.1–1 mM of CoCl₂, on the viability of SH-SY5Y cells, determined by MTT assay. The results represent the mean ± SEM of three independent experiments, expressed as the percentage of the vehicle (100%). Statistically significant ##### $p < 0.0001$ vs. vehicle.

Figure 64. Representative images (100 × total magnification) of SH-SY5Y cells treated with (A) vehicle (0.1% DMSO), (B) CoCl₂ 0.1 mM, (C) echinomycin 0.1 nM, (D) echinomycin 0.5 nM, (E) echinomycin 1 nM, (F) echinomycin 5 nM, (G) CoCl₂ 0.1 mM + echinomycin 0.1 nM, (H) CoCl₂ 0.1 mM + echinomycin 0.5 nM (I) CoCl₂ 0.1 mM + echinomycin 1 nM, and (J) CoCl₂ 0.1 mM + echinomycin 5 nM. Scale bar: 50 μm.

Figure 65. Effect of the incubation of CoCl₂ 0.1 mM, echinomycin 0.1 nM-5 nM, and the combination of CoCl₂ 0.1 mM with echinomycin 0.1 nM-5 nM on the viability of SH-SY5Y cells, determined by MTT assay. The results represent the mean ± SEM of three independent experiments, expressed as the percentage of the vehicle (100%). Statistically significant # $p < 0.05$ vs. vehicle.

Figure 66. Representative images (100 × total magnification) of SH-SY5Y cells treated with (A) vehicle (0.2% DMSO), (B) CoCl₂ 0.1 mM + mirtazapine 10 nM, (C) CoCl₂ 0.1 mM + mirtazapine 20 μM, (D) echinomycin 0.5 nM + CoCl₂ 0.1 mM + mirtazapine 10 nM, (E) echinomycin 0.5 nM + CoCl₂ 0.1 mM + mirtazapine 20 μM, (F) CoCl₂ 0.1 mM + dextromethorphan 10 nM, (G) CoCl₂ 0.1 mM + dextromethorphan 20 μM, (H) echinomycin 0.5 nM + CoCl₂ 0.1 mM + dextromethorphan 10 nM, (I) echinomycin 0.5 nM + CoCl₂ 0.1 mM + dextromethorphan 20 μM, (J) CoCl₂ 0.1 mM + quetiapine 10 nM, (K) CoCl₂ 0.1 mM + quetiapine 20 μM, (L) echinomycin 0.5 nM + CoCl₂ 0.1 mM + quetiapine 10 nM, (M) Echinomycin 0.5 nM + CoCl₂ 0.1 mM + quetiapine 20 μM, (N) CoCl₂ 0.1 mM + celecoxib 10 nM, (O) CoCl₂ 0.1 mM + celecoxib 20 μM, (P) echinomycin 0.5 nM + CoCl₂ 0.1 mM + celecoxib 10 nM, (Q) echinomycin 0.5 nM + CoCl₂ 0.1 mM + celecoxib 20 μM, (R) CoCl₂ 0.1 mM + TCB-2 10 nM, (S) CoCl₂ 0.1 mM + TCB-2 20 μM, (T) echinomycin 0.5 nM + CoCl₂ 0.1 mM + TCB-2 10 nM, (U) echinomycin 0.5 nM + CoCl₂ 0.1 mM + TCB-2 20 μM, (V) CoCl₂ 0.1 mM + ketamine 10 nM (W) CoCl₂ 0.1 mM + ketamine 20 μM, (X) echinomycin 0.5 nM + CoCl₂ 0.1 mM + ketamine 10 nM, (Y)

echinomycin 0.5 nM + CoCl₂ 0.1 mM + ketamine 20 μM, (Z) CoCl₂ 0.1 mM + scopolamine 10 nM, (AA) CoCl₂ 0.1 mM + scopolamine 20 μM, (AB) echinomycin 0.5 nM + CoCl₂ 0.1 mM + scopolamine 10 nM, (AC) echinomycin 0.5 nM + CoCl₂ 0.1 mM + scopolamine 20 μM, (AD) CoCl₂ 0.1 mM + lamotrigine 10 nM, and (AE) CoCl₂ 0.1 mM + lamotrigine 20 μM, (AF) echinomycin 0.5 nM + CoCl₂ 0.1 mM + lamotrigine 10 nM, and (AG) echinomycin 0.5 nM + CoCl₂ 0.1 mM + lamotrigine 20 μM. Scale bar: 50 μm.

Figure 67. Effect of the incubation of SH-SY5Y cells with CoCl₂ 0.1 mM in combination with either 10 nM or 20 μM of (A) mirtazapine, (B) dextromethorphan, (C) quetiapine, (D) celecoxib, (E) TCB-2, (F) ketamine, (G) scopolamine, and (H) lamotrigine on cell viability, and effect of incubating these cells with a combination of CoCl₂ 0.1 mM, echinomycin 0.5 nM, and either 10 nM or 20 μM of the same compounds (A-H) on cell viability, using the MTT assay. The results represent the mean ± SEM of three independent experiments, expressed as the percentage of the vehicle (100%). Statistically significant # p < 0.05, ### p < 0.001, vs. vehicle, and * p < 0.05, ** p < 0.01, *** p < 0.001, and **** p < 0.0001 vs. CoCl₂ 0.1 mM or CoCl₂ 0.1 mM combined with the different drugs.

Figure S1. Representative images (total magnification 100x) of SH-SY5Y cells morphology after exposure to mirtazapine, H₂O₂, and to the combination of mirtazapine with H₂O₂. Cells were incubated with (A) vehicle (0.1% methanol), (B) mirtazapine 0.01 μM, (C) mirtazapine 0.1 μM, (D) mirtazapine 1 μM, (E) mirtazapine 10 μM, (F) mirtazapine 20 μM, (G) H₂O₂ 132 μM, (H) H₂O₂ 132 μM + mirtazapine 0.01 μM, (I) H₂O₂ 132 μM + mirtazapine 0.1 μM, (J) H₂O₂ 132 μM + mirtazapine 1 μM, (K) H₂O₂ 132 μM + mirtazapine 10 μM, (L) H₂O₂ 132 μM + mirtazapine 20 μM. Scale bar: 179.3 μm.

Figure S2. Effect of increasing concentrations of (A) mirtazapine, and (B) mirtazapine in combination with H₂O₂, on the viability of SH-SY5Y cells, obtained by the MTT assay. The results are expressed as the percentage of the respective vehicles, and represent the mean ± SEM of three independent experiments.

Figure S3. Representative images (100 × total magnification) of SH-SY5Y and HT-22 cells after incubation of increasing concentrations of L-TRP. Cells were treated with (A,I) vehicle (0.1% H₂O) (B,J) 5-HT 0.1 nM, (C,K) 5-HT 1 nM, (D,L) 5-HT 10 nM, (E,M) 5-HT 100 nM, (F,N) 5-HT 1 μM, (G,O) 5-HT 10 μM, (H,P) 5-HT 100 μM. Scale bar: 179.3 μm.

Figure S4. Effect of the incubation of 0.1 nM-100 μM of 5-HT on the viability of (A) SH-SY5Y cells and (B) HT-22 cells, determined by MTT methodology. The results represent the mean ± SEM of three independent experiments, expressed as the percentage of the vehicle (100%).

Figure S5. Representative images (100 × total magnification) of SH-SY5Y and HT-22 cells after incubation of H₂O₂ in combination with 5-HT. Cells were treated with (A,I) vehicle (0.1% H₂O), (B,J) 5-HT 0.1 nM + H₂O₂ 132 μM/ 105 μM, (C,K) 5-HT 1 nM + H₂O₂ 132 μM/ 105 μM, (D,L) 5-HT 10 nM + H₂O₂ 132 μM/ 105 μM, (E,M) 5-HT 100 nM + H₂O₂ 132 μM/ 105 μM, (F,N) 5-HT 1 μM + H₂O₂ 132 μM/ 105 μM, (G,O) 5-HT 10 μM + H₂O₂ 132 μM/ 105 μM, (H,P) 5-HT 100 μM + H₂O₂ 132 μM/ 105 μM, (Q) H₂O₂ 132 μM, (R) H₂O₂ 105 μM. Scale bar: 179.3 μm.

Figure S6. Effect of the incubation of (A) 132 μM of H₂O₂ and (B) 105 μM of H₂O₂, in combination with 0.1 nM–100 μM of 5-HT, determined by MTT methodology. The results represent the mean ± SEM of three independent experiments, expressed as the percentage of the vehicle (100%). Statistically significant ### p < 0.001 vs. vehicle, * p < 0.05 vs. H₂O₂ 105 μM, and *** p < 0.001, **** p < 0.0001 vs. H₂O₂ 132 μM.

Figure S7. Representative images (100 × total magnification) of SH-SY5Y and HT-22 cells after incubation of corticosterone in combination with 5-HT. Cells were treated with (A,I) vehicle (0.1% methanol), (B,J) 5-HT 0.1 nM + corticosterone 322 μM/ 35 μM, (C,K) 5-HT 1 nM + corticosterone 322 μM/ 35 μM, (D,L) 5-HT 10 nM + corticosterone 322 μM/ 35 μM, (E,M) 5-HT 100 nM + corticosterone 322 μM/ 35 μM, (F,N) 5-HT 1 μM + corticosterone 322 μM/ 35 μM, (G,O) 5-HT 10 μM + corticosterone 322 μM/ 35 μM, (H,P) 5-HT 100 μM + corticosterone 322 μM/ 35 μM, (Q) corticosterone 322 μM, (R) corticosterone 35 μM. Scale bar: 179.3 μm.

Figure S8. Effect of the incubation of (A) 322 μM of corticosterone and (B) 35 μM of corticosterone, in combination with 0.1 nM–100 μM of 5-HT, determined by MTT methodology. The results represent the mean ± SEM of three independent experiments, expressed as the percentage of the vehicle (100%). Statistically significant ## p < 0.01, ### p < 0.001, #### p < 0.0001 vs. vehicle, and * p < 0.05 vs. corticosterone 322 μM.

Figure S9. Representative images (100 × total magnification) of SH-SY5Y after incubation of (A) vehicle (0.1% DMSO), (B) H₂O₂ 132 μM, (C) corticosterone 322 μM, (D) quetiapine 20 μM, (E) ketamine 20 μM, (F) dextromethorphan 20 μM, (G) celecoxib 20 μM, (H) TCB-2 20 μM. Scale bars: 50 and 179.3 μm.

Figure S10. Representative images (100 × total magnification) of SH-SY5Y after incubation of (A) quetiapine 20 μM + H₂O₂ 132 μM, (B) ketamine 20 μM + H₂O₂ 132 μM, (C) dextromethorphan 20 μM + H₂O₂ 132 μM, (D) celecoxib 20 μM + H₂O₂ 132 μM, (E) TCB-2 20 μM + H₂O₂ 132 μM, (F) quetiapine 20 μM + corticosterone 332 μM, (G)

ketamine 20 μM + corticosterone 332 μM , (H) dextromethorphan 20 μM + corticosterone 332 μM , (I) celecoxib 20 μM + corticosterone 332 μM , (J) TCB-2 20 μM + corticosterone 332 μM . Scale bars: 50 and 179.3 μm .

Figure S11. Effect of the incubation of 132 μM of H_2O_2 in combination with (A) quetiapine 20 μM , (B) ketamine 20 μM , (C) dextromethorphan 20 μM , (D) celecoxib 20 μM , and (E) TCB-2 20 μM , determined by MTT methodology. The results represent the mean \pm SEM of three independent experiments, expressed as the percentage of the vehicle (100%). Statistically significant # $p < 0.05$, ## $p < 0.01$ vs. vehicle, and * $p < 0.05$, ** $p < 0.01$ vs. H_2O_2 132 μM .

Figure S12. Effect of the incubation of 322 μM of corticosterone in combination with (A) quetiapine 20 μM , (B) ketamine 20 μM , (C) dextromethorphan 20 μM , (D) celecoxib 20 μM , and (E) TCB-2 20 μM , determined by MTT methodology. The results represent the mean \pm SEM of three independent experiments, expressed as the percentage of the vehicle (100%). Statistically significant # $p < 0.05$, ## $p < 0.01$, ### $p < 0.01$ vs. vehicle, and *** $p < 0.001$ vs. corticosterone 322 μM .

List of Tables

Table 1. Summary of the types of 5-HT receptors and their inhibitory/ excitatory potential.

Table 2. Most studied 5-HT receptors in depression, as well as their connection to this disease.

Table 3. Summary of BDNF main functions in the central nervous system.

Table 4. Summary of the BDNF and MDD connection.

Table 5. Main indication, known mechanism of action and relevance in depression of potential to be repurposed in the context of depression.

Table 6. Tested compounds, as well as their suppliers and solvent used in this work.

Table 7. Primary and secondary antibodies used in western blot and immunofluorescence methodologies.

Table 8. IC₅₀ values and average of IC₅₀ values for H₂O₂ and corticosterone in the viability of SH-SY5Y and HT-22 cells, obtained by MTT or NR. The results are rounded to the nearest integer.

Abbreviations

11 β -HSD: 11 Beta-Hydroxysteroid Dehydrogenase

3-HAA: 3-Hydroxyanthranilic Acid

3-HK: 3-Hydroxykynurenine

5-HIAA: 5-Hydroxyindoleacetic Acid

5-HT: 5-Hydroxytryptamine (Serotonin)

5-HTP: 5-Hydroxytryptophan

AA: Anthranilic Acid

AADC: Aromatic L-amino Acid Decarboxylase

AANAT: Arylalkylamine N-acetyltransferase

ACMSD: Aminocarboxymuconate-Semialdehyde Decarboxylase

aCSF: Artificial Cerebrospinal Fluid

ACTH: Adrenocorticotropic Hormone

ASMT: Acetylserotonin Methyltransferase

BCL-2: B-cell lymphoma 2

BDNF: Brain-Derived Neurotrophic Factor

cAMP: Cyclic Adenosine Monophosphate

CAT: Catalase

CBG: Corticosteroid Binding Globulin

CNS: Central Nervous System

COX: Cyclooxygenase

CREB: cAMP Response Element-Binding Protein

CRH: Corticotropin-Releasing Hormone

DA: Dopamine

DAG: Diacylglycerol

DCFDA: Dichlorodihydrofluorescein diacetate

ECD: Electrochemical detection

ERK: Extracellular-signal-Regulated Kinase

FDA: Food and Drug Administration

GABA: Gamma-Aminobutyric Acid

GAD: Glutamate Decarboxylase

GPx: Glutathione Peroxidase

GR: Glucocorticoid Receptor

HDAC: Histone Deacetylase

HIF-1: Hypoxia-inducible factor 1

HPA: Hypothalamic-Pituitary-Adrenal Axis

HPLC: High-performance liquid chromatography

IDO: Indoleamine 2,3-Dioxygenase

IL: Interleukin

IP3: Inositol Trisphosphate

KAT: Kynurenine Aminotransferase

KMO: Kynurenine 3-Monooxygenase

KYN: Kynurenine

KYNA: Kynurenic Acid

KYNU: Kynureninase

LPS: Lipopolysaccharide

MAO: Monoamine Oxidase

MAOI: Monoamine Oxidase Inhibitor

MDA: Malondialdehyde

MDD: Major Depressive Disorder

MR: Mineralocorticoid Receptor

MTT: 3-[4,5-dimethylthiazol-2-yl]-2,5 diphenyl tetrazolium bromide)

NA: Noradrenaline

NADPH: Nicotinamide Adenine Dinucleotide Phosphate

NAS: N-Acetylserotonin

NF-κB: Nuclear Factor Kappa-light-chain-enhancer of Activated B cells

NMDA: N-Methyl-D-Aspartate

NPC: Neural Progenitor Cell

NR: Neutral Red

Nrf-2: Nuclear Factor Erythroid 2-Related Factor 2

PA: Phosphatidic Acid

PFA: Paraformaldehyde

PFC: Prefrontal cortex

PKB: Protein Kinase B

PLC γ : Phospholipase C Gamma

PNS: Peripheral Nervous System

PPAR: Peroxisome Proliferator-Activated Receptor

PVN: Paraventricular Nucleus

QA: Quinolinic Acid

QPRT: Quinolate Phosphoribosyltransferase

RNS: Reactive Nitrogen Species

ROS: Reactive Oxygen Species

SERT: Serotonin Transporter

SNRI: Serotonin-Noradrenaline Reuptake Inhibitor

SOD: Superoxide Dismutase

SSRI: Selective Serotonin Reuptake Inhibitor

TCA: Tricarboxylic Acid Cycle

TDO: Tryptophan 2,3-Dioxygenase

TPH: Tryptophan Hydroxylase

TrkB: Tropomyosin Receptor Kinase B

TrkB – FL: Tropomyosin Receptor Kinase B – Full Length

TRP: Tryptophan

WHO: World Health Organization

XA: Xanthurenic Acid

I. Introduction

The introduction is based on the following review articles, published as first author:

- **Correia, A.S.**; Cardoso, A.; Vale, N. Highlighting Immune System and Stress in Major Depressive Disorder, Parkinson's, and Alzheimer's Diseases, with a Connection with Serotonin. *Int. J. Mol. Sci.* **2021**, *22*, 8525.
- **Correia, A.S.**; Vale, N. Antidepressants in Alzheimer's Disease: A Focus on the Role of Mirtazapine. *Pharmaceuticals* **2021**, *14*, 930.
- **Correia, A.S.**; Vale, N. Tryptophan Metabolism in Depression: A Narrative Review with a Focus on Serotonin and Kynurenine Pathways. *Int. J. Mol. Sci.* **2022**, *23*, 8493.
- **Correia, A.S.**; Cardoso, A.; Vale, N. Oxidative Stress in Depression: The Link with the Stress Response, Neuroinflammation, Serotonin, Neurogenesis and Synaptic Plasticity. *Antioxidants* **2023**, *12*, 470.
- **Correia, A.S.**; Cardoso, A.; Vale, N. BDNF Unveiled: Exploring Its Role in Major Depression Disorder Serotonergic Imbalance and Associated Stress Conditions. *Pharmaceutics* **2023**, *15*, 2081.

To the published content, some additional modifications, insights/ updates were also included.

1. The Contextual Landscape of Major Depressive Disorder

Depression is a multifaceted mental health condition, manifesting in various forms that impact individuals uniquely. Among the prevalent types of depression are Major Depressive Disorder (MDD), Persistent Depressive Disorder, Bipolar Disorder, Seasonal Affective Disorder, and Postpartum Depression [1]. Notably, the World Health Organization (WHO) reports that approximately 280 million people worldwide struggle with depression [2]. Particularly, Portugal occupies the 5th position among the countries with the most cases of depression: about 8% of the population suffers from the disease [3]. MDD, commonly only referred to depression, represents a debilitating condition characterized by at least one distinct depressive episode lasting a minimum of two weeks, marked by shifts in mood, interests, and pleasure, as well as cognitive symptom alterations [4]. Indeed, this condition is very heterogeneous, characterized by anhedonia and a depressed mood, with potential consequences extending to suicide and impairment of cognitive functions, including memory and learning [5,6]. People suffering from MDD also suffer from social stigma, elevated occurrences of physical health conditions like heart disease, obesity, and type 2 diabetes, as well as a more likelihood of adverse consequences concerning their educational, occupational, and interpersonal aspects of life [6]. The hereditary component contributing to MDD is roughly estimated at around 35% to 40%. Furthermore, environmental elements like childhood experiences of sexual, physical, or emotional abuse are closely linked to the likelihood of MDD development [6,7]. However, the comprehension of how these environmental factors interact with genetic and epigenetic influences remains incomplete. Some individuals with a high susceptibility may only need mild stressors to trigger MDD, while those with low vulnerability may only develop MDD when exposed to severe stressors [6]. Nevertheless, gaining a complete understanding of this condition is of extreme importance in the field of neuroscience because there is no singular established mechanism that can explain the entirety of its complexity.

A significant challenge in dealing with this disease is its frequent recurrence, treatment ineffectiveness, and the absence of diagnosis and treatment options, particularly in low- and middle-income countries [2,4,8]. Nevertheless, there are viable treatment approaches, particularly psychotherapy and/or the use of antidepressant medications [4]. Both psychotherapy and psychopharmacology demonstrate efficacy in addressing MDD. Still, it is noteworthy that approximately 30% of individuals affected by MDD do not experience remission, even after multiple treatments [4,9]. In fact, resistance to antidepressant medication can come from several aspects, such as variations in cytochrome P450 (CYP) enzymes genes affecting drug metabolism, the activity of drug

efflux transporters that are expressed at the blood-brain barrier (BBB), brain structure itself, neurotransmission system imbalances and other molecular aspects such as brain-derived neurotrophic factor (BDNF) secretion and intercellular trafficking [10]. This supports the significance of further research into this disorder. Nevertheless, it is important to note that the preclinical research of depression often involves animal models, facing several challenges and limitations that typically slow down the research of this disease. Particularly, besides the complexity of depression, developing animal models that accurately mimic the complex human condition of depression is challenging. Thus, bridging the gap between animal studies and human depression is a major obstacle. Also, ensuring the reproducibility of research findings is a fundamental challenge in laboratory research, often being an issue when studying depression [11]. This issue will be further explored in the discussion.

Depression comes from the overall impact of disturbed network regulation including numerous brain regions. It is not only attributed to any single brain region or neurotransmitter system but rather results from the complex connection among these regions [6]. The configurations of these implicated components are diverse, which relates to the significant variability and heterogeneity seen in the clinical manifestations of MDD [6]. Indeed, this disease involves a multitude of systems, ranging from the immune system to the neuroendocrine system, and encompasses diverse molecular components (Figure 1) [4,12]. Despite the complex nature of MDD, multiple studies consistently highlight the importance of various factors, including neurotransmitters (including serotonin (5-HT), dopamine (DA), noradrenaline (NA), glutamate and gamma-aminobutyric acid (GABA)), oxidative stress, exposure to hypoxia, neurotrophic factors (particularly BDNF) disturbances in gut microbiota, genetic predisposition, immunological factors, endocrine influences, and environmental factors in contributing to this condition [12,13]. Structural alterations, in brain regions such as the pre-frontal cortex, anterior cingulate cortex and hippocampus are also significant [14]. Indeed, previous studies have shown that the hippocampus is smaller in depressed patients than in healthy controls [15,16]. Possibly, these findings are due to abnormal axonal and dendritic growth, driven by, for example, alterations in the inflammatory status, dysregulation of the hypothalamic–pituitary–adrenal (HPA) axis and apoptosis [6].

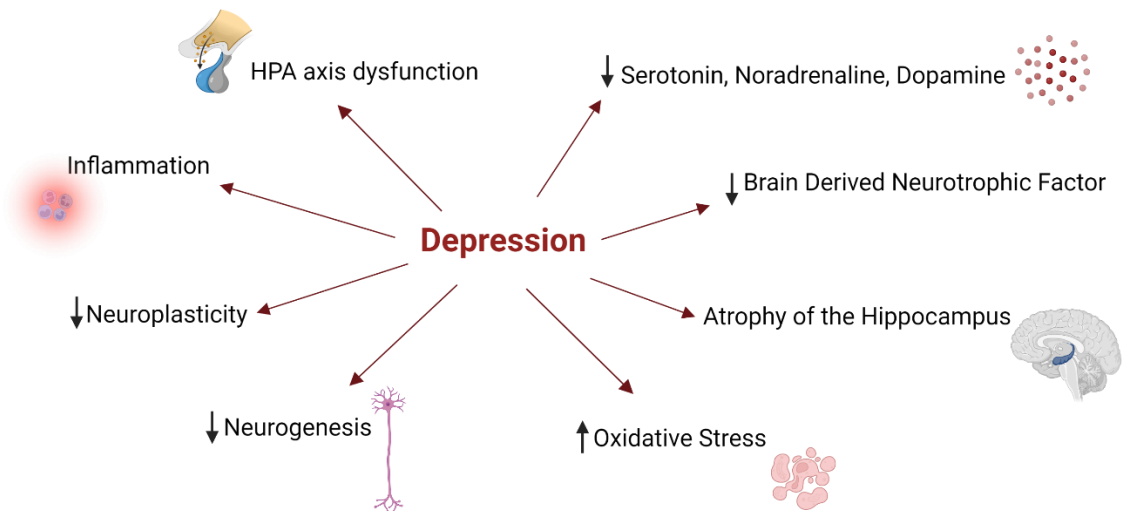


Figure 1. Depression is a multifaceted condition characterized by different underlying factors. These include dysfunction in the HPA axis, imbalanced levels of neurotransmitters like 5-HT, NA and DA, fluctuations in neurotrophic factors such as BDNF, shrinkage of certain brain regions like the hippocampus, high levels of inflammation and oxidative stress, and reduced levels of neurogenesis. Illustration created with BioRender [17].

This thesis's introduction will cover the following points:

- It will begin by discussing the general roles of oxidative stress, tryptophan metabolism (with special focus on 5-HT), BDNF, and HPA axis dysfunction in depression.
- After that, the interconnection between these systems in depression will be addressed.
- Finally, pharmacological interventions in the management of MDD will also be discussed.

2. Exploring the Role of Oxidative Stress, Tryptophan Metabolism, Brain-Derived Neurotrophic Factor, and Hypothalamic–Pituitary–Adrenal Axis Dysfunction in Major Depressive Disorder

2.1. Oxidative Stress Dysregulation: An Overlook

Oxidative stress arises from the disruption in the equilibrium between the generation of free radicals, notably reactive oxygen species (ROS), and antioxidant mechanisms. These mechanisms play an important role in the generation of free radicals by effectively neutralizing these reactive species, which are produced during various metabolic processes. Furthermore, the exposure to environmental stressors, such as smoking or ultraviolet radiation, can amplify these metabolic reactions, accentuating the challenge of maintaining this equilibrium [18]. Lifestyle factors such as diet, physical activity, and stress management significantly affect oxidative stress levels in the body. Indeed, a balanced diet rich in antioxidants, regular exercise, and effective stress reduction techniques can help maintain oxidative balance [19].

The main ROS, superoxide radicals ($O_2^{\cdot-}$), hydrogen peroxide (H_2O_2), hydroxyl radicals ($\cdot OH$), and singlet oxygen (1O_2), are generated through processes such as immunity, apoptosis, protein phosphorylation, and other cellular signaling processes [20]. Indeed, in the human body, ROS are mainly produced in mitochondria, peroxisomes, and the endoplasmic reticulum, being also continuously generated by enzymatic reactions that involve cyclooxygenases (COXs), nicotinamide adenine dinucleotide phosphate (NADPH) and xanthine oxidases, lipoxygenases and through the Fenton reaction, that is the reaction between iron and H_2O_2 , generating $\cdot OH$ [20]. At low quantities, ROS are important to the maintenance of homeostasis and cellular processes, being involved in the regulation of intracellular signaling pathways, acting as secondary messengers in various cellular processes, including cell proliferation, differentiation, and apoptosis. They are also important in the immune response [18,21–23]. However, when the production of these species increases in response to several stimuli, negative effects occur in cellular structures and processes: proteins, lipids, nucleic acids, enzymes, cellular division, and cellular metabolism are highly affected, being associated with the development and progression of several diseases, such as cancer and diabetes [18,21,24]. In fact, oxidative stress damages cells primarily through the oxidation of lipids, proteins, and DNA. This process can trigger a cascade of cellular events leading to apoptosis or necrosis, also by affecting unspecific targets, promoting an imbalance in the adaptive pathways, such as nuclear factor- κB (NF- κB) and nuclear factor erythroid 2-related factor 2 (Nrf-2), converging into pathological conditions [25].

To protect against the effects of increased ROS levels, cells have antioxidant defenses, with a particular focus on enzymatic systems such as superoxide dismutase (SOD), catalase (CAT), and glutathione peroxidase (GPx). These endogenous antioxidants have indispensable roles in preserving the overall health of an organism, being important to maintain ROS homeostasis [18,26]. Exogenous antioxidant defenses may also be introduced by diet or nutritional supplementation, such as vitamin C, vitamin E and carotenoids [18,27]. For instance, dietary antioxidants like vitamin C and E have been studied for their potential in reducing the risk of chronic diseases like heart disease and cancer [28]. The production of ROS must be counterbalanced by an equivalent rate of antioxidant consumption. However, in pathological scenarios, the production of ROS is increased, promoting deleterious effects within cells and tissues, catalyzing the progression of diseases, as mentioned earlier. Figure 2 summarizes the harmful effects of excessive ROS production.

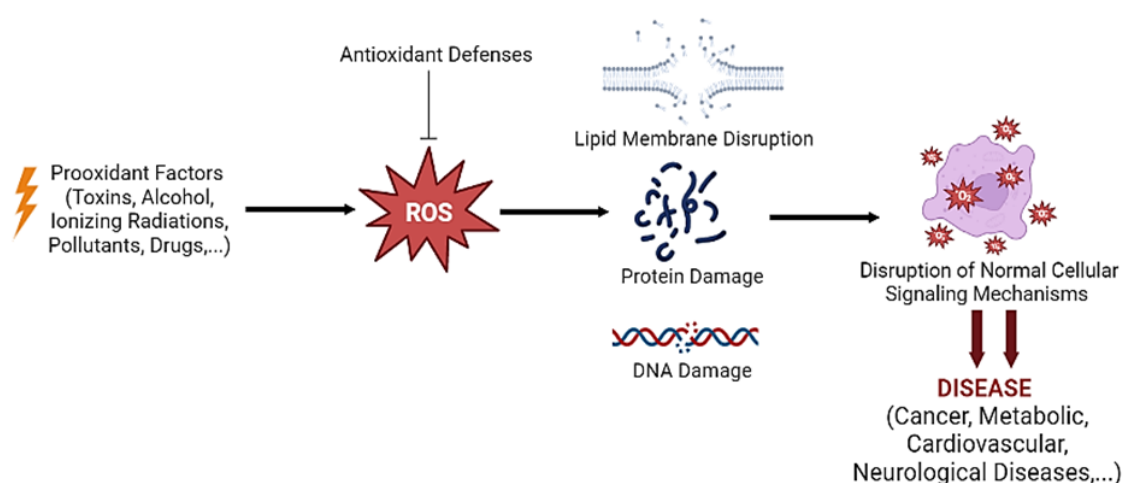


Figure 2. Prooxidant factors such as toxins and pollutants promote high levels of ROS production that are kept at low levels by the antioxidant defenses. However, when ROS production overwhelms antioxidant defenses, harmful effects such as membrane disruption, protein and DNA damage occur, disrupting the normal cell signaling mechanisms and culminating in diseases such as cancer or neurological diseases. Created with BioRender [17].

Research on oxidative stress in depression and antioxidant-associated mechanisms and potentialities may lead to more pharmacological success. Some examples in the context of depression will be described below.

2.1.1. Oxidative Stress As A Key Contributor to Major Depressive Disorder Pathogenesis

The several cellular and molecular mechanisms involved in MDD, such as an exacerbated stress response, presence of high levels of neuroinflammation, imbalance in the signaling mediated by neurotransmitters and, also, challenges in neurogenesis and synaptic plasticity, are intensified by the presence of high levels of oxidative stress [29,30]. Indeed, the overproduction of ROS, coupled with an inadequate antioxidant response, triggers a series of detrimental events, including inflammation, neurodegeneration, tissue damage, and cellular damage [31].

The impact of ROS on depression is well-documented. The brain, in particular, is vulnerable to oxidative stress due to its high oxygen consumption, lipid content, and relatively weaker antioxidative defense. Also, the brain neurons, astrocytes and microglia are rich in mitochondria and NADPH oxidase (NOX), being capable of generating high levels of ROS. This vulnerability makes oxidative stress a primary cause of neurodegeneration and a key factor in MDD. Addressing these changes with suitable antioxidants could be an effective strategy for managing MDD [30,32].

A recent longitudinal study indicated that depression is linked to reduced intake of antioxidants like vitamins A, C, and E, selenium, zinc, and B vitamins (B6, folate, and B12) [33]. There is also evidence that elevated levels of oxidative stress in the brain contribute to increased lipid peroxidation [30]. Indeed, a meta-analysis of lipid peroxidation markers in MDD (particularly malondialdehyde, MDA) demonstrated that lipid peroxidation was greater in MDD individuals than in controls, being also correlated with greater severity of symptoms [34]. When coupled with a decrease in antioxidant defenses, these mechanisms support the role of oxidative stress as an important player in the onset and progression of depression [30]. Targeting hypoxia-related pathways may be also a promising tool for depressive disorders in the context of mitigating high oxidative stress levels, known to be enhanced by hypoxia [13,35]. In fact, we have recently found that hypoxia–ischemia induced an increase in ROS in neuron-like cells, and that the drug edaravone increased cell viability and reduced ROS production, probably by its free radical-scavenging properties [36].

Various studies have also observed notable reductions in antioxidants (such as SOD and GSH) in both depressed patients and animal models [32,37]. Also, clinical investigations have consistently reported elevated levels of peroxidation biomarkers (MDA, 8-hydroxy-2'-deoxyguanosine (8-OHdG), and F2-isoprostanes) and reduced antioxidant activity in the plasma and serum of individuals with MDD [32,38,39]. Animal studies have further demonstrated stress-induced abnormalities in various brain regions,

such as decreased GSH and SOD activity, as well as increased levels of ROS, MDA, and carbonyl compounds, particularly in the prefrontal cortex (PFC) and hippocampus of depressed rats subjected to chronic unpredictable mild stress and chronic restraint stress [40,41]. Furthermore, it has been revealed that antidepressants have antioxidant properties and antioxidants exhibit antidepressant effects in both human subjects and rodents. For instance, antidepressants like fluoxetine and citalopram have been shown to enhance SOD activity and ascorbic acid levels, while reducing MDA and carbonyl levels in MDD patients [32,42]. Conversely, antioxidant compounds such as diallyl disulfide have been demonstrated to reverse lipopolysaccharide induced depressive-like behaviors in mice [43].

These findings collectively support the significant role of oxidative stress as a key factor in the pathogenesis of depression and suggest that augmenting antioxidant activity is a potential therapeutic approach. On the part 3, will be made a deeper analysis into the high levels of ROS associated with the stress response, neuroinflammation, imbalanced neurotransmitter function, and disturbances in neurogenesis and synaptic plasticity, all of which collectively contribute to the development and progression of MDD (Figure 3).

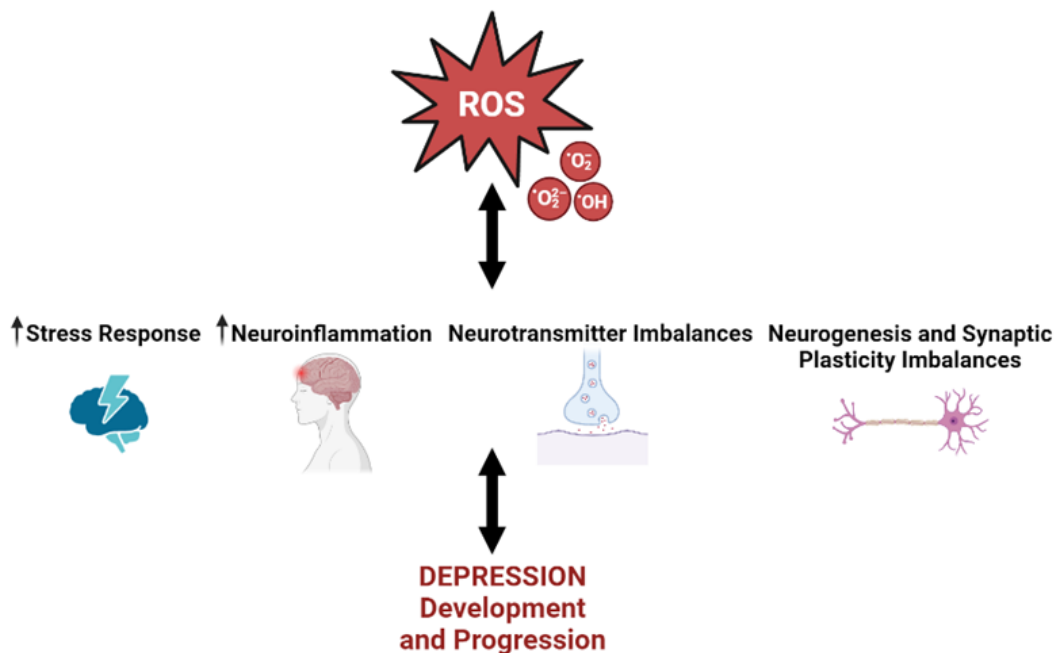


Figure 3. High levels of ROS promote and are promoted by the stress response, neuroinflammation, and imbalances in neurotransmitter-related pathways and neurogenesis/synaptic plasticity processes. All these features underlie the pathophysiology of depression, being critical in disease development and progression. Created with BioRender. [17].

2.2. A Closer Look On Hypothalamic–Pituitary–Adrenal Axis In The Control of Stress Response

The HPA axis plays a crucial role in various aspects of health and disease, being an important neuroendocrine complex involved in various physiological processes. Indeed, HPA axis is a complex system, important in regulating basic functions such as energy balance, reproduction, and response to stress [44,45]. The key elements of this axis are the hypothalamus, pituitary gland and adrenal glands. The hypothalamus contains neuroendocrine neurons which synthesize and secrete vasopressin and corticotropin-releasing hormone (CRH), mainly in the paraventricular nucleus (PVN). The pituitary gland is located just below the hypothalamus. In response to stress, CRH and vasopressin are released into hypophysial portal vessels that access the anterior lobe of the pituitary gland to secrete adrenocorticotrophic hormone (ACTH) by the activation of cyclic adenosine monophosphate (cAMP) pathway, after binding to CRH receptor 1 and vasopressin V1b (or V3) receptor, respectively. The adrenal glands cortex produces glucocorticoid hormones (mainly cortisol in humans) in response to stimulation by ACTH, that binds to the melanocortin type 2 receptor. These glucocorticoids regulate physiological responses and inhibit further HPA axis activation. The HPA axis is connected to both the central nervous system and the endocrine system, regulating the hormones in the body and affecting the stress response [46].

The stress response includes a complex connection of systems, with particular emphasis on the autonomic nervous system and the HPA axis. When this axis is triggered, it leads to an increase in glucocorticoid levels, a key component in the body's adaptation to stress [47,48]. Diverse reactions to stress are observed, depending on if it is of a short-term or long-term nature. The short-term is a natural physiological response, while the long-term tends to be detrimental, disrupting the normal, healthy stress response. Under physiological conditions and in a stress-free situation, healthy adults secrete between 10 and 20 mg of cortisol in the daily rhythm with regular peaks [49]. Initially, there's a surge in ACTH levels, which triggers the release of cortisol. However, when someone experiences prolonged, chronic stress, ACTH levels generally remain high due to impaired negative feedback, and cortisol levels remain high due to elevated adrenal sensitivity. Indeed, the hypothalamus changes the signaling from being mainly driven by CRH to being also driven by vasopressin. This shift contributes to the persistence of high cortisol levels, mainly to the decrease in the cortisol metabolism [50]. Thus, when faced with uncontrollable and prolonged stress, it can lead to a range of alterations in various aspects of the central nervous system, contributing to neuropsychiatric and neurodegenerative conditions [47,51]. In fact, elevated cortisol

secretion during stressful situations can significantly impact the functioning of the brain. This hormone has a particularly pronounced effect on the hippocampus due to the abundance of steroid receptors it possesses [49,52]. Recurrent exposure to stress triggers alterations in neuronal structures. When stress is brief and infrequent, the hippocampal atrophy that may occur is often reversible. However, chronic, long-term stress can result in the death of neurons within the hippocampus. Numerous studies have suggested that conditions like depression and post-traumatic stress disorder are associated with a reduction in the volume of the hippocampus, as well as that of the PFC and amygdala [49,53]. What remains uncertain is whether it is the increased cortisol secretion itself or the dysregulation of cortisol secretion that serves as the primary cause of this neuronal atrophy [49].

Glucocorticoid receptors (GRs) and mineralocorticoid receptors (MRs) are the intracellular nuclear receptors that respond to cortisol. GRs are found in the brain and peripheral tissues, while MRs are primarily located in cardiovascular tissues, the liver, kidneys, and certain brain regions like the corticolimbic areas (prefrontal cortex, amygdala, and hippocampus) [54]. These receptors can either activate or repress the transcription of genes in the cell nucleus and also mediate rapid, non-genomic effects [55]. During the day, nuclear MRs are typically occupied by cortisol, remaining active. However, during the night, when cortisol levels are very low, these MRs become unoccupied. When cortisol levels rise significantly, such as during the circadian peak or in response to acute or chronic stress, both nuclear GRs and membrane-associated MRs and GRs become occupied by this hormone, leading to changes in synaptic plasticity at the cellular level [54,56]. The regulation of GR sensitivity is linked to the activity of *FKBP5*, that encodes the FK 506 binding protein 51 (FKBP51). Upon bound with FKBP51, the GR exhibits reduced affinity for glucocorticoid binding and experiences impaired translocation into the nucleus. Importantly, the activation of the GR leads to an increase in both *FKBP5* mRNA and protein expression, establishing a negative feedback loop to modulate GR sensitivity [57].

The availability of cortisol in the body is also influenced by corticosteroid-binding globulin (CBG), a protein carrier. Under normal conditions, most cortisol is tightly bound to CBG, but small amounts are loosely bound to albumin, and a fraction remains "free" and biologically active [58]. Additionally, the body's clearance of cortisol involves two mechanisms: enzymic degradation in the liver and intracellular metabolism by two isoenzymes of 11 β -hydroxysteroid dehydrogenase (11 β -HSD). 11 β -HSD type 1 acts predominantly as a reductase, regenerating active glucocorticoids and amplifying the cellular actions of cortisol. It is found in various tissues and is implicated in regulating tissue sensitivity to cortisol. On the other hand, 11 β -HSD type 2 is a high-affinity

dehydrogenase that inactivates glucocorticoids [59]. These various levels of regulation in cortisol signaling, including receptor distribution, CBG levels, and enzyme activity, play crucial roles in maintaining homeostasis and responding to stressors in the body [50].

Research in neuropsychiatry indicates that abnormalities in the stress response play a significant role in the development of these types of diseases. Furthermore, additional research also highlights the importance of imbalances in the stress response in the context of neurodegenerative disorders [47].

2.2.1. Unraveling the Hypothalamic–Pituitary–Adrenal Axis Dysregulation in Major Depressive Disorder

Hyperactivity of the HPA axis is one of the most consistent biological findings in MDD [60].

In individuals with MDD, the functionality of the GR typically becomes compromised, resulting in a diminished capacity for negative feedback regulation: a dysfunction of the GR leads to an impaired HPA axis negative feedback, which in turn leads to the HPA axis hyperactivity [61]. Consequently, this dysregulation triggers an excessive secretion of CRH within the central nervous system and an increased synthesis of glucocorticoids [62]. Antidepressant drugs, on the other hand, also work by influencing the functioning of this system. These influences can take various forms, including the regulation of GR expression and post-translational modifications. As a result, the therapeutic effects of antidepressants involve, at least partially, the restoration of GR function [63]. Also, they can affect the release of CRH. By modulating the release of CRH, antidepressants can further help to restore the balance of the HPA axis and alleviate the symptoms of depression [62,64]. An interesting study revealed that when given with imipramine and fluoxetine, SN003 (a CRH receptor 1 blocker), potentiated the antidepressant-like effect of these drugs in depressed rats, being an advantageous combination in terms of safety, since it requires lower doses of the applied agents [65]. Research has also revealed that depressed individuals often exhibit elevated levels of CRH mRNA expression coupled with elevated levels in cerebrospinal fluid [47]. Beyond this, high stress levels have also been associated with disruptions in serotonergic pathways, alterations in the structural integrity of brain regions like the hippocampus and PFC, as well as epigenetic modifications in genes such as BDNF [66–68]. In fact, evidence supports the complex connection between the stress system and MDD across various features. Prolonged exposure to corticosterone (the equivalent of glucocorticoids in mice) has been demonstrated to induce structural modifications in neuronal dendrites, promoting atrophy [69,70]. Moreover, research on postmortem tissue from individuals with depression and

animal models has provided valuable insights into the alterations at the cellular level associated with this condition, including dendritic atrophy, neuronal loss, and alterations in glial elements [71]. Chronic exposure to corticosterone also leads to synapse loss and neuronal apoptosis through mechanisms such as glutamate excitotoxicity, a cell death mechanism triggered by excessive glutamate release from neurons and glial cells [72–74]. These neurobiological changes align with cognitive decline and the development of conditions like MDD. Additionally, studies have revealed that in stressed animals, concentrations of brain metabolites decrease, particularly affecting N-acetyl-aspartate (indicates neuronal viability and function), creatine and phosphocreatine (energy metabolites), and choline-containing compounds (representing formation/ degradation products of cell membranes). The administration of tianeptine, an antidepressant, has been shown to prevent these stress-induced effects [75]. Furthermore, stress-related epigenetic alterations in genes such as *GR*, *5-HT transporter*, *BDNF*, and *spindle and kinetochore-associated complex 2* have been linked to a diagnosis of MDD [68,76–81]. Moreover, polymorphic variations within the *FKBP5* gene have been associated with differential FKBP5 mRNA expression following GR activation and alterations in GR sensitivity, being implicated in MDD [82].

Both glucocorticoids and inflammation have been implicated in the pathogenesis of depression. The accepted glucocorticoid resistance model suggests that reduced sensitivity to cortisol's anti-inflammatory effects leads to increased inflammation in depression. Indeed, animal studies have revealed that repetitive social defeat, a form of chronic stress, can trigger glucocorticoid-resistant monocytes, elevated neuroinflammatory signaling, and depressive-like behaviors in animal models [83,84]. Human studies have observed reduced GR function/expression, HPA axis hyperactivity, and increased inflammation in depressed patients [61,83], despite the recognized property of glucocorticoids as important anti-inflammatory molecules. This apparent contradiction may be explained by the balance between the coexistence of the glucocorticoid system and the inflammatory system. Chronic stress may disrupt this equilibrium, favoring inflammatory processes and impairing glucocorticoid signaling. Moreover, the actions of glucocorticoids may vary depending on the context and concentration, further complicating the relationship between glucocorticoids and inflammation. Understanding this interaction is crucial for identifying treatment targets in depression [85].

Stressors have the power to either augment or suppress immune functions [86]. Stress-induced proinflammatory cytokine production activates the indoleamine 2,3-dioxygenase (IDO)/kynurenine (KYN) pathway in cells such as glial cells and macrophages, further connecting stress with the immune system. IDO plays a critical

role in the catabolism of tryptophan (TRP), resulting in reduced 5-HT levels, explored in the next sections [87]. Particularly notorious is the link between high concentrations of interleukin (IL)-1 and IL-6 and the stress response—a connection of high importance in strengthening the immune system and facilitating survival [88,89]. Indeed, an elevated production of IL-6 in individuals with MDD has been observed to play a role in MDD prognosis and how individuals respond to treatment, possibly through activation of HPA axis: the dysregulated cortisol levels can lead to chronic activation of the immune system, including the production of IL-6 [90].

Research also establishes the central role of microglial cells in the modulation of stress-induced depression [91]. Preclinical research has reported inflammatory activation in microglia within specific brain regions that are important in mood regulation (such as the PFC, nucleus accumbens, amygdala, and hippocampus). Nevertheless, the precise pathways that modulate stress-induced microglial activation remain unclear [92]. However, in response to stress-induced neuroinflammation, microglia release proinflammatory cytokines and metabolic byproducts, influencing the function of neurons and astrocytes [93]. In fact, antidepressants, including selective 5-HT reuptake inhibitors (SSRIs) and 5-HT-NA reuptake inhibitors (SNRIs) have been shown to inhibit microglial activation [94]. There is also evidence of the relationship between stress and immune responses by the investigation of the knockout of the *Cx3cr1* gene in microglia—a gene crucial in microglial regulation. Results demonstrated that this gene plays a significant role in the microglia-mediated stress response, and its knockdown prevents the effects of stress and depressive behaviors in mice [95]. Thus, microglia play a complex role in depression, and their impact can be both beneficial and detrimental depending on if these cells are dysregulated or overactivated. Understanding the complex relationship between stress and the microglia has the potential to provide valuable insights and significant breakthroughs in MDD understanding [96].

The exploration of the stress response, primarily mediated by the HPA axis, provides a pathway to understand the fundamental biological mechanisms that underlie depression, opening the possibility of developing more effective treatments tailored to this system.

2.3. An Overlook on Tryptophan Metabolism

TRP is an essential dietary component with important implications in various physiological reactions. There are two major pathways of TRP metabolism: the KYN pathway and the 5-HT pathway (Figure 4).

The KYN pathway is the principal branch for TRP metabolism, accounting for approximately 95% of free TRP utilization [97]. This pathway plays an important role in various physiological processes, including production of cellular energy, modulation of inflammation, and facilitation of neurotransmission. Notably, it exerts influences on physical exercise outcomes and mental health, with established connections to diseases such as MDD, schizophrenia, cancer, and diabetes [97–99]. The KYN pathway is active in a variety of cell types and tissues, including the liver, brain, and immune cells [98].

The initial and rate-limiting step within the KYN pathway involves the conversion of TRP to KYN, facilitated by the enzymes IDO1 and IDO2, as well as TRP 2,3-dioxygenase (TDO). Subsequently, KYN predominantly transforms into 3-hydroxykynurenine (3-HK) through the catalytic action of KYN 3-monooxygenase (KMO). 3-HK, in turn, undergoes conversion into xanthurenic acid (XA) by KYN aminotransferase (KAT) and into 3-hydroxyanthranilic acid (3-HAA) via the enzyme kynureninase (KYNU). Following this, 3-HAA undergoes further metabolism into picolinic acid (PA) through the enzymatic activity of aminocarboxymuconate-semialdehyde decarboxylase (ACMSD) and into quinolinic acid (QA) via non-enzymatic processes. Subsequently, QA is transformed into NAD⁺ through the action of quinolinate phosphoribosyl transferase (QPRT). Additionally, to a lesser extent, KYN can be metabolized into kynurenic acid (KYNA) through the enzymatic activity of KAT and into anthranilic acid (AA) through the actions of KYNU [98,100].

The serotonergic pathway of TRP metabolization is extremely important in human physiology, having a profound influence on several physiological functions. Indeed, 5-HT networks are important players in behavioral aspects, including mood regulation, sexual function, appetite control and stress response modulation. Moreover, these networks also influence motor coordination, circadian rhythm synchronization, and thermoregulation. The 5-HT pathway has also influence on diverse physiological processes such as gastrointestinal regulation, nociception, mammary gland development, regulation of blood vessel constriction and dilation, control of heart rate, and modulation of platelet aggregation [101].

This pathway's first and rate-limiting step is the conversion of TRP to 5-hydroxytryptophan (5-HTP) by the enzymes TRP hydroxylase 1 or 2 (TPH1 or 2, mostly expressed in peripheral and in the central nervous tissues, respectively). Subsequently,

5-HTP undergoes decarboxylation mediated by aromatic acid decarboxylase (AADC) to yield 5-HT, which can further be metabolized. Specifically, 5-HT can be converted to N-acetylserotonin (NAS) by the enzyme arylalkylamine N-acetyltransferase (AANAT), and then, by N-acetylserotonin O-methyltransferase (ASMT), into melatonin. Alternatively, monoamine oxidase (MAO) catalyzes the transformation of 5-HT into its major metabolite, 5-hydroxyindoleacetic acid (5-HIAA) [100,102,103]. In humans, there are two types of MAO: MAO-A and MAO-B. Whereas MAO-A primarily metabolizes 5-HT, NA, and DA and is involved in the catabolism of these neurotransmitters in the brain and peripheral tissues, specifically in regions associated with mood regulation, MAO-B predominantly breaks down phenylethylamine and benzylamine, but it can also metabolize DA at higher concentrations, being also present in significant amounts in the brain, particularly in areas linked to motor control and movement [104].

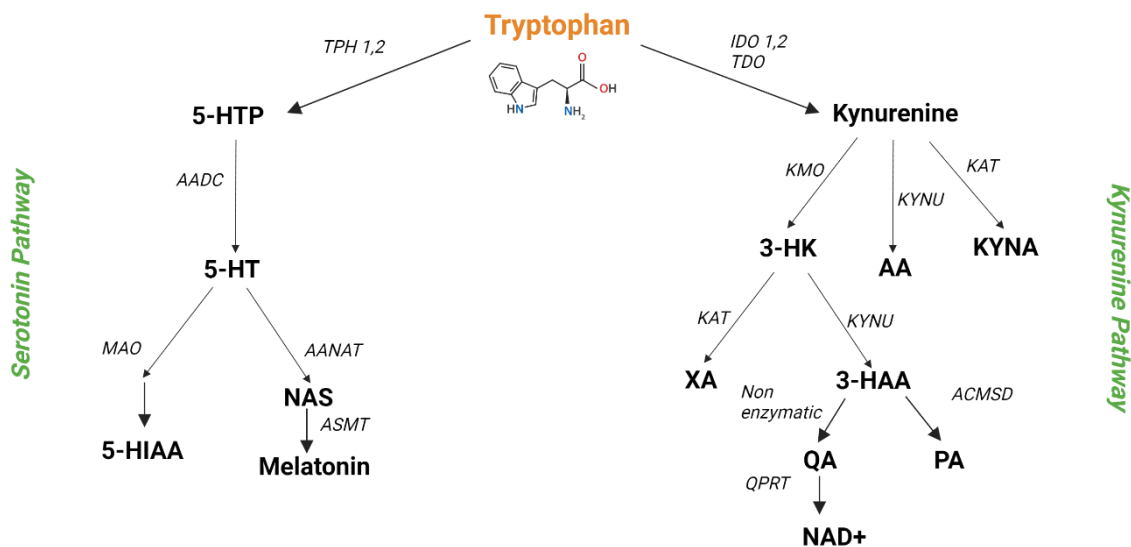


Figure 4. Summary of the two major metabolic pathways of the amino acid TRP: 5-HT and Kyn pathways. Illustration created with BioRender [17].

Thus, overall, TRP metabolism is a complex and highly regulated process that influences a wide range of physiological functions, including mood and immune responses, highlighting the interconnections of biochemical pathways in the human body.

2.3.1. Tryptophan Metabolism as A Player in the Development of Major Depressive Disorder

Depression is a multifaceted condition influenced by several factors, as previously referred. Among these, exposure to chronic stress, neuroinflammation, and dysregulation of critical neurotransmitters, such as 5-HT, are prominent contributors [4,8]. The metabolism of the amino acid TRP has a high participation in all these processes. Indeed, TRP metabolism plays a pivotal role in the context of depression and various neuropsychiatric disorders by contributing to the production of essential neuroactive compounds [102]. Particularly its transformation into both 5-HT and KYN plays an important role in depression [102]. Thus, the maintenance of TRP's homeostatic balance and its regulation during these metabolic processes is extremely important. Consequently, the research of TRP metabolism is critical for the comprehension of MDD.

In depression research, the 5-HT pathway is extensively studied, and it will be further explored on the next subtopic. Generally, imbalance in 5-HT levels, along with disruptions in its receptors and associated pathways, are strongly correlated with the disease [101,105]. Regarding the KYN pathway, excessive activation of this pathway tends to suppress the 5-HT pathway. The KYN pathway divides into two significant branches: the neurotoxic and the neuroprotective branches. In the context of depression, an imbalance occurs towards the neurotoxic branch, exacerbating the condition [98,99].

High levels of stress has been shown to suppress TPH expression, leading to reduced 5-HT levels [106]. To underscore the significance of this enzyme in depression, various TPH1 inhibitors, designed for managing conditions characterized by elevated 5-HT levels in peripheral tissues, have been found to induce depression as a side effect. In fact, the clinical advancement of *p*-chlorophenylalanine was discontinued due to this specific side effect [107]. Furthermore, postmortem studies have established a correlation between TPH2 enzyme expression in individuals who committed suicide, revealing overexpression of this enzyme. Indeed, the compensatory increase in TPH2 may be involved in cases of suicide when the level of 5-HT is decreased [108,109].

5-HTP also plays significant roles in depression, having the potential to elevate 5-HT levels, thereby alleviating depressive symptoms. Evidence suggests that the transport of 5-HTP into the brain is impaired in depression [110,111]. Interestingly, combining 5-HTP with nialamide, an antidepressant that inhibits MAO, has proven more beneficial than using nialamide alone [112]. A similar synergistic effect is observed when L-deprenil, another MAO inhibitor (MAOI), is combined with 5-HTP [113].

Imbalances in MAO enzyme activity are also associated with depressive pathology. Indeed, MAOIs have demonstrated efficacy in treating depression [114]. Notably, MAO-

A is more deeply implicated in the pathophysiology of depression, with elevated MAO-A activity and expression observed in depressed individuals and animal models of depression [115]. However, MAO-B activity is also altered in depression, as evidenced by elevated MAO-B levels in the PFC of individuals experiencing major depressive episodes [116].

Other crucial metabolites within the 5-HT pathway include 5-HIAA and melatonin. Reduced levels of 5-HIAA in cerebrospinal fluid have been associated with suicidal attempts in individuals with depression, largely owing to its connection with decreased 5-HT levels [117]. Moreover, depressed patients often exhibit lower levels of melatonin, although some inconsistencies exist in the literature. While some studies correlate depression with lower nocturnal serum/saliva melatonin levels, others report no differences or even elevated levels compared to non-depressed individuals [118,119]. Nevertheless, animal studies have shown that melatonin can reduce neuroinflammation induced by lipopolysaccharides (LPS), as well as NF- κ B expression in the cortex and hippocampus, leading to improved autophagy function and amelioration of depressive symptoms [120].

As mentioned above, the KYN pathway is also involved in the complexity of depression. It is activated to a significant degree in individuals suffering from depression, and this enhanced activity may contribute to the advancement of the disorder [121]. Both the enzymes IDO and TDO are excessively activated during depression, suggesting that inhibitors targeting these enzymes could potentially serve as therapeutic agents for treating depressive disorders [121]. It's essential to recognize that within the KYN pathway, the metabolite KYNA is regarded as a neuroprotective compound, whereas 3-HK is neurotoxic. In cases of depression, there is an imbalance between these two compounds. Astrocytes primarily produce KYNA because they lack the enzyme KMO, while microglia and macrophages predominantly generate the neurotoxin QA via the 3-HK pathway [109,122,123]. Indeed, depression is associated with a loss of astrocytes, which contributes to the overactivation of the 3-HK pathway. This, in turn, exacerbates astrocyte and neuronal apoptosis, leading to reduced levels of critical neuroprotective factors produced by these cells, such as glial-derived neurotrophic factor [109]. Therefore, the activation of KMO is closely linked to depression. Furthermore, increased levels of QA in depression have been observed to result in reduced levels of important neurotransmitters like DA, choline, and γ -aminobutyric acid (GABA), along with disturbances in glutamatergic pathways, which are also known to be dysfunctional in depression [109,124,125]. In fact, QA exerts numerous harmful impacts on the brain through various mechanisms, which include N-methyl-D-aspartate (NMDA) receptor excitotoxicity, astrocyte degeneration, neuronal death, and oxidative stress [126].

Evidence also suggests that the overproduction of proinflammatory cytokines in depression triggers the IDO enzyme, promoting the KYN pathway and reducing the activation of the 5-HT pathway [127]. In studies involving mice exposed to chronic unpredictable mild stress, a diet rich in TRP shifted TRP metabolism more toward the 5-HT pathway rather than the KYN pathway, which had been enhanced in these mice before TRP supplementation [128]. Thus, evidence underscores the important role of the KYN pathway in depression, making it a potential target for therapeutic interventions.

Interestingly, a lot of studies also support the role of gut microbiota in the pathogenesis of depression. Briefly, the changes in the gut microbiota observed in depression affect the HPA-axis, neurotransmitter levels, and inflammatory processes [129]. In the context of the role of microbiota in TRP metabolism, several studies support this connection. For example, a study that involved a murine model of chronic restraint stress revealed that these animals had depressive-like behavior, as well as strong activation of the KYN pathway. Indeed, IDO was overactivated in the brain and the gut. In these animals, the microbiome profile was altered, and the treatment with *Parabacteroides* elevated the 5-HT concentration, supporting the connection between 5-HT/KYN pathways and the microbiome [130]. Another study demonstrated that, in stressed mice, there were reduced levels of *Lactobacillus* and high levels of KYN, reflected in behavioral alterations. In these mice, when the *Lactobacillus* population was restored, KYN metabolism was suppressed by IDO1 inhibition in the intestine, particularly by the ROS produced by these microorganisms [131]. The evaluation of the antidepressant activity of probiotics such as *Bifidobacteria infantis* in rats also revealed that, compared with controls, these rats had a marked increase in plasma concentrations of TRP and KYNA, as well as reduced 5-HIAA levels, especially in the frontal cortex [132]. In another study that involved rats with depressive-like behavior exposed to chronic unpredictable mild stress, the microbiota of these rats differed significantly from healthy controls. Indeed, in the depressive animals, the levels of 5-HT and TPH2 were low in the brain, contrasting with high levels of IDO expression [133]. The comparison of germ-free and conventional animals also indicated that the plasma levels of 5-HT in conventional animals were 2.8-fold higher than in germ-free animals, supporting the role of microorganisms in 5-HT production [134].

Studying TRP metabolism in depression is crucial for understanding the biochemical basis of this disorder, with the potential to enhance diagnosis and treatment. Figure 5 demonstrates the information presented in this topic. Despite being present in the figure, the connection between TRP metabolism and BDNF will be explored later in the part 3.5.

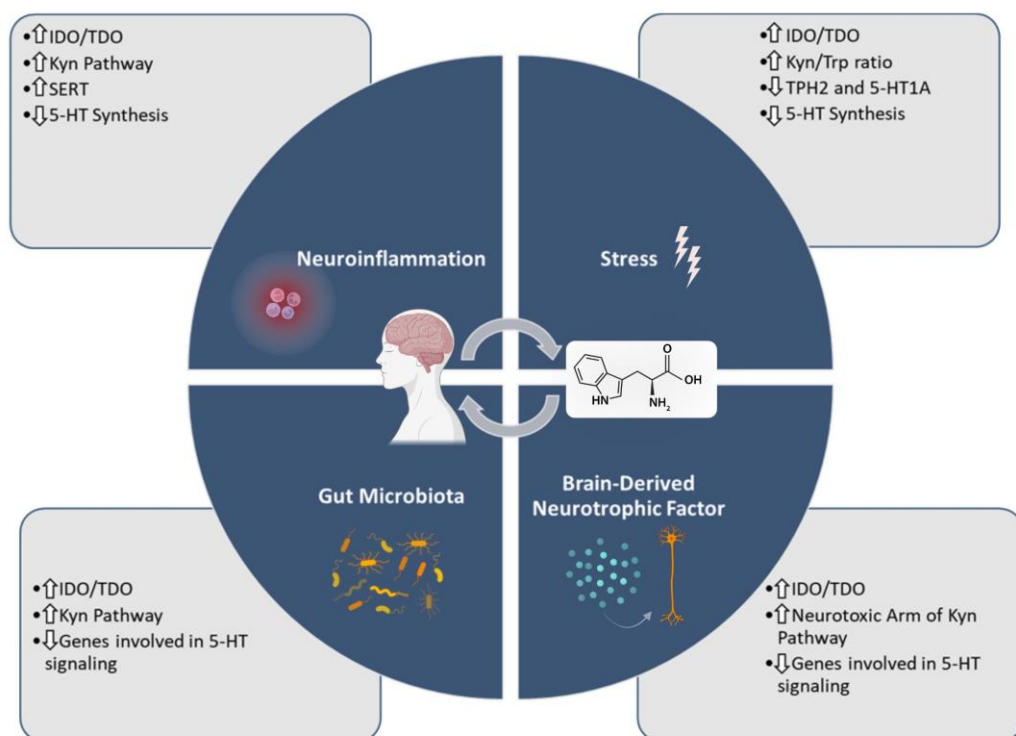


Figure 5. The TRP metabolism is important in several processes connected with depression, particularly neuroinflammation, stress response, gut microbiota dysregulation, and BDNF activity. Illustration created with BioRender [17].

2.3.2 Exploring Serotonin's Role in Major Depressive Disorder

5-HT is important in diverse functions that include behavior, mood, memory, and gastrointestinal equilibrium [101]. Serotonergic neurons origin primarily within the raphe nuclei of the brainstem, from which they have ascending and descending projections placing their influence over the entirety of the central nervous system [135]. Additionally, 5-HT is produced in the enterochromaffin cells located in the intestinal mucosa, contributing to its multifaceted role in the body. Indeed, these cells synthesize ~95% of total body 5-HT [101,136].

The activity of 5-HT is subject to control mechanisms regulating its synthesis, release, and metabolism. The majority of 5-HT is intracellular, ensuring a tight regulation of its concentration. Stored in intracellular vesicles, 5-HT is released into the synaptic cleft upon neuronal depolarization, where it binds to receptors on both presynaptic and postsynaptic membranes [137]. These receptors are distributed in the central nervous system, peripheral nervous system, and peripheral tissues such as smooth muscles and heart. Modulating these receptors can have significant impacts on various conditions, including mood disorders, gastrointestinal issues, and cardiovascular health [138]. A summary of 5-HT receptors is presented in Table 1.

Presynaptic receptors are self-regulators, inhibiting the release of additional 5-HT. In contrast, postsynaptic receptors modulate either excitatory or inhibitory signaling pathways, depending on the specific receptor subtype involved, through the activation of second messenger cascades. 5-HT that is reabsorbed into the originating cell via the serotonin transporter (SERT) is subsequently stored in intracellular vesicles or undergoes metabolism through the action of MAO within the cytoplasm. On the other hand, 5-HT that circulates in the periphery is metabolized by the liver and lungs [137].

Table 1. Summary of the types of 5-HT receptors and their inhibitory/ excitatory potential [139].

5-HT Receptor	Type/ Mechanism	Potential
5-HT1 (5-HT1A-F)	Gi/o -protein coupled; Decrease cellular levels of cAMP	Inhibitory
5-HT2 (5-HT2A, 5-HT2B, 5-HT2C)	Gq /11- protein coupled; Increase cellular levels of inositol 1,4,5-trisphosphate (IP ₃) and diacylglycerol (DAG)	Excitatory
5-HT3	Ligand-gated Na + and K + cation channel; Depolarize plasma membrane	Excitatory
5-HT4	Gs -protein coupled; Increase cellular levels of cAMP	Excitatory
5-HT5 (5-HT5A-B)	Gi/o -protein coupled; Decrease cellular levels of cAMP	Inhibitory
5-HT6	Gs- protein coupled; Increase cellular levels of cAMP	Excitatory
5-HT7	Gs -protein coupled; Increase cellular levels of cAMP	Excitatory

The involvement of monoamines in the context of depression has been extensively researched. In the present day, antidepressants designed to enhance the availability of 5-HT in the synaptic cleft (SSRIs), have proven to be effective and rank among the most widely prescribed medications in the world [140]. Nevertheless, as depression is an extraordinarily complex disorder, and while impaired 5-HT activity can contribute to its development, it neither represents a sole causative factor nor is it sufficient on its own [105].

Evidence from several studies supports the diverse roles played by 5-HT receptor subtypes in the development of MDD. The diverse functions of these distinct receptors offer the potential to introduce new antidepressants that could be greater than SSRIs in both effectiveness and advantages. Indeed, in a general way, antagonists of 5-HT_{2A}, 5-

HT2C, 5-HT3, 5-HT6, and 5-HT7 receptors, in addition to agonists of 5-HT1A, 5-HT1B, 5-HT2C, 5-HT4, and 5-HT6 receptors, have demonstrated the ability to evoke antidepressant-like responses [141]. Nevertheless, it is important to note that, for example, in the case of 5-HT2A receptor, both agonists and antagonists have desired properties valuable in the treatment of mood disorders, being unclear the exact mechanisms of their action. Therefore, the effects can vary depending on the individual's specific neurobiology and the context in which the receptor is activated, as well as the location of the receptor (pre or post-synaptic) [142]. 5-HT1A-B and 5-HT2A are the most studied 5-HT receptors in the context of depression, despite the role of other 5-HT receptors being also a target of studies in MDD, especially 5-HT3 [143]. Table 2 represents a short summary of the connection between these three receptors and depression.

Table 2. Most studied 5-HT receptors in depression, as well as their connection to this disease.

5-HT Receptor Subtype	Functions Known in Depression
5-HT1A	Activation of 5-HT1A receptors is generally considered to have an antidepressant effect. Agonists of 5-HT1A receptors are often used in the treatment of depression, enhancing 5-HT signaling. Stimulation of the 5-HT1A receptor is an existing therapeutic target for treating depression and anxiety, using drugs such as buspirone and tandospirone [144].
5-HT2A	The 5-HT2A receptor has been implicated in the response to antidepressant treatment. It can control neuronal excitability in most networks involved in depression through interactions with the monoaminergic, GABAergic, and glutamatergic neurotransmissions [145]. Preclinical studies show that 5-HT2A receptor antagonists have antipsychotic and antidepressant properties, whereas agonist ligands possess cognition-enhancing and hallucinogenic properties [146].
5-HT3	Studies suggest that 5-HT3 antagonists may have potential antidepressant effects by modulating 5-HT transmission. However, this is an area of ongoing research. 5-HT3 receptor antagonists inhibit the binding of 5-HT to postsynaptic 5-HT3 receptor and might increase its availability to other receptors like 5-HT1A, 1B and 1D as well as 5-HT2 receptors, producing anti-depressant-like effect [147].

The 5-HT1A receptor is an abundant 5-HT receptor in the brain with presynaptic and postsynaptic subtypes. When 5-HT binds to these receptors, it induces neuronal hyperpolarization and reduces its firing rate, but the response to sustained stimulation

differs between these subtypes. In depression, the 5-HT_{1A} receptor is increased presynaptically, causing a decrease in the release of 5-HT [148]. Indeed, 5-HT_{1A} autoreceptors act as a feedback mechanism to regulate 5-HT release, being located on the 5-HT neurons in the brainstem (specifically in the raphe nuclei). When 5-HT_{1A} receptor agonists are administered, it can inhibit the firing of serotonergic neurons and thus reduce the release of 5-HT, but in short term. With chronic administration, there's a desensitization of these presynaptic receptors, leading to an overall increase in the release of 5-HT in the brain to bind to postsynaptic heteroreceptors, modulating the activity of the receiving neuron. The exact effect can vary depending on the location and type of neuron, playing an important role in regulating mood and other aspects of brain function [149].

Stimulation of the 5-HT_{2A} receptor in neurons can lead to several effects through various signaling pathways, such as modulation of GABA and glutamate, mainly due to the high presence of this receptor in glutamatergic and GABAergic neurons [150]. In most cases, activating the 5-HT_{2A} receptor leads to an increase in the levels of intracellular calcium. Additionally, the activation of the 5-HT_{2A} receptor results in the phosphorylation of ERK through a variety of intracellular signaling mechanisms, mostly promoted by Src and calmodulin, a process that regulates downstream signaling components [146,151]. The ERK pathway is involved in the regulation of various cellular processes that can influence mood and behavior, playing a crucial role in neuroplasticity. Indeed, dysregulation of this pathway has been linked to depressive symptoms [152]. These receptors also interact with β -arrestin proteins, that are multifunctional intracellular proteins with an ability to directly interact with many cellular components, contributing to multiple aspects of, for example, GPCR signaling [150,153]. Previous studies have revealed that these receptors coexist with β -arrestin-1 and -2 in cortical neurons. In mice lacking β -arrestin-2, where 5-HT_{2A} receptors predominantly remain on the cell surface, 5-HT fails to induce behavioral responses, including head-twitching. This implies that β -arrestin-2 plays an important role in mediating the internal movement of 5-HT_{2A} receptors within cells and that this intracellular process is connected to the manifestation of head-twitching in response to high 5-HT levels. However, the selective 5-HT_{2A} receptor agonist DOI can still induce head-twitching in mice lacking β -arrestin-2, suggesting that β -arrestins are not indispensable for DOI-mediated responses [154,155]. These findings support the role of the specific ligand in determining how the receptor's signaling pathway is triggered [150]. Additionally, the regulation of signal intensity and duration in 5-HT_{2A} receptor signaling is known to be managed through the swift endocytosis mediated by β -arrestins [156]. Another mechanism through which 5-HT_{2A} receptor subtypes can modulate their signaling involves their capacity to form complexes

with other types of GPCRs, such as metabotropic glutamate receptor type 2 (mGluR2) and dopamine D2 receptors. Although the consequences of these receptor complexes in living organisms are not fully understood, this process probably have an influence on how the receptors bind to molecules and how they interact with various signaling pathways [150].

The 5-HT₃ receptors have permeability to various ions, namely Na⁺, K⁺, and Ca²⁺. Activation of these receptors initiates the opening of ion channels, triggering swift membrane depolarization through the influx of cations [157,158]. The roles of 5-HT₃ receptors are linked to their specific localization. Indeed, activation of nerve-terminal 5-HT₃ receptors modulates the release of diverse neurotransmitters, such 5-HT, DA, or GABA. In contrast, the activation of postsynaptic 5-HT₃ receptors primarily participates in rapid synaptic transmission [158,159]. Furthermore, the 5-HT₃ receptor can be formed by five identical 5-HT_{3A} subunits (homopentameric) or a mixture of 5-HT_{3A} and one of the other four 5-HT_{3B}, 5-HT_{3C}, 5-HT_{3D}, or 5-HT_{3E} subunits (heteropentameric). The homomeric 5-HT_{3A} receptors are equally permeable to both monovalent and divalent cations, while heteromeric 5-HT₃ receptors display reduced calcium permeability [158]. Additionally, heteromeric receptors have faster activation and deactivation kinetics compared to homomeric receptors. It is worth mentioning that the affinity and efficacy of 5-HT₃ receptor agonists and antagonists are connected to the specific receptor structure, whether it is heteromeric or homomeric, as specified in previous research [158].

Despite all the evidence that connects 5-HT signaling pathways to MDD, it is important to note that a recent comprehensive systematic umbrella review revealed that there is no robust evidence that depression is caused by lower 5-HT concentrations or activity [160], despite other very recent review was published with the aim of contradicting this review [161]. However, over the past few years, selective alterations in 5-HT neurotransmission have remained a viable therapeutic way for managing mood disorders. Indeed, the effectiveness of SSRIs is well-established, as previously mentioned. However, a heterogeneous condition like clinical depression can not be attributed only to the deficient functioning of a single neurotransmitter [162]. In fact, evidence reveals that depleting TRP in healthy individuals, who exhibit no apparent risk factors for depression, does not result in a significant decline in mood [163]. Thus, the idea that decreasing brain 5-HT levels alone is sufficient to induce depression seems unreasonable. However, in individuals who have recovered from depression and have remained free from both pharmaceutical and psychological treatments for extended periods, TRP depletion can indeed lead to a substantial reduction in mood, suggesting that in individuals with a history of depression, prior episodes render them vulnerable,

and reductions in brain 5-HT levels can trigger clinical relapses [163]. Possibly, decreased activity of 5-HT pathways interacts with important pre-existing neurobiological vulnerabilities [162,164]. Indeed, all the inconsistencies and complexity of serotonergic system and depression highlight the importance of further research to understand the effects of different drugs on the 5-HT system in MDD.

2.4 The Multifaceted Roles of Brain-Derived Neurotrophic Factor

BDNF is a neurotrophic factor that plays a crucial role in supporting the survival and differentiation of neurons during their development [165]. BDNF expression is observed in both the central nervous system (CNS) and the peripheral nervous system (PNS), with synthesis occurring in neurons, oligodendrocytes, as well as other cell types like platelets, T and B lymphocytes [166]. In the human and rodent brain, BDNF is widely and abundantly expressed, particularly in regions such as the hippocampus and cerebral cortex. Hippocampal neurons exhibit the highest levels of BDNF, while lower levels are detected in organs like the liver and lungs [165].

Neurons are the primary producers of BDNF [167]. The production process begins in the endoplasmic reticulum, where the precursor protein, proBDNF, is first synthesized. Following the removal of the signal peptide, it transforms into proBDNF, which is around 32-35 kDa in size. The peptide is known to play a significant role in the development and plasticity of neuromuscular synapses [168]. Later in the process, proBDNF undergoes further modifications to become its mature form, a smaller 14 kDa polypeptide. BDNF forms dimers (28 kDa), and biologically active BDNF generally consists of a dimer, that is constructed from two identical mature peptide chains held together by noncovalent interactions [169]. BDNF expression is regulated at the transcriptional level through various mechanisms. In humans, the BDNF gene comprises nine promoters, all encoding the same protein but producing different noncoding exons. The human *BDNF* gene has a total of 11 exons (I–IX, Vh, and VIIIh), and the expression of BDNF transcripts is characterized by cell and activity specificity, with distinct transcripts playing unique roles in both molecular processes and behavioral outcomes [170,171]. Among these exons, exon IV is the most extensively studied, being important in the modulation of mood, cognition, and behavior [172]. Notably, the methylation status of the promoter associated with this exon has emerged as a potential biomarker for antidepressant therapy in individuals with MDD [173]. Furthermore, there is evidence suggesting that miR-182 may serve as a potential regulatory microRNA for BDNF. This discovery implies that serum levels of BDNF and related miRNAs may have the potential

to serve as valuable biomarkers for diagnosing depression or as promising therapeutic targets for addressing this condition [174].

This neurotrophic factor interacts with two types of receptors. One belongs to the family of receptors characterized by tyrosine kinase activity, specifically full length tropomyosin receptor kinase B (TrkB-FL), while the other is the p75 neurotrophic factor receptor (p75 NTR), which has a low binding affinity for mature BDNF [166]. When BDNF binds to the TrkB-FL, it primarily initiates three intracellular signaling pathways: ERK, PI3K/Akt, and phospholipase C γ (PLC γ) signaling. These signaling pathways are vital for mediating the diverse functions of BDNF [175].

BDNF is known to play an important role in several physiological processes (Table 3). In fact, reduced levels of BDNF contribute to cerebral atrophy, cognitive decline, and the increased risk of psychiatric disorders [176]. The release and activity of various neurotransmitters, including glutamate, GABA, and DA, are also influenced by BDNF, which can modulate the balance and function of neurotransmitter systems, affecting neuronal communication and overall brain function [177]. This neurotrophic factor is also important in processes such as the development of dendrites and synaptic specializations, maturation and refinement of dendritic arbors, and axon growth and differentiation [178].

Table 3. Summary of BDNF main functions in the central nervous system.

Know Function	Explanation
Neuronal Development	Promotes the growth and development of neurons during early brain development, contributing to the formation of neuronal connections and neural circuits [178].
Synaptic Plasticity	Regulates synaptic plasticity. It facilitates the strengthening and formation of new synapses [179].
Learning, Memory, and Mood Regulation	Supports the formation of long-term memories and promotes the consolidation of newly acquired information. BDNF is also implicated in mood regulation, being associated with the pathophysiology of psychiatric disorders, such as MDD [176,180].

Continuation of the Table 3.

Function	Description
Neurogenesis	Promotes the generation of new neurons, replenishing and maintaining a healthy population of neurons [181].
Neuroprotection	Helps to mitigate damage caused by oxidative stress, inflammation, and other harmful processes in the brain [182].

One of the most studied and characterized roles of BDNF is the regulation of postsynaptic and presynaptic transmission, regulating synaptic plasticity [179]. This process is the capability of modifying the strength or efficacy of synaptic transmission at preexisting synapses [183]. Multiple research studies have confirmed that BDNF is important in hippocampal long-term potentiation, which is a sustained improvement in synaptic effectiveness, important in the foundation of learning and memory [179]. Indeed, it is known that modifications in synaptic connections contribute to the retention of memories. Studies demonstrate that compromised BDNF function is associated with memory impairment, being associated with dementia [180]. BDNF is, thus, important for enhancing synaptic efficacy, by regulating the trafficking, phosphorylation, and expression levels of the AMPA receptor, a type of G protein-coupled ionotropic glutamate receptor that is a key player on synaptic plasticity [184]. Additionally, BDNF also influences dendritic spine characteristics and promotes neurogenesis through effects on cell survival and proliferation [165,185]. Moreover, evidence demonstrate that BDNF plays an important role in adult neurogenesis [181], which is the creation of fully functional neurons from neural precursors in adult organisms in specific areas of the mammalian brain, particularly in the hippocampus [186]. An example that highlights the connection between BDNF and neurogenesis is the treatment with *Panax notoginseng* saponins, used in the context of cerebral ischemia injury, that stimulated hippocampal neurogenesis in rats by inducing different pathways, such as the upregulation of BDNF [187]. Research has also demonstrated that BDNF can enhance the multiplication of neural progenitor cells (NPCs) and facilitate the prolonged viability of their progeny [188]. Also, BDNF administration to the dentate gyrus of adult rats led to the increased neurogenesis of granule cells [189]. BDNF also presents various protective effects on the brain, such as preventing cell death, reducing oxidative damage, and inhibiting autophagy [182]. Indeed, based on the functions of this neurotrophic factor, there are several treatments and strategies that have been shown to increase the levels

of BDNF, such as regular physical exercise, omega-3 fatty acid intake and some antidepressant drugs, such as SSRIs [165,190].

Being implicated in the pathophysiology of disorders such as Alzheimer's disease and Parkinson's disease, BDNF is an active area of investigation in neuroscience and related fields. Conversely, BDNF is inversely linked to mood disorders, including MDD, which will be discussed further.

2.4.1. Exploring Brain-Derived Neurotrophic Factor in Major Depressive Disorder

BDNF has been associated with numerous psychiatric and neurological conditions. These conditions encompass MDD, anxiety disorders, schizophrenia, Rett syndrome and other neurodegenerative diseases [167,191].

The link between BDNF and MDD is an extensive area of research, with much left to understand. Nevertheless, the neurotrophic hypothesis of depression relies on the connection between decreased BDNF levels and an increased probability of developing depression [192]. Malfunctions in BDNF contribute to disturbances in synaptic plasticity, leading to a reduction in excitatory neurons and glutamate levels, ultimately leading to depressive states [188]. As mentioned previously, BDNF also assumes a critical function in hippocampal neurogenesis, and depression is closely linked to the impairment of this process. Indeed, adult-generated hippocampal neurons are important for mood control and antidepressant efficacy [193]. Table 4 represents a summary of the connection between BDNF and MDD. The connection between BDNF and oxidative stress, 5-HT/TRP metabolism and HPA axis dysfunction will be further explored.

Individuals suffering from depression often display characteristics indicative of reduced neurogenesis. This is evidenced by a diminished volume of the dentate gyrus and decreased vascularization in the neurogenic niche [194–196]. Treatment with SSRIs in depressed individuals has been linked to increased markers of neurogenesis in the hippocampus, particularly the proliferation of NPCs within the dentate gyrus [194,197]. Furthermore, human studies have demonstrated a positive correlation between peripheral blood levels of BDNF and both hippocampal size and cognitive function [198,199]. Low BDNF levels are consistently associated with an increased prevalence of depressive symptoms, neuronal loss, and atrophy in key brain regions [200]. A recent study highlighted that patients experiencing their first episode drug-free MDD and responding to SSRI treatments (including escitalopram, paroxetine, and duloxetine) exhibited elevated serum BDNF levels [201]. Moreover, antidepressant-treated individuals have shown increased BDNF expression in the hippocampus when

compared to the untreated patients [202]. Postmortem examinations of brains from depressed patients, including suicide cases, have revealed reduced BDNF mRNA levels, confirming this trend [203,204]. Animal models of depression have further corroborated these findings, showing that depression lead to diminished BDNF levels, increased cell death, and reduced neurogenesis in the hippocampus [205,206]. Several other studies have reported lower serum BDNF levels in individuals with depression compared to those without the condition [207]. A recent study indicated that after 100 days of SSRI treatment, methylation changes in specific sites of the BDNF gene's promoter region were observed, leading to a reduction in depression scores [208]. Interestingly, a genetic variation known as Val66Met, which naturally occurs in the BDNF gene, is also connected with MDD. This genetic variation involves the substitution of valine (Val) with methionine (Met) at position 66 [209]. Recent research has linked this polymorphism to MDD and its potential use as a biomarker for predicting a patient's response to antidepressants and electroconvulsive therapy. Thus, the presence of the Met allele could serve as an indicator for the likelihood of developing MDD [210]. Behavioral tests in another study demonstrated antidepressant effects and elevated serum BDNF levels following prolonged use of allopurinol, a drug that increases the level of TRP in the body by inhibiting xanthine oxidase [211]. Additionally, modulation of depressive-like behaviors in chronically stressed mice through upregulating BDNF/TrkB signaling via δ opioid receptor agonist SNC80 in the hippocampus and amygdala has shown promising antidepressant effects [212]. A compound known as luteolin-7-O-glucuronide has also demonstrated efficacy in improving depression-like behavior in mice by activating BDNF signaling pathways [213]. Interestingly, fecal microbiota transplantation in rat models of depression has shown an antidepressant effect by increasing the expression levels of BDNF and other components such as 5-HT [214]. Various forms of physical exercise have also been found to stimulate the production of this neurotrophin, leading to cognitive enhancement and a reduction in symptoms associated with depression and anxiety [215]. For instance, interval training has been shown to elevate BDNF concentrations in the serum and plasma of healthy young individuals [216].

TrkB phosphorylation and expression also undergo changes in individuals with depression. Indeed, antidepressants such as imipramine and fluoxetine enhanced TrkB signaling in the cerebral cortex of mice, a process dependent on BDNF to produce the behavioral benefits often associated with these drugs. Notably, the tyrosine residues in the TrkB autophosphorylation site are phosphorylated in response to antidepressants [217]. Indeed, activated phosphorylated forms of TrkB have been found to be reduced in brain samples from depressed patients [218]. Several antidepressants, including SSRIs

and ketamine, directly bind to this receptor, activating or enhancing the TrkB-BDNF signaling pathway [219].

Table 4. Summary of the BDNF and MDD connection.

Feature	BDNF and Major Depressive Disorder Connection
Levels of BDNF	Reduced BDNF levels have been observed in individuals with MDD [192].
Changes in structure and function	Deficiencies or imbalances in BDNF levels may contribute to the development of depression by promoting structural and functioning changes [220].
5-HT influence	BDNF is influenced by 5-HT, and 5-HT activation can stimulate BDNF synthesis and release. 5-HT receptors can also modulate BDNF expression, influencing neuronal function and, consequently, mood regulation [221].
Neuroplasticity	BDNF is involved in neuroplasticity, which is crucial for synaptic connections and structural changes in the brain related to MDD [188].
Antidepressant effects	Different antidepressants can enhance BDNF gene expression, contributing to their therapeutic effects [220].
Oxidative stress	Oxidative stress can lower BDNF production and damage its signaling pathways. The connection between oxidative stress and BDNF levels plays a significant role in the development and progression of depression [222].
HPA axis dysregulation	Stress-induced HPA axis hyperactivity and the resulting increase in glucocorticoid levels diminish BDNF expression, playing an important role in the development of depression [223].

3. Intersecting Pathways in Major Depressive Disorder: Oxidative Stress, Tryptophan Metabolism, Brain-Derived Neurotrophic Factor, and Hypothalamic–Pituitary–Adrenal Axis Dysfunction

3.1. Exploring the Connection Between Oxidative Stress and Major Depressive Disorder's Associated Stress Response

The exploration of the connection between oxidative stress and MDD's associated stress response is an area of study that holds promise for advancing the understanding of the underlying mechanisms of MDD [224]. Indeed, increased production of ROS leads to hyperactivation of the HPA axis [225]. Furthermore, the release of glucocorticoids triggered by HPA axis activation amplifies the activity of cellular reduction-oxidation

systems. When stress induces the activation of GRs, there is a rise in mitochondrial membrane potential, calcium-holding capacity, and mitochondrial oxidation [226]. Consequently, it leads to the generation of superoxide, hydrogen peroxide, and hydroxyl radicals, culminating in oxidative damage [227].

In vivo studies have provided evidence that exposure to corticosterone leads to an increase in oxidative markers, such as lipid peroxidation, accompanied by a decrease in antioxidant enzymatic systems, like catalase. Notably, these findings demonstrate that oxidative injury in the hippocampus of rats impairs their cognitive function [228]. Another study, in mice, also revealed that after the induction of depressive and anxiety-like behaviors with pressure injury, the plasmatic levels of corticosterone and brain oxidative stress markers such as MDA were increased [229]. Moreover, the introduction of vitamin D3 to mice effectively mitigated depressive-like behavior and the oxidative stress induced by the repeated administration of corticosterone. Remarkably, this intervention resulted in a decrease in lipid peroxidation, protein carbonyl formation, and nitrite levels, ameliorating depressive symptoms [230]. Another study in mice corroborated the induction of elevated oxidative stress markers by corticosterone, which were subsequently reversed by lutein, exhibiting antidepressant-like effects in these animal subjects [231]. Administering the carotenoid crocin-I demonstrated a notable ability to alleviate neuroinflammation and oxidative damage induced by corticosterone, underscoring its antidepressant potential. This compound also effectively stimulated the activity of essential antioxidants, including SOD-2 and glutathione reductase, contributing to its therapeutic effects [232]. Similarly, the administration of catalpol to mice exhibited inhibition of HPA axis hyperactivity, evidenced by reduced levels of corticosterone, ACTH, and CRH. This treatment not only alleviated central inflammation but also ameliorated oxidative damage through the regulation of the NF- κ B and Nrf2 pathways, yielding antidepressant effects in mice subjected to corticosterone injection [233]. The administration of *Myrcia pubipetala* Miq in mice subjected to corticosterone treatment also exhibited antioxidant effects, addressing the imbalance in antioxidant enzyme activities within the hippocampus and cerebral cortex [234]. In a recent study involving 60 nurses, the impact of day and night shift work on stress, anxiety, quality of life, and oxidative stress parameters was also assessed. This investigation supported a direct correlation between increasing stress and anxiety levels, rising oxidant markers, and elevated cortisol levels, ultimately leading to a diminished quality of life among the nurses [235]. In another study, the antidepressant effects of L-cysteine on corticosterone-induced oxidative stress in rats were evident. L-cysteine effectively lowered plasmatic corticosterone levels while boosting antioxidant defenses, mitigating the oxidative stress caused by corticosterone [236]. In vitro experiments involving the addition of *Hericium*

erinaceus to rat pheochromocytoma cells (PC-12) demonstrated strong neuroprotective effects. This intervention successfully alleviated the oxidative stress induced by high doses of corticosterone. The neuroprotective action was further substantiated by elevated endogenous antioxidant enzyme activities, reduced intracellular levels of ROS, and protection against apoptosis triggered by elevated ROS levels [237].

Collectively, these studies provide evidence of a direct link between the hyperactivation of the HPA axis during stressful conditions and the occurrence of oxidative stress in depression. High stress levels are consistently associated with a reduction in antioxidant levels and an increase in prooxidant levels, facilitating the emergence and progression of depression. In sum, prolonged exposure to chronic stress overstimulates the HPA axis, and this overstimulation can lead to high cortisol levels, which in turn can cause oxidative stress [227]. Furthermore, oxidative stress can intensify the hyperactivity of the HPA axis.

3.2. The Interplay Between Oxidative Stress and Serotonin in Major Depressive Disorder

One mechanism commonly discussed in the context of depression is based in the monoamine hypothesis. This theory defends that depression is linked to disruptions in the levels of monoamine neurotransmitters, specifically 5-HT, NA, and DA [238] (Figure 6).

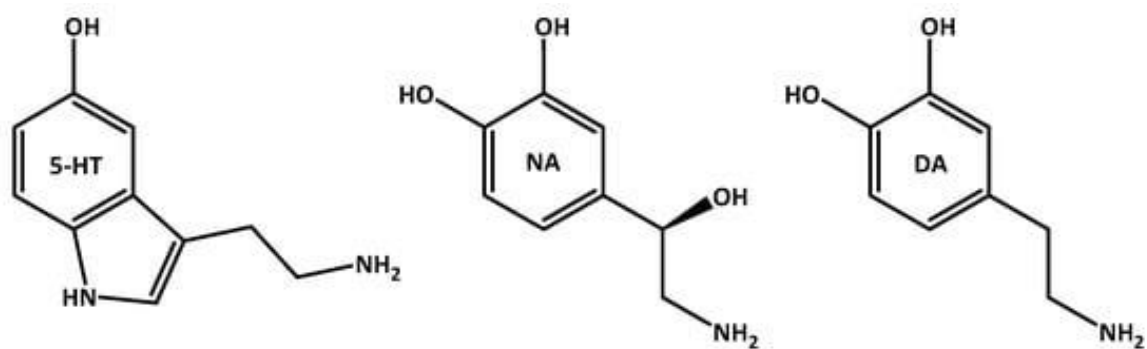


Figure 6. Molecular structure of the neurotransmitters 5-HT, NA and DA.

Research into the relationship between oxidative stress and 5-HT signaling dysfunction in MDD is ongoing, being important for a deeper understanding of the disorder and the development of novel treatment approaches. By targeting oxidative stress as a potential therapeutic avenue, a research aim is to restore 5-HT balance [239]. In fact, a study found that lipopolysaccharide increased oxidative stress in both the brain and liver of mice. Antidepressant drugs had varying effects on oxidative stress. In the

brain, SSRIs (sertraline, fluoxetine, fluvoxamine) reduced oxidative stress, while the TCA imipramine increased it. In the liver, all these antidepressants reduced oxidative stress. Thus, there is still a lot to uncover between the connection of different antidepressants with oxidative stress [240]. Nevertheless, most of animal studies suggest that antidepressant drugs indeed decrease oxidative stress and modulate the activity of antioxidant enzymes [241].

Oxidative stress generates numerous neurotoxic substances through the oxidation of TRP. Among these substances, oxidation-specific epitopes such as MDA are recognized for their potent proinflammatory properties, and their correlation with depression is evident as they interact with pathways like the TRP/KYN system. Indeed, TRP can undergo metabolism into KYN, both via the influence of proinflammatory cytokines and direct action by ROS. This metabolic pathway can then give rise to prooxidant compounds, namely 3-HK and QA, which are associated with the pathogenesis of depression, as previously mentioned [242,243].

In a recent investigation, selenium-modified fluoxetine derivatives were found to inhibit 5-HT reuptake, contributing to their antidepressant effects, and reduce oxidative stress, producing promising results and thus highlight the connection between 5-HT and oxidative stress in depression [244]. Additionally, we demonstrated that both mirtazapine and TRP, players in serotonergic pathways, effectively countered cellular stress induced by hydrogen peroxide, highlighting the significant role played by these pathways in mitigating oxidative stress [245] (further explored in the results/ discussion). Another study revealed that saffron intake also protected human neurons from oxidative stress, stimulating the production of DA, 5-HT, and BDNF. In addition, saffron inhibited the expression of SERT. Indeed, all these data provided support into the context of oxidative stress related to depression [246]. Moreover, the application of nacre extract from pearl oysters has shown efficacy in reducing LPS-induced depression and anxiety in mice. This effect is accompanied by a reduction in elevated oxidative stress levels triggered by LPS, coupled with notable alterations in 5-HT receptors (specifically 5-HT_{1A} and 5-HT_{2A}) and BDNF levels, highlighting its antidepressant properties [247]. Persimmon leaf extract, known for its antioxidant properties, has also exhibited promise. In depressed mice, the administration of this extract prevented dendritic spine loss by inhibiting 5-HT reuptake, thereby increasing 5-HT levels in the brain and alleviating depressive-like behaviors in the animals [248]. Additionally, another study further bolsters the connection between 5-HT and oxidative stress. In murine RAW264.7 macrophages, it was demonstrated that 5-HT and its metabolites not only reduced oxidative stress but also prevented the production of inflammatory cytokines by macrophages, underlining the multifaceted nature of 5-HT's impact [249]. In a postpartum depression rat model,

supplementation with the probiotic *Lactobacillus casei* exhibited significant improvements in depression-like behaviors. Notably, this probiotic induced positive alterations in the gut microbiota of the rats, which in turn led to several beneficial processes, including enhanced expression of monoamines and the BDNF/ERK1/2 pathway, along with a reduction in oxidative stress levels (marked by the suppression of MDA and the promotion of SOD activity) [250]. Antidepressant treatment with SSRIs also reduced DNA and RNA damage from oxidation in patients with depression. Indeed, treating patients with these drugs (specifically escitalopram, with some switching to duloxetine) for 8 weeks resulted in a significant reduction (25% for DNA damage marker 8-oxodG and 10% for RNA damage marker 8-oxoGuo) in the levels of these markers in urine, indicating that SSRIs may reduce DNA and RNA damage from oxidation in patients with depression [251].

Collectively, these studies support the connection between the 5-HT imbalance observed in depression and the consequential oxidative stress.

3.3. Oxidative Stress's Impact on Synaptic Plasticity and Neurogenesis in Major Depressive Disorder

Oxidative stress has the capacity to decrease the production of BDNF and impair its signaling pathways, thereby reducing BDNF levels. Conversely, low levels of BDNF can worsen oxidative stress by compromising the brain's antioxidant defenses. Numerous studies suggest that reduced BDNF levels contribute to increased oxidative stress, highlighting a potential protective role for BDNF in mitigating neuronal oxidative damage [222,252].

Several research findings provide substantial evidence for the connection between oxidative stress and impairments in neurogenesis and synaptic plasticity in depression, with a primary focus on their association with BDNF. Indeed, BDNF is recognized for its role in increasing the expression of antioxidant enzymes, particularly superoxide dismutase and glutathione peroxidase, enzymes that actively counteract oxidative stress by neutralizing ROS and limiting oxidative damage [252]. A recent study supported this connection by demonstrating that stress-induced depressive symptoms in mice, characterized by diminished neurogenesis, were effectively ameliorated through the upregulation of the mitochondrial antioxidant sirtuin 3. This promising intervention not only restored stress resilience but also improved overall depressed behavior, offering a potential way for treatment [253]. Furthermore, the administration of tilapia skin peptides to mice exhibited notable effects on depression-like behavior, as it modulated oxidative stress and neurogenesis. These findings strongly suggested the involvement of the

BDNF pathway in the antidepressant properties of these peptides, facilitating enhanced neurogenesis and the prevention of neural apoptosis. Additionally, this compound enhanced the Nrf2/HO-1 pathway, which is important in the expression of numerous antioxidant genes, emphasizing its potential as a therapeutic agent [254]. The flower essential oil of *Tagetes minuta* was found to restore the signaling pathway BDNF, protein kinase B (PKB) and signal-related kinase 2 (ERK2). This resulted in a reduction in oxidative stress and a decrease in depressive-like behavior in mice [255]. Another research demonstrated that melatonin enhanced antioxidant markers and stimulated neurogenesis in the hippocampus and PFC of rats previously exposed to methotrexate. Melatonin improved the animals' antioxidant defenses by enhancing the expression of Nrf2 and BDNF. Furthermore, it enhanced synaptic plasticity and the expression of doublecortin, an indicator of neurogenesis [256]. When the antioxidant carvedilol was administered to depressed mice, it led to elevated levels of brain glutathione and BDNF, while decreasing MDA levels, resulting in antidepressant-like effects [257]. A similar outcome was observed when mice were given luteolin-7-O-glucuronide, a compound known for its antioxidant properties. This compound improved depression-like behavior by activating the BDNF signaling pathway, modulating neurogenesis and neuroplasticity [213]. Rosmanic acid reversed depressive behaviors induced by LPS in mice by promoting the expression of the BDNF/Nrf2 pathway. This, in turn, led to increased expression of antioxidant enzymes like heme oxygenase-1 and NADPH quinone dehydrogenase 1 and a decrease in proinflammatory gene expression [258]. Additionally, both celastrol and thymoquinone alleviated depressive and anxiety behaviors in rats by restoring the concentrations of acetylcholine, DA, and 5-HT, which had been previously depleted due to exposure to aluminum chloride. These compounds also upregulated BDNF expression and downregulated oxido-inflammatory markers like MDA and IL-6 in the rats' brains [259]. In SH-SY5Y cells, walnut polyphenols, and the active compound urolithin A protected against oxidative damage caused by hydrogen peroxide. They achieved this by enhancing the BDNF signaling pathway, thereby promoting neuroprotection [260]. Moreover, several antidepressants have demonstrated the ability to raise BDNF levels while concurrently reducing markers of oxidative stress. For example, drugs like mirtazapine [261–263] and escitalopram [264,265] exhibit this dual effect. Further evidence supporting this connection includes the high vulnerability to stress-induced oxidative stress observed in the cerebral cortex of mice lacking BDNF [266]. Additional research has shown promising interventions. In PC-12 cell cultures, exposure to 1-(1-propanoylpiperidin-4-yl)-3-[4-(trifluoromethoxy)phenyl]urea (TPPU) was effective in reducing oxidative stress damage caused by hydrogen peroxide and promoting BDNF expression [267]. In studies involving rats, omega-3 fatty acids were

found to restore the balance of oxidative stress, dampen the inflammatory response, bolster BDNF production, and regulate 5-HT metabolism, all contributing to the prevention of nicotine withdrawal-induced anxiety and depression [268]. Another recent study explored the potential of the antioxidant hesperetin, found in citrus peels, in a depression model induced by reserpine in male rats. The findings revealed that hesperetin significantly improved BDNF levels in the hippocampus, reduced oxidative stress levels by increasing antioxidative markers, particularly superoxide dismutase and glutathione peroxidase, and consequently ameliorated depressive-like symptoms [269]. Similar positive outcomes were observed when administering red raspberry extract to rats using a chronic unpredictable mild stress-induced depression model. This extract demonstrated potential efficacy in reducing depressive-like behavior and histological damage to hippocampus tissue. It achieved this by modulating neuroinflammation, the oxidative stress response and enhancing BDNF/TrkB signaling pathway [270].

This evidence strongly substantiates the link between the dysregulation of ROS production, and the consequential impairment of neurogenesis and synaptic plasticity. These interconnected factors play an important role in the development of MDD.

3.4. Tryptophan Metabolism Players and Depression's Associated Chronic Stress

Exploring the complex connections between TRP metabolism and the chronic stress observed in depression have the potential to yield valuable insights that could lead to new therapeutic strategies [271].

Studies indicate that elevated levels of cortisol are correlated with lower plasma TRP levels and a higher KYN/TRP ratio, particularly in individuals who have attempted suicide [272]. Cortisol is known to activate TDO, leading to increased KYN production and a shift in TRP metabolism away from 5-HT production toward KYN production [273]. Indeed, chronic stress, mainly characterized by elevated cortisol and pro-inflammatory cytokine levels, activates the IDO and TDO enzymes, facilitating the conversion of TRP into KYN [274]. Notably, treatment with allopurinol, a xanthine oxidase inhibitor that decreased the activity of TDO (used to decrease high blood uric acid levels), has been shown to prevent stress-related reductions in brain 5-HT concentrations by interfering with TDO activity. This intervention results in a reduction in the activation ratio of the KYN pathway [275,276]. Furthermore, the administration of 1-methyl-TRP, an inhibitor of the IDO enzyme, has been found to alleviate depressive-like behavior in rodents exposed to stress induced by LPS [277]. Exposure to LPS also increased the expression of IDO mRNA in the brains of rodents, leading to the overactivation of the KYN pathway [278].

Physical exercise also plays a role in modulating the effects of the KYN pathway in stress-associated depression. It induces the activity of skeletal muscle peroxisome proliferator-activated receptor gamma coactivator-1 alpha isoform 1 (PGC-1 α 1), which, in turn, promotes the expression of KAT, facilitating the conversion of KYN into KYNA, a neuroprotective metabolite of the KYN pathway. This conversion helps maintain the KYN/KYNA balance, reducing the levels of free KYN and protecting the brain against stress-induced depressive behaviors [279]. PGC-1 α 1 activity is known to decline with age and in conditions such as diabetes, potentially contributing to depression associated with these factors [275].

Focusing on 5-HT, the functioning of serotonergic signaling in the brain is connected with the stress response, and drugs that target serotonergic pathways can significantly impact the effects of stress [280]. Indeed, chronic excess cortisol can lead to 5-HT deficiency by reducing TRP availability and can also reduce the density and reactivity of 5-HT receptors [49]. This connection was demonstrated with an experiment conducted on cynomolgus monkeys, which were categorized based on their resilience to stress, falling into high, medium, and low resilience groups. In this experiment, the animals more susceptible to stress exhibited reduced expression of several critical genes crucial for the normal operation of the serotonergic system. These genes included *Plasmacytoma expressed transcript 1* (Pet-1), TPH2, SERT, and 5-HT1A. These proteins play pivotal roles in the development of brain serotonergic systems, the production and transportation of 5-HT, as well as the functioning of 5-HT itself. Moreover, in the same study, animals having higher vulnerability to stress demonstrated an increase in the expression of CRH compared to their more resilient counterparts [281]. Consequently, these findings strongly suggest a significant interplay between 5-HT and stress sensitivity. Other studies provide further support for the link between cortisol and serotonergic pathways. For example, the administration of crocin reduced cortisol levels and increased 5-HT levels, ameliorating depressive-like behavior in mice [282]. Similar results were observed with the administration of gossypetin [283], aqueous extracts of miswak and date palm [284]. Diets enriched with TRP oligopeptides led to lower levels of HPA axis hormones and increased levels of 5-HT and BDNF, promoting positive effects on anxious depression in mice [285].

Several studies have also been focused to understand the connection between SSRIs and various components of the HPA axis [280,286]. Compelling evidence has indicated that the acute administration of fluoxetine, a widely prescribed SSRI for MDD, produces a significant increase in extracellular 5-HT concentration within the hypothalamus. This effect extends to regions like the PVN, which is rich in CRH-containing neurons. Consequently, these findings substantiate that the acute use of

fluoxetine augments HPA axis activity. This augmentation is evident through increased levels of CRH mRNA, high expression of transcription factors, and elevated concentrations of ACTH and corticosterone in the bloodstream [287]. Indeed, a pilot study examined the baseline response to metyrapone and 6-week response to fluoxetine in premenopausal women with MDD. The results suggested that overactivity of the HPA axis may be one factor associated with slower response to fluoxetine [288]. However, it's important to note that 5-HT's impact on the HPA axis varies based on dosage, duration of action, and the specific subtype of serotonergic receptor involved. For instance, the administration of 5-HT_{1A} agonists into the PVN can inhibit HPA axis activity at lower dosages while eliciting the opposite effect at higher dosages [289]. In addition to acute effects, evidence suggests that chronic administration of SSRIs decrease HPA axis activity, resulting in reduced plasma levels of ACTH and decreased CRH mRNA expression in the PVN [290]. This supports the complex and context-dependent nature of 5-HT's influence on the stress response.

Collectively, this body of evidence underscores the complex relationship between TRP metabolism and the stress response present in MDD.

3.5. Linking Tryptophan Metabolism with Brain-Derived Neurotrophic Factor Expression in Major Depressive Disorder

Understanding the relationship between TRP metabolism and BDNF expression provides a promising way for the development of novel therapeutic interventions in MDD. In fact, TRP metabolism plays a crucial role in modulating BDNF function.

A noteworthy study revealed that when TRP levels were depleted in healthy individuals, there was a compensatory increase in serum BDNF levels. This compensatory response was absent in individuals dealing with depression, where BDNF levels, along with plasma TRP levels, remained persistently low [291]. In a separate study conducted on mice subjected to chronic unpredictable stress, TRP supplementation likewise demonstrated an improvement in BDNF expression, supporting the interplay between TRP metabolism and BDNF in the context of depression [128].

The relationship between the KYN pathway and the expression of BDNF is also connected within the context of depression. Indeed, QA plays a role by interacting with the NMDA receptor, which triggers signaling pathways that ultimately reduce BDNF expression [292]. Notably, other neurotoxic metabolites produced along the KYN pathway also have the capacity to disrupt the crucial glial-neuronal networks that are important in the synthesis of neurotrophic factors, particularly BDNF [109]. In fact, there

is evidence to suggest that BDNF can exert a regulatory influence on the Kyn pathway. For instance, when mice with reduced BDNF expression (heterozygous mice with BDNF+/-, experiencing approximately a 50% reduction in BDNF levels) were exposed to stressful conditions, they exhibited high activation in the neurotoxic arm of the KYN pathway. This resulted in an increase in the levels of neurotoxic metabolites such as 3-HK, a contrast to the response observed in wild-type animals [293]. In another study involving mice with the BDNF Val66Met polymorphism, which is associated with an increased susceptibility to psychiatric disorders, these mice presented an overactivation of the KYN pathway [294]. Further supporting this connection, a study demonstrated that the blockade of IDO1 attenuated depressive-like behavior in mice subjected to chronic unpredictable mild stress. Simultaneously, this blockade resulted in an increase in hippocampal BDNF expression and enhanced neurogenesis in the hippocampus [295]. This collectively emphasizes the complex relationship between the KYN pathway and BDNF expression in the context of depression.

Research has shown that BDNF and 5-HT are also interconnected in several ways. Indeed, serotonergic pathways influence the expression and release of BDNF in the central nervous system, and BDNF is involved in the regulation of the development and function of serotonergic neurons, promoting their development, maintenance, and plasticity, influencing 5-HT synthesis and availability. Also, imbalances in 5-HT levels can impact BDNF levels in the central nervous system [296–299]. Additionally, both 5-HT and BDNF contribute to the modulation of synaptic connections and structural changes in the brain during neuroplasticity, both being important in the context of mood disorders such as depression [300]. Within raphe neurons, BDNF promotes the expression of TPH and enhances the uptake of 5-HT. Moreover, this neurotrophic factor fosters the development and function of serotonergic neurons [300]. The association between BDNF and serotonergic pathways is further validated by interactions with 5-HT receptors, such as 5-HT1A and 5-HT2A. These interactions are compromised in conditions where the BDNF gene is deleted [300–302]. Another evidence supporting this connection is the observation that elevated levels of 5-HT can, in turn, raise BDNF levels, as seen when different SSRI antidepressants are administered. In fact, the inhibition of SERT by SSRIs amplifies 5-HT pathways through interactions with various 5-HT receptors. This subsequently increases phosphorylation of the cAMP Response Element-Binding protein (CREB), leading to elevated levels of BDNF transcription [300]. A meta-analysis of the comparative efficacy of antidepressants on peripheral BDNF concentrations in patients with MDD revealed that both SSRIs and 5-HT and NA reuptake inhibitors (SNRIs) boosted BDNF levels after a period of treatment, and sertraline outperformed the other three medications (venlafaxine, paroxetine, or escitalopram) regarding BDNF

concentration rise [265]. Several psychedelics, agonists of the 5-HT_{2A} receptor, promote plasticity by directly binding to TrkB. Indeed, these drugs exhibit rapid and long-lasting antidepressant effects while promoting neuroplasticity that bears similarities to the impact of conventional antidepressant treatments. For example, it was demonstrated that lysergic acid diethylamide (LSD) and psilocin directly bind to TrkB with affinities 1000-fold higher than fluoxetine and ketamine [303]. Evidence also revealed that the fast and prolonged antidepressant-like effects of the activation of 5-HT_{1A} require BDNF signaling. This was demonstrated by the intra-medial PFC infusion of the 5-HT_{1A} receptor agonist 8-OH-DPAT, that induced rapid and long-lasting antidepressant-like effects in animals tests, such as forced swim and novelty-suppressed feeding, being blocked by the co-infusion of an anti-BDNF neutralizing antibody [304]. In addition, a recent study highlighted that BDNF and the 5-HT₇ receptor are interconnected. Indeed, when activated, these receptors increase the level of BDNF and TrkB affinity [305]. Interestingly, a study in rodents demonstrated that a single injection of BDNF improved the activity of SERT in the hippocampus of these animals. These acute BDNF effects would be predicted to counteract the early effects of SSRIs, that produce rapid blockade of the SERT, which could explain some of the delay in their therapeutic effects [306]. Other study demonstrated that after a prolonged treatment with SSRIs, the methylation of promoter CpG sites of BDNF was considerably reduced, improving treatment and reducing depression scores after treatment [208]. Another research based on reserpine-induced depressive-like behaviors in rodents demonstrated that scopolamine attenuated the induced depression in mice partially by the regulation of the SERT, BDNF, and TPH1 in the hippocampus and PFC [307]. A study examining the effects of gardening in elderly individuals found an increase in TRP metabolism in the gardening group, which correlated with elevated BDNF levels [308]. A recent study also explored the relationship between TPH2 expression and BDNF levels. In this study, the administration of pargyline (MAOI) to zebrafish treated with an irreversible TPH2 inhibitor, resulted in reduced BDNF levels, highlighting the interdependence between the 5-HT and BDNF systems. In fact, pargyline reduced *Bdnf* gene mRNA concentration only in the zebrafish-treated with the TPH2 inhibitor. In other words, alterations in 5-HT levels can influence BDNF levels, which may impact the effectiveness of antidepressant treatments [309]. Moreover, the interaction between 5-HT neurotransmission and BDNF-related pathways is supported by another study. This research found that increased TRP intake led to high activation of 5-HT pathways, which in turn modulated the BDNF system. This protective effect was observed against cognitive decline in aged rats [310]. Additionally, physical exercise is known to upregulate the BDNF-5-HT system, with 5-HT actively participating in BDNF-mediated neuroplasticity stimulated by aerobic physical exercise in rats [311].

Thus, in sum, 5-HT and BDNF have a complex interaction. In fact, serotonergic pathways control BDNF expression, and BDNF, in turn, regulates the development and function of serotonergic neurons. Understanding the relationship between 5-HT and BDNF is crucial for advancing the knowledge of MDD, and recent studies have explored this connection, offering insights into potential therapeutic approaches for depression. Figure 7 represents a simplified summary of the BDNF and 5-HT connection in MDD. Future directions may include a focus on personalized approaches to identify patient most likely to benefit from BDNF-related treatment, as well as studies to identify biomarkers and long-term efficacy and safety [312].

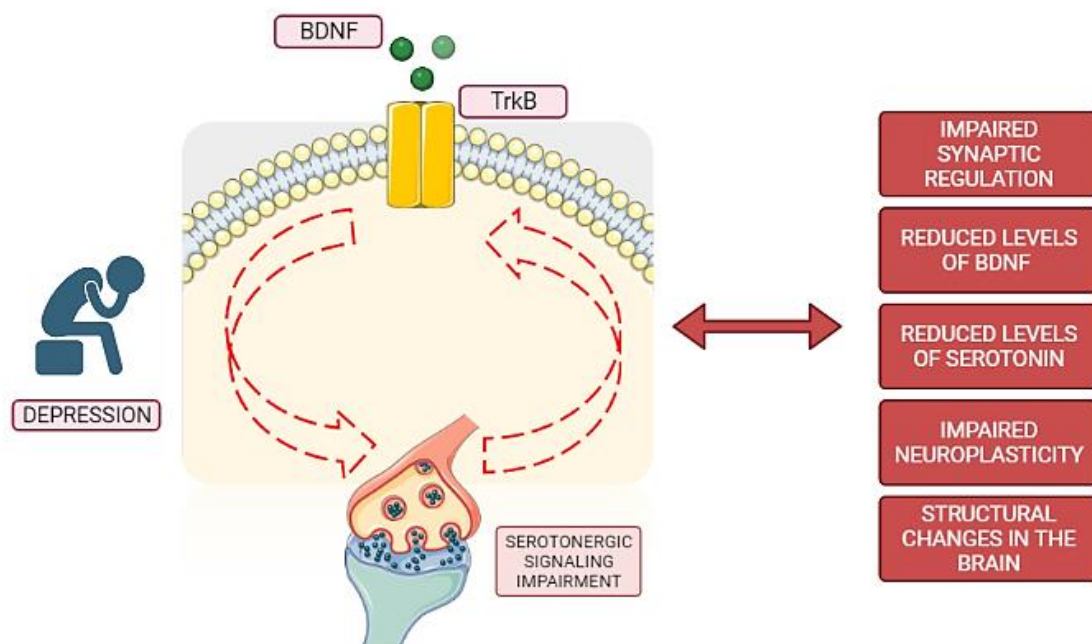


Figure 7. Simplified scheme of BDNF and 5-HT interaction in depression. In depression, there exists a complex interplay between BDNF and 5-HT. BDNF interacts with the TrkB receptor, thereby exerting its influence on serotonergic signaling pathways. Conversely, these pathways also impact BDNF signaling. Disruptions within these pathways, indicated by red dashed arrows, are observed in MDD. Consequently, these disruptions contribute to structural changes in the brain, impaired neuroplasticity, compromised synaptic regulation, and reduced levels of both serotonin and BDNF. These cumulative effects ultimately promote or contribute to the development of depressive symptoms. Illustration created with BioRender [17].

3.6. Bridging Brain-Derived Neurotrophic Factor with Hypothalamic–Pituitary–Adrenal Axis Dysregulation in Major Depressive Disorder

Research is also trying to understand the complex relationship between the activity of the HPA axis and BDNF. Indeed, dysregulation of the HPA axis contributes to a suppression of transcription of the *bdnf* gene [49]. On the other side, BDNF has been found to regulate the HPA axis, potentially leading to reduced HPA axis activity and, consequently, lower glucocorticoid levels [313]. It is worth noting that acute or chronic stress-induced activation of the HPA axis has distinct impacts on various BDNF signaling pathways. Short-term stress, for instance, triggers temporary HPA axis activation that can yield positive effects on neurotransmission and synaptic plasticity in the PFC. These effects are thought to enhance processes related to emotional memory and bolster the ability to cope with future stressors. Conversely, chronic stress exerts detrimental effects on neuroplasticity in the PFC and disrupts the usual regulation of the HPA axis. These adverse effects increase the risk of developing mental health disorders, including MDD [314]. Moreover, there are BDNF gene polymorphisms (rs2049046 and rs11030094) that have been associated with the modulation of the HPA axis in individuals with MDD, influencing their response to antidepressant treatments [315]. In a study involving mice, chronic administration of corticosterone induced depressive-like behaviors and reduced the expression of BDNF in the dentate gyrus of the hippocampus [316]. In female mice, the administration of oxytocin alleviated depression-like symptoms induced by dexamethasone by increasing hippocampal CREB-BDNF signaling [317]. Another study, conducted in HT-22 cells (mouse hippocampal cells), demonstrated that the total alkaloids of *Fibraurea recisa* protected these cells from corticosterone-induced damage, increasing cell viability significantly while elevating BDNF levels [318]. Kolaviron, a biflavonoid compound, shielded mice from anxiety and sadness induced by chronic unpredictable mild stress by enhancing antioxidant defense mechanisms. This intervention resulted in a rise in the levels of BDNF in the PFC and hippocampus and a decrease in corticosterone levels, which had risen after exposure to stress [319]. Another study involving mice found that corticosterone treatment caused distinct alterations in proBDNF and mature BDNF levels in different brain areas. Notably, both proBDNF and mature BDNF levels substantially increased in the pituitary gland, while proBDNF was reduced in the adrenal gland. These findings underscore the complex effects of corticosterone on proBDNF processing and behavior in mice [320].

In summary, chronic stress-induced hyperactivity of the HPA axis and elevated glucocorticoid levels can lead to a reduction in BDNF expression, while BDNF can

modulate HPA axis activity, thereby influencing glucocorticoid levels. Recent studies have highlighted the correlation between the HPA axis and BDNF, particularly on the impact of corticosterone on BDNF levels and behavior in animal models. This knowledge is important in advancing the understanding of MDD and its treatment strategies.

4. Pharmacological Interventions in the Management of Major Depressive Disorder

4.1. An Overlook of Pharmacotherapy for Major Depressive Disorder

The global economic impact of depression is significant, and it is the third leading contributor to the worldwide disease burden, according to WHO, since 2008. It is anticipated to ascend to the top by 2030 [321]. Hence, there is the need for advancements in research and the practical integration of novel findings.

The first breakthrough in the treatment of depression was made in the early 1950s, when researchers developed iproniazid as a drug for tuberculosis, also proved to be effective in alleviating symptoms of depression, being a type of MAOI [322]. Around the same time, another class of antidepressants known as tricyclics (TCAs) emerged. Indeed, imipramine was the first TCA, approved in 1959 by the Food and Drug Administration (FDA) for the treatment of MDD. Like MAOIs, TCAs were developed in the 1950s and were found to increase monoamine levels, primarily by blocking the reuptake of 5-HT and NA [145,323]. While these discoveries represented important advancements, the acceptance and use of these early antidepressants were hindered by public stigma and the potential for severe side effects [323]. By the late 1980s, a new generation of antidepressants, SSRIs, offered a more targeted approach to depression treatment. As previously referred, they function by inhibiting the reuptake of 5-HT into neurons within the raphe nuclei, resulting in increased 5-HT. These drugs were found to have improved side effect profiles. Indeed, the introduction of SSRIs led to an increase in the use of antidepressants among adults. Today, despite being developed several decades ago, SSRIs remain some of the most prescribed drugs in the world [145,324]. However, data reveals that approximately 33% of patients with MDD do not respond to treatment with these commonly used drugs, and 67% do not achieve remission with this first-line approach. Despite not recent data, this supports the diverse underlying causes of depression [145]. Today, several classes of antidepressants are present in the market. Besides the previously mentioned, SNRIs such as venlafaxine, block 5-HT and NA reuptake in the synapse; 5-HT modulators (e.g.: vilazodone) and atypical antidepressants (e.g.: mirtazapine, that will be further explored in this section) are also

widely used [325]. In recent years, research has shifted its focus towards potential new therapies, including noncompetitive NMDA receptor antagonists [145].

Depression treatment approaches include both pharmaceutical interventions and non-pharmaceutical options, such as psychotherapy, electroconvulsive therapy, and transcranial magnetic stimulation [321]. Psychotherapy has demonstrated its efficacy in alleviating depressive symptoms and enhancing the overall quality of life for individuals with depression [326]. Consequently, numerous clinical guidelines are progressively including the use of psychotherapy either as a standalone treatment or in combination with antidepressants [321].

4.2. Antidepressant Breakthroughs: Advancements in Pharmacotherapy for Depression

Most antidepressants are generally considered safe and effective, but they have certain limitations, including a delayed onset of action and side effects that can impact a patient's adherence to treatment, such as including weight gain, sexual dysfunction, dizziness, headaches, anxiety, psychosis, and cognitive impairments. Thus, over the past few decades, most efforts in antidepressant research have been directed towards discovering drugs that act more rapidly, with greater safety [321,327]. Currently, there are a total of 9687 clinical trials related to all forms of depression, with 1414 of these trials currently in the recruitment phase. However, despite a significant number of trials, the development of new depression drugs is in urgent need [321,328].

The most common type of new drugs is based on NMDA receptor properties [321,327,329]. The great interest in these receptors comes from the role of glutamate in depression. Glutamate is a key excitatory neurotransmitter in the brain, playing a vital role in synaptic plasticity, cognitive functions, and emotional and reward processes. Ionotropic receptors (NMDA, AMPA, and kainate receptors), as well as metabotropic receptor mGluR, have been demonstrated to play a role in regulating mood and related functions that are compromised in individuals with depression [330]. Indeed, numerous clinical investigations and animal research have consistently observed dysfunction within the glutamatergic system in diverse limbic and cortical regions of the brains of individuals experiencing depression [331].

GABAergic modulators are also promising novel targets for antidepressants. GABA, the primary inhibitory neurotransmitter, plays a crucial role in balancing brain function by counteracting glutamate [321]. Studies have revealed that individuals with depression often exhibit GABA-related neurotransmission impairments [332]. Indeed, a recent study revealed that GABA levels in the PFC, anterior cingulate cortex, and occipital lobe are

decreased in patients with MDD [333]. Nonetheless, while GABAergic ligands have shown effectiveness in treating depression, directly influencing the GABA pathway, they can lead to side effects like drowsiness or sedation, which can impede daily functioning. Therefore, the balance seems to be shifting in favor of glutamate receptor ligands [327].

New advances regarding the future of MDD pharmacotherapy surged with the discovery of the antidepressant activity of intravenous ketamine, a dissociative anesthetic and NMDA receptor antagonist [329]. This drug blocks NMDA receptors on GABA interneurons, releasing the inhibition of glutamate release, a process that activates AMPA receptors on glutamatergic cells and increases BDNF and glutamate, increasing synaptic efficiency [334]. Indeed, the administration of ketamine to depressed patients resulted in a sustained three-day reduction in depressive symptoms [335]. This discovery led to the search for related medications like S-ketamine (esketamine), which was developed for intranasal use and FDA-approved as an adjunctive treatment for treatment-resistant depression in 2019. Notably, both intravenous ketamine and intranasal esketamine have shown promise in rapidly alleviating MDD symptoms, leading to esketamine's second FDA-approved indication in 2020. Despite these promising aspects, the benefits of ketamine and esketamine must be weighed against their costs and potential side effects, such as sedation and dissociation [329,336]. Additionally, combining electroconvulsive therapy with antidepressants has been a known approach, and recent findings regarding its use with esketamine have shown great promise and high effectiveness, particularly in cases of drug-resistant depression [327,337].

The combination of bupropion and dextromethorphan also resulted in a significant reduction in depression scores. Dextromethorphan is an uncompetitive NMDA receptor antagonist and sigma-1 receptor agonist, a class of drugs that is recognized for their potential to facilitate synaptic plasticity and neuronal resilience, primarily through their capacity to upregulate BDNF secretion and activate the TrkB receptor signaling cascade [338]. Bupropion inhibits the reuptake of both NA and DA, as well as CYP2D6 enzymes, increasing dextromethorphan bioavailability. Indeed, this drug combination was approved only in the USA in August 2022 for the treatment of MDD in adults (currently, is used only off-label in Europe [339]). In clinical trials, this combination was generally well tolerated, and was not associated with a signal for increased psychotomimetic effects or weight gain [340].

Another trial explored the use of adjunctive esmethadone, another uncompetitive NMDA receptor antagonist [341]. This trial demonstrated rapid and effective reductions in depressive symptoms, although this was not consistently replicated in a subsequent phase 3 trial. Additional phase 3 studies are currently underway to confirm the initial findings [329,342].

Neurosteroids like brexanolone and zuranolone represent another class of potential antidepressants [329]. These drugs modulate GABA neurotransmission. Brexanolone, which was approved by the FDA in 2019 for postpartum MDD, demonstrated rapid and long-lasting reductions in depression symptoms [343]. Zuranolone is also being studied across various MDD cases, with positive results from clinical trials. Indeed, this drug demonstrated enhanced efficacy in alleviating depressive symptoms by day 15, exhibiting a swift onset of action by day 3, having a favorable safety profile [344].

A new category of antidepressants includes orexin receptor antagonists and compounds, that act through two neuropeptides (orexin-A and orexin-B) and two GPCRs (the orexin type 1 and the orexin type 2 receptor). Dysfunction of the orexin system has been implicated in the pathophysiology of depression in human and animal studies, although the exact mechanism of this dysfunction remains unclear. Nevertheless, ligands for type 1 and 2 receptors can modulate various aspects such as feeding, sleep, motivated behavior, anxiety, and addiction, making them potentially influential in regulating different features of depression. Indeed, orexin receptor antagonists are being investigated as potential treatments for MDD, with several ongoing clinical trials [345].

New drugs like ansofaxine (a potential triple reuptake inhibitor of 5-HT, NA, and DA) exhibit side effects that are similar to traditional antidepressants. These side effects are generally mild to moderate, with slightly different frequency patterns compared to drugs like SSRIs or NRIs. Notably, this drug doesn't seem to cause the sexual dysfunctions typically associated with conventional antidepressants [327,346]. In September of 2023, FDA also approved gepirone, for the treatment of MDD. This drug is a 5-HT_{1A} receptor agonist, and an active metabolite of gepirone, 1- (2-pyrimidinyl)piperazine, is an α 2 -adrenergic receptor antagonist. This drug has the big advantage of not causing sexual dysfunction nor weight gain, as well as less sedation and minimal withdrawal symptoms [347].

Psychedelic drugs have also gained attention as potential alternative antidepressants. Preliminary findings suggest that psilocybin, derived from mushrooms, may lead to sustained antidepressant effects in patients with treatment-resistant depression and terminal cancer [329]. In individuals suffering from treatment-resistant depression, the administration of a single dose of psilocybin, combined with psychological support in conjunction with SSRI treatment, exhibited a positive safety profile and displayed significant therapeutic effectiveness [348]. Indeed, a recent study suggests that a single, moderate dose of psilocybin significantly reduces depressive symptoms compared to a placebo, for at least two weeks [349].

The cholinergic system is increasingly recognized as having a significant role in mood regulation. Indeed, acetylcholine, a neurotransmitter, is implicated in mood

disorders with depressive symptoms, although its exact role remains unclear. Recent evidence, such as the rapid and sustained antidepressant effects of scopolamine in depressed individuals, has induced the interest in the cholinergic system's involvement in MDD and bipolar disorder, being suggested that excessive cholinergic activity can trigger MDD. This hypothesis is supported by studies showing that drugs increasing acetylcholine activity can induce depressive symptoms [350]. However, understanding of the efficacy and mechanism of treatments targeting the reversal of acetylcholinesterase increase using acetylcholinesterase inhibitors (AChEIs) remains limited [351].

Regarding other targets, previous studies have found that treatments aimed at regulating the HPA axis, such as GR antagonists, do not effectively alleviate the symptoms of depressed patients [327]. Nevertheless, this is a subject of research interest, and a recent study revealed that antalarmin, a CRH receptor 1 antagonist, alleviated LPS-induced depression-like behavior in mice [352]. Therapies regarding the direct manipulation of KYN pathways are also still not available in the common medical practice for MDD [353].

A promising approach for identifying new uses for existing drugs available in the market, drug repurposing, is increasingly applied in research, given that these medications have undergone safety evaluations and as they have successfully subjected to preclinical and clinical testing, the risk of failure is substantially reduced [354]. Table 5 represents examples of widely studied drugs with potential to be repurposed in the context of depression and some of them explored in this work, their original indication, as well as evidence in depression that support their potential use in this disease.

Table 5. Main indication, known mechanism of action and relevance in depression of potential to be repurposed in the context of depression.

Drug	Main Indication and Mechanism of Action	Relevance in Depression
Statins	Management of hypercholesteremia. Selective, competitive inhibitor of hydroxymethylglutaryl-CoA (HMG-CoA) reductase [355].	Demonstrated anti-depressant effects, useful as add-on therapy in patients with cardiovascular disease, with MDD [356]. Related beneficial effect particularly through positive actions on serotonergic neurotransmission, neurogenesis, and neuroplasticity, HPA axis regulation and modulation of inflammation [357].
Scopolamine	Postoperative nausea/vomiting and motion sickness. Competitive antagonist of 5-HT ₃ receptors and nonselective muscarinic antagonist [358].	Evidence of antidepressant effects in patients with MDD and bipolar depression [359]. Added to antidepressants can effectively relieve the symptoms of patients with severe depression [360]. Currently, 2 clinical trials in MDD and bipolar disorder are ongoing (NCT04719663 and NCT04211961 [361]). In rodents, studies have shown that the antidepressant-like effects are linked to mTORC1 signaling in the PFC. This activation of mTORC1 seems to be initiated by a glutamate surge in the PFC, resulting from the disinhibition of glutamatergic neurons. This increased glutamate transmission leads to the activation of AMPA receptors, that ultimately raises the levels of BDNF, which then stimulates mTORC1 signaling and promotes synaptogenesis processes [362].

Continuation of the Table 5.

Drug	Main Indication and Mechanism of Action	Relevance in Depression
Valproic Acid	Management of epilepsy. Mechanism of action not fully understood: Inhibits voltage-gated sodium channels, GABA transaminase, increases the expression and activity of glutamic acid decarboxylase (GAD), inhibits the action of histone deacetylases (HDAC) enzymes, notably HDAC1, modulates the activity of various calcium channels [363].	Demonstrated efficacy in preventing mood recurrence and enhancing the quality of life for individuals with bipolar disorder when used as a maintenance therapy [364]. Supplementary use of this drug resulted in significant and sustained clinical enhancement over an extended duration in individuals dealing with severe treatment resistant depression [365].
Lamotrigine	Anti-seizure/anti-epilepsy drug. Mechanism of action for lamotrigine is not entirely understood. Selectively binds and inhibits voltage-gated sodium channels, stabilizing presynaptic membranes and inhibiting presynaptic glutamate release [366].	Used off-label for bipolar disorder [366]. Could potentially offer an effective approach in addressing individuals with treatment-resistant persistent depressive disorder, being a viable substitute for the combination of antidepressant and benzodiazepine therapies in this disorder [367].
Pioglitazone	Treatment of type 2 diabetes mellitus. Peroxisome proliferator-activated receptor (PPAR)-gamma and PPAR-alpha agonist [368].	Alone or as add-on therapy to conventional treatments, could induce remission of depressive episodes [369]. Evidence of enhancing antidepressant response among people with comorbid MDD and type 2 diabetes [370]. Induced the neuroprotective phenotype of microglia in CMS-treated mice, mediated by PPAR γ [371], and anti-depressant effect in LPS injected rats [372].

Continuation of the Table 5.

Drug	Main Indication and Mechanism of Action	Relevance in Depression
N-acetyl cysteine	Therapy for acetaminophen toxicity. Serves as a prodrug to L-cysteine, a precursor to the biologic antioxidant glutathione [373].	Evidence as an adjunctive therapy to reduce symptoms of Bipolar disorder, MDD, and schizophrenia [374]. Enhanced coping mechanisms, not only for addressing acute stressors but possibly also for mitigating the impact of persistent stress-inducing factors, which are primarily implicated in the pathogenesis of stress-related disorders [375].
Minocycline	Tetracycline antibiotic, anti-infectious activity against both gram-positive and gram-negative bacteria. Bind to the 30S ribosomal subunit of bacteria, preventing protein synthesis [376].	Potential novel treatment for MDD, in particular for treatment-resistant depression [377]. May improve depressive symptoms and augment response to treatment in patients with treatment-resistant depression [378]. Inhibits both the IDO and the p-38 components of inflammation-induced depression [379].
Nimodipine	Prevent vasospasm secondary to subarachnoid hemorrhage. Blocks voltage-gated L-type calcium channels [380].	This drug has been shown to be effective in treating mood symptoms in case reports and treatment trials of bipolar and unipolar depression [381]. An old clinical trial revealed that this drug in the context of vascular depression, augmentation of fluoxetine with nimodipine led to better treatment results and lower rates of recurrence [382].

Continuation of the Table 5.

Drug	Main Indication and Mechanism of Action	Relevance in Depression
Quetiapine	Schizophrenia and acute manic episodes. Antagonist for D2 receptors and 5-HT _{2A} receptors [383].	Quetiapine monotherapy in older adults with MDD was found to be effective [384]. Quetiapine augmentation may be a useful intervention for MDD with comorbid anxiety [385]. Adjunctive quetiapine was effective in patients with MDD who had shown an inadequate response to antidepressant treatment [386].
Celecoxib	First-line analgesics for patients with osteoarthritis and rheumatoid arthritis. Selective inhibition of COX-2 [387].	A recent meta-analysis demonstrated that celecoxib could be effective for improving depressive symptoms [388]. Antidepressant efficacy was demonstrated when used as an add-on treatment for MDD and mania, possibly by reducing inflammatory markers [389].

Drug repurposing in the treatment of depression represents a promising strategy, aiming to improve the lives of individuals who are affected by this disease.

4.4. Mirtazapine: A Classic Antidepressant's Ongoing Relevance

In this subtopic, mirtazapine's role is going to be explored, a drug that has played a central role in this project mainly because this is an atypical, very effective antidepressant present in clinical practice. This drug was initially synthesized in 1987 in the Netherlands [90], and exerts its therapeutic action on both the serotonergic and noradrenergic systems. It is an atypical antidepressant, more specifically referred to as a noradrenergic and specific serotonergic antidepressant [390]. Primarily, mirtazapine is indicated for the treatment of MDD, but it has a range of other therapeutic applications, such as post-traumatic stress disorder, obsessive-compulsive disorder and migraine [391]. Commonly associated with mirtazapine are sedative effects, antiemetic properties, an increased appetite (hyperphagia), and the potential occurrence of nightmares [390,392,393]. Due to its side effects, mirtazapine might not be the preferred option in many situations.

In clinical practice, mirtazapine is often prescribed for MDD when initial treatments like SSRIs prove ineffective. It has demonstrated efficacy in various stages of MDD and can also help manage associated symptoms such as insomnia and generalized agitation

[90]. Furthermore, the combination of Mirtazapine with SSRIs like paroxetine and fluoxetine, or with SNRIs like venlafaxine, is a common therapeutic approach and, in some severe cases, is recommended for the treatment of MDD [394,395]. In comparison to SSRIs like sertraline, mirtazapine exhibits a swifter onset of action, presenting a distinct advantage [90]. Notably, mirtazapine possesses a notably favorable safety profile with minimal anticholinergic or 5-HT-related side effects [90]. While several studies suggest that there's no established difference in the efficacy of mirtazapine versus other antidepressants for treating depression, some investigations indicate a higher likelihood of remission with mirtazapine treatment [396]. Furthermore, when compared to a range of 21 different antidepressants, mirtazapine emerges as one of the most effective options for managing MDD [397]. In a more recent study encompassing various SSRIs (fluoxetine, paroxetine, sertraline, citalopram, and escitalopram), venlafaxine, and mirtazapine in MDD treatment, mirtazapine demonstrated effectiveness and excellent tolerability at lower doses, minimizing the risk of significant side effects. Particularly, when compared to venlafaxine, the efficacy of mirtazapine increased at doses up to 30 mg, whereas venlafaxine's dose-efficacy relationship extended to doses between 75–150 mg [398]. Thus, mirtazapine remains a widely prescribed option for MDD treatment, though it necessitates personalized patient assessment.

This drug exerts its effects by acting as an antagonist on several key 5-HT receptors, including 5-HT₂ (specifically 5-HT_{2A} and 5-HT_{2C}) and 5-HT₃. Because of this receptor modulation, it facilitates the stimulation of 5-HT_{1A} receptors. This interplay is instrumental in the antidepressant mechanisms of action associated with this drug [399,400]. Regarding noradrenergic transmission, this drug functions by blocking central α_2 hetero and auto-receptors, which, in turn, promotes noradrenergic signaling. This augmentation leads to an increased release of both 5-HT and NA, a pivotal aspect of mirtazapine's antidepressant efficacy [400]. This activation in the sympathetic nervous system is also important in the antidepressant activity of mirtazapine [390]. In addition to its interactions with 5-HT and NA receptors, mirtazapine also exerts a sedative effect through its antagonistic activity on histamine receptors (H₁) [390,401]. Furthermore, the drug exhibits low affinity for muscarinic cholinergic receptors and peripheral α_2 receptors. More details about this drug will be addressed in the discussion. The mechanism of action of mirtazapine is succinctly summarized in Figure 8.

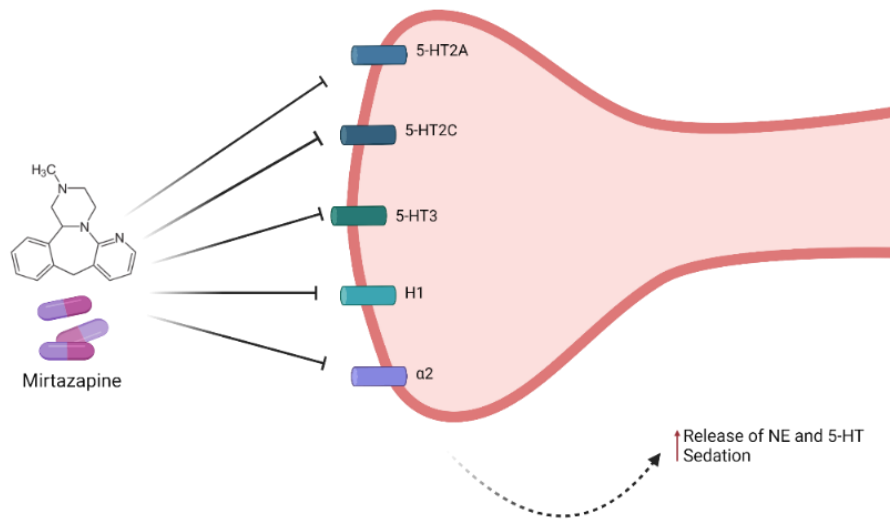


Figure 8. Summary of the mechanism of action of mirtazapine. This drug is an antagonist of 5-HT_{2A}, 5-HT_{2C}, 5-HT₃, H₁, and α₂ receptors, resulting in antidepressant and sedative effects. Illustration created with BioRender [17].

II. Aim

As highlighted in the introduction, MDD is one of the most prevalent psychiatric diseases worldwide. Understanding the complexities of this condition remains a challenge for the field of neuroscience, as it lacks an established mechanism to explain its complex nature. Indeed, managing this disease presents substantial difficulties due to its frequent recurrence, treatment inefficacies, and the considerable variability between individuals.

From a research perspective, it is essential to recognize that investigating depression often employs animal models, which in turn brings obstacles and constraints that impede progress in understanding this disease. Beyond the inherent complexity of depression, creating animal models that faithfully replicate the multifaceted human experience of depression is a considerable challenge. Consequently, bridging the gap between animal studies and human depression is a major obstacle. Additionally, ensuring the replicability of research findings is a fundamental challenge in research, frequently presenting issues when exploring depression. Taking this into consideration, the adoption of cellular models based on established mechanisms can serve as an initial screening platform for identifying potential antidepressant agents. When using cell models, it is important to focus on biomarkers associated with depression, enabling the examination of these molecular mechanisms at the cellular level. Indeed, cell models provide a controlled environment to study the cellular and molecular mechanisms underlying depression, and are crucial for drug discovery and testing, enabling to screen potential antidepressant compounds quickly and efficiently, identifying those with promising therapeutic effects in more initial stages.

Thus, within this thesis, the central aim was to investigate the role of mirtazapine, L-TRP, and drugs with potential to be repurposed (scopolamine, lamotrigine, dextromethorphan, celecoxib, quetiapine, TCB-2, ketamine) for the treatment of depression, using diverse types of cellular models. Indeed, we aimed to understand their capacity to mitigate the effects of high glucocorticoid exposure and oxidative stress. Additionally, this study focused on understanding the ways in which some of these drugs interact with the TRP/5-HT metabolic pathways and influence BDNF and pTrkB levels. Moreover, we also aimed to conduct an exploratory study about the involvement of hypoxia in the response to different drugs that have the potential for use as antidepressants.

III. Materials and Methods

1. Materials

An inventory of the tested compounds, and their solvents are presented in Table 6. Additionally, Table 7 provides a detailed list of the primary and secondary antibodies used in Western blot and immunofluorescence methodologies. Single compounds were dissolved in either H₂O, DMSO or methanol, with a maximum solvent concentration of 0.1% and in some cases 1% for H₂O. When combining two drugs in DMSO, the highest allowable DMSO concentration was 0.2%. The different biological models used were exposed to the test drugs or equivalent amount of solvent (controls: vehicle-treated conditions). The text points out material suppliers when they are first referenced.

Table 6. Tested compounds, as well as their suppliers and solvent used in this work.

Compound	Supplier	Solvent
Mirtazapine	Cayman Chemical Company (Ann Arbor, Michigan, USA. Catalog number (#) 19994)	Dimethyl sulfoxide (DMSO), Methanol
Hydrocortisone	Sigma-Aldrich (Merck KGaA, Darmstadt, Germany. #H0888)	DMSO
Hydrogen peroxide (30%; Perhydrol™)	Merck Milipore (Burlington, Massachusetts, USA. #1.07209)	H ₂ O
Corticosterone	Sigma-Aldrich (#27840)	DMSO
Scopolamine hydrobromide	Sigma-Aldrich (#PHR1470)	H ₂ O
Lamotrigine	Cayman Chemical Company (#15428)	DMSO
5-HTP	Sigma-Aldrich (#H9772)	H ₂ O
5-HT	Sigma-Aldrich (#H9523)	H ₂ O
L-TRP	Sigma-Aldrich (#T0254)	H ₂ O
5-HIAA	Sigma-Aldrich (#H8876)	H ₂ O
Dextromethorphan hydrobromide	Sigma-Aldrich (#D9684)	DMSO

Continuation of the Table 6.

Compound	Supplier	Solvent
Celecoxib	Sigma-Aldrich (#PZ0008)	DMSO
Methyl methanesulfonate (MMS)	Sigma-Aldrich (#129925)	H ₂ O
Cobalt (II) chloride hexahydrate	Sigma-Aldrich (#255599)	H ₂ O
Quetiapine hemifumarate	Cayman Chemical Company (#14152)	DMSO
TCB-2	Sigma-Aldrich (#2592)	DMSO
Ketamine hydrochloride	LGC Standards (Teddington, Middlesex, UK. #DRE-C14531000)	DMSO
Echinomycin	Sigma-Aldrich (#SML0477)	DMSO

Table 7. Primary and secondary antibodies used in western blot and immunofluorescence methodologies.

Antibody	Supplier	Dilution	Experiment
Primary Antibodies			
Rabbit recombinant anti-BDNF	Abcam (Cambridge, UK. #ab108319)	1:1500	Western blot analysis of rat hippocampal slices and neuronal cortical cell cultures from mice
Mouse anti-GAPDH	Invitrogen (Waltham, Massachusetts, USA. #AM4300)	1:5000	Western blot analysis of rat hippocampal slices
Rabbit anti-phospho-TrkB (Tyr816)	Merck Millipore, (Burlington, Massachusetts, USA. #ABN1381)	1:300	Immunofluorescence of neuronal hippocampal cell cultures from mice
Mouse anti-BDNF, BDNF#9	Developmental Studies Hybridoma Bank (Iowa City, Iowa, USA. #AB_2617199)	1:25	Immunofluorescence neuronal hippocampal cell cultures from mice
Rabbit polyclonal anti-5-HT3AR	Abcam (#ab13897)	1:500	Immunofluorescence of SH-SY5Y and HT-22 cells

Continuation of the Table 7.

Antibody	Supplier	Dilution	Experiment
Secondary Antibodies			
Horseradish peroxidase (HRP)-conjugated goat anti-mouse	Santa Cruz Biotechnology (#sc-2005)	1:10000	Western blot analysis of rat hippocampal slices
HRP-conjugated goat anti-rabbit	Santa Cruz Biotechnology (#sc-2004)	1:10000	Western blot analysis of rat hippocampal slices
Donkey anti-rabbit IgG (H+L)	Jackson ImmunoResearch (West Grove, Pennsylvania, USA. #AB_2340585)	1:5000	Western blot analysis of neuronal cortical cell cultures from mice
Goat anti-mouse 488	Invitrogen (#A11008)	1:1000	Immunofluorescence of neuronal hippocampal cell cultures from mice
Donkey anti-rabbit 568	Invitrogen (#A10042)	1:1000	Immunofluorescence of neuronal hippocampal cell cultures from mice
Donkey anti-rabbit 488	Molecular Probes (Eugene, Oregon, USA. #A-21206)	1:1000	Immunofluorescence of SH-SY5Y and HT-22 cells

2. SH-SY5Y and HT-22 Cell Culture

SH-SY5Y human neuroblastoma cell line was obtained from American Type Culture Collection, (Manassas, Virginia, USA), and HT-22 mouse hippocampal cell line were gently provided by Professor Ana Cristina Rego's group (University of Coimbra, Coimbra, Portugal). Both cell lines were incubated at 37 °C (with 5% CO₂) and cultured in Dulbecco's Modified Eagle's Medium (DMEM; Millipore Sigma, Merck KGaA, Darmstadt, Germany) supplemented with 10% Fetal Bovine Serum (FBS; Millipore Sigma) and 1% penicillin (1000 U/mL)/ streptomycin (10 mg/mL) solution (Sigma-Aldrich). These are adherent cell lines, subcultured when confluences of 75–80% were obtained. Before each new assay, both cell lines were trypsinized (TrypLE express, Gibco® Life Technologies, Grand Island, NY, USA), centrifuged (5 min., 800 and 1100 rpm for HT-22 and SH-SY5Y, respectively; Hettich, Tuttlingen, Germany), and seeded at a density of 62500 cells/cm² (SH-SY5Y cells) and 9375 cells/cm² (HT-22 cells).

3. Morphological Analysis of SH-SY5Y and HT-22 cells

Leica DMI6000 B Automated Microscope (Leica, Wetzlar, Germany) was used to observe and capture images of SH-SY5Y and HT-22 cells after all the treatment conditions, previously to the cellular viability assays.

4. Cellular Viability Assays

Cellular viability was evaluated by using thiazolyl blue tetrazolium bromide (MTT) and/or neutral red (NR) assays. For the MTT assays, following the removal of the culture medium, 100 μ L of MTT (0.5 mg/mL in phosphate buffered saline (PBS); Sigma-Aldrich) was added to each plate well. Then, protected from the light, the cells were incubated for 3h. Next, MTT was removed and 100 μ L of DMSO was added to each well. Finally, absorbance values (570 nm) were obtained in the automated microplate reader (Tecan Infinite M200, Zurich Switzerland). For the NR assay, following the removal of the culture medium, 100 μ L of NR medium (1:100 in culture medium; NR solution was purchased from Sigma-Aldrich) was added to each well. Then, the cells were incubated for a period of 3h, also protected from the light. After that, the cells were washed in PBS (150 μ L), and NR destain solution (50% of 96% ethanol, 49% deionized water and 1% glacial acetic acid; 150 μ L per well) was added to the cells. Absorbance at 540 nm was obtained in the automated microplate reader.

5. Alkaline Comet Assay

Assessment of DNA damage subsequent to exposure to the tested agents was obtained by using the alkaline comet assay, as previously described [402]. Cells exposed to MMS (0.5 mM, 1h) served as positive controls. Briefly, after treatment exposure, cells were washed with pH 7.4 PBS (without calcium/magnesium), detached by using trypsinization (150 μ L/well for 5 min) and suspended in pH 7.4 PBS (without calcium/magnesium). Cells were then centrifuged (300 \times g for 5 min), the supernatant was discarded, and the pellets were resuspended in ice-cold pH 7.4 PBS (without calcium/magnesium). After that, 6.0×10^3 cells were transferred to a microcentrifuge tube, centrifuged at 400 \times g for 5 min and then embedded in 100 μ L of 0.6% low melting point (LMP) agarose (Sigma-Aldrich). Next, 5 μ L of each sample was placed on the slides precoated with 1% normal melting point (NMP) agarose (Lonza, Basel, Switzerland), using a high-throughput system of 12-minigel comet assay unit (Severn Biotech Ltd.[®], Kidderminster, UK). After agarose polymerization (4 $^{\circ}$ C for 10 min), the slides were incubated at 4 $^{\circ}$ C for 1h, protected from light in lysis solution (2.5 M of NaCl, 100 mM of Na₂EDTA, 10 mM of Tris-base, 250 mM of NaOH at pH of 10 and 1% Triton-X 100). Next,

the slides were washed with cold H₂O (4°C for 3×5 min) and then immersed in electrophoresis buffer (1 mM of Na₂EDTA and 300 mM of NaOH at pH of 13) for 30 min at 4 °C in the electrophoresis platform for DNA unwinding. After that, the electrophoresis ran for 20 min at constant 30 V (0.9 v/cm). At the end of the electrophoresis, the slides were washed with PBS (pH of 7.4; 2×5 min) and deionized H₂O (1×10 min), followed by fixations in 70% and 96% ethanol (5 min each). The slides were dried overnight and protected from light at room temperature. Finally, all the slides were stained with a 1:10000 dilution of SYBR® Gold (Invitrogen) in TE buffer (Tris-HCl (10 mM) and EDTA (1 mM) at pH of 7.5–8) for 20 min, observed in the BA410 ELITE series microscope (Motic, Hong Kong, China), equipped with a complete EPI fluorescence kit, and analyzed using the image analysis software Comet Assay IV (Perceptive Instruments, Staffordshire, UK). The DNA percentages in the comet tails (% tail intensity) were obtained for 100 cells per experimental condition.

6. 2',7'-Dichlorofluorescein Diacetate Assay

Intracellular oxidative activity was evaluated by 2',7'-dichlorofluorescein diacetate (DCFDA) assay (Sigma-Aldrich). After cell adhesion (24h), cells were incubated with 100 µL/well of 100 µM DCFDA, dissolved in PBS for 30 min before exposure to the drugs. At the end of the incubation period, the supernatant was rejected, and the cells were incubated with the test compounds for 1h, 3h, 6h, 24h, and 48h at 37°C. Finally, the fluorescence was obtained using a fluorescence plate reader (SpectraMax Gemini EM Microplate Reader; Molecular Devices, San Jose, California, USA), 485 nm excitation and 530 nm emission.

7. High-Performance Liquid Chromatography Analysis

For the high-performance liquid chromatography with electrochemical detection (HPLC-ECD) procedure, after being filtrated and centrifugated, the analysis of 5-HT content in the samples was performed using the 3030 Reagent kit® for HPLC analysis of 5-HT in the serum (Waters Corporation, Milford, Massachusetts, USA), following the specific recommendations of the manufacturer, as previously described [403]. The calibration curve was generated with concentrations between 1–1000 nM of 5-HT ($y = 493146x$; $R^2 = 0.9963$), and all the samples were collected after 48h of the cell treatments. The decade electrochemical detector (Antec Scientific, Zoeterwoude, The Netherlands) contained a glassy carbon electrode programmed to a potential of 50 mV. Empower Pro software 3 (Waters Corporation) was used for controlling the produced current.

For HPLC with UV/Vis detection procedure, samples were subjected to the HPLC (Flexar FX-10 Ultra High-Performance LC 10,000 PSI; Perkin Elmer), and the separation was carried out at a flux of 2 mL/min. Optical density of all the tested compounds was recorded at 280 nm. Quantification was performed based on standard curves for L-TRP ($y = 750,542x$; $R^2 = 0.9971$), 5-HTP ($y = 804,860x$; $R^2 = 0.9986$), 5-HT ($y = 782,455x$; $R^2 = 0.9977$), and 5-HIAA ($y = 595,569x$; $R^2 = 0.9919$), generated with concentrations between 1 μ M–1 mg/mL. Results were analyzed using Chromera[®] software, version 3.2.0 (Perkin Elmer).

8. Hypoxia Induction of Cells

For the induction of hypoxia to cells, CoCl₂ or the hypoxia chamber (StemCell, Vancouver, British Columbia, Canada) was used. For hypoxia induced with the chamber, each plate was placed in the hypoxia incubator chamber with a 2% O₂, 10% CO₂, and 88% N₂ atmosphere, following manufacturer recommendations. For hypoxia induced with CoCl₂, this compound was added to cells for a period of 48h in a range of concentrations (0.1 mM – 1 mM) before finding the ideal concentration (0.1 mM) to proceed with the experiment.

9. Animals

For the experiments with hippocampal slices, male adult Wistar rats (about 6 - 8 weeks old) were used. Wistar rats were purchased from Charles River (Barcelona, Spain) and kept under standardized temperature (22-24 °C), humidity (55±10%) and lighting conditions, with *ad libitum* access to water and food at the Rodent Facility of Instituto de Medicina Molecular João Lobo Antunes. This project was also approved by the internal committee (ORBEA) of Instituto de Medicina Molecular João Lobo Antunes and the Portuguese Animal Ethics Committee (DGAV - Direção Geral de Alimentação e Veterinária). Throughout the experimental work, every effort was made to reduce the number of animals sacrificed. Under profound isoflurane anesthesia, rats were sacrificed by decapitation.

For the experiments with primary neuronal cortical or hippocampal cell cultures, C57BL/6 mice embryos at E16.5 were collected through caesarean section of pregnant C57BL/6 mice, euthanized by cervical dislocation. C57BL/6 mice purchased from Charles River (Barcelona, Spain) were maintained under a 12h light/12h dark cycle with free access to food and water at the Animal Facility of Instituto de Investigação e Inovação em Saúde (i3S). All procedures were approved by DGAV and carried out with the permission of the i3S's animal ethical committee.

All animals were handled in accordance with Portuguese legislation (DL 113/2013) and European Community Guidelines for Animal Care (European Union Council Directive – 2010/63/ EU).

10. Acute Hippocampal Slices Preparation

After decapitation of the animal, the brain was quickly removed and maintained in an ice-cold, oxygenated artificial cerebrospinal fluid (aCSF; 3.5 mM KCl, 1.25 mM NaH₂PO₄, 124 mM NaCl, 26 mM NaHCO₃, 2 mM CaCl₂, 1.3 mM MgSO₄, and 10 mM glucose, with a pH of ~7.4 when aerated with 95% O₂-5% CO₂) for a few mins. before further dissections. Then, the hippocampi were isolated and cut into 300- μ m thick slices using the McIlwain Tissue Chopper (Campden Instruments, Loughborough, England). The slices were maintained in aCSF for 1h for energy charge recovery and then exposed for 6h to the test drugs or equivalent amount of solvent (controls), which were added to the aCSF. Throughout the dissection process, the brain tissue and hippocampal slices were kept in ice-cold, oxygenated aCSF and visualized under a dissecting scope.

11. Neuronal Cortical and Hippocampal Cell Culture From Mice

Primary neuronal cortical and hippocampal cell cultures were obtained, respectively, from the cortex and hippocampus of C57BL/6 mice embryos. More specifically, in this study, prenatal mice at embryonic day 16.5 (E16.5) were used, a stage where neurons have minimal innervation and limited axonal and dendritic development.

The isolated cortex and hippocampus were digested with trypsin (1.5 mg/mL), washed with HBSS (Gibco® Life Technologies) containing 10% (v/v) FBS and then washed only with HBSS to remove FBS. The tissue was then dissociated in neurobasal medium (Gibco® Life Technologies) using a pipette and cells were plated at a density of 90 \times 10⁴ cells/cm² in pre-coated plates with poly-D-lysine (Sigma-Aldrich). Cells were cultured in neurobasal medium supplemented with 2% (v/v) NeuroCult™ SM1 neuronal supplement (StemCell), GlutaMAX (0.5 mM), glutamate (0.025 mM) and gentamycin (50 μ g/mL) (Gibco® Life Technologies), at 37 °C with 5% CO₂, for 4 days before the exposure to the different treatments.

12. Immunofluorescence Analysis

For the immunofluorescence of HT-22 and SH-SY5Y cells, they were grown on 24-well plates, covered with 13-mm coverslips, and coated with poly-D-lysine 20 μ g/mL in PBS-1x (Thermo Fisher Scientifics, Waltham, Massachusetts, USA) and laminin 5

µg/mL in PBS-1x (Sigma-Aldrich). After that, the cells were washed with PBS-1x and plated at a seeding density of 6500 cells/well. Then, cells were fixed with 4% paraformaldehyde (PFA) at room temperature for 10 min and washed 3 × 5 min with 0.1% Triton X-100 in PBS-1x. Next, cells were blocked with donor horse serum (Biowest, Nuaille, France) 5% in PBST (PBS-Tween 20 0.1%), for 1h, at room temperature. The primary antibody was diluted in donor horse serum 5% in PBST and added to the cells, following an overnight period of incubation. Cells were washed with 0.1% Triton X-100 in PBS-1x (3×5 min) and incubated for 1h at room temperature with the secondary antibody, diluted in donor horse serum 5% in PBST. Antibodies used are present in Table 7. Finally, cells were washed with 0.1% Triton X-100 in PBS-1x (3×5 min), incubated with DAPI (Sigma-Aldrich) 1:1000 in PBS-1x for 10 min, and washed twice with PBS-1x. For mounting, ProLong™ gold antifade mountant (Invitrogen) was used on each slide. Images were acquired on ApoTome Slider (Zeiss®, Oberkochen, Germany) fluorescence microscope coupled to the AxioVision Rel. 4.8. software (Zeiss®).

For the immunofluorescence of primary neuronal hippocampal cell cultures, after the exposure to different treatments, primary neuronal hippocampal cell cultures were fixed in 4% PFA for 10 min, followed by PBS washes and Triton X-100 0.1% in PBS for permeabilization for 10 min. After that, the cells were blocked with 5% bovine serum albumin (BSA; nzytech, Lisbon, Portugal) for 1h and then treated with primary antibodies overnight at 4°C. Afterwards, cells were washed again with PBS, and secondary antibodies were added for 1h in blocking solution. Antibodies used are present in Table 7. Then, Alexa Fluor™ 647 Phalloidin (1:40 dilution; Invitrogen) was added to the cells for 30 min, and the nuclei were stained with Hoechst 33342 (1:5000 dilution; Thermo Fisher Scientific), for 10 min. Finally, mounting medium (ibidi, Gräfelfing, Germany) was added to each well. Immunostaining assessment was conducted using the Operetta CLS™ High-Content Analysis System (PerkinElmer, Waltham, Massachusetts, USA), using a 20x objective to acquire 25 images for each well. Following image acquisition, fluorescence intensity was quantified through analysis in the Ilastik 1.3.3 and CellProfiler 4.2.6 softwares.

13. Western Blot Analysis

For the experiment with rat hippocampal slices, after the treatment exposure, total proteins were extracted from these slices using acid-extraction buffer (50 mmol/L sodium acetate, 1 mol/L NaCl, 0.1% Triton x100, glacial acetic acid until pH 4.0 is reached), containing 1:100 diluted protease inhibitors cocktail (Mini-Complete EDTA-free; Roche Applied Science, Penzberg, Germany). Protein concentrations were measured using DC protein assay (Bio-Rad, Hercules, CA, USA). Equal amounts of protein (20 µg) were

separated on 15% polyacrylamide gels and subsequently transferred to a polyvinylidene fluoride (PVDF) membrane (GE Healthcare, Buckinghamshire, UK). After that, membranes were blocked with 3% BSA in TBS-T (TBS/0.1% Tween 20) for 1h, at RT. Protein detection from the membrane was performed with specific primary antibodies, incubated overnight at 4 °C with blocking solution. Then, the membranes were washed with TBS-T and incubated for 1h (RT) with the secondary antibodies, in blocking solution. Antibodies used are present in Table 7. Finally, membranes were washed with TBS-T and developed with an enhanced chemiluminescence (ECL) Western Blot Detection Reagent (Bio-Rad), visualized using the chemiluminescence detection imager Amersham 800 (GE Healthcare). The relative intensities of protein bands were analyzed using ImageJ Software.

For the experiment with mice neuronal cortical cell culture, after the treatment exposure, total proteins were extracted using RIPA buffer (50 mM Tris HCl pH 8.0, 150 mM NaCl, 1% NP-40, 0.5% sodium deoxycholate, 0.1% SDS), with 1:100 protease inhibitors cocktail and phosphatase inhibitors (Bimake, Huissen, The Netherlands). Protein concentrations were measured in the supernatant of the protein extracts after 10 min centrifugation at 14,000 rpm, using Pierce BCA protein assay kit (Thermo Fisher Scientific). Equal amounts of protein (15 µg) were separated on 15% polyacrylamide gels, and subsequently transferred using iBlot™ 2 Dry Blotting System (Thermo Fisher Scientific). After that, membranes were blocked with 5% BSA in TBS-T (TBS/0.1% Tween 20) for 1h, at RT. Protein detection from the membrane was performed with specific primary antibodies, incubated overnight at 4°C in 1% BSA blocking solution. Then, the membranes were washed with TBS-T and incubated for 1h (RT) with the secondary antibody, in 0.5% blocking solution. Antibodies used are present in Table 7. To finalize, membranes were washed with TBS-T and developed with WesternBright Quantum (Chemiluminescent HRP Substrate, Advansta, San Jose, California, USA), visualized using the chemiluminescence detection imager Chemidoc (Bio-Rad). The relative intensities of protein bands were quantified using ImageJ Software.

14. Statistical Analysis

The obtained data were quantitatively presented as the mean ± standard error of the mean (SEM) based on a minimum of three independent experiments, unless otherwise noted. Particularly, for HPLC, results denote the compositional analysis of the extracellular medium of a minimum of three independently conducted experiments. The normality of the data was assessed using the Shapiro-Wilk test. If the data followed a normal distribution, statistical analysis was performed using a one-way Analysis of Variance (ANOVA), followed by Dunnett's multiple comparisons test or Tukey's multiple

comparisons test for post hoc analysis. In cases where the data did not follow a normal distribution, Dunn's multiple comparisons were carried out using the Kruskal-Wallis test. Regarding to the findings from the DCFDA assay, a two-way ANOVA was used to determine statistical differentiations, considering each time point, followed by Tukey's post hoc analysis (aggressors and drug combinations, versus vehicle-treated condition; and aggressors versus drug combinations). The differences were considered statistically significant when p value <0.05. Statistical analysis, graphical construction, and calculations of IC₅₀ values were carried out using software GraphPad Prism 9 (San Diego, California, USA).

IV. Results

The results in this thesis will be divided into distinct parts, based on the following original articles, as first author:

- **Correia, A.S.**; Fraga, S.; Teixeira, J.P.; Vale, N. Cell Model of Depression: Reduction of Cell Stress with Mirtazapine. *Int. J. Mol. Sci.* **2022**, *23*, 4942.
- **Correia, A.S.**; Cardoso, A.; Vale, N. Significant Differences in the Reversal of Cellular Stress Induced by Hydrogen Peroxide and Corticosterone by the Application of Mirtazapine or L-Tryptophan. *Int. J. Transl. Med.* **2022**, *2*, 482-505.
- **Correia, A.S.**; Silva, I.; Oliveira, J.C.; Reguengo, H.; Vale, N. Serotonin Type 3 Receptor Is Potentially Involved in Cellular Stress Induced by Hydrogen Peroxide. *Life* **2022**, *12*, 1645.
- **Correia, A.S.**; Silva, I.; Reguengo, H.; Oliveira, J.C.; Vasques-Nóvoa, F.; Cardoso, A.; Vale, N. The Effect of the Stress Induced by Hydrogen Peroxide and Corticosterone on Tryptophan Metabolism, Using Human Neuroblastoma Cell Line (SH-SY5Y). *Int. J. Mol. Sci.* **2023**, *24*, 4389.
- **Correia, A.S.**; Marques, L.; Cardoso, A.; Vale, N. Exploring the Role of Drug Repurposing in Bridging the Hypoxia-Depression Connection. *Membranes.* **2023**, *13*, 800.
- **Correia, A.S.**; Torrado, M.; Coelho, T.; Carvalho, E.; Inteiro-Oliveira, S.; Diógenes, M.J.; Pêgo, A.P.; Santos, S.; Sebastião, A.; Vale, N. BDNF Modulation in Response to Oxidative Stress and Corticosterone: Role of Scopolamine and Mirtazapine. Submitted in *Life Sciences*, January **2024**.

To the published content, some additional insights, modifications/ updates were also included.

The organization of this section aims to enhance clarity, making it easier for readers to comprehend the research findings. Furthermore, the final part of this section includes a compilation of some supplementary/ unpublished results. These additional findings are intended to enhance comprehension of the main results discussed earlier.

1. Investigating the Effects of Mirtazapine and Cellular Stressors on Cellular Viability

In this study, the aim was to uncover the effects of mirtazapine and cellular stressors (H_2O_2 and the glucocorticoids hydrocortisone and corticosterone) on the human neuroblastoma SH-SY5Y and mouse hippocampal HT-22 cellular viability, using MTT and NR assay. Both assays are commonly used to assess cellular viability and cytotoxicity, and some differences between the assays will be further expanded in the discussion. To complement the cellular viability methodologies, cellular morphology assessment was also carried out after the exposure to the different compounds for a period of 48h.

Mirtazapine was used in anticipation of its minimal cytotoxicity, aiming to use it in combination with the cell stressors and effectively mitigate the cytotoxic effects induced by these agents.

1.1. Effect of Mirtazapine on SH-SY5Y and HT-22 Cellular Viability

To study the effect of mirtazapine on SH-SY5Y and HT-22 cellular viability, this antidepressant was added to both cell lines in concentrations ranging from 0.01–20 μM , based on previous studies [263,404,405]. Cellular morphology was assessed right after the 48h of treatment (Figure 9). After that, cellular viability values were obtained by MTT (Figure 10A, C) and NR (Figure 10B, D).

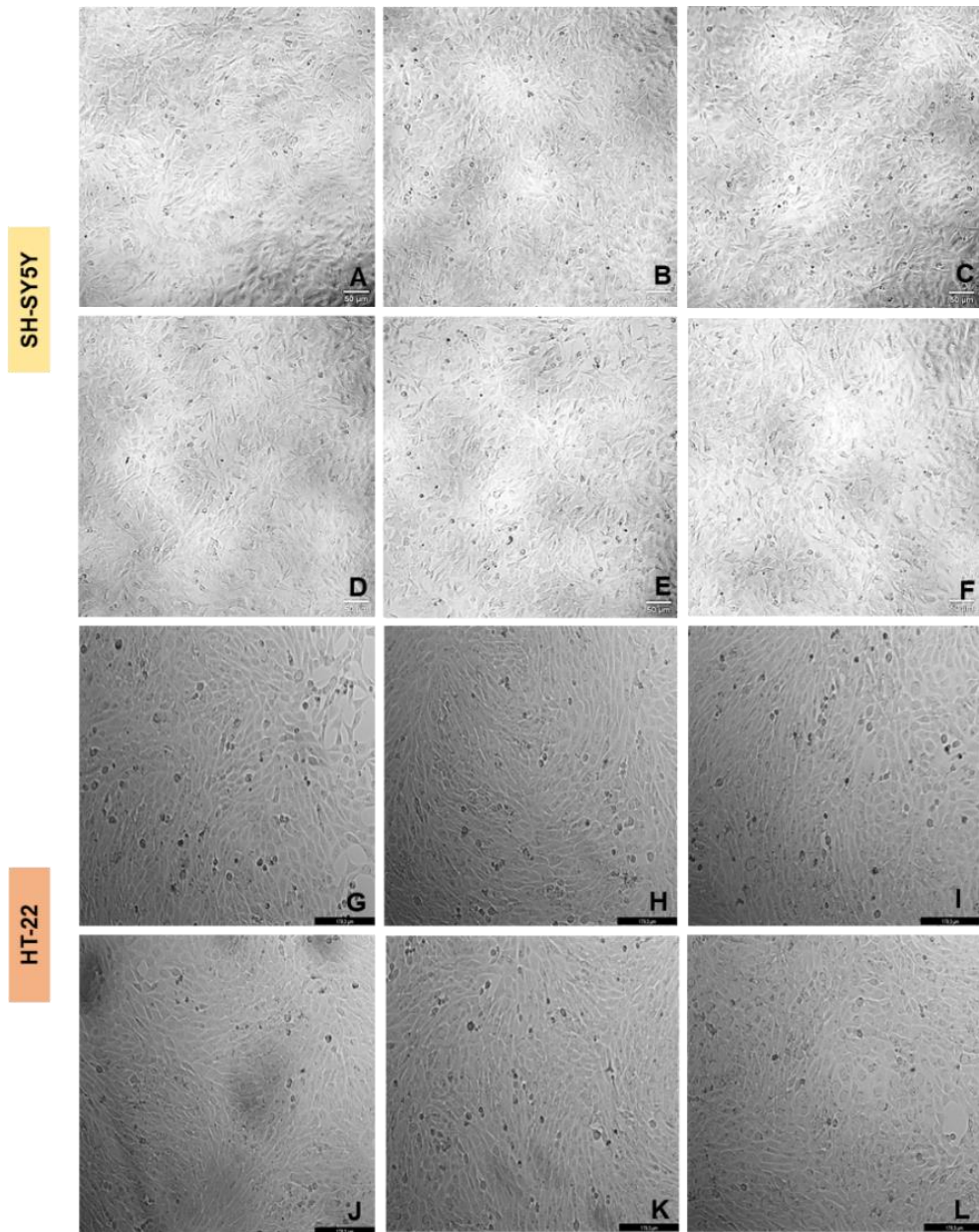


Figure 9. Representative images (total magnification 100x) of SH-SY5Y and HT-22 cells morphology after exposure to different concentrations of mirtazapine. Cells were incubated with (A, G) vehicle (0.1% DMSO), (B, H) mirtazapine 0.01 μ M, (C, I) mirtazapine 0.1 μ M, (D, J) mirtazapine 1 μ M, (E, K) mirtazapine 10 μ M, and (F, L) mirtazapine 20 μ M. Scale bar: 50 μ m.

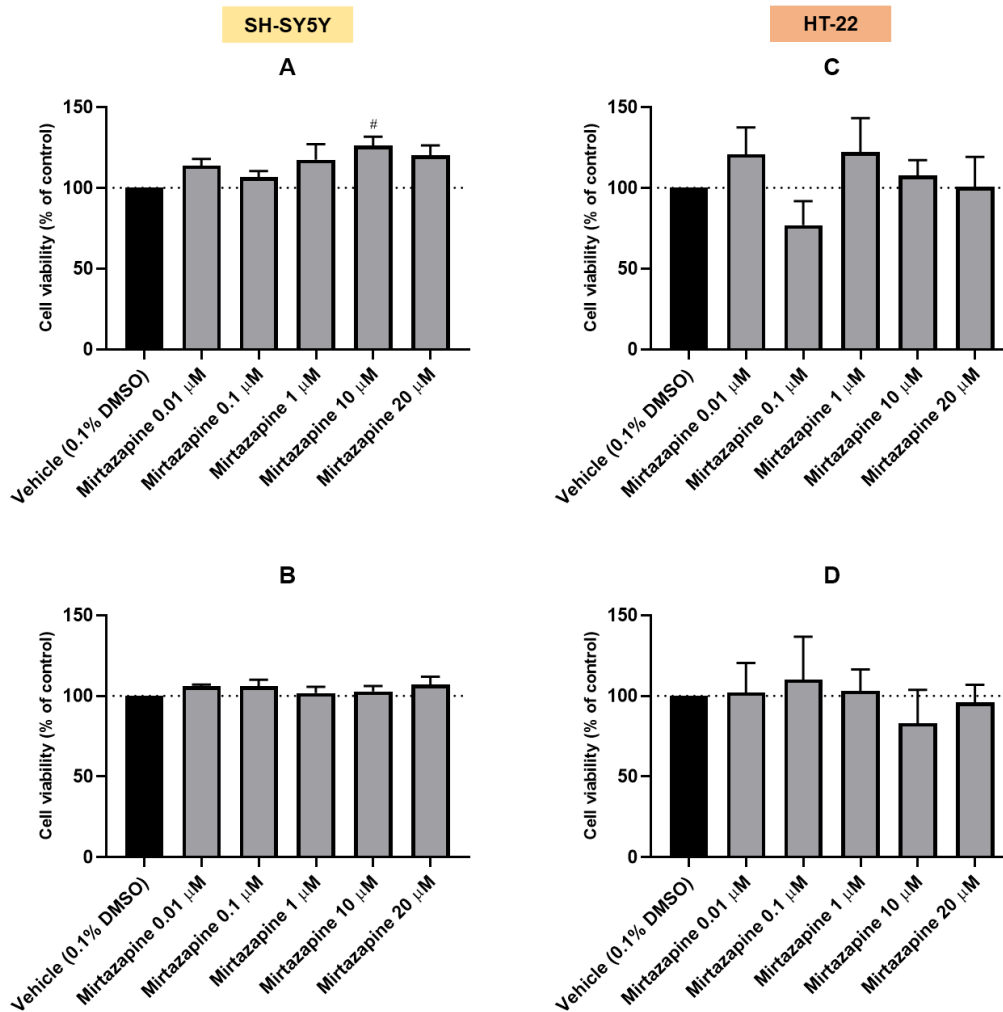


Figure 10. Effect of increasing concentrations of mirtazapine on the viability of SH-SY5Y and HT-22 cells, obtained by (A, C) MTT and (B, D) NR assays. The results are expressed as the percentage of the vehicle and represent the mean \pm SEM of three independent experiments. Statistically significant # $p < 0.05$ vs. vehicle.

These findings confirm that mirtazapine showed no toxicity at any tested concentrations, substantiated by both viability and morphological assessments. This suggests its potential to mitigate cellular stress in both SH-SY5Y and HT-22 cell lines. In HT-22 cells, the results showed greater variability, though they did not reach statistical significance.

Collectively, these findings underscore its promising role as a stress-reversal agent when combined with cellular stressors, that will be explored later.

1.2. Effect of Hydrogen Peroxide, Hydrocortisone and Corticosterone on SH-SY5Y and HT-22 Cellular Viability

H₂O₂, hydrocortisone and corticosterone were added to these cells in concentrations ranging from 50–300 μM, and 100-500 μM, respectively, based on previous research studies [263,406–412]. Additionally, for H₂O₂ and corticosterone, the concentration-response curves (Figures 13 and 18) and half-maximal inhibitory concentrations (IC₅₀) values on the cellular viability were determined (Table 8). Following the 48h treatment period, cellular morphology assessments were conducted (Figures 11, 14 and 16), and subsequent cellular viability evaluations were performed using both MTT and NR assays (Figures 12, 15 and 17).

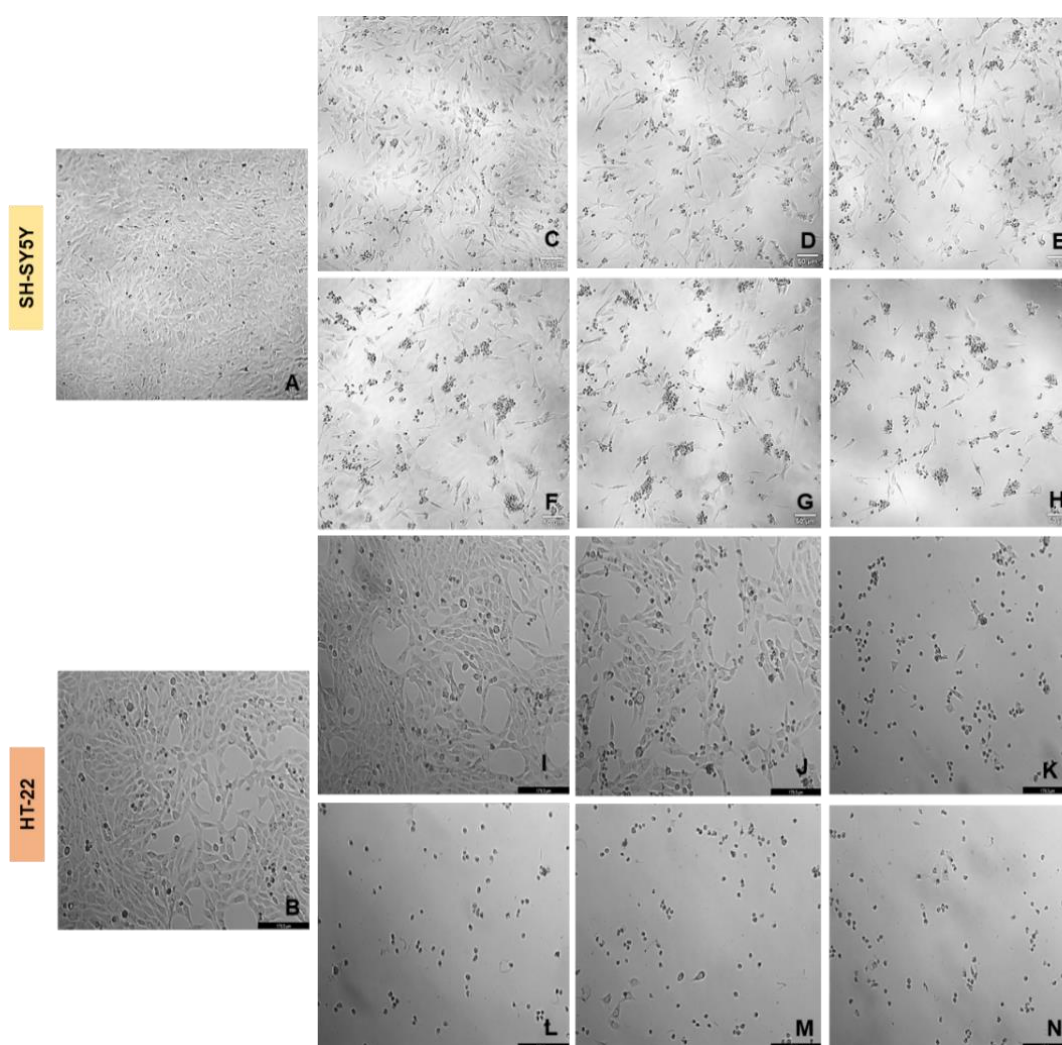


Figure 11. Representative images (100 × total magnification) of SH-SY5Y and HT-22 cells after incubation of increasing concentrations of H₂O₂. Cells were treated with (A, B) vehicle, (0.1% H₂O), (C, I) H₂O₂ 50 μM, (D, J) H₂O₂ 100 μM, (E, K) H₂O₂ 150 μM, (F, L) H₂O₂ 200 μM, (G, M) H₂O₂ 250 μM, (H, N) H₂O₂ 300 μM. Scale bar: 50 μm.

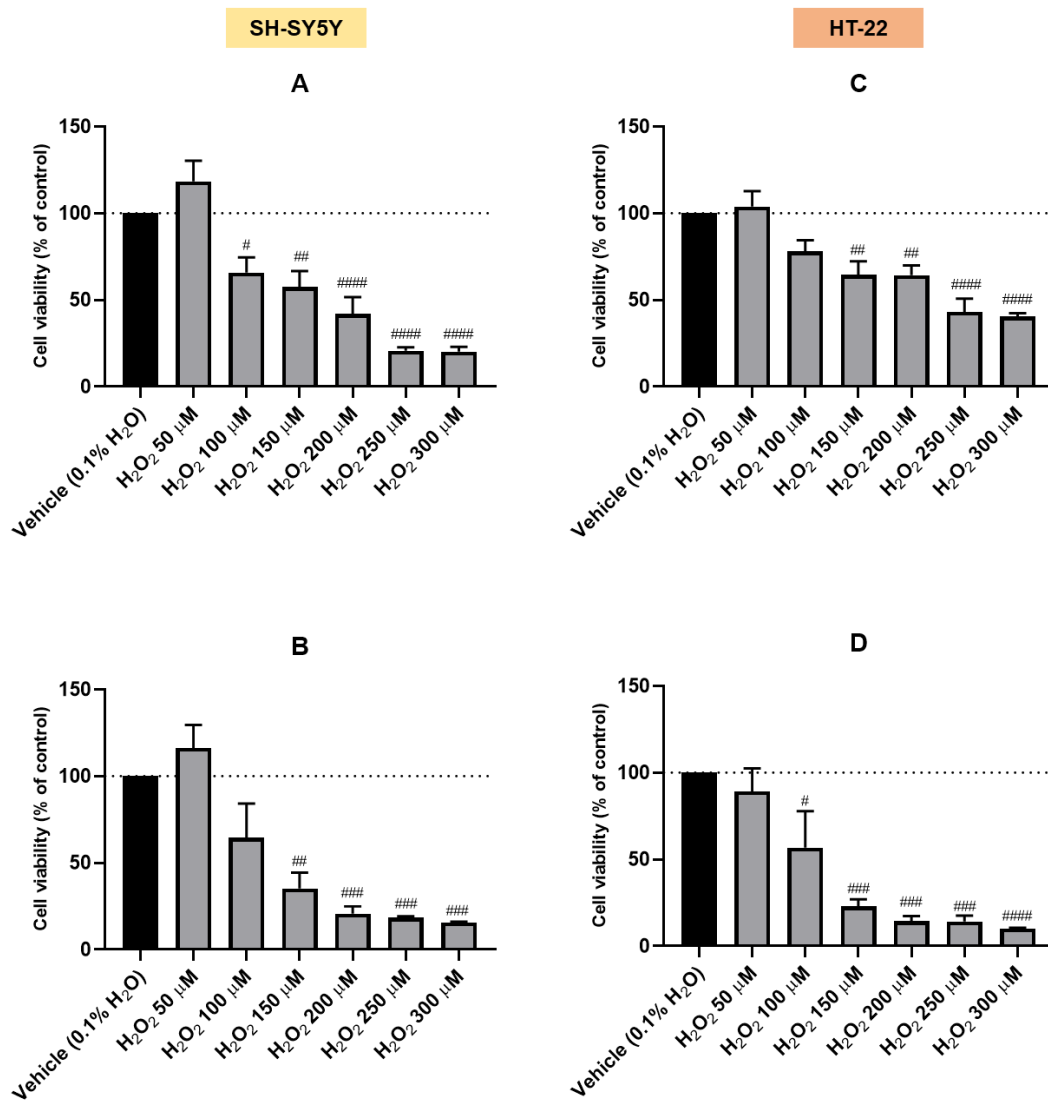


Figure 12. Effect of increasing concentrations of H₂O₂ on the viability of SH-SY5Y and HT-22 cells, obtained by (A, C) MTT and (B, D) NR assays. The results are expressed as the percentage of the vehicle and represent the mean ± SEM of three-six independent experiments. Statistically significant # p<0.05, ## p<0.01, ### p<0.001, #### p<0.0001 vs. vehicle.

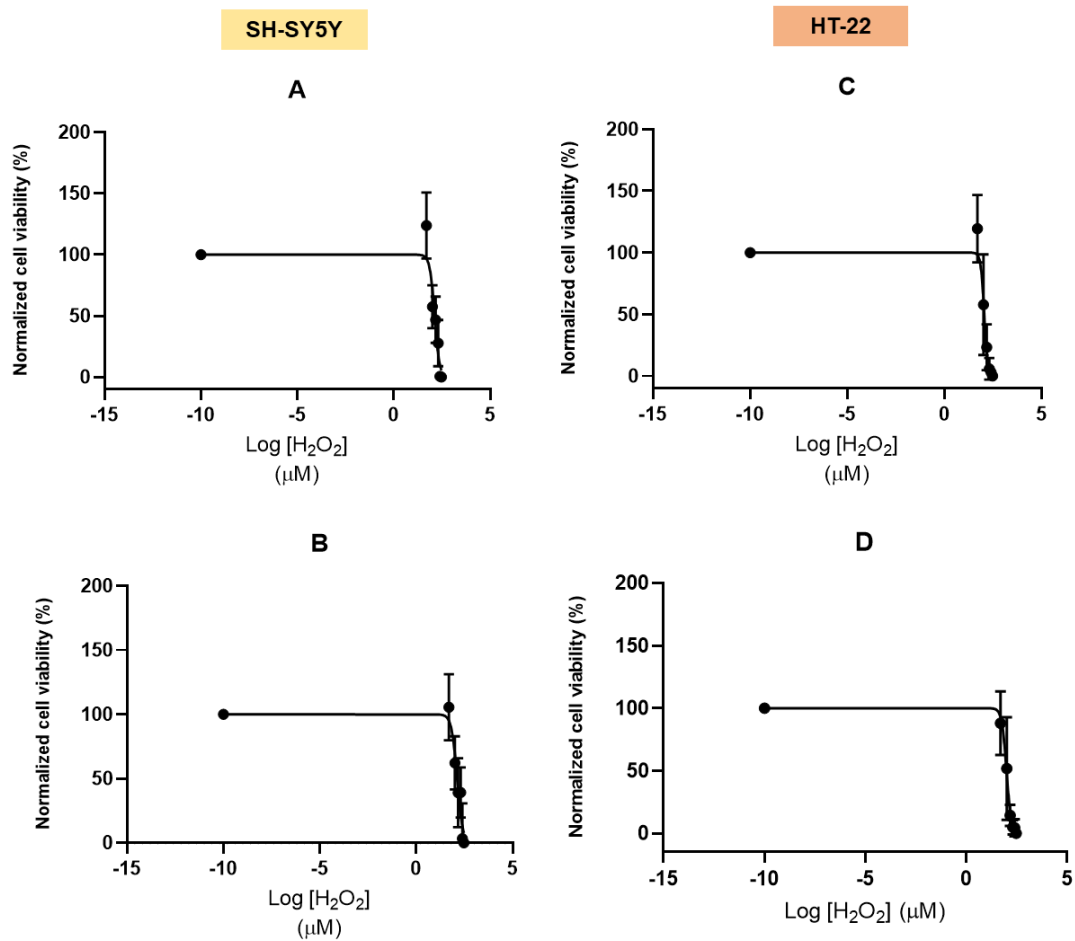


Figure 13. Concentration-response curves for increasing concentrations of H₂O₂ on the viability of SH-SY5Y cells and HT-22 cells, obtained by (A, C) MTT and (B, D) NR assays. The results are expressed as the percentage of each respective vehicle and represent the mean ± SEM of three-six independent experiments.

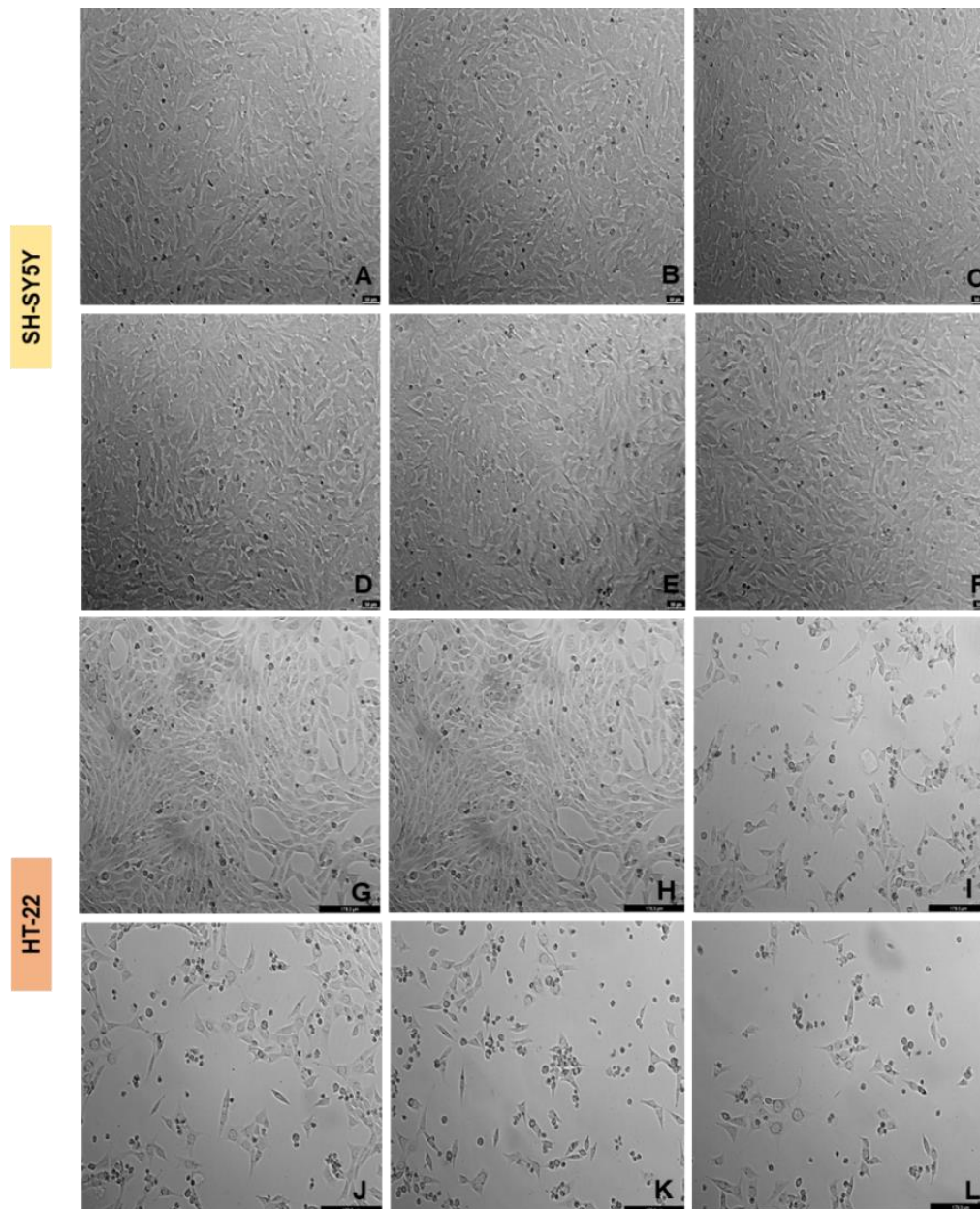


Figure 14. Representative images (100 × total magnification) of SH-SY5Y and HT-22 cells after incubation of increasing concentrations of hydrocortisone. Cells were treated with (A,G) vehicle (0.1% DMSO), (B, H) hydrocortisone 100 μM, (C, I) hydrocortisone 200 μM, (D, J) hydrocortisone 300 μM, (E, K) hydrocortisone 400 μM, (F, L) hydrocortisone 500 μM. Scale bar: 50 μm.

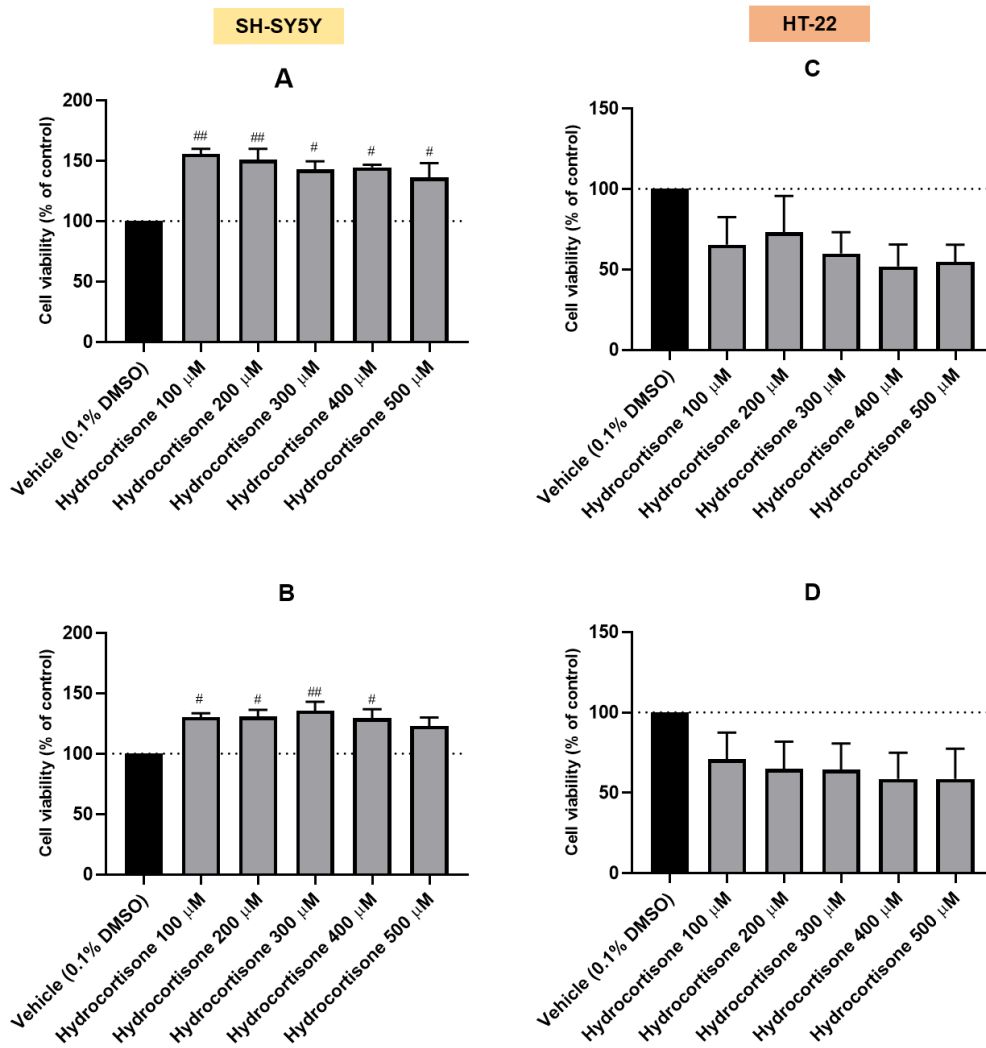


Figure 15. Effect of increasing concentrations of hydrocortisone on the viability of SH-SY5Y and HT-22 cells, obtained by (A, C) MTT and (B, D) NR assays. The results are expressed as the percentage of the vehicle and represent the mean \pm SEM of three independent experiments. Statistically significant # $p < 0.05$, ## $p < 0.01$ vs. vehicle.

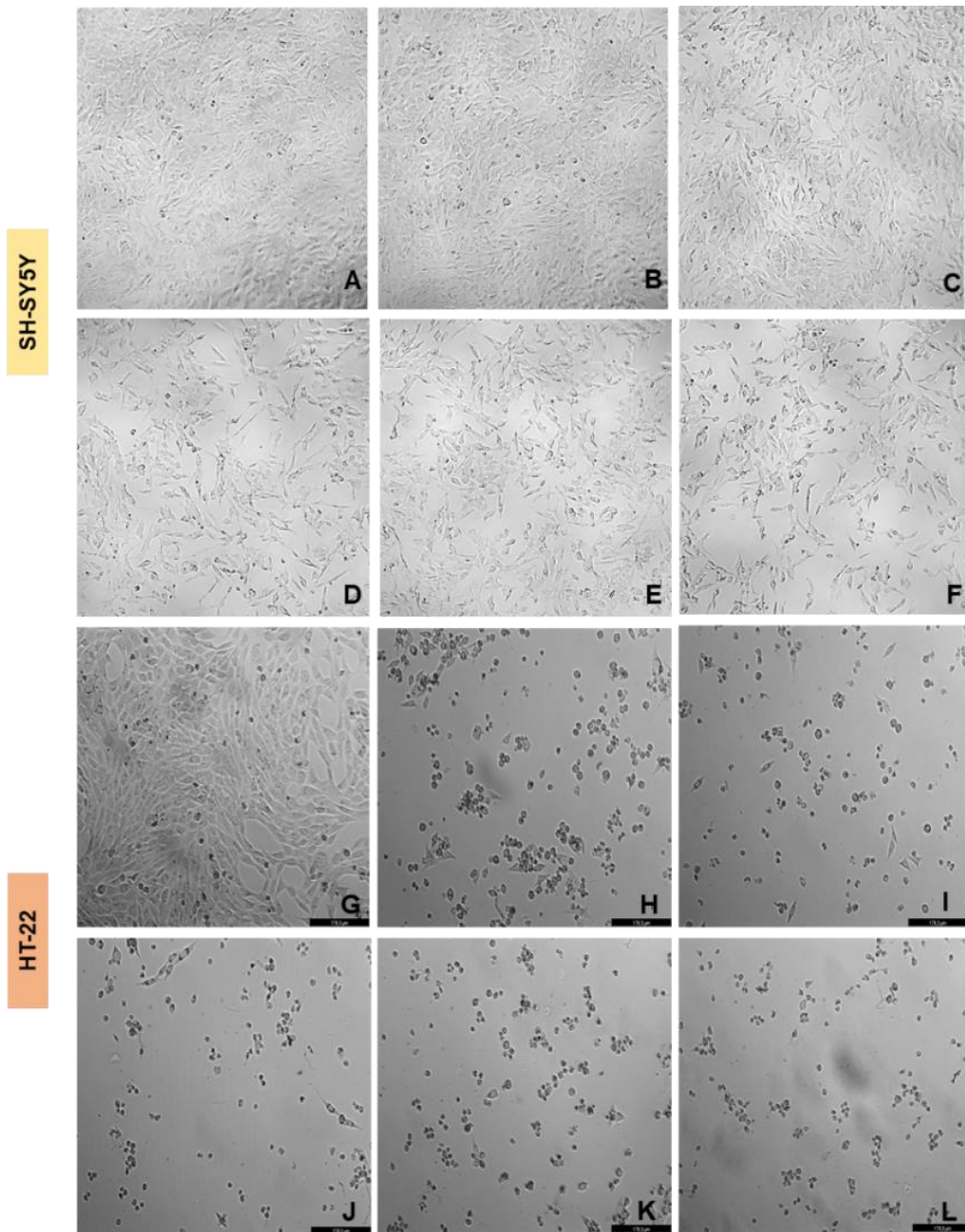


Figure 16. Representative images (100 × total magnification) of SH-SY5Y and HT-22 cells after incubation of increasing concentrations of corticosterone. Cells were treated with (A,G) vehicle (0.1% DMSO), (B, H) corticosterone 100 μM, (C, I) corticosterone 200 μM, (D, J) corticosterone 300 μM, (E, K) corticosterone 400 μM, (F, L) corticosterone 500 μM. Scale bar: 50 μm.

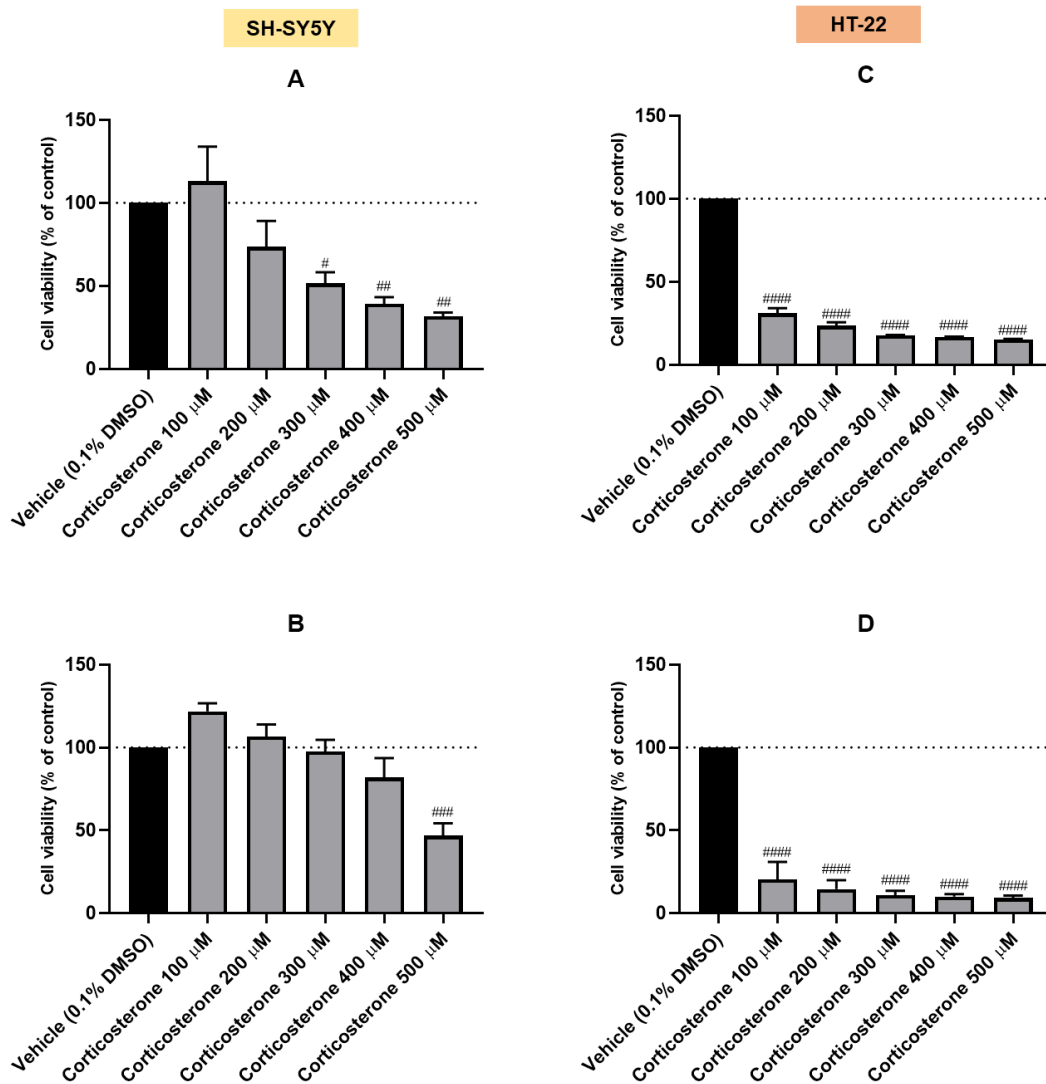


Figure 17. Effect of increasing concentrations of corticosterone on the viability of SH-SY5Y and HT-22 cells, obtained by (A, C) MTT and (B, D) NR assays. The results are expressed as the percentage of the vehicle and represent the mean \pm SEM of three-six independent experiments. Statistically significant # $p < 0.05$, ## $p < 0.01$, ### $p < 0.001$, #### $p < 0.0001$ vs. vehicle.

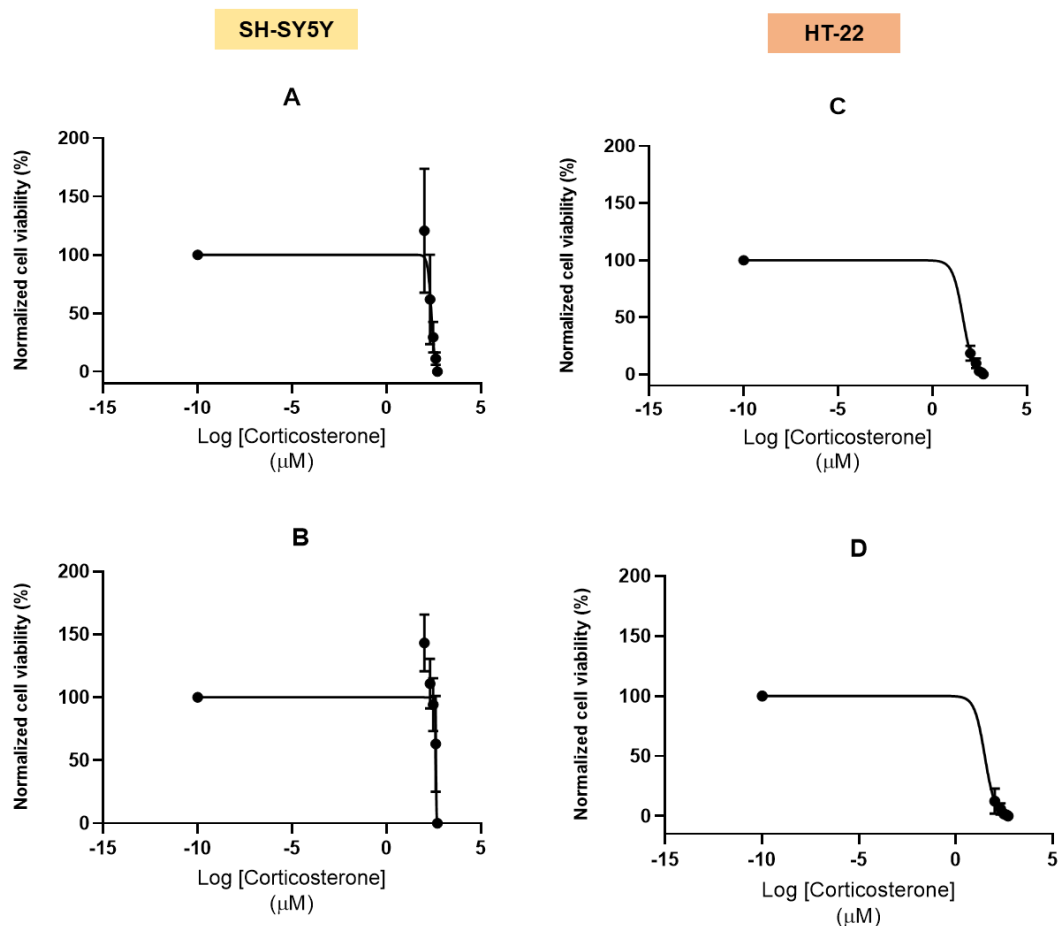


Figure 18. Concentration-response curves for increasing concentrations of corticosterone on the viability of SH-SY5Y cells and HT-22 cells, obtained by (A, C) MTT and (B, D) NR assays. The results are expressed as the percentage of each respective vehicle and represent the mean \pm SEM of three-six independent experiments.

Collectively, these results demonstrated that H_2O_2 and corticosterone led to a concentration-dependent reduction in cellular viability, as observed in both cellular viability methodologies, in both cell lines (Figures 12 and 17). The obtained IC_{50} values for these compounds in both cell lines are provided in Table 8, derived from the analysis of concentration-response curves (Figures 13 and 18). Furthermore, the examination of cellular morphology (Figures 11 and 16) demonstrated that higher concentrations of both compounds led to a decrease in cell number and induced notable cellular damage. This damage was characterized by fragmentation into smaller apoptotic bodies and cell shrinkage, resulting in a condensed and diminished appearance compared to the typical healthy cell morphology [413].

Table 8. IC₅₀ values and average of IC₅₀ values for H₂O₂ and corticosterone in the viability of SH-SY5Y and HT-22 cells, obtained by MTT or NR. The results are rounded to the nearest integer.

Cell line	Compound	Methodology	IC ₅₀ value (μM)	Average (μM)
SH-SY5Y	H ₂ O ₂	MTT	132; 95% CI [107.3, 158.8]	132
		NR	132; 95% CI [103.9, 161.8]	
	Corticosterone	MTT	236; 95% CI [183.4, 297.9]	322
		NR	408; 95% CI [365.7, undetermined]	
HT-22	H ₂ O ₂	MTT	111; 95% CI [93.1, 132.0]	105
		NR	98; 95% CI [78.3, 116.7]	
	Corticosterone	MTT	39; 95% CI [24.1, 55.3]	35
		NR	31; 95% CI [5.1, 64.6]	

In the context of hydrocortisone, it was noteworthy that this compound, across all concentrations tested, did not result in a decline in cell viability within SH-SY5Y cells (Figures 14A-F, and 15A, B). This finding rejects hydrocortisone as a viable stress-inducing agent for these cells. Interestingly, this glucocorticoid overall increased cellular viability in SH-SY5Y cells. Conversely, when applied to HT-22 cells (Figures 14G-L, and 15C, D), hydrocortisone did exhibit a reduction in cellular viability, although this decrease did not reach statistical significance. These findings will be subject to further exploration in the discussion.

Collectively, these results suggest that H₂O₂ and corticosterone, and not hydrocortisone, are better-suited candidates for inducing cellular damage, thus providing a cellular model to induce the oxidative stress and exacerbated HPA axis response conditions observed in individuals with depression, aiming to explore these responses in a molecular/ cellular way. This type of study facilitates an exploration of depression at the cellular level, opening up the potential for future screenings of compounds that could

be used in the treatment of depression, particularly in the context of mechanisms such as oxidative stress protection. In the discussion, this will be explored in further detail.

2. Exploring the Effects of Mirtazapine and L-Tryptophan on the Damage Induced by Stressors in Neuronal Cell Lines

The results from the previous part indicated that the exposure to high levels of oxidative stress (H_2O_2) and glucocorticoids (corticosterone) induce cytotoxicity. On the other hand, the exposure of cells to mirtazapine did not induce cytotoxic effects.

Hence, in this part 2, the primary goal was to examine the potential mitigation of corticosterone and H_2O_2 -induced stress responses by exposing both cell lines to mirtazapine and L-TRP. The focus encompassed the assessment of cell morphology, cell viability determination by MTT assay, and ROS levels using the DCFDA assay, as key measures.

Noteworthy, L-TRP, as well as mirtazapine, is involved in the regulation of 5-HT levels. As mentioned in the introduction, this amino acid is a precursor to 5-HT synthesis, while mirtazapine modulates 5-HT receptors, both being relevant in the context of mood regulation and depression.

2.1. Effect of the Combination of Mirtazapine with Hydrogen Peroxide on SH-SY5Y and HT-22 Cellular Viability

To first evaluate the effect of mirtazapine in combination with the aggressor H_2O_2 on the viability of SH-SY5Y and HT-22 cells, mirtazapine was added to the cells in crescent concentrations (0.01 μM – 20 μM), in combination with H_2O_2 , that was added to the cells in a concentration of 132 μM or 105 μM (representing the IC_{50} value obtained for SH-SY5Y and HT-22 cell viability, respectively, as shown in Table 8), for 48h. Subsequently, it was conducted a morphological examination of the cells exposed to this drug combination (Figure 19). Then, cellular viability was determined using the MTT assay (Figure 20).

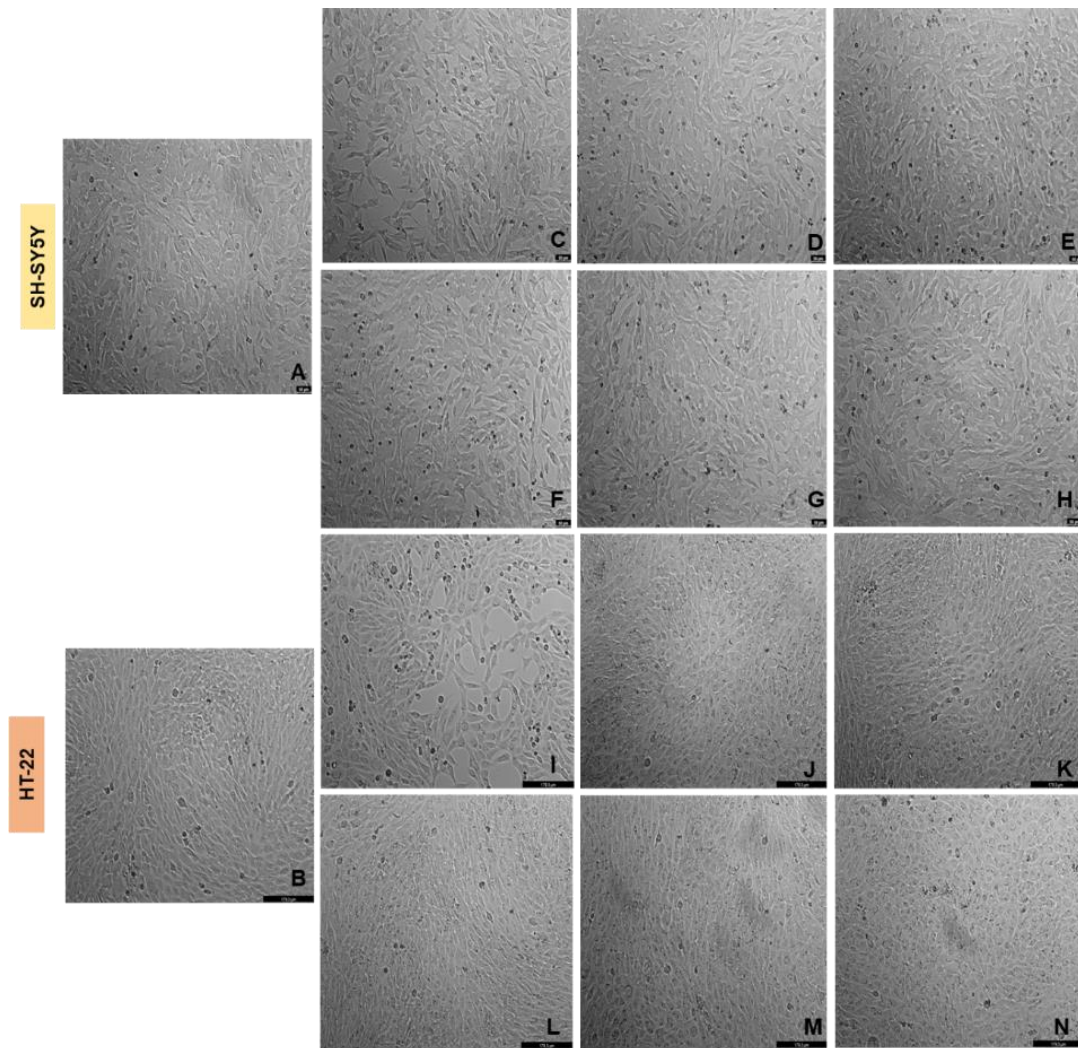


Figure 19. Representative images (total magnification 100x) of SH-SY5Y and HT-22 cells morphology after exposure to H₂O₂ and to the combination of mirtazapine with H₂O₂. Cells were incubated with (A,B) vehicle (0.1% DMSO), (C, I) H₂O₂ 132 μM and 105 μM, respectively, (D, J) H₂O₂ 132 μM + mirtazapine 0.01 μM and H₂O₂ 105 μM + mirtazapine 0.01 μM, respectively, (E, K) H₂O₂ 132 μM + mirtazapine 0.1 μM and H₂O₂ 105 μM + mirtazapine 0.1 μM, respectively, (F, L) H₂O₂ 132 μM + mirtazapine 1 μM and H₂O₂ 105 μM + mirtazapine 1 μM, respectively, (G, M) H₂O₂ 132 μM + mirtazapine 10 μM and H₂O₂ 105 μM + mirtazapine 10 μM, respectively, (H, N) H₂O₂ 132 μM + mirtazapine 20 μM and H₂O₂ 105 μM + mirtazapine 20 μM, respectively. Scale bars: 50 μm and 179.3 μm.

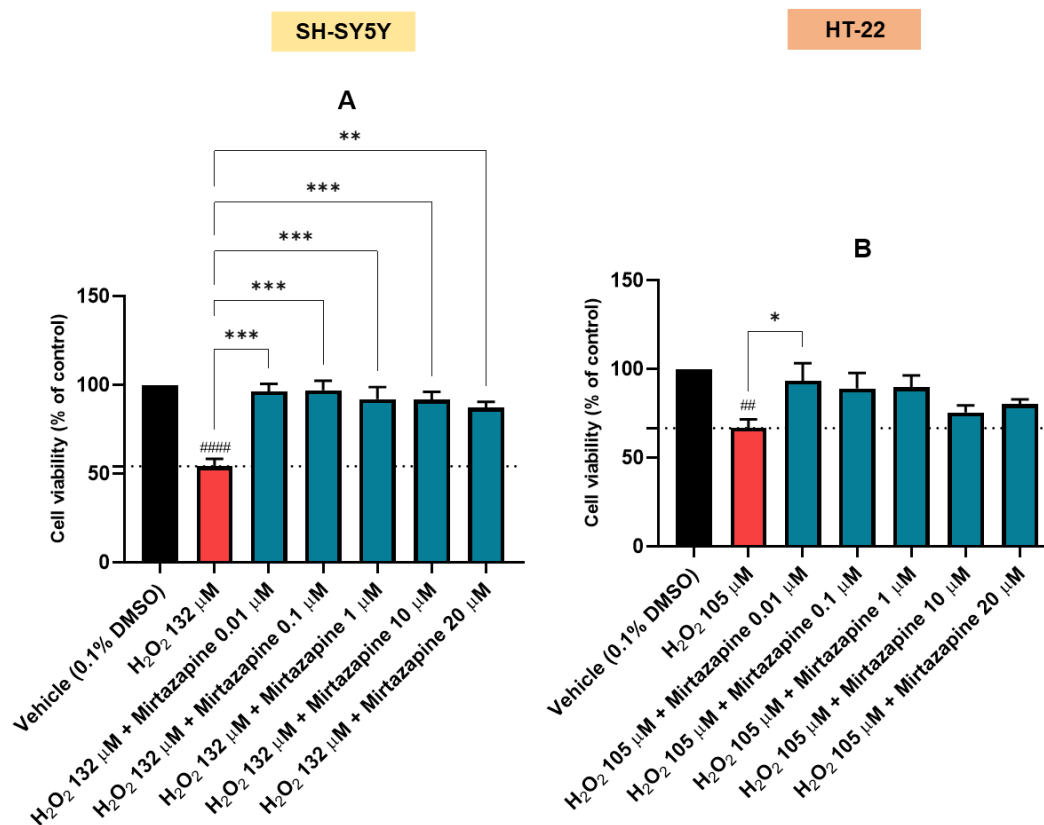


Figure 20. Effect of increasing concentrations of mirtazapine, in combination with H₂O₂, on the viability of (A) SH-SY5Y cells and (B) HT-22 cells, obtained by the MTT assay. The results are expressed as the percentage of the vehicle and represent the mean ± SEM of three independent experiments. Statistically significant # p<0.05 and ##### p < 0.0001 vs. vehicle, ** p < 0.01 and *** p < 0.001 vs. H₂O₂ 132 μM, * p<0.05 vs. H₂O₂ 105 μM.

Through the analysis of the obtained data, it was apparent that mirtazapine consistently counteracted the decrease in cell viability induced by H₂O₂, regardless of the concentrations tested, especially in SH-SY5Y cells (Figures 19C-H and 20A), in which the damage caused by H₂O₂ was more accentuated than in HT-22 cells (Figures 19I-N and 20B). This attenuation resulted in a significant increase in cell viability, ultimately restoring it to levels comparable to those observed in the vehicle-treated group. In summary, these findings provide evidence of mirtazapine's activity on counteracting the cytotoxicity induced by H₂O₂ in both cells, especially in SH-SY5Y cells.

2.2. Effect of the Combination of Mirtazapine with Corticosterone on SH-SY5Y and HT-22 Cellular Viability

Then, to investigate the impact of mirtazapine in combination with corticosterone on the viability of SH-SY5Y and HT-22 cells, mirtazapine was once again introduced to the cells in concentrations ranging from 0.01 μM to 20 μM . Simultaneously, corticosterone was added to the cells at either 322 μM or 35 μM concentrations, representing the respective IC_{50} values obtained for SH-SY5Y, and HT-22 cell viability, respectively (as detailed in Table 8). After 48h, it was conducted a morphological analysis of the cells incubated with these drug combinations (Figure 21). The assessment of cellular viability was subsequently carried out using the MTT assay (Figure 22).

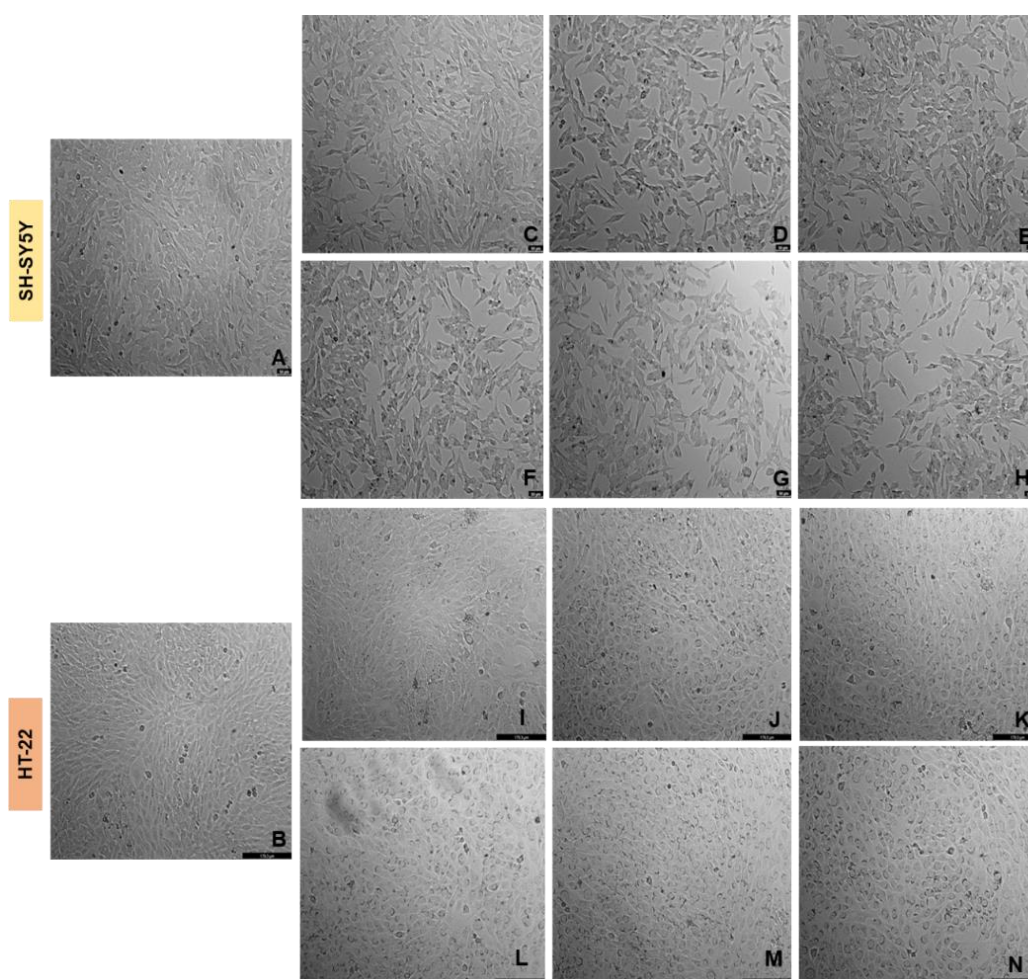


Figure 21. Representative images (total magnification 100x) of SH-SY5Y and HT-22 cells morphology after exposure to corticosterone and to the combination of mirtazapine with corticosterone. Cells were incubated with (A,B) vehicle (0.2% DMSO), (C, I) corticosterone 322 μM and 35 μM , respectively, (D, J) corticosterone 322 μM + mirtazapine 0.01 μM and corticosterone 35 μM + mirtazapine 0.01 μM , respectively, (E, K) corticosterone 322 μM + mirtazapine 0.1 μM and corticosterone 35 μM + mirtazapine 0.1 μM , respectively, (F, L) corticosterone 322 μM + mirtazapine 1 μM and corticosterone 35 μM + mirtazapine 1 μM , respectively,

(G, M) corticosterone 322 μM + mirtazapine 10 μM and corticosterone 35 μM + mirtazapine 10 μM , respectively, (H, N) corticosterone 322 μM + mirtazapine 20 μM and corticosterone 35 μM + mirtazapine 20 μM , respectively. Scale bars: 50 μm and 179.3 μm .

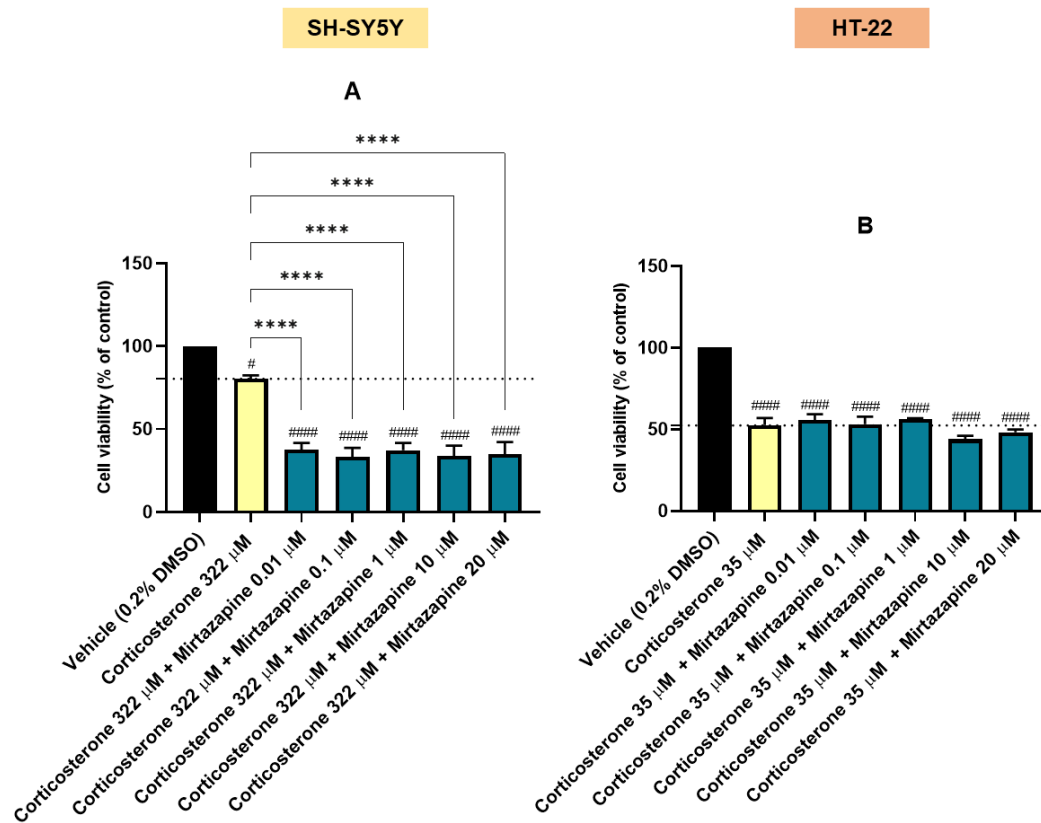


Figure 22. Effect of increasing concentrations of mirtazapine, in combination with corticosterone, on the viability of (A) SH-SY5Y cells and (B) HT-22 cells, obtained by the MTT assay. The results are expressed as the percentage of the vehicle and represent the mean \pm SEM of three independent experiments. Statistically significant # $p < 0.05$ and ##### $p < 0.0001$ vs. vehicle, **** $p < 0.0001$ vs. corticosterone 322 μM .

These findings indicate that for SH-SY5Y cells, mirtazapine did not mitigate the effects of corticosterone. In fact, the combination of mirtazapine with corticosterone led to a further decline in cell viability compared to corticosterone alone (Figures 21C-H and 22A). This finding will be further discussed. Likewise, for HT-22 cells, mirtazapine did not mitigate the detrimental effects of corticosterone (Figure 22B). It's worth noting that there were some seemingly contradictions by analyzing the morphology images (especially Figure 21I). This apparent contradiction could be attributed to the possibility that this figure was captured in a region of the well with more concentrated cells, making it less representative of the overall viability values. Nevertheless, in HT-22 cells, the impact of

the combination of mirtazapine with corticosterone did not significantly differ from that of corticosterone alone.

In summary, these results collectively demonstrate that mirtazapine did not effectively counteract the effects of corticosterone on the cells, opposing to what was observed with H₂O₂.

2.3. Effect L-Tryptophan on SH-SY5Y and HT-22 Cellular Viability

To explore the potential of L-TRP to attenuate H₂O₂ or corticosterone-induced stress on both cell lines, this amino acid was first added to the cells in concentrations ranging from 0.1 nM to 100 µM for 48h. After that, it was conducted a morphological analysis of the cells (Figure 23). The assessment of cellular viability was subsequently carried out using the MTT assay (Figure 24).

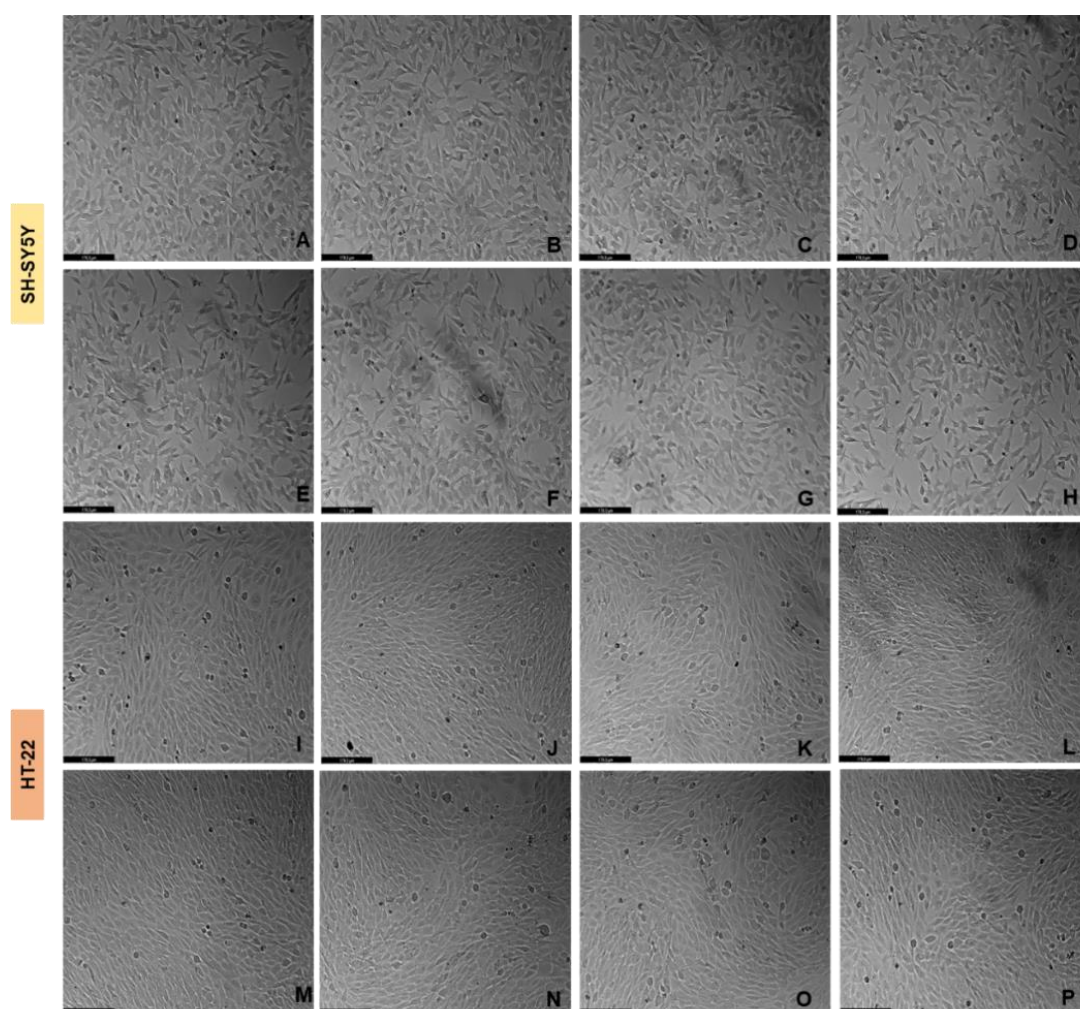


Figure 23. Representative images (100 × total magnification) of SH-SY5Y and HT-22 cells after incubation of increasing concentrations of L-TRP. Cells were treated with (A, I) vehicle (1% H₂O), (B, J) L-TRP 0.1 nM, (C, K) L-TRP 1 nM, (D, L) L-TRP 10 nM, (E, M) L-TRP 100 nM, (F, N) L-TRP 1 µM, (G, O) L-TRP 10 µM, (H, P) L-TRP 100 µM. Scale bar: 179.3 µm.

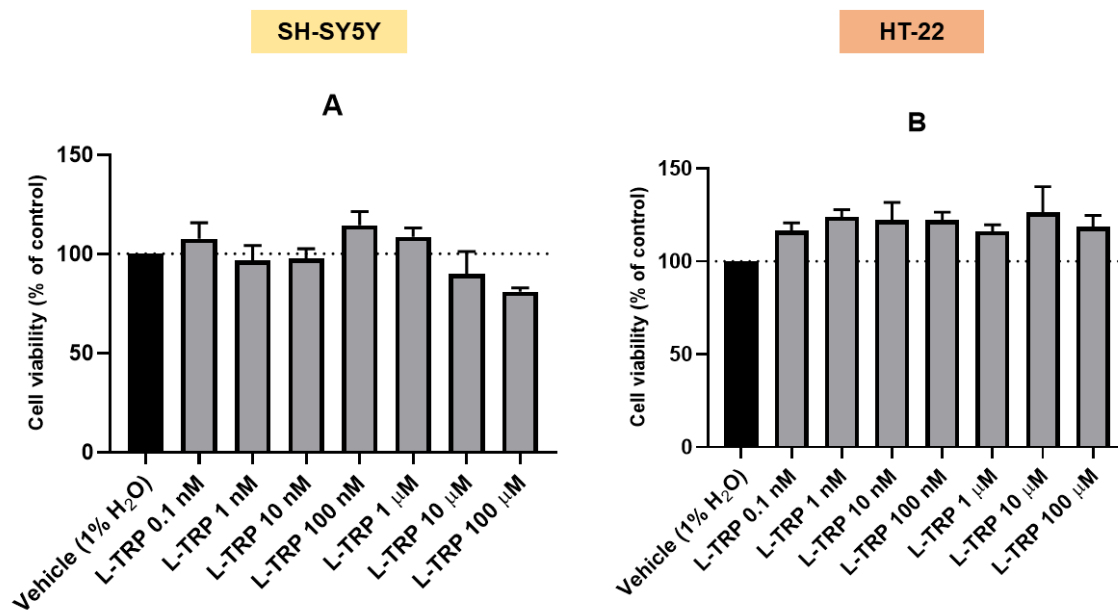


Figure 24. Effect of the incubation of 0.1 nM-100 μM of L-TRP on the viability of (A) SH-SY5Y cells and (B) HT-22 cells, determined by MTT methodology. The results represent the mean ± SEM of three independent experiments, expressed as the percentage of the vehicle (100%).

Analyzing the results obtained for both cell lines, it can be concluded that, like mirtazapine, L-TRP did not exhibit any toxicity toward the cells at any of the concentrations tested. This suggests that L-TRP holds promise as a potential cytoprotective agent for both HT-22 and SH-SY5Y cells. However, it is noteworthy that, in the case of SH-SY5Y cells, the highest concentration of L-TRP (100 μM) appeared to have a minor, non-statistically significant, impact on cell viability, resulting in an approximately 80.1 ± 1.8 % cell viability.

Thus, the findings from this study demonstrate that L-TRP does not induce a decrease in cell viability in both cell lines, as evidenced by both viability (Figure 24) and morphological assays (Figure 23). These results highlight the potential utility of L-TRP as an agent for mitigating oxidative stress and glucocorticoid-induced stress.

2.4. Effect of the Combination of L-Tryptophan with Hydrogen Peroxide on SH-SY5Y and HT-22 Cellular Viability

Next, to understand the effect of L-TRP combined with H₂O₂ on SH-SY5Y and HT-22 cellular viability, this amino acid was added to the cells in concentrations of 0.1 nM–100 μM. Once again, H₂O₂ was added to the cells at a fixed concentration of 132 μM for SH-SY5Y cells and 105 μM for HT-22 cells, for a period of incubation of 48h.

Following this, a morphological analysis of the cells was undertaken (Figure 25). Subsequently, the evaluation of cellular viability was conducted using the MTT assay (Figure 26).

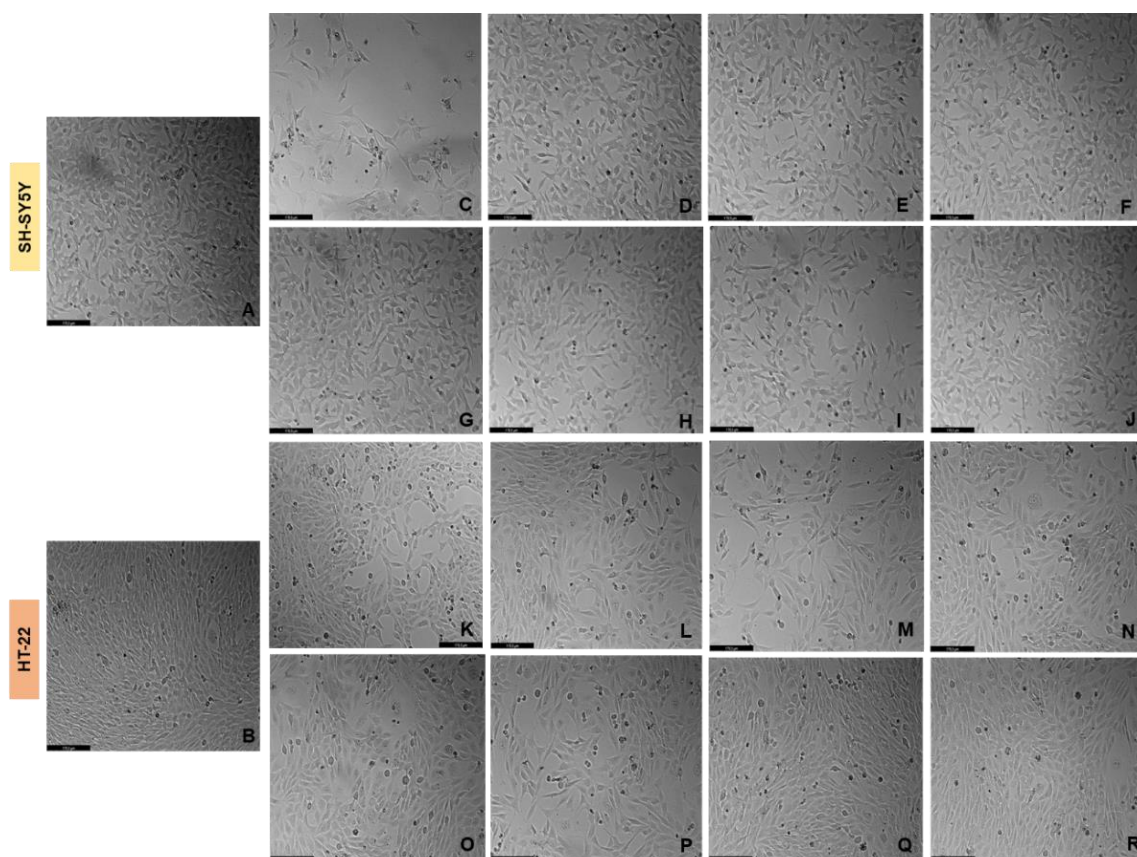


Figure 25. Representative images (100 × total magnification) of SH-SY5Y and HT-22 cells after incubation of H₂O₂ in combination with L-TRP. Cells were treated with (A,B) vehicle (1% H₂O), (C, K) H₂O₂ 132 μM and 105 μM, respectively, (D, L) L-TRP 0.1 nM + H₂O₂ 132 μM and L-TRP 0.1 nM + H₂O₂ 105 μM, respectively, (E, M) L-TRP 1 nM + H₂O₂ 132 μM and L-TRP 1 nM + H₂O₂ 105 μM, respectively, (F, N) L-TRP 10 nM + H₂O₂ 132 μM and L-TRP 10 nM + H₂O₂ 105 μM, respectively, (G, O) L-TRP 100 nM + H₂O₂ 132 μM and L-TRP 100 nM + H₂O₂ 105 μM, respectively, (H, P) L-TRP 1 μM + H₂O₂ 132 μM and L-TRP 1 μM + H₂O₂ 105 μM, respectively, (I, Q) L-TRP 10 μM + H₂O₂ 132 μM and L-TRP 10 μM + H₂O₂ 105 μM, respectively, (J, R) L-TRP 100 μM + H₂O₂ 132 μM and L-TRP 100 μM + H₂O₂ 105 μM, respectively. Scale bar: 179.3 μm.

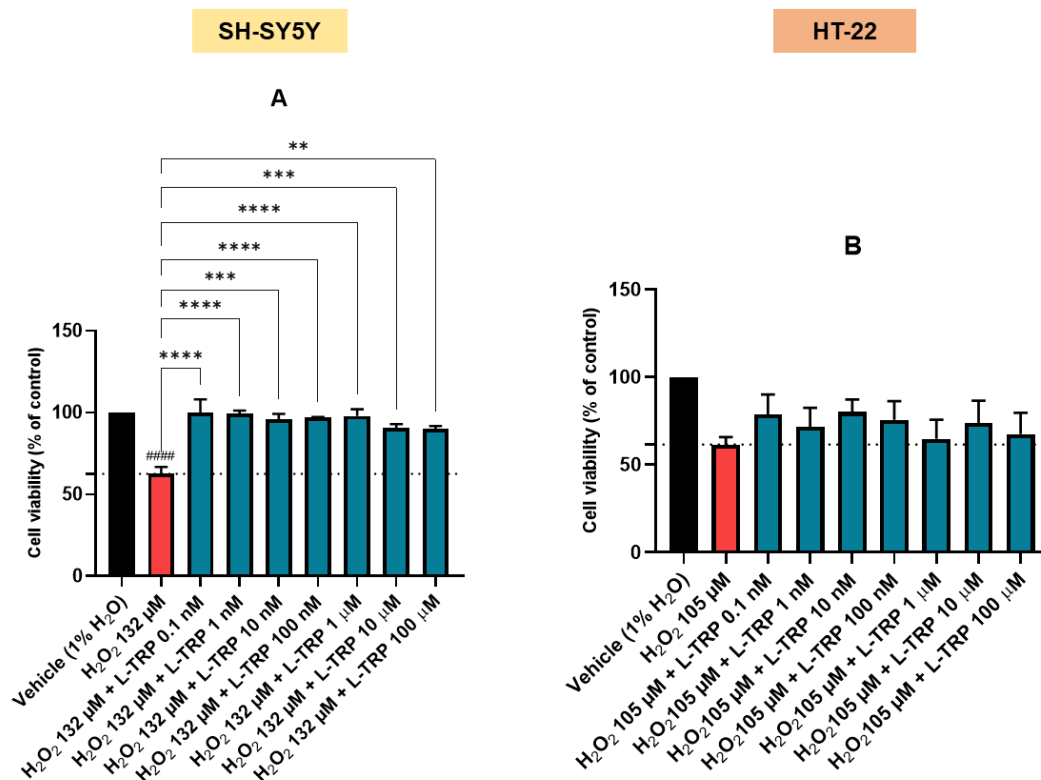


Figure 26. Effect of the incubation of (A) 132 μM of H₂O₂ and (B) 105 μM of H₂O₂, in combination with 0.1 nM–100 μM of L-TRP, determined by MTT methodology. The results represent the mean ± SEM of three independent experiments, expressed as the percentage of the vehicle (100%). Statistically significant ##### p < 0.0001 vs. vehicle, ** p < 0.01, *** p < 0.001, **** p < 0.0001 vs. H₂O₂ 132 μM.

The obtained results demonstrated that L-TRP, across all concentrations tested, mitigated the decline in cellular viability induced by H₂O₂ exposure in SH-SY5Y cells. In the case of HT-22 cells, a discernible trend of stress modulation by L-TRP was observed, particularly highlighted by the morphological analysis (especially in Figure 25K, R).

Collectively, these findings provide compelling evidence that L-TRP overall counteracted the deleterious effects of H₂O₂-induced stress on cellular viability, with a particularly notable impact on SH-SY5Y cells. These findings will be explored in the discussion.

2.5. Effect of the Combination of L-Tryptophan with Corticosterone on SH-SY5Y and HT-22 Cellular Viability

To elucidate the impact of L-TRP in combination with corticosterone on the viability of SH-SY5Y and HT-22 cells, a range of L-TRP concentrations spanning from 0.1 nM to 100 μM was introduced to the cell cultures. Once again, a fixed concentration of corticosterone was added to the cells, specifically 322 μM for SH-SY5Y cells and 35

μM for HT-22 cells (previously calculated IC_{50} values, Table 8), and the cells were incubated for a period of 48h. After this incubation, a morphological analysis of the cells was conducted (Figure 27). Following the morphological analysis, an assessment of cellular viability was carried out by the MTT assay (Figure 28).

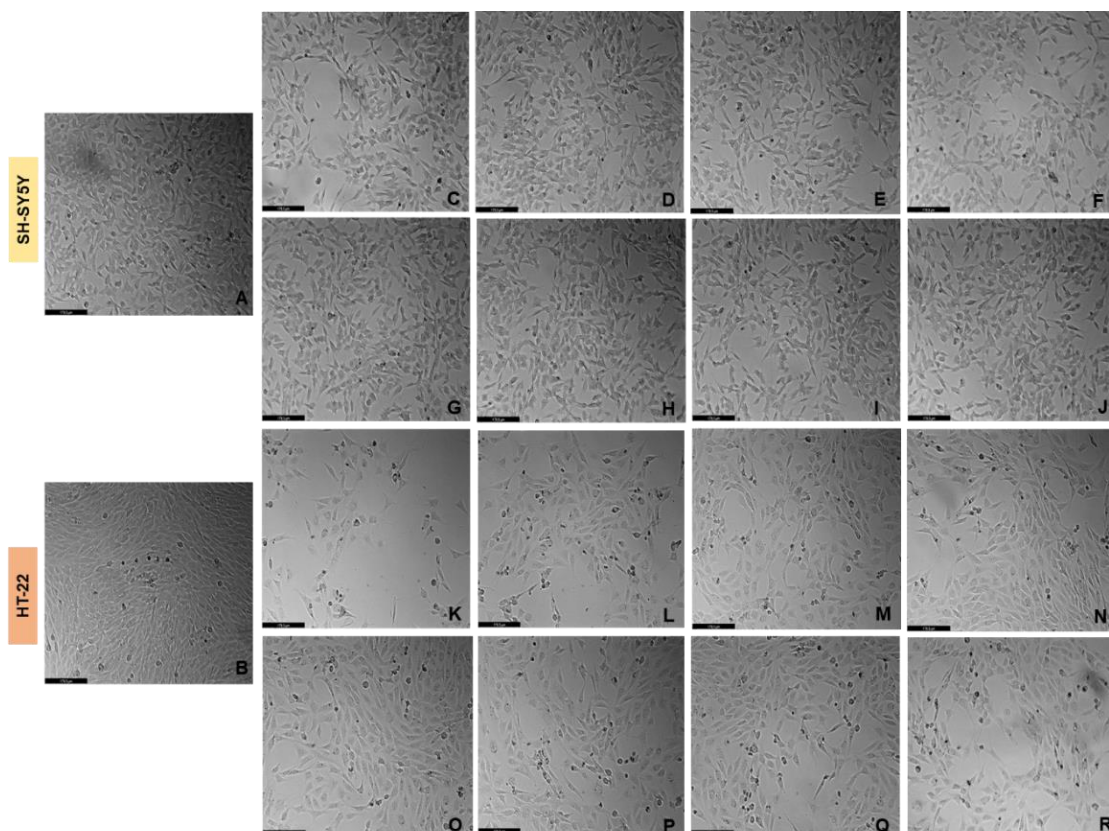


Figure 27. Representative images (100 × total magnification) of SH-SY5Y and HT-22 cells after incubation of corticosterone in combination with L-TRP. Cells were treated with (A,B) vehicle (0.1% DMSO / 1% H₂O), (C, K) corticosterone 322 μM and 35 μM , respectively, (D, L) L-TRP 0.1 nM + corticosterone 322 μM and L-TRP 0.1 nM + corticosterone 35 μM , respectively, (E, M) L-TRP 1 nM + corticosterone 322 μM and L-TRP 1 nM + corticosterone 35 μM , respectively, (F, N) L-TRP 10 nM + corticosterone 322 μM and L-TRP 10 nM + corticosterone 35 μM , respectively, (G, O) L-TRP 100 nM + corticosterone 322 μM and L-TRP 100 nM + corticosterone 35 μM , respectively, (H, P) L-TRP 1 μM + corticosterone 322 μM and L-TRP 1 μM + corticosterone 35 μM , respectively, (I, Q) L-TRP 10 μM + corticosterone 322 μM and L-TRP 10 μM + corticosterone 35 μM , respectively, (J, R) L-TRP 100 μM + corticosterone 322 μM and L-TRP 100 μM + corticosterone 35 μM , respectively. Scale bar: 179.3 μm .

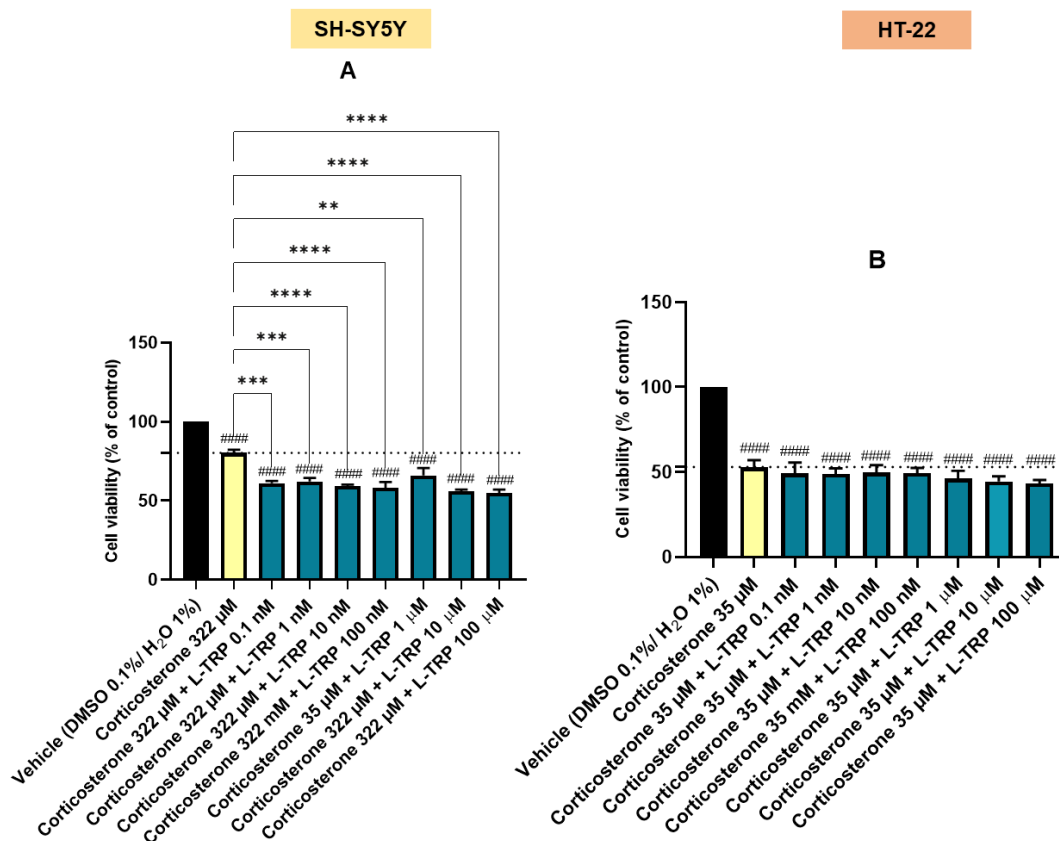


Figure 28. Effect of the incubation of (A) 322 µM of corticosterone and (B) 35 µM of corticosterone in combination with 0.1 nM–100 µM of L-TRP, determined by MTT methodology. The results represent the mean ± SEM of three independent experiments, expressed as the percentage of the vehicle (100%). Statistically significant ##### $p < 0.0001$ vs. vehicle, ** $p < 0.01$, *** $p < 0.001$, **** $p < 0.0001$ vs. corticosterone 322 µM.

These findings indicate that L-TRP was ineffective in mitigating the consequences of corticosterone exposure. In fact, when L-TRP was combined with corticosterone, it exacerbated the reduction in cell viability, particularly evident in SH-SY5Y cells, where the combination yielded a more pronounced decrease compared to corticosterone alone (Figures 27C-J and 28A). Similarly, in the case of HT-22 cells, L-TRP did not demonstrate any ability to counteract the cytotoxic effect of corticosterone exposure (Figures 27K-R, and 28B). However, it is worth noting that in HT-22 cells, the combination of L-TRP with corticosterone did not yield significantly different effects compared to corticosterone alone. These outcomes mirror the findings observed when mirtazapine was combined with corticosterone (Figure 22).

In summary, these results demonstrate that L-TRP did not possess the capacity to offset the deleterious effects of corticosterone on the cellular viability of both cell lines.

2.6. Effect of the Combination of Mirtazapine with Hydrogen Peroxide and Corticosterone on SH-SY5Y and HT-22 Reactive Oxygen Species Production

To further investigate the impact of the stimuli H_2O_2 and corticosterone, mirtazapine in isolation, and the effect of this drug in combination with the stimuli (Figure 29 and 30) on the production of ROS in SH-SY5Y and HT-22 cells, mirtazapine was applied to both cell lines at two distinct concentrations: 0.01 μM and 20 μM , representing the lower and upper extremes of concentrations tested in the previous cell viability studies. H_2O_2 was introduced to SH-SY5Y and HT-22 cells at fixed concentrations of 132 μM and 105 μM , respectively, corresponding to the mean IC_{50} values for both cell lines (Table 8). Corticosterone was added to SH-SY5Y cells at a concentration of 322 μM and to HT-22 cells at a concentration of 35 μM , again reflecting the mean IC_{50} values previously obtained. These compounds were incubated with the cells for periods of 1h, 3h, 6h, 24h, and 48h. The assessment of ROS production, relative to respective control groups, was conducted using the DCFDA assay. Briefly, this assay used DCFDA, a fluorogenic dye that diffuses into cells, where it is deacetylated by cellular esterases to a non-fluorescent compound. This compound is then oxidized by ROS into 2',7'-dichlorofluorescein (DCF), which is highly fluorescent. The fluorescence intensity of DCF indicates ROS levels [414].

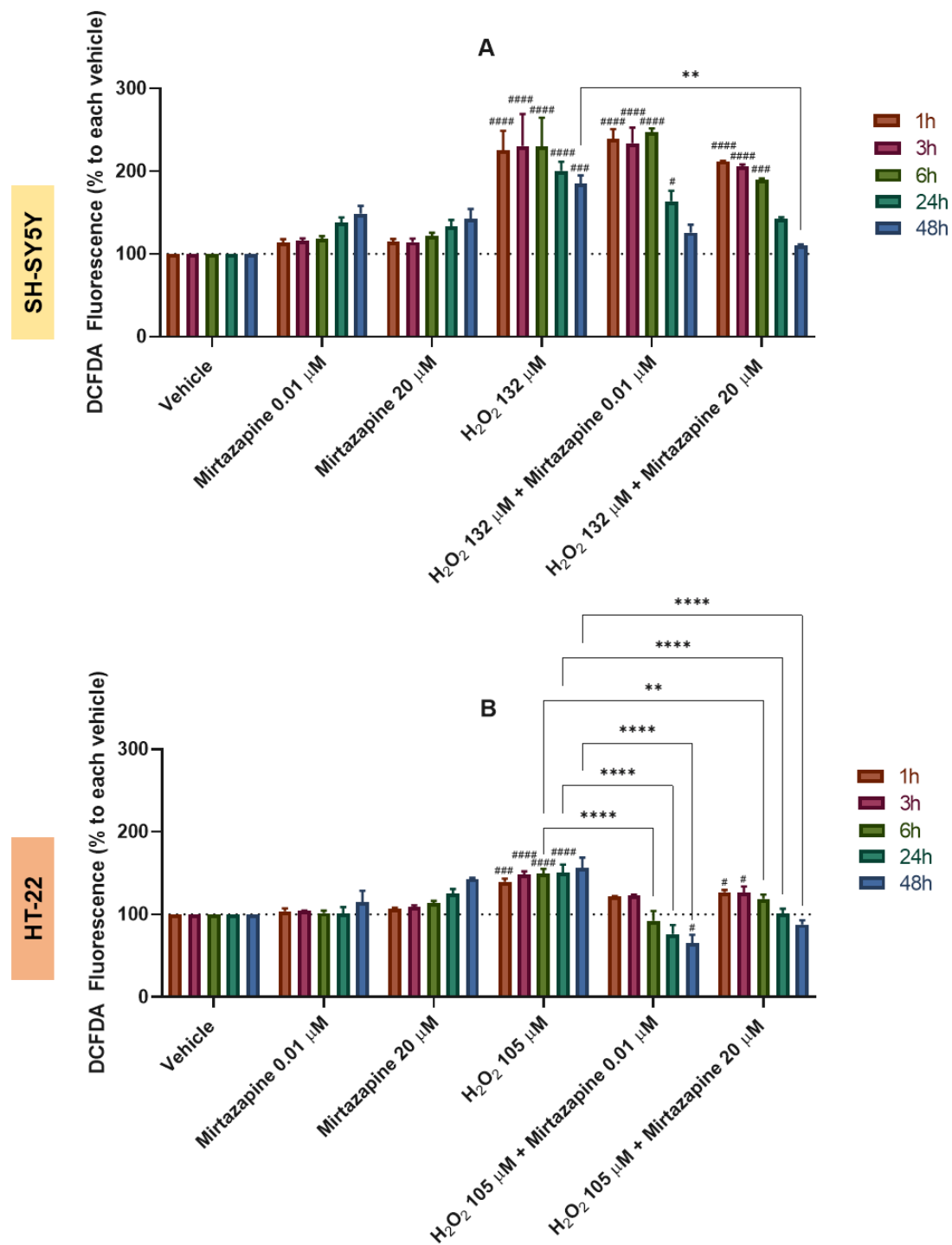


Figure 29. Effect on ROS production of 1h, 3h, 6h, 24h, and 48h-incubation of (A) 132 μM of H_2O_2 , 0.01 μM /20 μM of mirtazapine and 132 μM of H_2O_2 + 0.01 μM /20 μM of mirtazapine (SH-SY5Y cells) and (B) 105 μM of H_2O_2 , 0.01 μM /20 μM of mirtazapine and 105 μM of H_2O_2 + 0.01 μM /20 μM of mirtazapine (HT-22 cells), determined by DCFDA assay. The results are expressed as the percentage of each vehicle (100%) for each period (two-six independent experiments). Statistically significant # $p < 0.05$, ### $p < 0.001$, and #### $p < 0.0001$ vs. vehicle, for each time point, and * $p < 0.05$, ** $p < 0.01$, and **** $p < 0.0001$ vs. H_2O_2 132 μM (SH-SY5Y cells) and H_2O_2 105 μM (HT-22 cells).

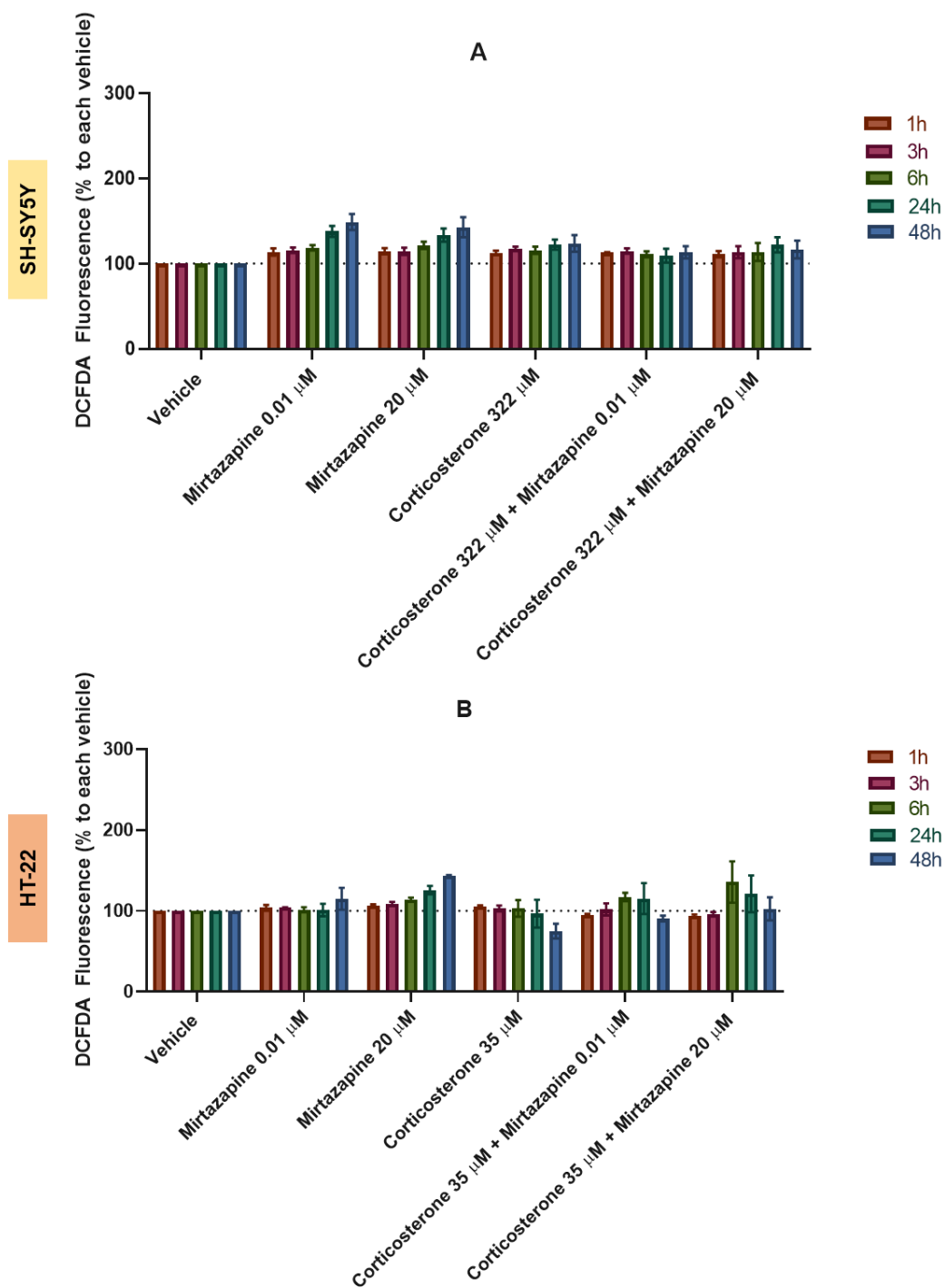


Figure 30. Effect on ROS production of 1h, 3h, 6h, 24h, and 48h-incubation of (A) 322 μ M of corticosterone, 0.01 μ M/20 μ M of mirtazapine and 322 μ M of corticosterone + 0.01 μ M/20 μ M of mirtazapine (SH-SY5Y cells) and (B) 35 μ M of corticosterone, 0.01 μ M/20 μ M of mirtazapine and 35 μ M of corticosterone + 0.01 μ M/20 μ M of mirtazapine (HT-22 cells), determined by DCFDA assay. The results are expressed as the percentage of each vehicle (100%) for each period (two-six independent experiments).

Analyzing the obtained results, several conclusions can be drawn. When mirtazapine was added in isolation, it elicited DCFDA fluorescence levels comparable to those of the vehicle control. However, especially notorious at 48h, in both concentrations, a slight increase in ROS production was observed for both cell lines.

The H₂O₂ stimulus resulted in a significant elevation in DCFDA fluorescence, indicating a marked increase in ROS production in both cell lines. This effect was even more marked on SH-SY5Y cells. Notably, in both cells, the combination of mirtazapine with H₂O₂ reduced DCFDA fluorescence when compared to H₂O₂ treatment alone, more significant in HT-22 cells (Figure 29). In HT-22 cells, it was noteworthy that both concentrations of mirtazapine appeared to be effective in reducing DCFDA fluorescence. On the other hand, in SH-SY5Y cells, the significant decrease in DCFDA fluorescence was observed only when the highest concentration of mirtazapine (20 µM) was combined with H₂O₂, specifically at the 48h time point (110.5%± 1.2% vs. 184.9%± 9.8% with H₂O₂ treatment alone).

Conversely, adding corticosterone alone or in combination with mirtazapine had little impact on DCFDA fluorescence levels in HT-22 and SH-SY5Y cells compared to the vehicle control group (Figure 30).

In summary, these findings collectively emphasize mirtazapine's capacity to mitigate ROS production and mitigate the impact of H₂O₂. It was evident that mirtazapine does not effectively counteract the effects of corticosterone, which do not appear to be associated with the induction of oxidative stress. This will be further explored in the discussion.

2.7. Effect of the Combination of L-Tryptophan with Hydrogen Peroxide and Corticosterone on SH-SY5Y and HT-22 Reactive Oxygen Species Production

Finally, to investigate the impact of the stimuli H₂O₂ and corticosterone, L-TRP in isolation, and the effect of this compound in combination with the stimuli (Figure 31 and 32) on the ROS levels in SH-SY5Y and HT-22 cells, L-TRP was applied to both cell lines at two distinct concentrations: 0.1 nM and 100 µM, representing the lower and upper extremes of concentrations tested in the cell viability studies. Similar to the study with mirtazapine, H₂O₂ was introduced to SH-SY5Y and HT-22 cells at fixed concentrations of 132 µM and 105 µM, respectively, and corticosterone was added to SH-SY5Y cells at a concentration of 322 µM and to HT-22 cells at a concentration of 35 µM. Again, these compounds were incubated with the cells for periods of 1h, 3h, 6h, 24h, and 48h. The

assessment of ROS production, relative to respective vehicle controls, was carried out using the DCFDA assay.

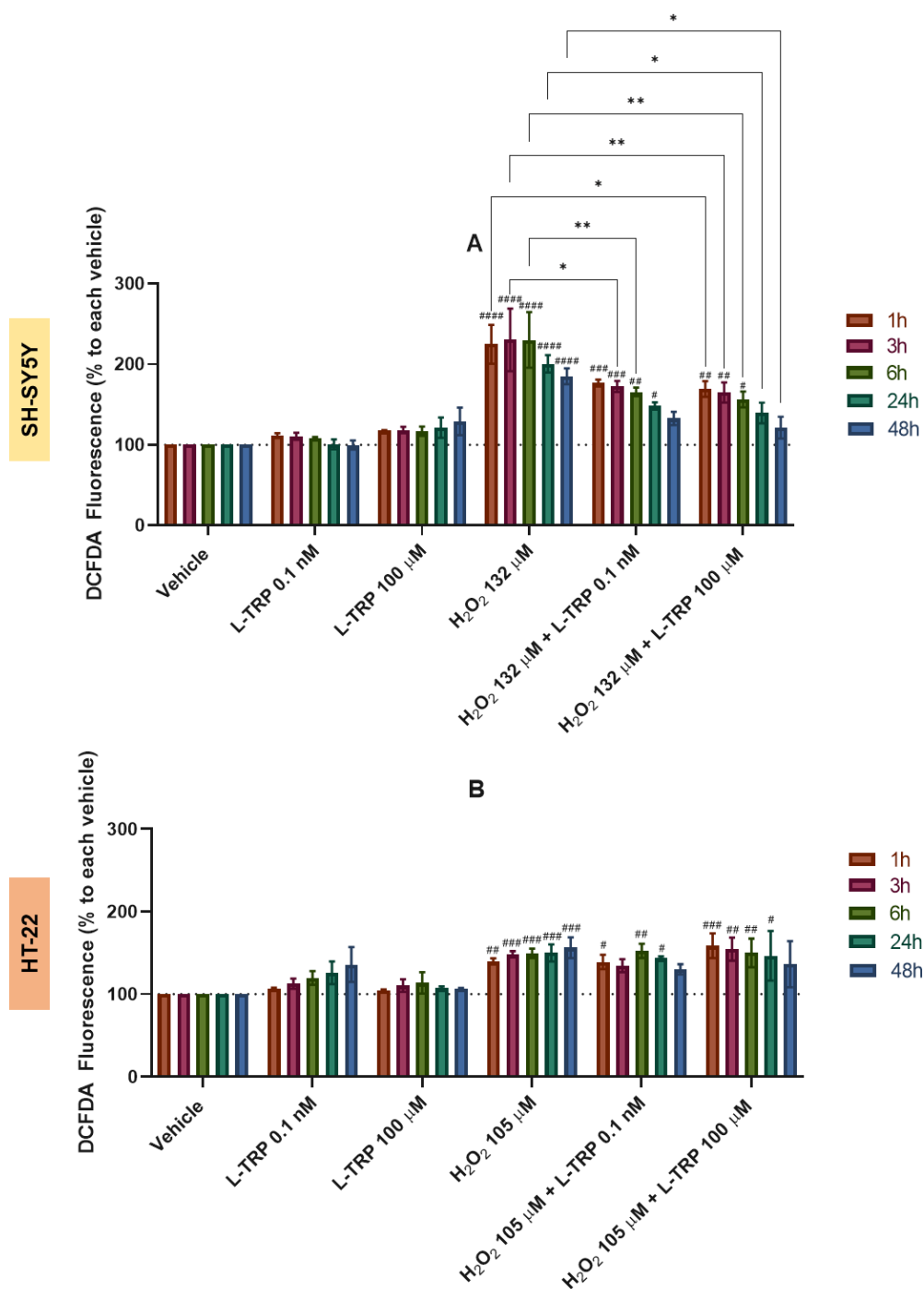


Figure 31. Effect on ROS production of 1h, 3h, 6h, 24h, and 4 h-incubation of (A) 132 μ M of H₂O₂, 0.01 μ M/100 μ M of L-TRP and 132 μ M of H₂O₂ + 0.1 nM/100 μ M of L-TRP (SH-SY5Y cells) and (B) 105 μ M of H₂O₂, 0.1 nM/100 μ M of L-TRP and 105 μ M of H₂O₂ + 0.1 nM/100 μ M of L-TRP (HT-22 cells), determined by DCFDA assay. The results are expressed as the percentage of each vehicle (100%) for each period (two-six independent experiments). Statistically significant # $p < 0.05$, ## $p < 0.01$, ### $p < 0.001$, and #### $p < 0.0001$ vs. vehicle, for each time point, and * $p < 0.05$, ** $p < 0.01$ vs. H₂O₂ 132 μ M.

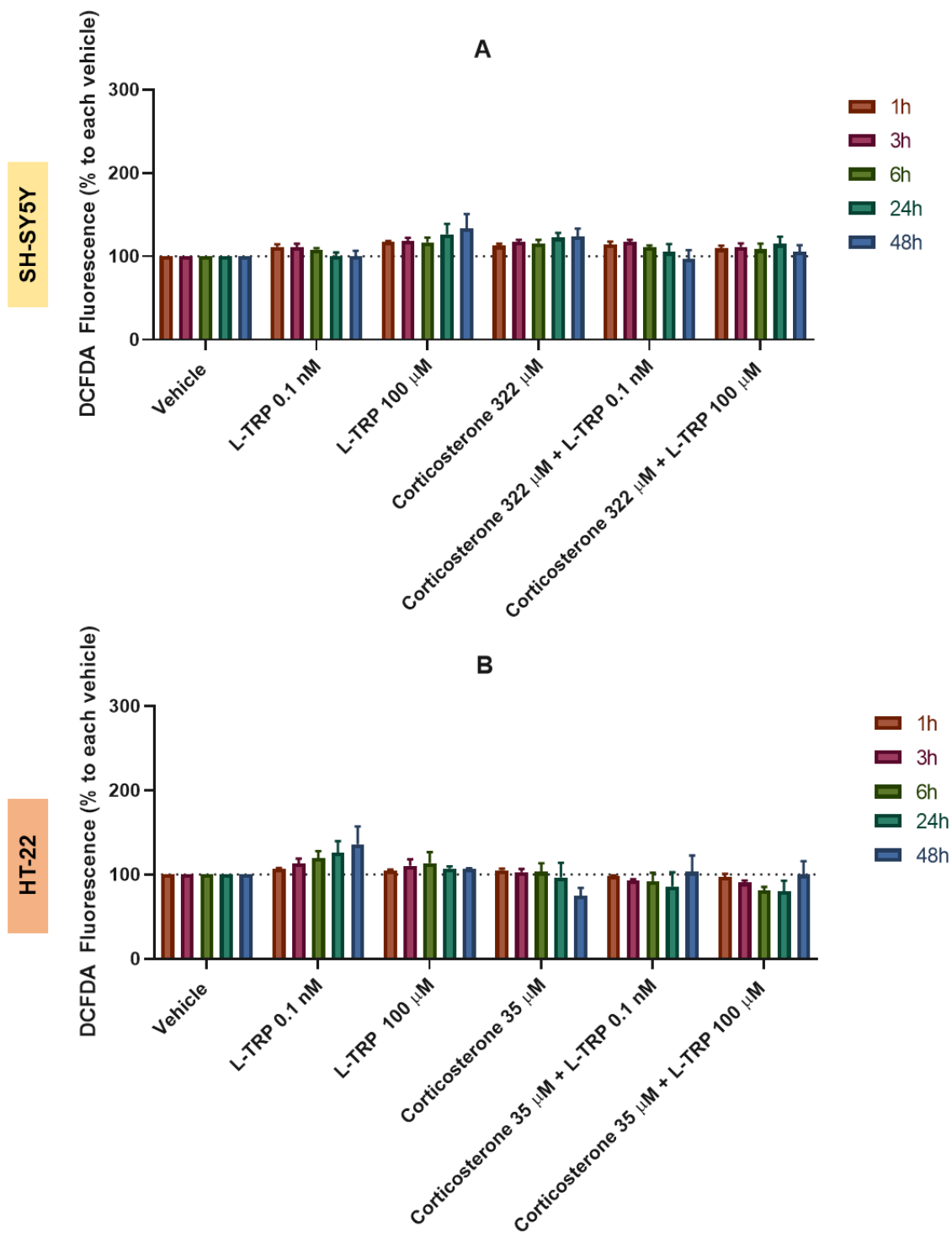


Figure 32. Effect on ROS production of 1h, 3h, 6h, 24h, and 48 h-incubation of (A) 322 μM of corticosterone, 0.1 nM/100 μM of L-TRP and 322 μM of corticosterone + 0.1 nM/100 μM of L-TRP (SH-SY5Y cells) and (B) 35 μM of corticosterone, 0.1 nM/100 μM of L-TRP and 35 μM of corticosterone + 0.1 μM/100 μM of L-TRP (HT-22 cells), determined by DCFDA assay. The results are expressed as the percentage of each vehicle (100%) for each period (two-six independent experiments).

These findings demonstrate that overall, L-TRP alone did not significantly change ROS levels, compared to the control group, for all time points. Especially in SH-SY5Y cells, the combination of L-TRP with H₂O₂ resulted in a reduction in DCFDA fluorescence compared to H₂O₂ treatment alone, in both concentrations of L-TRP, but more markedly with L-TRP 100 μM (121.3%± 13.5% vs. 184.9%± 9.8% with H₂O₂ treatment alone, at 48h; Figure 31A). These results underscore the effectiveness of L-TRP in mitigating the effects of H₂O₂, which aligns with the findings from the cell viability assays (Figure 26A). For HT-22 cells, this effect was less pronounced, although there was a discernible trend of L-TRP reducing DCFDA fluorescence when combined with H₂O₂ (Figure 31B). Once more, these outcomes are in accordance with the viability studies (Figure 26), wherein L-TRP did not exhibit the same level of effectiveness in enhancing cell viability in HT-22 cells as it did in SH-SY5Y cells when H₂O₂ was present.

Conversely, in both cells, the combination of L-TRP with corticosterone did not induce significant changes in DCFDA fluorescence levels, similar to what was observed in Figure 30.

In summary, these results collectively emphasize that L-TRP holds potential as a compound for attenuating the effects of H₂O₂-induced oxidative stress but may not be as effective in counteracting the effects of corticosterone. Figure 33 summarizes the main conclusions of these results presented in part 2.

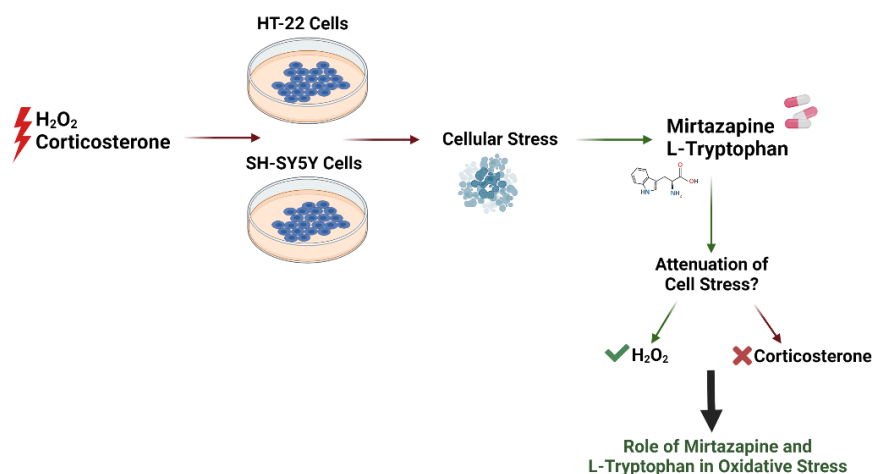


Figure 33. Schematic illustration of the main findings of this work. In sum, our main findings evidence that both mirtazapine and L-TRP can counteract the harmful effects caused by H₂O₂ but not by corticosterone, revealing that these agents may have an important protective role in oxidative stress. Created with Biorender [17].

3. Assessing the DNA Integrity of SH-SY5Y Cells Following Exposure to Stress-Inducing Agents and Mirtazapine

This part is dedicated to the exploration of the interplay between H_2O_2 and mirtazapine, focusing on assessing DNA damage using the alkaline comet assay. Furthermore, the effect on DNA damage after exposing cells to hydrocortisone was also explored. Briefly, the comet assay, also known as single cell gel electrophoresis, is a technique for evaluating DNA damage at the level of individual cells. It detects breaks in DNA strands, which are visualized under a microscope as a comet with a distinct head (intact DNA) and tail (damaged or fragmented DNA), being widely used for assessing the impact of various agents on DNA integrity [415]. Figure 34 visually represents the underlying hypothesis of this study. To conduct this study, only SH-SY5Y cells were used.

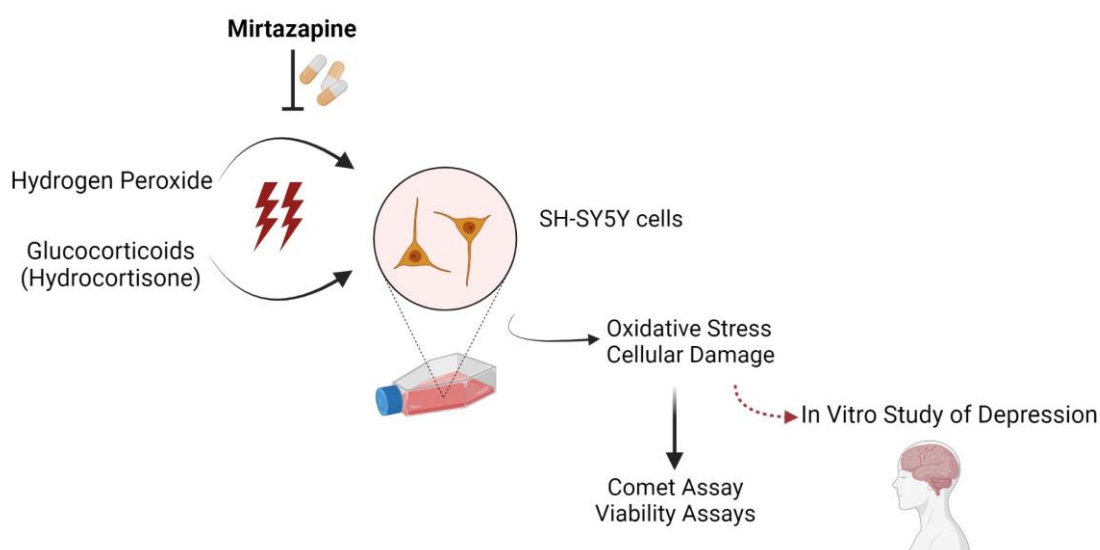


Figure 34. In this study, to explore an in vitro model of depression in SH-SY5Y cells, two stress inducers (H_2O_2 and glucocorticoids, namely hydrocortisone) were used, and the mirtazapine effectiveness against the induced oxidative stress was tested. Created with Biorender [17].

3.1. Effect of Hydrocortisone, Hydrogen Peroxide, Mirtazapine, and the Combination of Mirtazapine with Hydrogen Peroxide on DNA integrity

In the Figure 20, it was demonstrated that mirtazapine consistently counteracted the decrease in cell viability induced by H₂O₂, regardless of the concentrations tested. Additionally, it was also notorious the mirtazapine's potential as an effective agent for mitigating the ROS levels in SH-SY5Y cells, especially the concentration of 20 μM (Figure 29A).

To explore the role of these compounds on DNA damage, H₂O₂ stimulus was added to the cells in increasing concentrations, for 48h (10 – 200 μM). For mirtazapine, the testing was limited to the two extreme concentrations previously examined (0.01 μM and 20 μM). Following the incubation period, the extent of DNA damage (% tail intensity) was assessed in each cell using the alkaline comet assay. Additionally, hydrocortisone was introduced to the cells in incremental concentrations for a 48h period (50 – 300 μM), also with the goal of quantifying the percentage of DNA damage, to better understand how this glucocorticoid works. MMS, an alkylating agent, was used as a positive control.

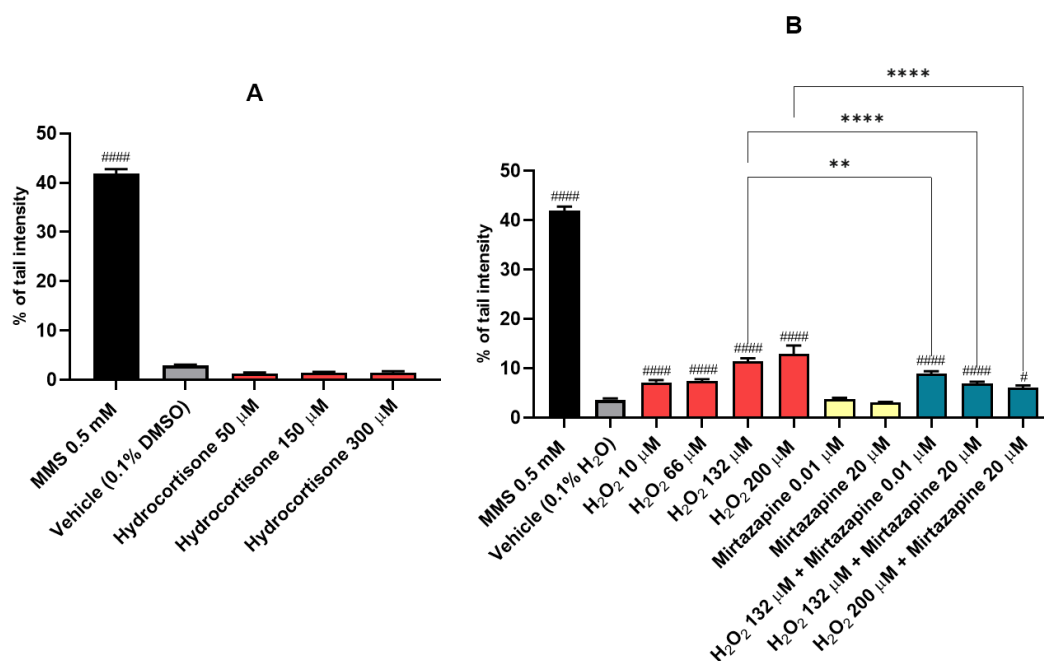


Figure 35. Effect of (A) hydrocortisone, and (B) H₂O₂, mirtazapine and the combination of mirtazapine with H₂O₂ on the DNA integrity of SH-SY5Y cells, assessed by the alkaline comet assay. The results are expressed as the percentage of the tail intensity and represent the mean ± SEM of three independent experiments. Statistically significant # p < 0.05 and #### p < 0.0001 vs. vehicle, and ** p < 0.01 and **** p < 0.0001 vs. H₂O₂ (single agent, in the concentration exposed in each combination with mirtazapine).

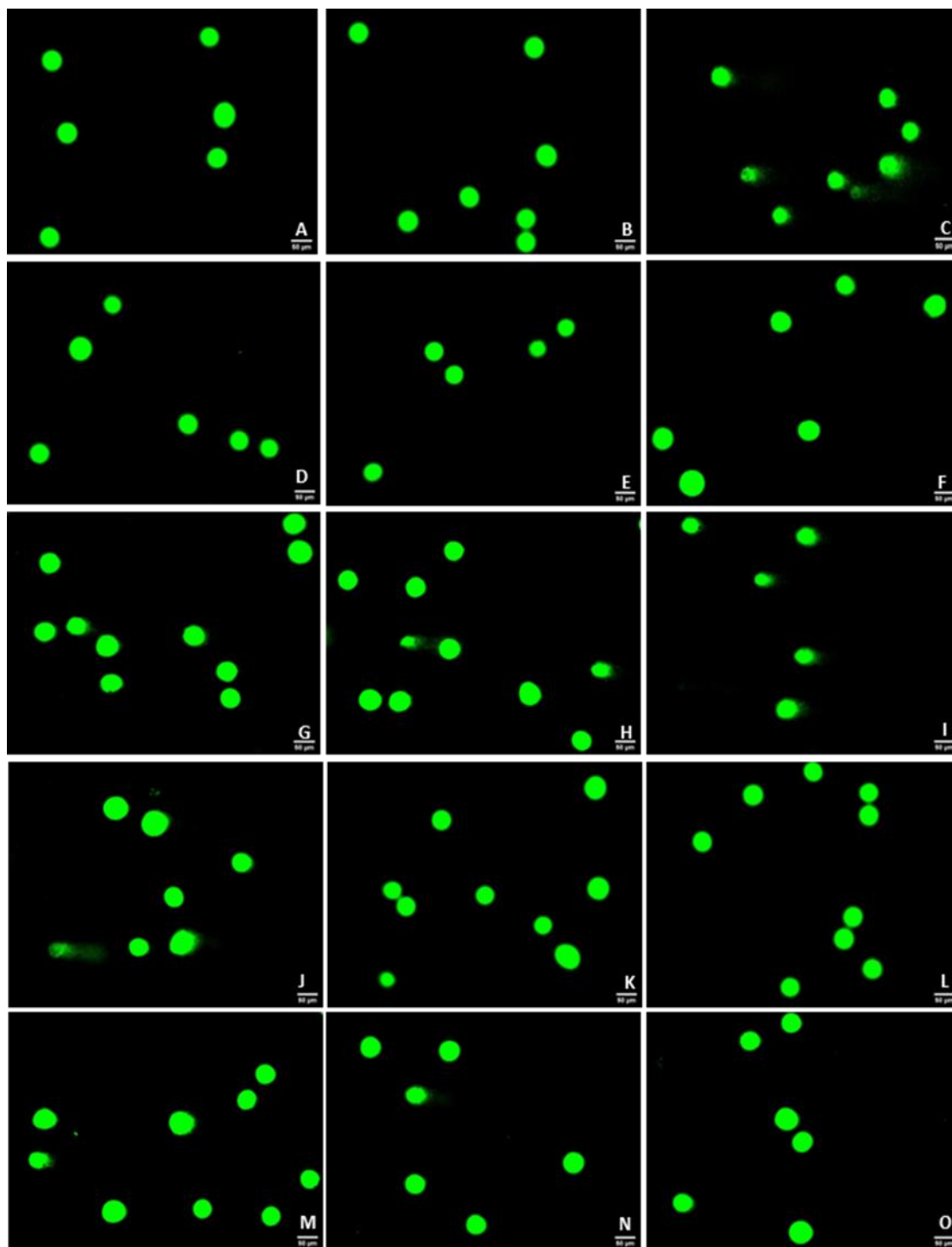


Figure 36. Representative images (total magnification 200x) of SH-SY5Y cells after application of increasing concentrations of hydrocortisone, H₂O₂, mirtazapine, and the combination of mirtazapine with hydrogen peroxide. These cells were stained with SYBR Gold, as described in the materials and methods section. Cells were treated with (A) vehicle (0.1% H₂O), (B) vehicle (0.1% DMSO), (C) MMS 0.5 mM (positive control), (D) hydrocortisone 50 µM, (E) hydrocortisone 100 µM, (F) hydrocortisone 150 µM, (G) H₂O₂ 10 µM, (H) H₂O₂ 66 µM, (I) H₂O₂ 132 µM, (J) H₂O₂ 200 µM, (K) mirtazapine 0.01 µM (L) mirtazapine 20 µM, (M) H₂O₂ 132 µM + mirtazapine 0.01 µM, (N) H₂O₂ 132 µM + mirtazapine 20 µM, and (O) H₂O₂ 200 µM + mirtazapine 20 µM. Scale bar: 50 µm.

The obtained results with hydrocortisone (Figure 35A and 36D-F) are aligned with the previously obtained results with this glucocorticoid, revealing that this agent does not affect DNA integrity of the cells. However, regarding H₂O₂, our results revealed that this compound led to higher levels of DNA damage in comparison with the vehicle-treated group, in a concentration-dependent manner (Figure 35B). Indeed, more pronounced comet tails can be observed in the cells, representing more DNA damage (Figure 35G-J), being consistent with previously obtained results on cell viability. Additionally, mirtazapine did not lead to significant DNA damage, presenting similar values with the vehicle-treated group (Figure 35B and 36K,L), consistent with the previous results regarding the protective effects of mirtazapine.

Regarding the combination of mirtazapine with H₂O₂, these findings validate that mirtazapine effectively attenuated DNA damage induced by both H₂O₂ concentrations of 132 μM and 200 μM (Figures 35B and 36M-O). In fact, we also explored whether mirtazapine could even reverse DNA damage caused by high a H₂O₂ concentration (200 μM) surpassing the IC₅₀ value (132 μM). Notably, when the lower and higher concentrations of mirtazapine were combined with H₂O₂ at 132 μM, the resulting tail intensity values were 8.9% ± 0.5% and 6.9% ± 0.4%, respectively, as compared to 11.4% ± 0.6% for H₂O₂ alone at 132 μM. Similarly, the combination of the higher mirtazapine concentration with H₂O₂ at 200 μM yielded a tail intensity value of 6.1% ± 0.5%, in contrast to 12.9% ± 1.7% for H₂O₂ alone at 200 μM.

These observations highlight the significant DNA-protective effects of mirtazapine in the presence of high oxidative stress levels.

4. Investigating Drugs that Modulate Serotonin Type 3 Receptors in Hydrogen Peroxide and Corticosterone-Induced Cellular Stress

The previous results clearly indicate that the exposure to high levels of oxidative stress (H₂O₂) induces cytotoxicity, observed by high levels of ROS production, DNA damage and overall loss of cell viability. On the other hand, the exposure of cells to mirtazapine induces cytoprotective effects that could counteract these effects produced by H₂O₂, but not from corticosterone, that also led to overall loss of cell viability, not reflected by high levels of ROS production.

In this part, we aimed to conduct a preliminary study about the potential role of drugs that interact with the 5-HT₃ receptor (mirtazapine, scopolamine, and lamotrigine, explored in more detail in the discussion and already mentioned in the introduction) in the modulation of H₂O₂/ corticosterone-induced stress to HT-22 and SH-SY5Y cells, mainly by using cell morphology, cell viability and HPLC assays. Briefly, while there is

evidence suggesting a potential link between 5-HT₃ receptors (particularly antagonists) and depression, the precise role of these receptors in the development and treatment of depression is still a subject of ongoing research.

4.1. Presence of Serotonin Type 3 Receptors in SH-SY5Y cells and HT-22 cells

Before subjecting the cells to drug testing, immunofluorescence experiments were conducted on both SH-SY5Y, and HT-22 cell lines to validate the presence of the 5-HT₃ receptor in these cells (Figure 37).

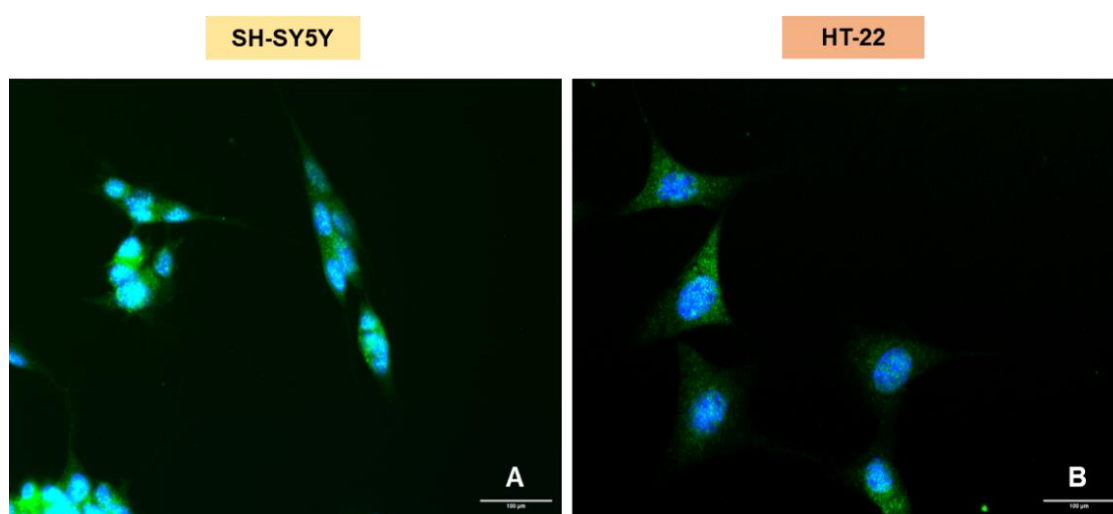


Figure 37. Representative images (400× total magnification) of (A) SH-SY5Y cells and (B) HT-22 cells after immunostaining with DAPI (stains nuclei, blue) and primary antibody rabbit polyclonal anti-5-HT_{3A}/ donkey anti-rabbit 488 secondary antibody (green), as previously described in the materials and methods section. Scale bar: 100 µm.

These findings provide evidence of the presence of the 5-HT₃ receptor, presented in green, in both HT-22 and SH-SY5Y cell lines. This reinforces the receptor's presence across these specific cell types, supporting its potential roles and significance in these cellular functions and pathways.

4.2. Effect of Scopolamine and Lamotrigine on SH-SY5Y and HT-22 Cell Viability

To investigate the impact of scopolamine (Figures 38C-G, M-Q, and 39) and lamotrigine (Figures 38H-L, R-V, and 40) on cellular viability, these drugs were introduced to SH-SY5Y cells and HT-22 cells for 48h, using a range of concentrations spanning from 0.01 µM to 20 µM. The evaluation of the results encompassed the use of both MTT and

NR assays, complemented by the morphological analysis of both cell lines. It is worth noting that earlier, as illustrated in Figures 9 and 10, this study was performed with mirtazapine, which holds significance within the context of this study due to its interaction with the 5-HT₃ receptor.

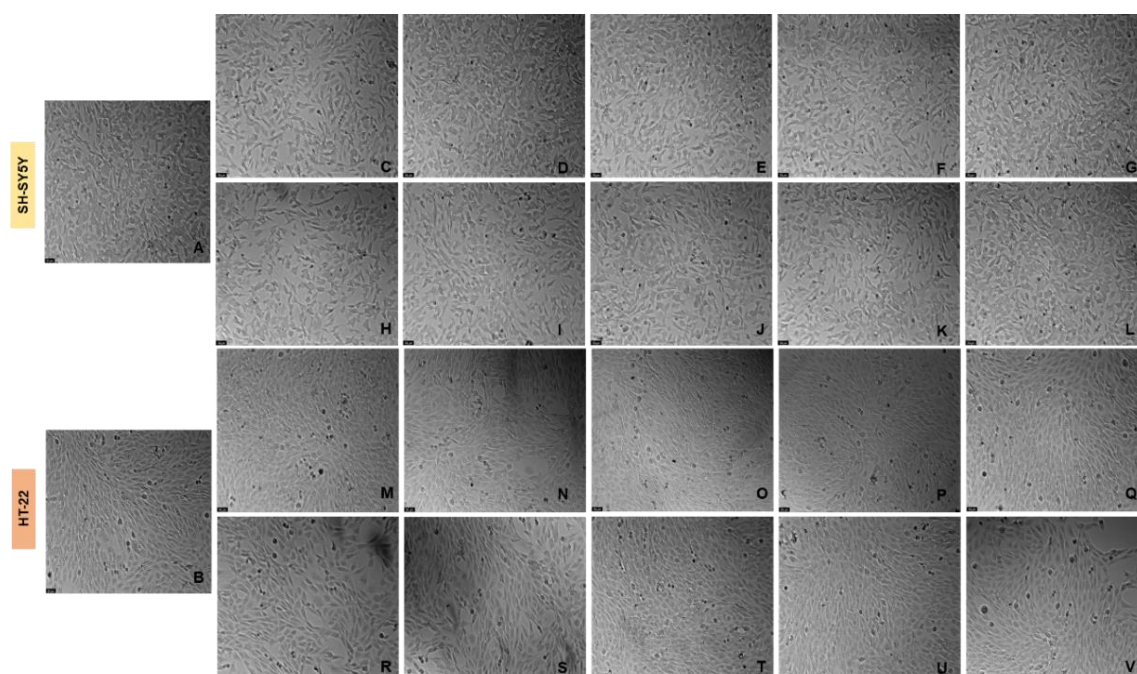


Figure 38. Representative images (100 × total magnification) of SH-SY5Y and HT-22 cells after incubation of (A,B) vehicle (0.1% DMSO), (C, M) scopolamine 0.01 μM, (D, N) scopolamine 0.1 μM, (E, O) scopolamine 1 μM, (F, P) scopolamine 10 μM, (G, Q) scopolamine 20 μM, (H, R) lamotrigine 0.01 μM, (I, S) lamotrigine 0.1 μM, (J, T) lamotrigine 1 μM, (K, U) lamotrigine 10 μM, (L, V) lamotrigine 20 μM. Scale bar: 50 μm.

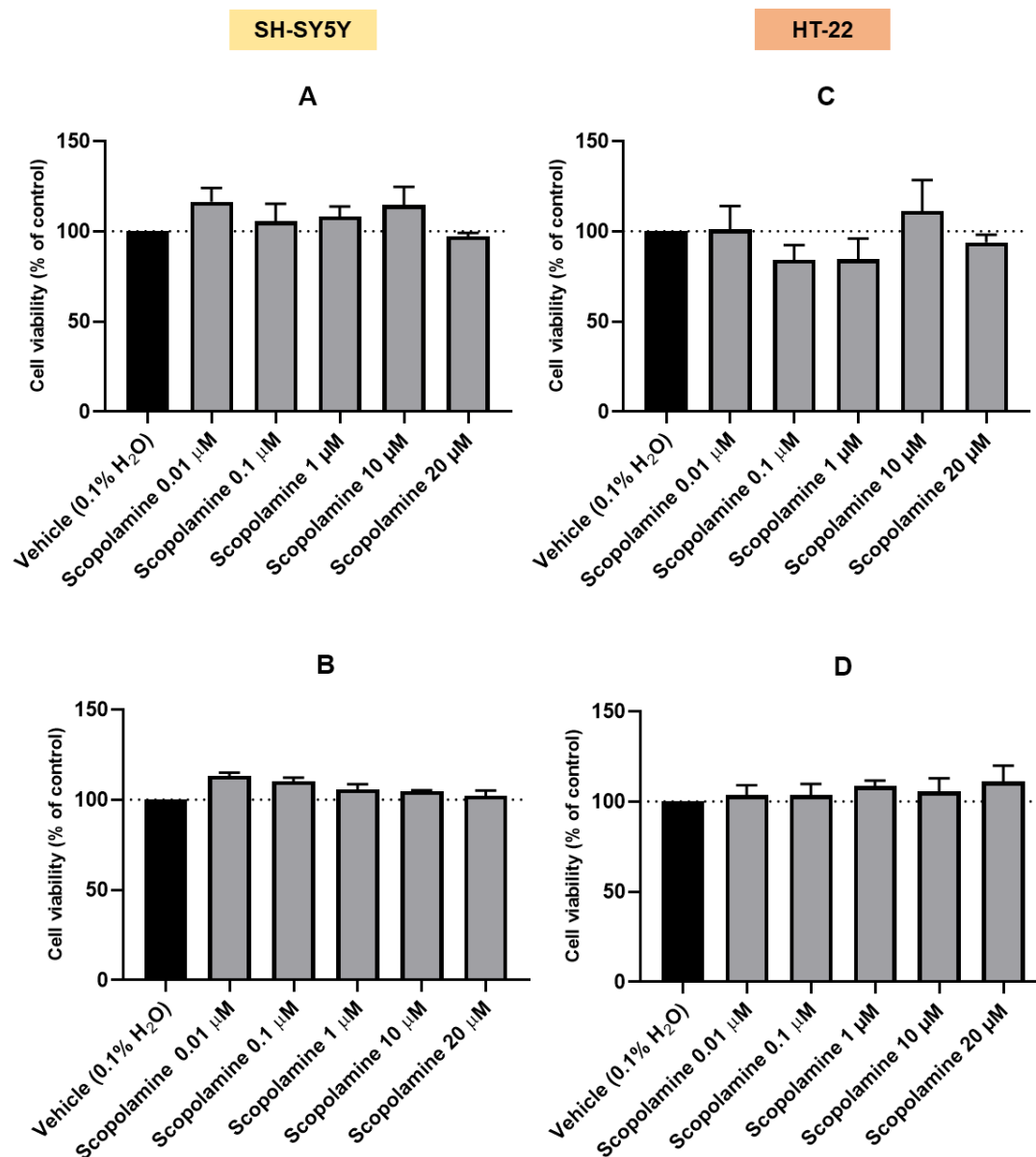


Figure 39. Effect of increasing concentrations of scopolamine on the viability of SH-SY5Y and HT-22 cells, obtained by (A, C) MTT and (B, D) NR assays. The results are expressed as the percentage of the vehicle and represent the mean \pm SEM of three independent experiments.

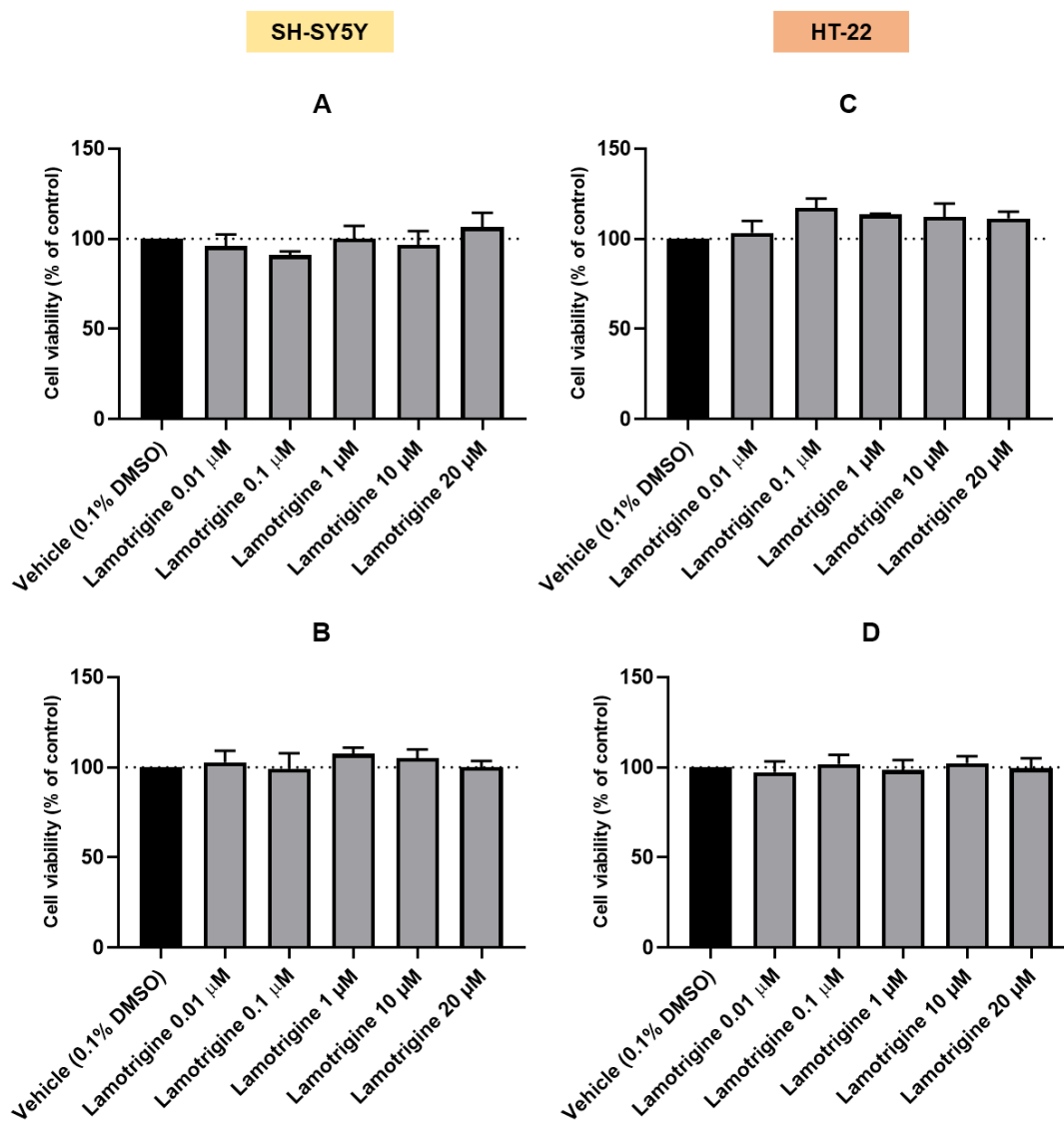


Figure 40. Effect of increasing concentrations of lamotrigine on the viability of SH-SY5Y and HT-22 cells, obtained by (A, C) MTT and (B, D) NR assays. The results are expressed as the percentage of vehicle and represent the mean \pm SEM of three independent experiments.

These findings demonstrate that such as mirtazapine (Figures 9 and 10), scopolamine and lamotrigine demonstrated non-toxicity across all tested concentrations, displaying the potential to effectively modulate cellular stress in both SH-SY5Y and HT-22 cell lines.

Collectively, these results provide compelling evidence that these drugs do not compromise cell viability in either cell line, as substantiated by both viability and morphological assessments, being suitable for further tests in combination with stress inducers.

4.3. Effect of Mirtazapine, Scopolamine and Lamotrigine in Combination with Hydrogen Peroxide and Corticosterone on SH-SY5Y and HT-22 Cell Viability

To investigate the impact of scopolamine and lamotrigine in combination with H₂O₂ (Figures 41B-D, J-L, and 42A, C) and corticosterone (Figures 41F-H, N-P, and 42B, D) on cellular viability, these drug combinations were applied to SH-SY5Y cells and HT-22 cells for 48h. Following this incubation period, a morphological assessment was conducted, and the cellular viability was determined using MTT assay. Scopolamine and lamotrigine were introduced to the cellular cultures at a concentration of 20 µM (the highest concentrations previously tested). H₂O₂ was applied to SH-SY5Y cells at a concentration of 132 µM and to HT-22 cells at a concentration of 105 µM, both of which corresponded to the mean IC₅₀ values for the respective cell lines, as already mentioned (Table 8). Similarly, corticosterone was applied to the cells at concentrations 322 µM (for SH-SY5Y cells) and 35 µM (for HT-22 cells). Again, it is worth noting that earlier, as detailed in Figures 21 and 22, this study was performed with mirtazapine. However, for the purposes of this specific analysis, the study was repeated with mirtazapine at a concentration of 20 µM.

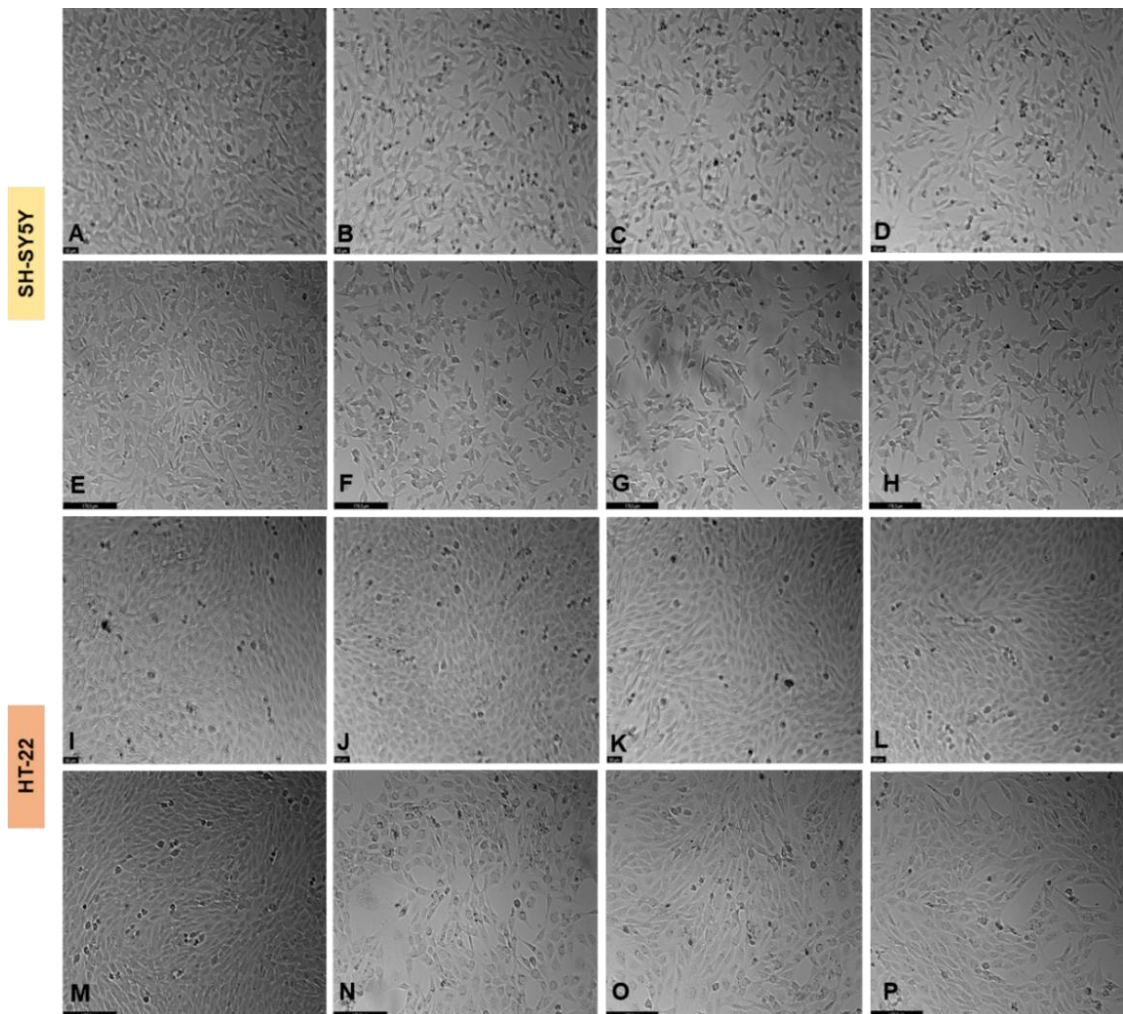


Figure 41. Representative images (100 × total magnification) of SH-SY5Y and HT-22 cells after incubation of H₂O₂ and corticosterone in combination with mirtazapine, scopolamine, and lamotrigine. Cells were treated with (A,I) vehicle (0.1% H₂O /0.1% DMSO), (B,J) H₂O₂ 132 μM (for SH-SY5Y cells) and H₂O₂ 105 μM (for HT-22 cells) + mirtazapine 20 μM, (C, K) H₂O₂ 132 μM (for SH-SY5Y cells) and H₂O₂ 105 μM (for HT-22 cells) + scopolamine 20 μM, (D, L) H₂O₂ 132 μM (for SH-SY5Y cells) and H₂O₂ 105 μM (for HT-22 cells) + lamotrigine 20 μM, (E, M) vehicle (0.1% DMSO), (F, N) corticosterone 322 μM (for SH-SY5Y cells) and corticosterone 35 μM (for HT-22 cells) + mirtazapine 20 μM, (G, O) corticosterone 322 μM (for SH-SY5Y cells) and corticosterone 35 μM (for HT-22 cells) + scopolamine 20 μM, (H, P) corticosterone 322 μM (for SH-SY5Y cells) and corticosterone 35 μM (for HT-22 cells) + lamotrigine 20 μM. Scale bar: 50 μm and 179.3 μm.

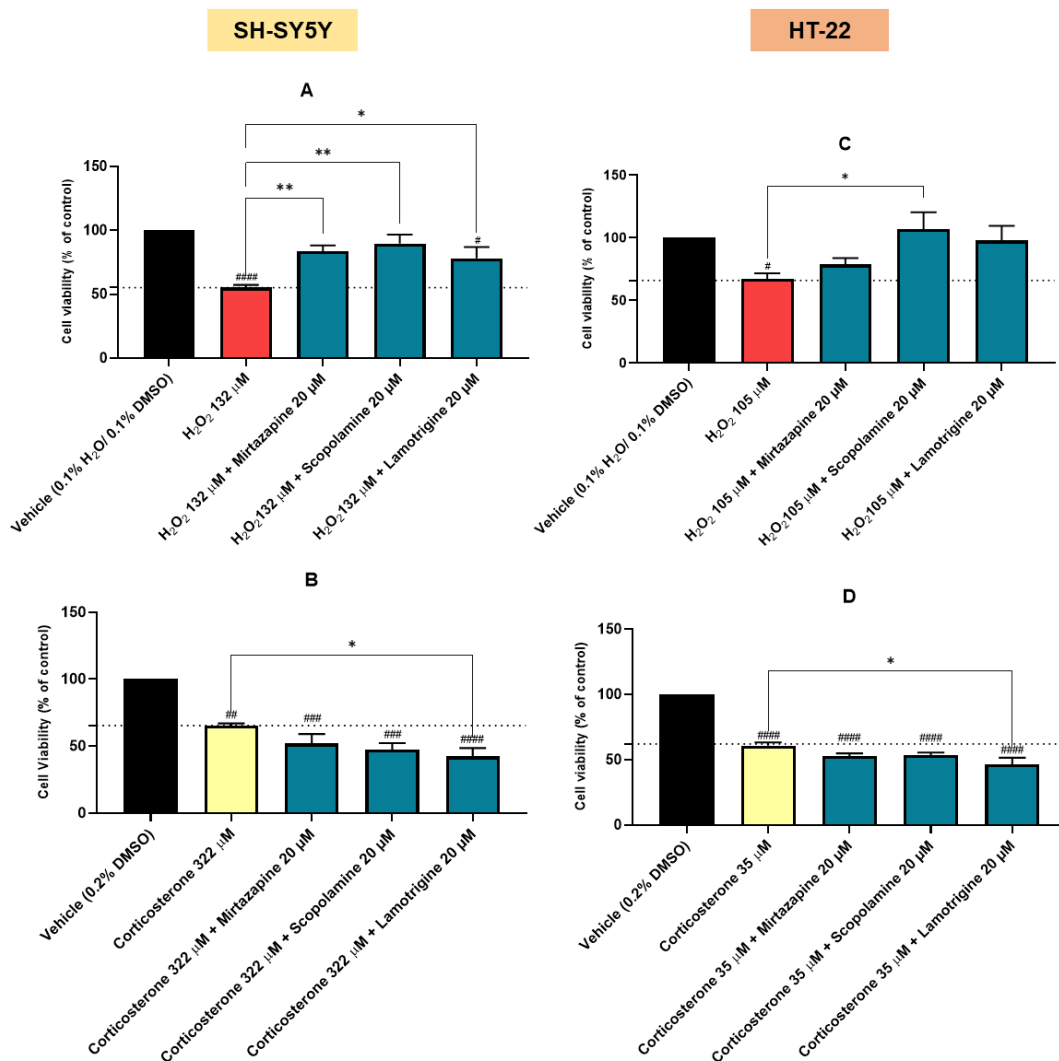


Figure 42. Effect of the incubation of (A) 132 μM of H₂O₂ and (C) 105 μM of H₂O₂, in combination with 20 μM of mirtazapine, scopolamine and lamotrigine, (B) 322 μM of corticosterone and (D) 35 μM of corticosterone, in combination with 20 μM of mirtazapine, scopolamine and lamotrigine, determined by MTT methodology. The results represent the mean ± SEM of three-six independent experiments, expressed as the percentage of the vehicle (100%). Statistically significant # p < 0.05, ## p < 0.01, ### p < 0.001, ##### p < 0.0001 vs. vehicle, and * p < 0.05, ** p < 0.01 vs. H₂O₂ 132 μM, H₂O₂ 105 μM, corticosterone 322 μM, or corticosterone 35 μM.

Our findings provide compelling evidence demonstrating the capacity of mirtazapine, scopolamine, and lamotrigine to significantly mitigate the deleterious effects of H₂O₂-induced stress in SH-SY5Y cells. Notably, scopolamine exhibited the most pronounced enhancement in cell viability, with a substantial increase to 89.6% ± 7.1% as compared to 55.2% ± 2.1% viability observed under H₂O₂ exposure alone (Figures 41C and 42A). Furthermore, the protective effect of scopolamine extended to HT-22 cells, where this drug, again, displayed the highest viability values, reaching 107.1% ± 13.4% in contrast to the 66.9% ± 4.8% viability observed in the absence of scopolamine

(Figures 41K and 42C). While mirtazapine and lamotrigine exhibited a discernible trend towards ameliorating H₂O₂-induced stress in HT-22 cells, these effects did not reach statistical significance (Figures 41B,D, J, L and 42C).

In contrast, these results revealed that mirtazapine, scopolamine, and lamotrigine failed to mitigate the stress imposed by corticosterone treatment in both HT-22 and SH-SY5Y cells (Figures 41F-H, N-P and 42B,D). In fact, these compounds yielded viability values similar to those observed under corticosterone-induced stress alone, with lamotrigine even exacerbating the cytotoxic effects. Specifically, in SH-SY5Y cells, lamotrigine led to a reduction in viability to 42.3% ± 6.1%, in contrast to the 65.3% ± 1.6% viability observed with corticosterone treatment alone. Similarly, in HT-22 cells, lamotrigine led to a diminished viability of 46.3% ± 5.1%, a significant decrease from the 60.8% ± 2.4% viability observed in the absence of lamotrigine.

These findings underscore the differential impact of mirtazapine, scopolamine, and lamotrigine on cellular stress responses, particularly in the context of cellular stress induced by H₂O₂ and corticosterone.

4.4. Effect of Mirtazapine, Scopolamine and Lamotrigine in Combination with Hydrogen Peroxide and Corticosterone on Extracellular Serotonin Levels

Aiming to investigate the modulatory effects of the studied pharmaceutical agents and their combinations with H₂O₂ and corticosterone stimuli on the extracellular levels of 5-HT, a neurotransmitter highly connected with the pathophysiology of depression, the effect of these drugs and drug combinations in the extracellular 5-HT levels of SH-SY5Y and HT-22 cells was explored (Figures 43 and 44). The quantification of 5-HT concentrations was performed using electrochemical detection coupled with high-performance liquid chromatography (ECD-HPLC), following a 48h incubation period with the respective treatments. Briefly, ECD is a highly selective and sensitive technique used in HPLC for analyzing a variety of compounds, including neurotransmitters. ECD functions by detecting the electrical current that correlates to the concentration of analytes in the HPLC system [416].

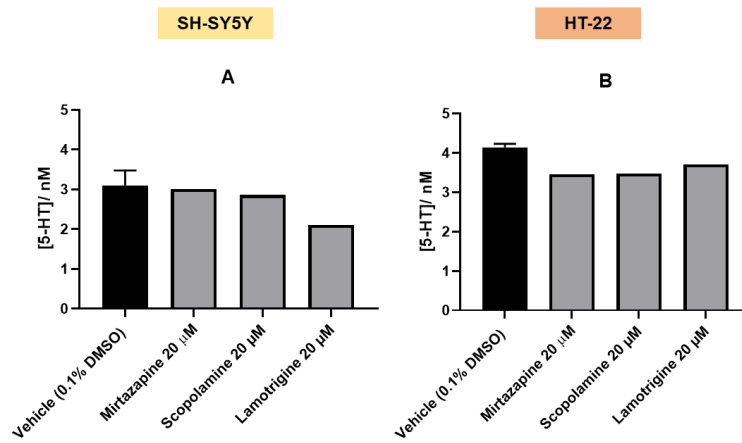


Figure 43. Concentrations of 5-HT (nM) in the extracellular medium of mirtazapine, scopolamine, and lamotrigine-treated SH-SY5Y and HT-22 cells, determined by ECD-HPLC. Results are derived from the analysis of the extracellular medium across a minimum of three separate and independently conducted experiments.

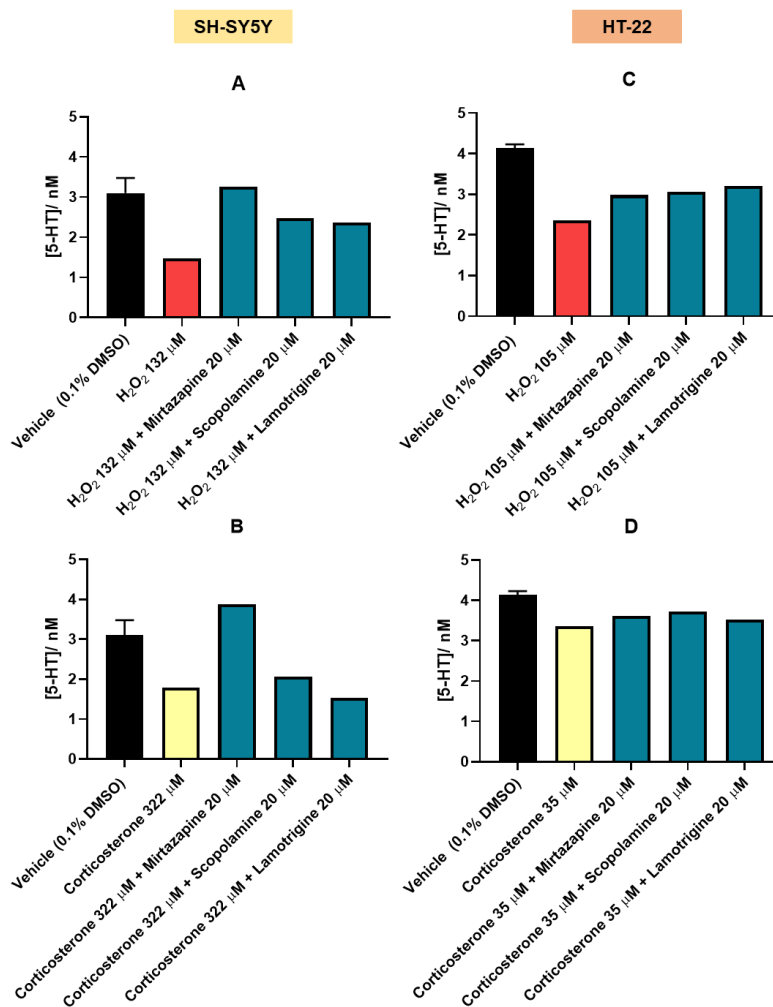


Figure 44. Concentrations of 5-HT (nM) in the extracellular medium of SH-SY5Y and HT-22 cells, treated with corticosterone, H₂O₂, and their combinations with mirtazapine, scopolamine, and lamotrigine

determined by ECD-HPLC. Results are derived from the analysis of the extracellular medium across a minimum of three separate and independently conducted experiments.

Upon analyzing the results, it is possible to conclude that the extracellular concentration of 5-HT did not exhibit significant variations when mirtazapine, scopolamine, and lamotrigine were individually applied to both cell types (Figure 43). However, in SH-SY5Y cells, lamotrigine appeared to cause a reduction in 5-HT concentration (2.1 nM) compared to the cells treated with the vehicle (3.1 nM) (Figure 43A).

Regarding the results involving the combination of these drugs with H₂O₂ stimulus in SH-SY5Y cells (Figure 44A), it was apparent that mirtazapine, scopolamine, and lamotrigine increased extracellular 5-HT levels when compared to cells treated with H₂O₂ alone (1.5 nM). Notably, mirtazapine produced the most substantial increase in 5-HT levels when combined with H₂O₂, reaching 3.3 nM. In contrast, in HT-22 cells (Figure 44C), the values obtained with these drug combinations and H₂O₂ were not significantly different from those obtained with H₂O₂ alone (2.4 nM). HT-22 cells displayed less fluctuation in response compared to SH-SY5Y cells.

Concerning corticosterone, in SH-SY5Y cells (Figure 44B), it appears that this agent reduced extracellular 5-HT levels, reducing them to 1.8 nM compared to the control cells (3.1 nM). This response was not significantly attenuated by scopolamine and lamotrigine, in contrast to mirtazapine. In fact, the combination of mirtazapine with corticosterone appeared to increase extracellular 5-HT levels (3.9 nM compared to 1.8 nM with corticosterone alone). On the other hand, in HT-22 cells, it was observed that extracellular 5-HT concentrations remained relatively stable when exposed to corticosterone and the combination of corticosterone with mirtazapine, scopolamine, and lamotrigine, as there were no observed substantial fluctuations (Figure 44D).

These findings highlight the cell-specific and drug-specific effects on extracellular 5-HT concentrations, highlighting the interplay between these compounds and their potential implications.

5. Exploring the Impact of Hydrogen Peroxide and Corticosterone-Induced Stress on Tryptophan Metabolism in SH-SY5Y Cells

The preceding part of our study has underscored the cell-dependent and compound-specific influences on extracellular 5-HT levels, without external addition of this neurotransmitter to the cells.

In this subsection of the study, the primary goal was to investigate the impact of H₂O₂ and corticosterone-induced stress on the levels of 5-HT, as well as on the level of

other metabolites in the L-TRP/5-HT metabolic pathway within SH-SY5Y cells. Thus, this study aims to investigate the impact of applying elevated concentrations of L-TRP, 5-HTP, 5-HT, and 5-HIAA (Figure 45) within a cellular context. These specific compounds were added to the SH-SY5Y cells, both individually and in combination with either H₂O₂ or corticosterone, to understand their impact on cellular viability, determined by the MTT assay. Additionally, cellular morphology was also evaluated, and the extracellular levels of the metabolites were determined by HPLC analysis.

This experimental approach allowed the elucidation of the interplay between oxidative stress and corticosterone-induced stress on the L-TRP/5-HT metabolic pathway, exploring potential mechanisms underlying cellular responses to such stressors.

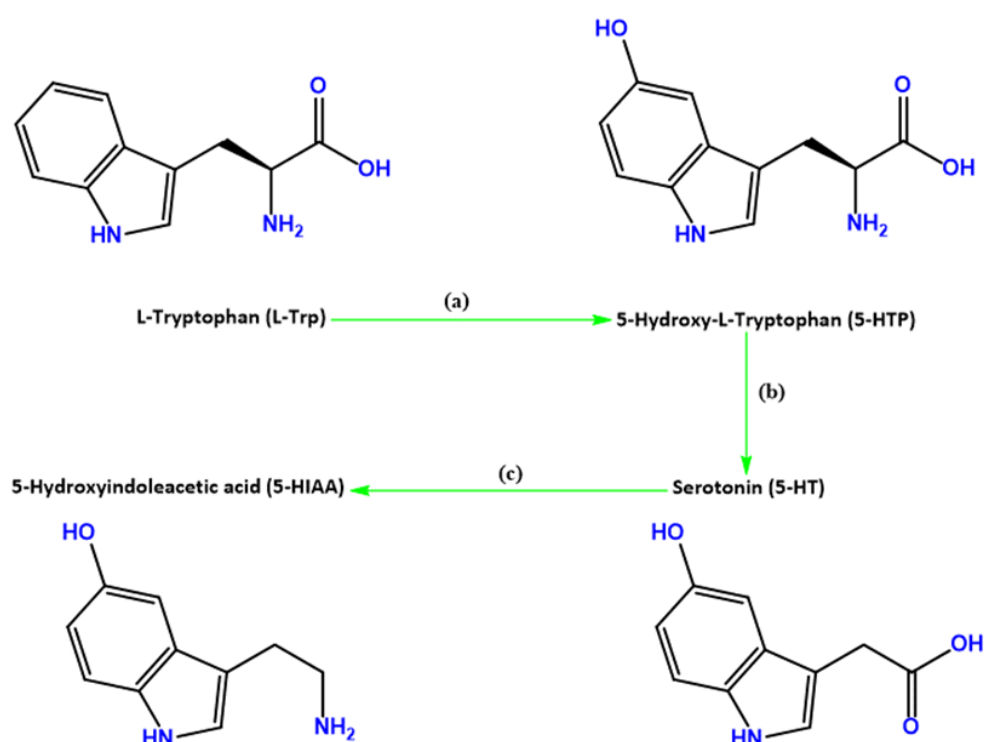


Figure 45. Summary of 5-HT's branch of L-L-TRP biotransformation. This amino acid is (a) metabolized into 5-HTP, that is (b) converted into 5-HT, and finally (c) metabolized into 5-HIAA.

5.1. Effect of L-TRP, 5-HTP, 5-HT, 5-HIAA and Their Combinations with H₂O₂ or Corticosterone on SH-SY5Y Cell Viability and Extracellular L-TRP, 5-HTP, 5-HT, 5-HIAA Concentration

To assess the 48h impact of L-TRP, 5-HTP, 5-HT and 5-HIAA and its combinations with H₂O₂ or corticosterone on SH-SY5Y cell viability and extracellular levels of each metabolite, L-TRP, 5-HTP, 5-HT and 5-HIAA were applied into the cell culture at a concentration of 500 μM. Similarly, H₂O₂ and corticosterone were introduced at

concentrations of 300 μM and 500 μM , respectively. It is important to emphasize that the selection of these elevated concentrations was intentional, done to ensure a discernible cellular response to these compounds, especially when subjected to extraordinarily high levels of stress, notably within the HPLC. Previously (Figures 26 and 28), the effects of L-TRP at lower concentrations when combined with H_2O_2 and corticosterone were also explored. Indeed, our findings indicated that L-TRP was ineffective in mitigating the detrimental consequences of corticosterone exposure, but effectively counteracted the effects of H_2O_2 exposure.

After exposing the cells to their respective treatment conditions, the evaluation of their impact on the morphology and viability of SH-SY5Y cells was carried out (Figures 46 and 47). Furthermore, extracellular media were collected from three independent experiments to assess their impact on L-TRP, 5-HTP, 5-HT and 5-HIAA extracellular concentration (Figure 48).

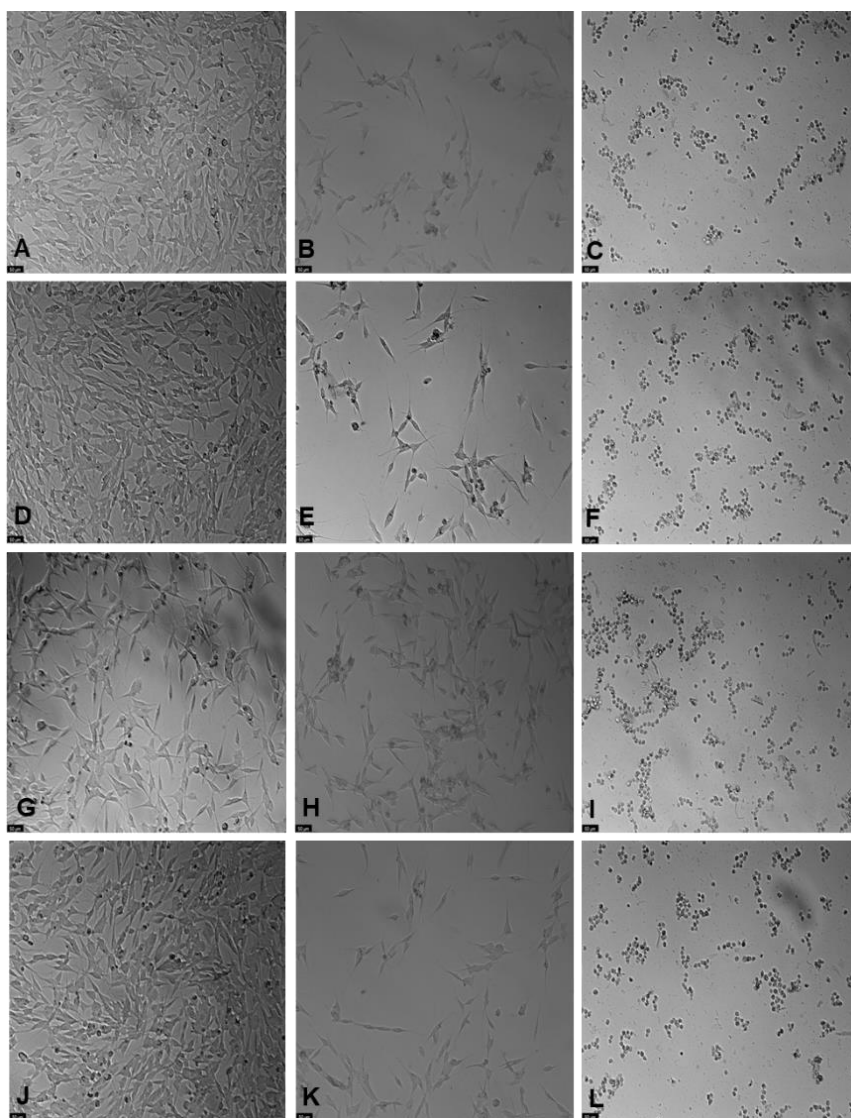


Figure 46. Representative images (100 × total magnification) of SH-SY5Y exposed to (A) L-TRP 500 μM, (B) L-TRP 500 μM + H₂O₂ 300 μM, and (C) L-TRP 500 μM + corticosterone 500 μM, (D) 5-HTP 500 μM, (E) 5-HTP 500 μM + H₂O₂ 300 μM, and (F) 5-HTP 500 μM + corticosterone 500 μM, (G) 5-HT 500 μM, (H) 5-HT 500 μM + H₂O₂ 300 μM, and (I) 5-HT 500 μM + corticosterone 500 μM, (J) 5-HIAA 500 μM, (K) 5-HIAA 500 μM + H₂O₂ 300 μM, and (L) 5-HIAA 500 μM + corticosterone 500 μM. Scale bar: 50 μm.

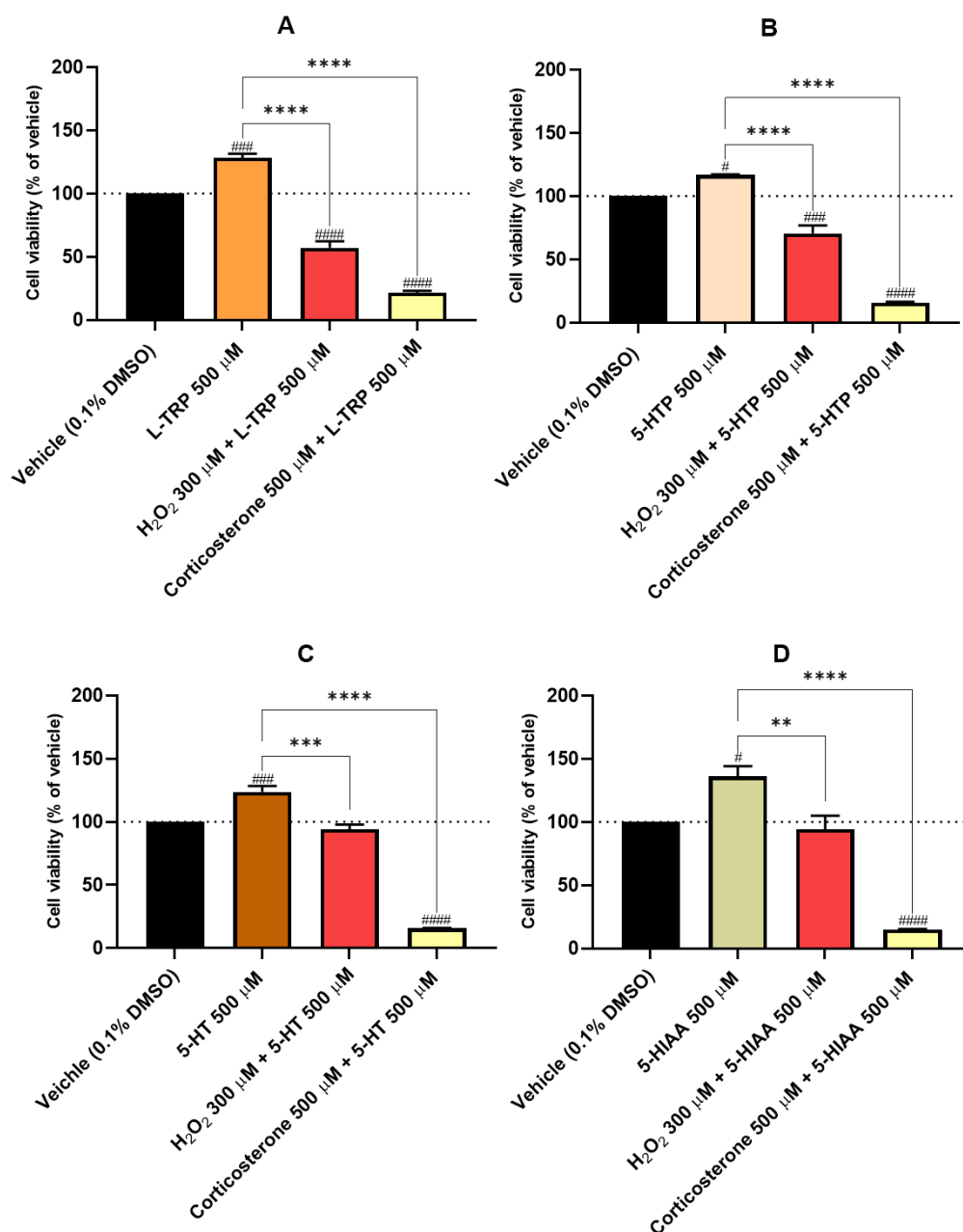


Figure 47. Effect of the incubation of 500 μM of (A) L-TRP, (B) 5-HTP, (C) 5-HT, (D) 5-HIAA, 500 μM of each metabolite in combination with 300 μM of H₂O₂, and 500 μM of each metabolite in combination with 500 μM of corticosterone on the SH-SY5Y cellular viability, determined by MTT assay. The results represent the mean ± SEM of three independent experiments, expressed as the percentage of the vehicle (100%). Statistically significant # p < 0.05, ### p < 0.001, #### p < 0.0001 vs. vehicle, and ** p < 0.01, *** p < 0.001, **** p < 0.0001 vs. L-TRP 500 μM, 5-HTP 500 μM, 5-HT 500 μM and 5-HIAA 500 μM.

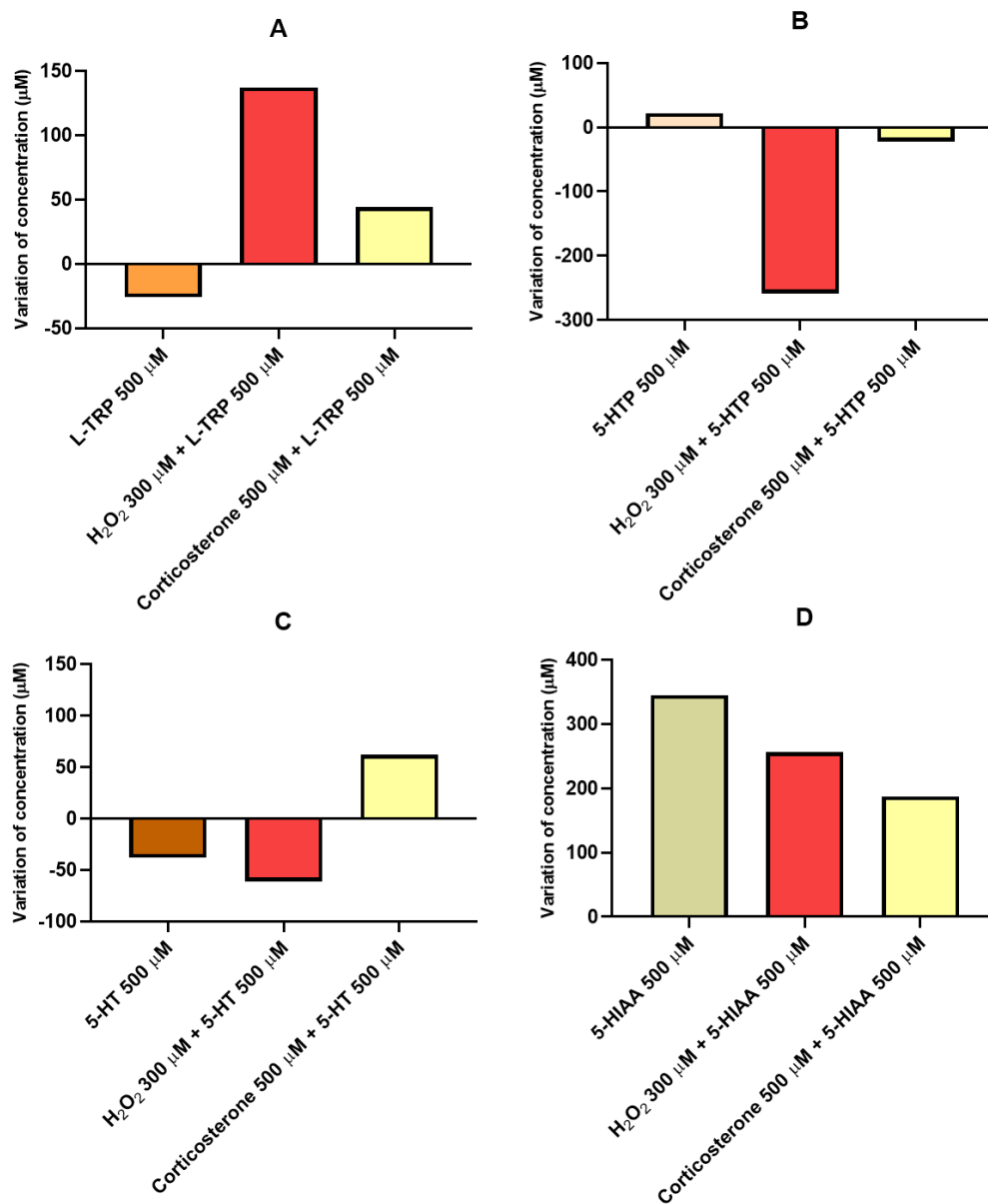


Figure 48. Variation of concentration (μM) of (A) L-TRP, (B) 5-HTP, (C) 5-HT and (D) 5-HIAA in the extracellular medium of SH-SY5Y cells, in which the baseline represents (A) L-TRP, (B) 5-HTP, (C) 5-HT and (D) 5-HIAA 500 μM . These cells were treated with H₂O₂ and corticosterone combined with these metabolites and analyzed by HPLC. Results are derived from the analysis of the extracellular medium across a minimum of three separate and independently conducted experiments.

These results indicate that L-TRP as a single compound enhanced cell viability ($128.4\% \pm 3.1\%$ compared to the vehicle control). Conversely, the combination of L-TRP with high levels of H₂O₂ and corticosterone significantly reduced cell viability ($57.1\% \pm 5.1\%$ for H₂O₂ and $21.6\% \pm 1.5\%$ for corticosterone, compared to vehicle treated cells), primarily due to their high stress-inducing effects (Figures 46A-C, 47A). Viability values and morphology assessment were concordant. Indeed, lower viability values were

accompanied by observable changes in cell morphology, characterized by a rounded appearance, shrinkage, and a reduced cell count. Interestingly, HPLC analysis revealed contrasting results (Figure 48A). Following a 48h exposure to L-TRP alone, the extracellular L-TRP concentration decreased by 26 μM . In contrast, when combined with both H_2O_2 and corticosterone, L-TRP levels in the extracellular medium increased by 137 μM and 44 μM , respectively.

For 5-HTP, similar to L-TRP, it increased cell viability ($116.8\% \pm 0.4\%$ compared to the vehicle). However, when 5-HTP was combined with H_2O_2 and corticosterone, cell viability declined significantly ($70.5\% \pm 6.3\%$ and $15.8\% \pm 1.1\%$ compared to the vehicle, respectively), attributed to the influence of H_2O_2 and corticosterone (Figure 47B). Morphological assessment supported these viability findings (Figure 46D-F). HPLC results (Figure 48B) showed that after 48h of exposure to 5-HTP alone, extracellular levels of this compound increased 22 μM . However, when combined with H_2O_2 or corticosterone, 5-HTP levels decreased 259 μM and 22 μM , respectively, in contrast to the trend observed with L-TRP in the extracellular medium.

Regarding the obtained results involving 5-HT, once again, they indicate distinct effects on cell viability based on different conditions (Figure 47C). When 5-HT was applied in isolation, it resulted in an increase in cell viability ($123.7\% \pm 4.7\%$ compared to the vehicle control). However, in combination with H_2O_2 , cellular viability exhibited only a slight deviation from the vehicle control ($94.2\% \pm 3.7\%$). Conversely, in the presence of corticosterone, cell viability declined markedly ($15.9\% \pm 0.3\%$, compared to vehicle control). It is noteworthy that the assessments of viability and morphology are consistent with these findings. However, when examining Figure 46G, it seems that cells do not exhibit a high level of confluence. Concerning HPLC results, following a 48h exposure of SH-SY5Y cells to 5-HT alone, the concentration of this compound in the extracellular medium decreased 38 μM . Interestingly, in contrast to the behavior of other analyzed compounds, a different pattern in extracellular levels of 5-HT emerged when it was combined with both H_2O_2 and corticosterone. Specifically, in combination with H_2O_2 , 5-HT levels in the extracellular medium decreased 61 μM . Conversely, when combined with corticosterone, these values increased 62 μM .

Finally, these findings indicate that when 5-HIAA was applied isolated, it led to an increase in cell viability ($136.1\% \pm 8.2\%$, compared to the vehicle control), as observed with the other metabolites. However, when combined with both H_2O_2 and corticosterone, cell viability exhibited a slight decrease with H_2O_2 treatment ($94.3\% \pm 10.7\%$, compared to the vehicle) and a substantial decline with corticosterone treatment ($15.1\% \pm 0.3\%$, compared to the vehicle), exhibiting a similar response to 5-HT in combination with these agents. Moreover, although viability analysis and morphology assessments appeared to

align, it is important to highlight that in the context of the combination of 5-HIAA with H_2O_2 , the elevated viability values do not seem to correlate with the observed alterations in cellular morphology. In HPLC results, a notable increase in extracellular 5-HIAA levels was observed following all treatments. Specifically, after exposing the cells to 5-HIAA isolated, the concentration of this compound in the extracellular medium significantly increased 345 μ M. When combined with both H_2O_2 and corticosterone, extracellular 5-HIAA levels rose 256 μ M and 187 μ M, respectively.

5.2. Effect of H_2O_2 and Corticosterone on Extracellular 5-HT Concentration

Given the significance of 5-HT in the context of depression and the findings from our previous experiments, the cells were exposed to several concentrations of H_2O_2 (50–300 μ M) and corticosterone (100–500 μ M) for a duration of 48h. The aim of this experiment was to elucidate the impact of different concentrations of these treatments on the extracellular levels of 5-HT. To achieve this, a highly sensitive electrochemical HPLC method was used to accurately measure the concentrations of 5-HT in the extracellular medium of the cells. The results of these experiments are present in Figure 49.

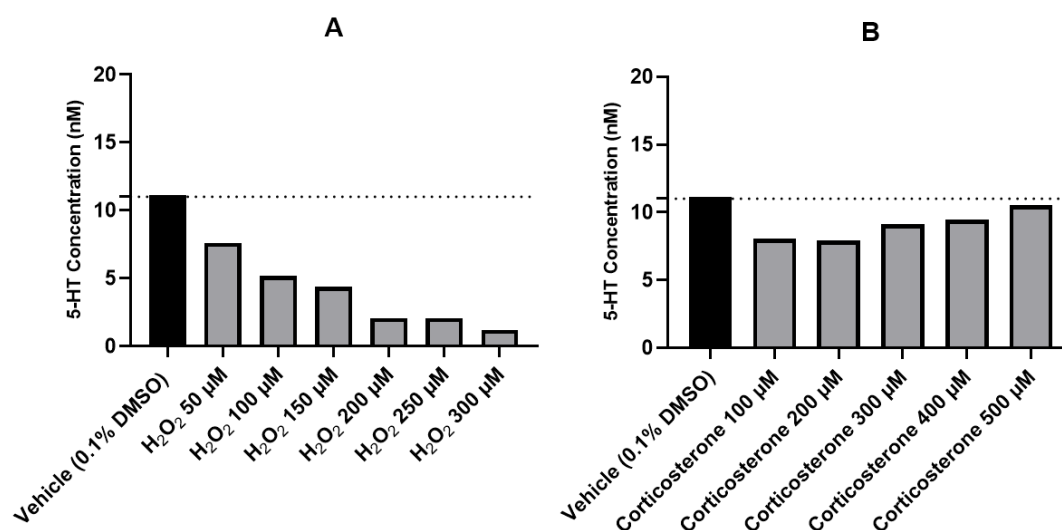


Figure 49. Concentrations of 5-HT (nM) in the extracellular medium of SH-SY5Y cells treated with (A) H_2O_2 50–300 μ M and (B) corticosterone 100–500 μ M, determined by HPLC (electrochemical method). The results represent the analysis of the supernatant collected from the three independent experiments.

These findings reveal a concentration-dependent reduction in extracellular 5-HT levels in SH-SY5Y cells following a 48h exposure to increasing concentrations of H_2O_2 . Notably, 5-HT levels ranged from 11.1 nM (vehicle) to 1.2 nM (H_2O_2 300 μ M). Conversely,

exposure to corticosterone did not result in notorious alterations in extracellular 5-HT concentrations. Specifically, treatment with corticosterone 100 μM yielded 5-HT values of 8.1 nM, and this value showed a gradual increase with higher corticosterone concentrations, nearing the vehicle baseline (11.1 nM) when exposed to corticosterone 500 μM (10.5 nM).

6. Neurotrophic Responses in Different Neuronal Models: BDNF Levels After Mirtazapine, Scopolamine, and Cellular Stress Exposure

To elucidate the impact of mirtazapine and scopolamine on BDNF levels, we used primary neuronal cell cultures and acute hippocampal slices for expression analysis. Specifically, BDNF levels in mice neuronal hippocampal cells were examined using immunofluorescence, while also assessing mice neuronal cortical cells and acute hippocampal slices through Western blot analysis. Additionally, we expanded our study to include the assessment of phosphorylated TrkB (pTrkB) levels in mice neuronal hippocampal cells using immunofluorescence. All the rationale of these studies and interpretation of the obtained results are presented in the discussion.

6.1. BDNF Levels After Mirtazapine, Scopolamine, and Cellular Stress Exposure in Acute Hippocampal Slices

To investigate the impact of mirtazapine, scopolamine, H_2O_2 , and corticosterone on the mature BDNF levels in acute hippocampal slices, mirtazapine and scopolamine were used at a concentration of 20 μM for 6h. H_2O_2 and corticosterone stimulus were applied at concentrations of 105 μM and 35 μM , respectively, corresponding to their medium IC_{50} values determined in HT-22 cellular viability assays, as previously determined (Table 8). Figures 50 and 51 present the results of the western blot analysis for the BDNF monomeric and dimeric forms, respectively.

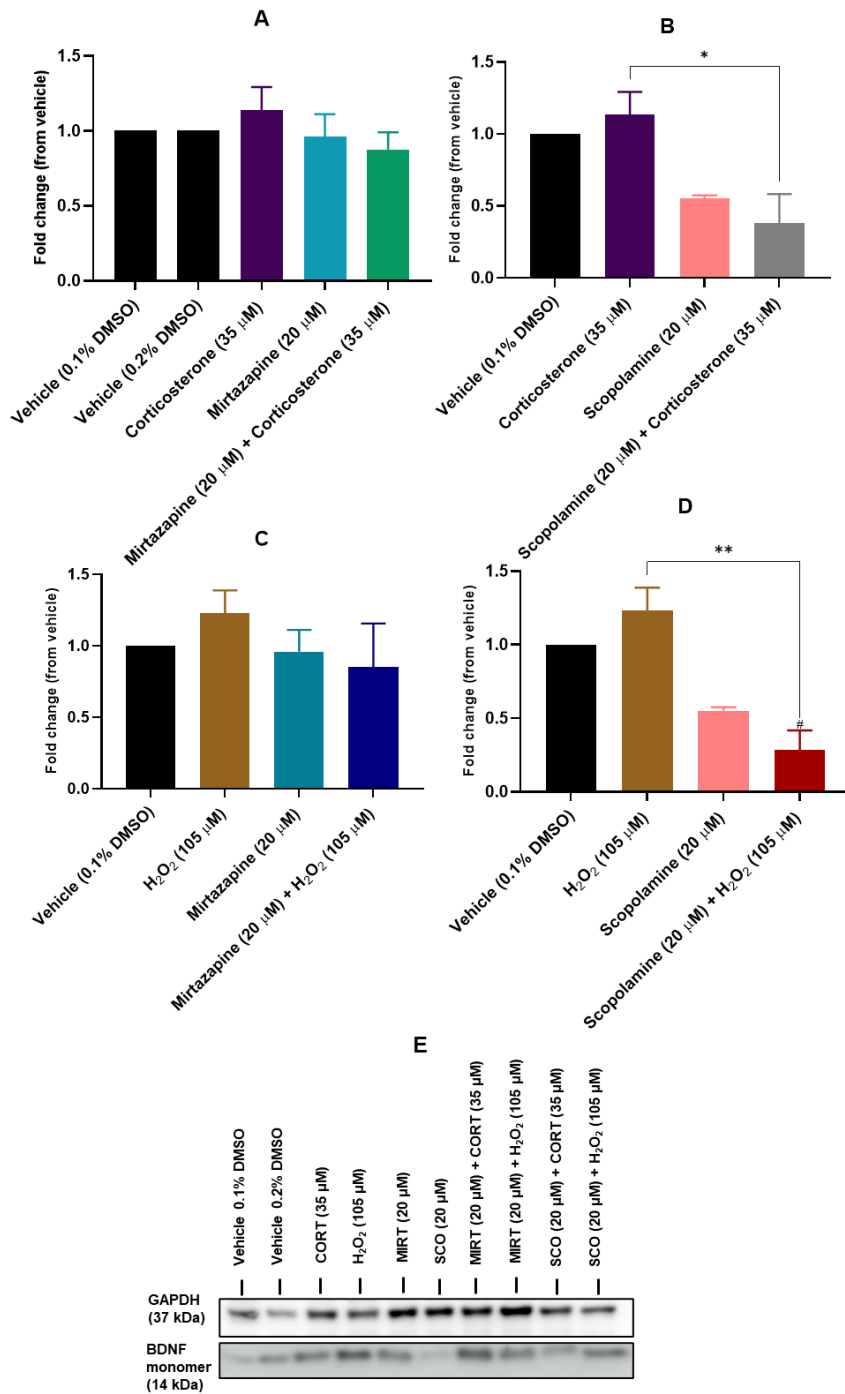


Figure 50. Western blot analysis of BDNF monomer levels in acute hippocampal slices treated for 6h with mirtazapine 20 μ M combined with (A) corticosterone 35 μ M and (C) H₂O₂ 105 μ M, and scopolamine 20 μ M combined with (B) corticosterone 35 μ M and (D) H₂O₂ 105 μ M, after incubation with anti-BDNF primary antibody, previously detailed in the materials and methods section. Representative blot represented in (E). CORT: corticosterone; MIRT: mirtazapine; SCO: scopolamine. For clearer understanding and analysis, the results obtained for H₂O₂, mirtazapine, scopolamine, and corticosterone (for the same timepoint) are repeated in separate graphs. Statistically significant * $p < 0.05$ and ** $p < 0.01$ vs. the aggressor (H₂O₂ 105 μ M or corticosterone 35 μ M), and # $p < 0.05$ vs. vehicle.

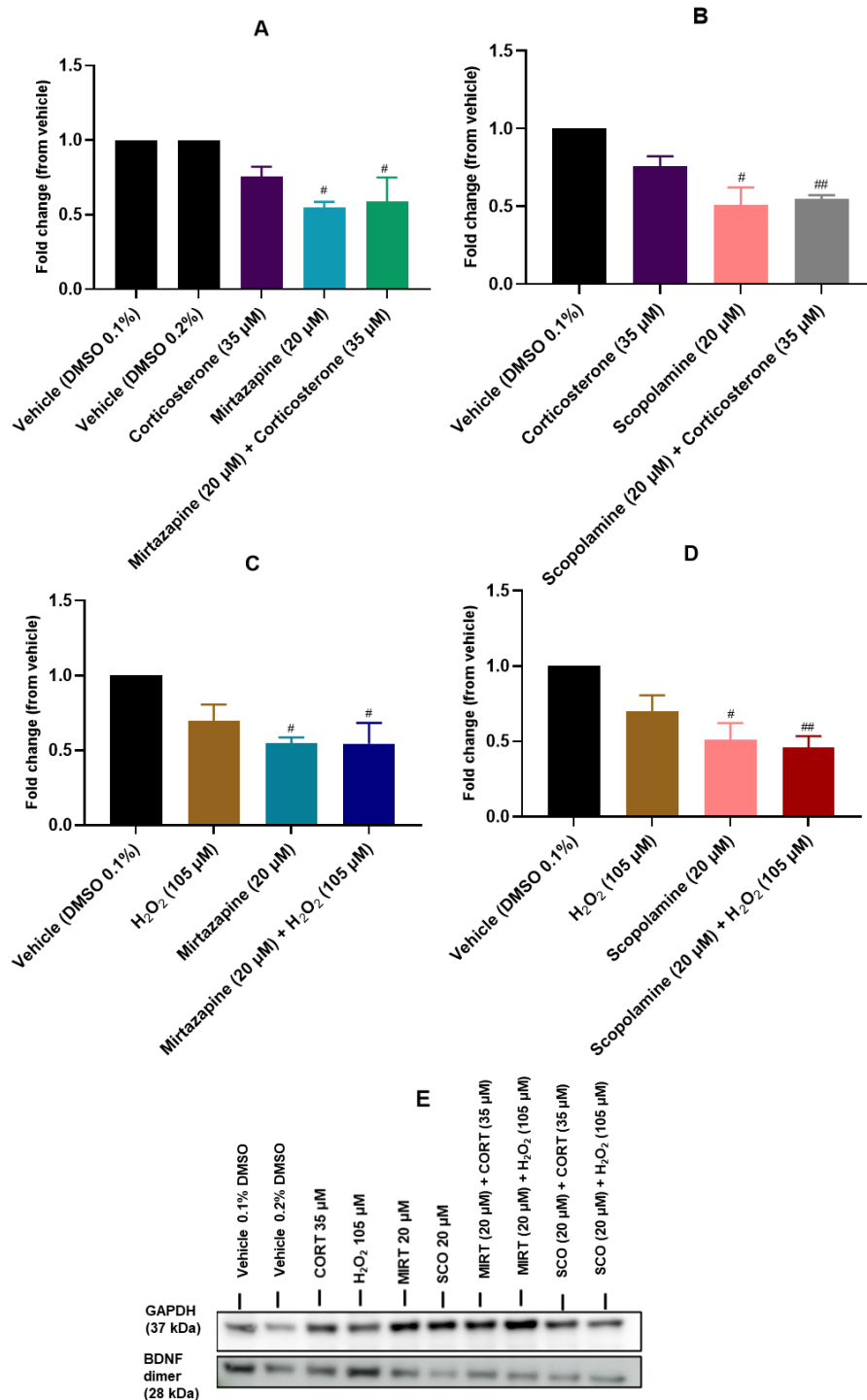


Figure 51. Western blot analysis of BDNF dimer levels in acute hippocampal slices treated for 6h with mirtazapine 20 μ M combined with (A) corticosterone 35 μ M and (C) H₂O₂ 105 μ M, and scopolamine 20 μ M combined with (B) corticosterone 35 μ M and (D) H₂O₂ 105 μ M, after incubation with anti-BDNF primary antibody, previously detailed in the materials and methods section. Representative blot represented in (E). CORT: corticosterone; MIRT: mirtazapine; SCO: scopolamine. For clearer understanding and analysis, the results obtained for H₂O₂, mirtazapine, scopolamine, and corticosterone (for the same timepoint) are repeated in separate graphs. Statistically significant # p<0.05 and ## p < 0.01 vs. vehicle.

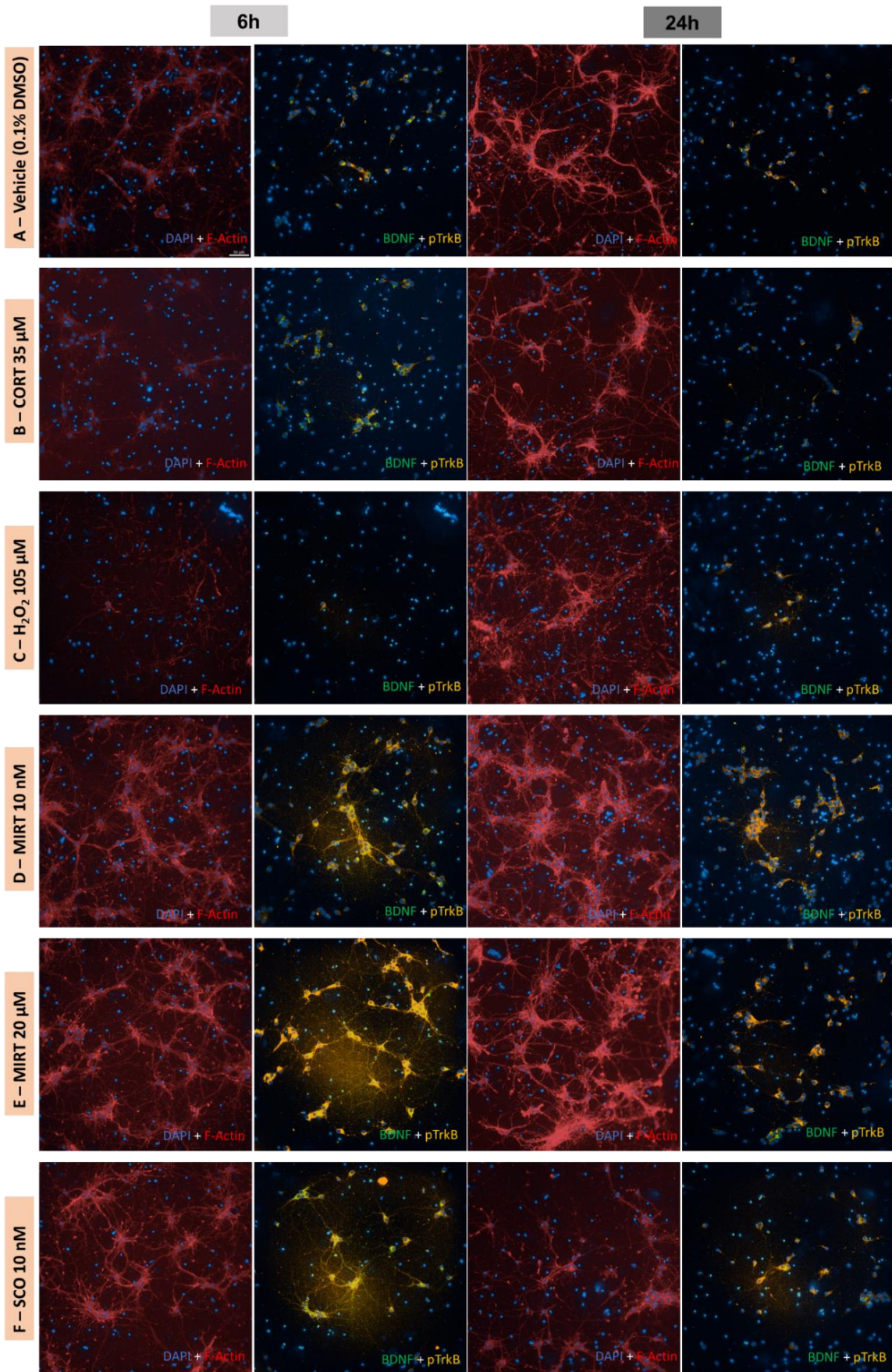
In the hippocampal slices, we analyzed the monomeric and dimeric forms of the mature BDNF.

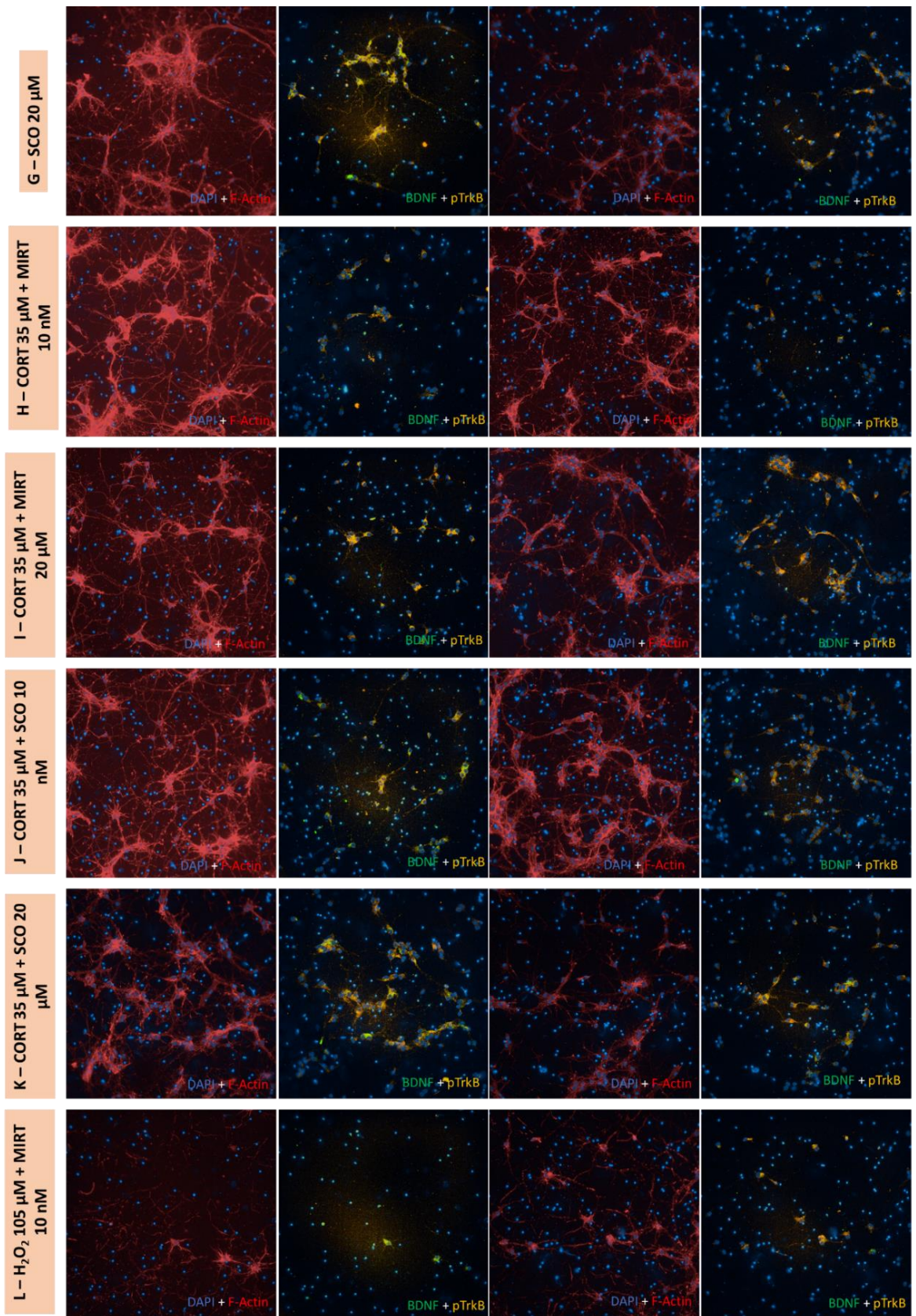
Collectively, these findings indicate that scopolamine either alone or combined with corticosterone or H₂O₂, reduced BDNF levels, a pronounced effect which was not observed when using corticosterone or H₂O₂ by themselves (Figures 50B, D). However, mirtazapine did not demonstrate a significant impact on BDNF monomer levels (Figures 50A, C), despite a reduction in BDNF dimer levels (Figures 51A, C).

These findings indicate that scopolamine, whether applied alone or in combination with corticosterone or H₂O₂, significantly reduced BDNF levels. This suggests that, even under stressful conditions, the presence of stressors did not impede the effects of scopolamine on the modulation of BDNF levels. On the other hand, the impact of mirtazapine in mature BDNF levels was less pronounced.

6.2. BDNF and phosphorylated TrkB Levels After Mirtazapine, Scopolamine, and Cellular Stress Exposure in Neuronal Hippocampal Cell Culture

To explore the 6h and 24h effect of mirtazapine, scopolamine, H₂O₂ and corticosterone on BDNF (Figures 52-54) and pTrkB (Figures 52, 55 and 56) levels in mice neuronal hippocampal cells, mirtazapine and scopolamine were added to the cells in a concentration of 10 nM and 20 μM. H₂O₂ and corticosterone were added in a concentration of 105 μM and 35 μM, respectively, representing the medium IC₅₀ values on HT-22 cellular viability. The immunofluorescence results are presented in Figures 52-56. Specifically, Figure 52 features representative images of the stained cells, while Figures 53 to 56 depict the quantitative data derived from the analysis.





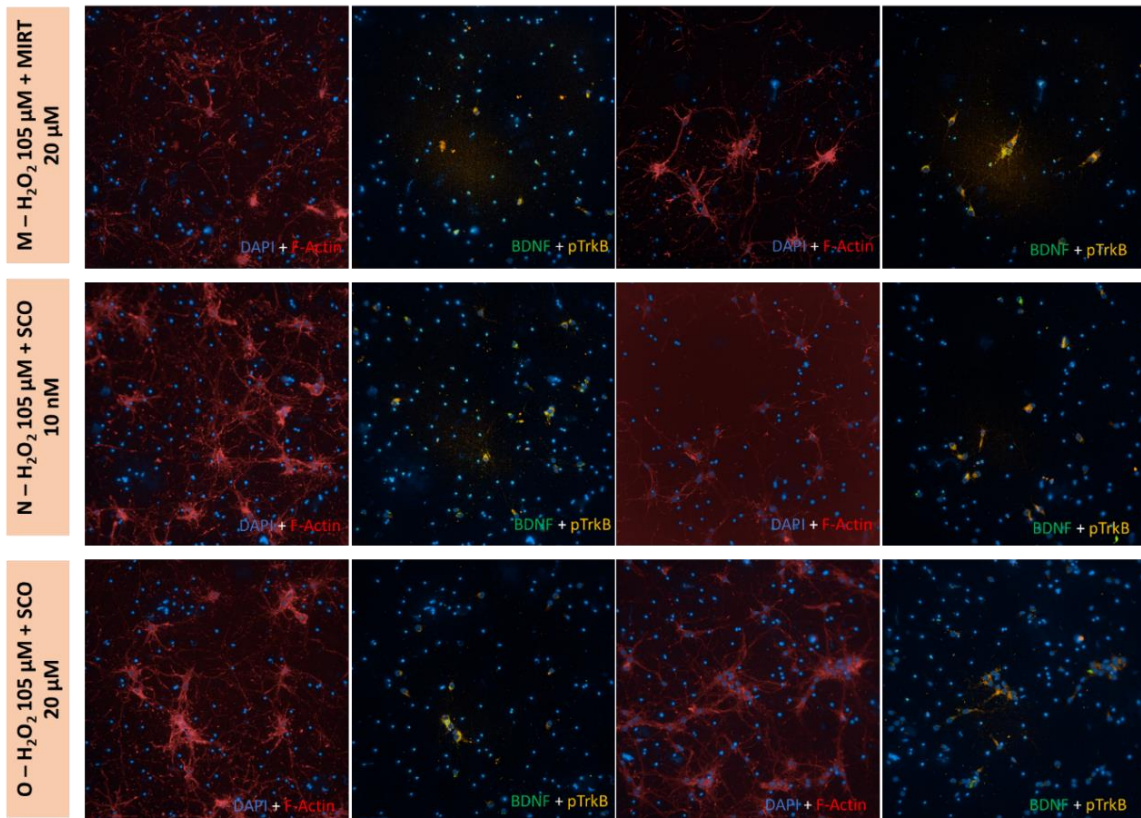


Figure 52. Representative images (200× total magnification) of neuronal hippocampal cell culture incubated for 6h (left) or 24h (right) with (A) vehicle (0.1% DMSO), (B) corticosterone 35 μM, (C) H₂O₂ 105 μM, (D) mirtazapine 10 nM, (E) mirtazapine 20 μM, (F) scopolamine 10 nM, (G) scopolamine 20 μM, (H) corticosterone 35 μM + mirtazapine 10 nM, (I) corticosterone 35 μM + mirtazapine 20 μM, (J) corticosterone 35 μM + scopolamine 10 nM, (K) corticosterone 35 μM + scopolamine 20 μM, (L) H₂O₂ 105 μM + mirtazapine 10 nM, (M) H₂O₂ 105 μM + mirtazapine 20 μM, (N) H₂O₂ 105 μM + scopolamine 10 nM, (O) H₂O₂ 105 μM + scopolamine 20 μM, after immunostaining with Hoechst 33342 (blue), Alexa Fluor™ 647 Phalloidin (red), anti-BDNF (conjugated with Alexa Fluor™ 488, green) and anti- pTrkB (conjugated with Alexa Fluor™ 568, orange) primary antibodies. CORT: corticosterone; MIRT: mirtazapine; SCO: scopolamine. Scale bar (present in the first image): 50 μm.

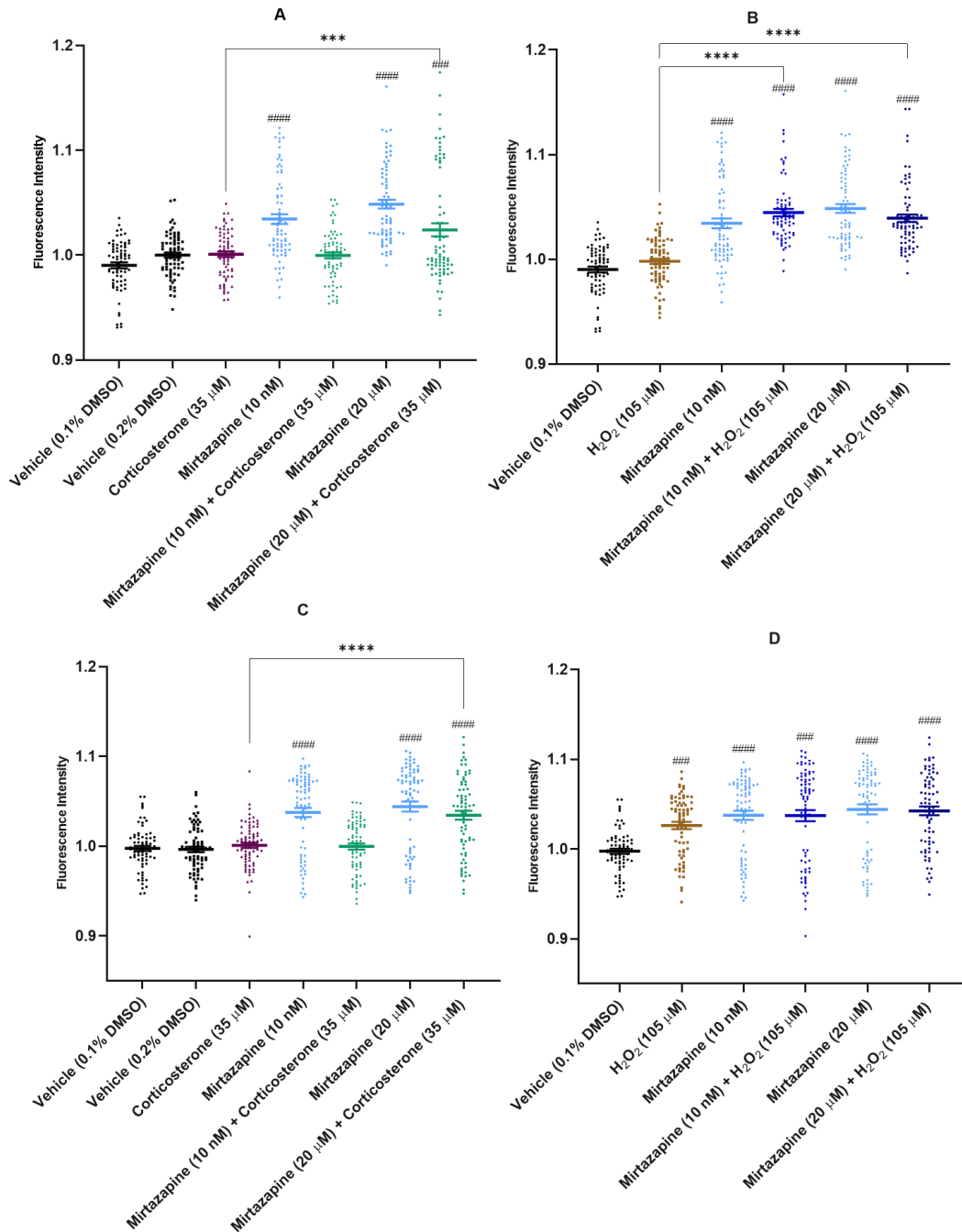


Figure 53. Fluorescence intensity of BDNF expressed in neuronal hippocampal cell culture incubated for 6h (A, B) or 24h (C,D) with mirtazapine 10 nM or 20 μ M combined with (A, C) corticosterone 35 μ M and (B, D) H₂O₂ 105 μ M, after immunostaining, as previously detailed in the materials and methods section. For clearer understanding and analysis, the results obtained for H₂O₂, mirtazapine, scopolamine, and corticosterone (for the same timepoint) are repeated in separate graphs. Statistically significant ### p<0.001 and #### p < 0.0001 vs. vehicle, *** p<0.001 and **** p < 0.0001 vs. the aggressor (H₂O₂ 105 μ M or corticosterone 35 μ M).

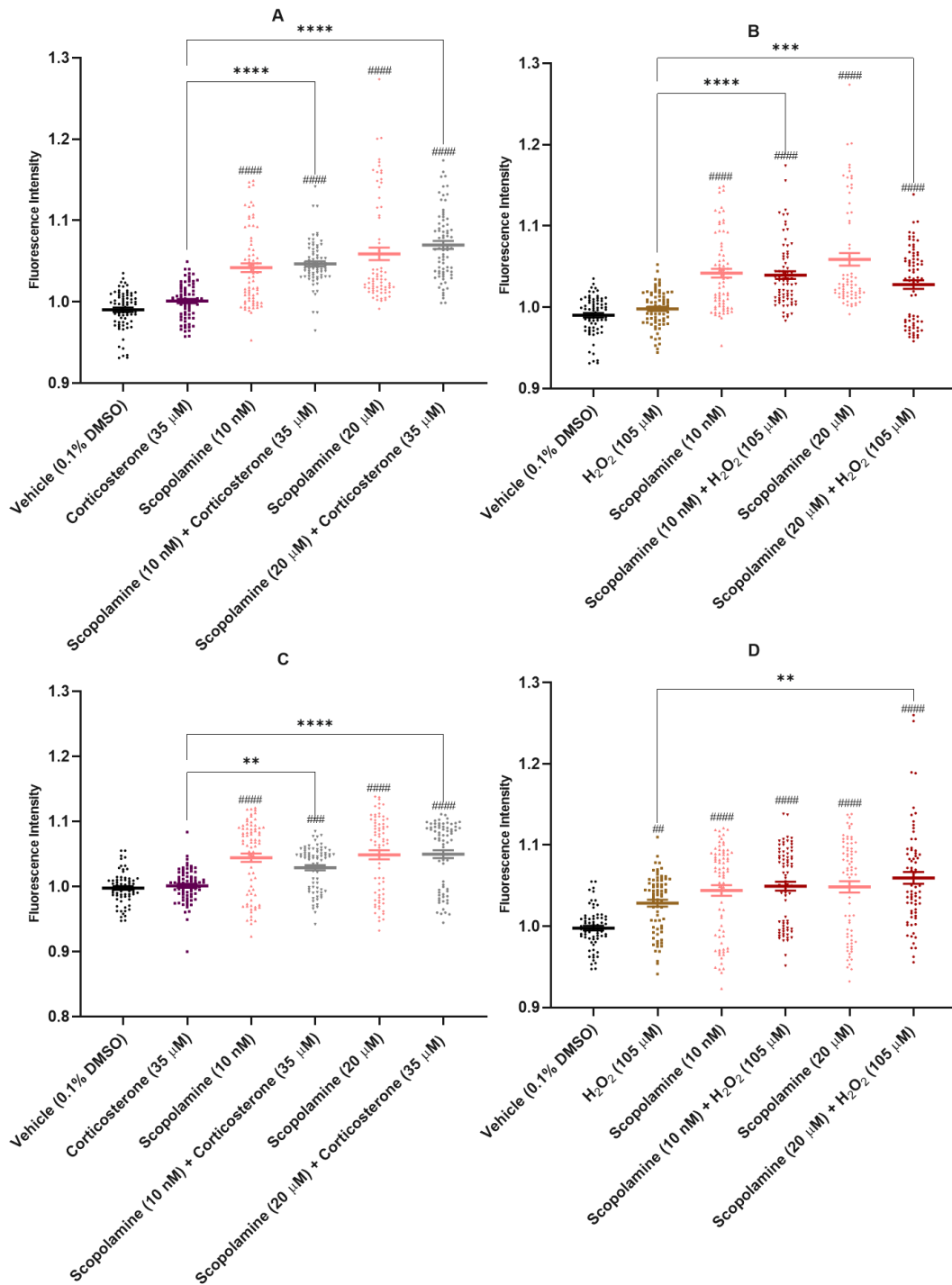


Figure 54. Fluorescence intensity of BDNF expressed in neuronal hippocampal cell culture incubated for 6h (A, B) or 24h (C,D) with scopolamine 10 nM or 20 μ M combined with (A, C) corticosterone 35 μ M and (B, D) H₂O₂ 105 μ M, after immunostaining, as previously detailed in the materials and methods section. For clearer understanding and analysis, the results obtained for H₂O₂, mirtazapine, scopolamine, and corticosterone (for the same timepoint) are repeated in separate graphs. Statistically significant ## p<0.01, ### p<0.001 and #### p < 0.0001 vs. vehicle, ** p<0.01, *** p<0.001 and **** p < 0.0001 vs. the aggressor (H₂O₂ 105 μ M or corticosterone 35 μ M).

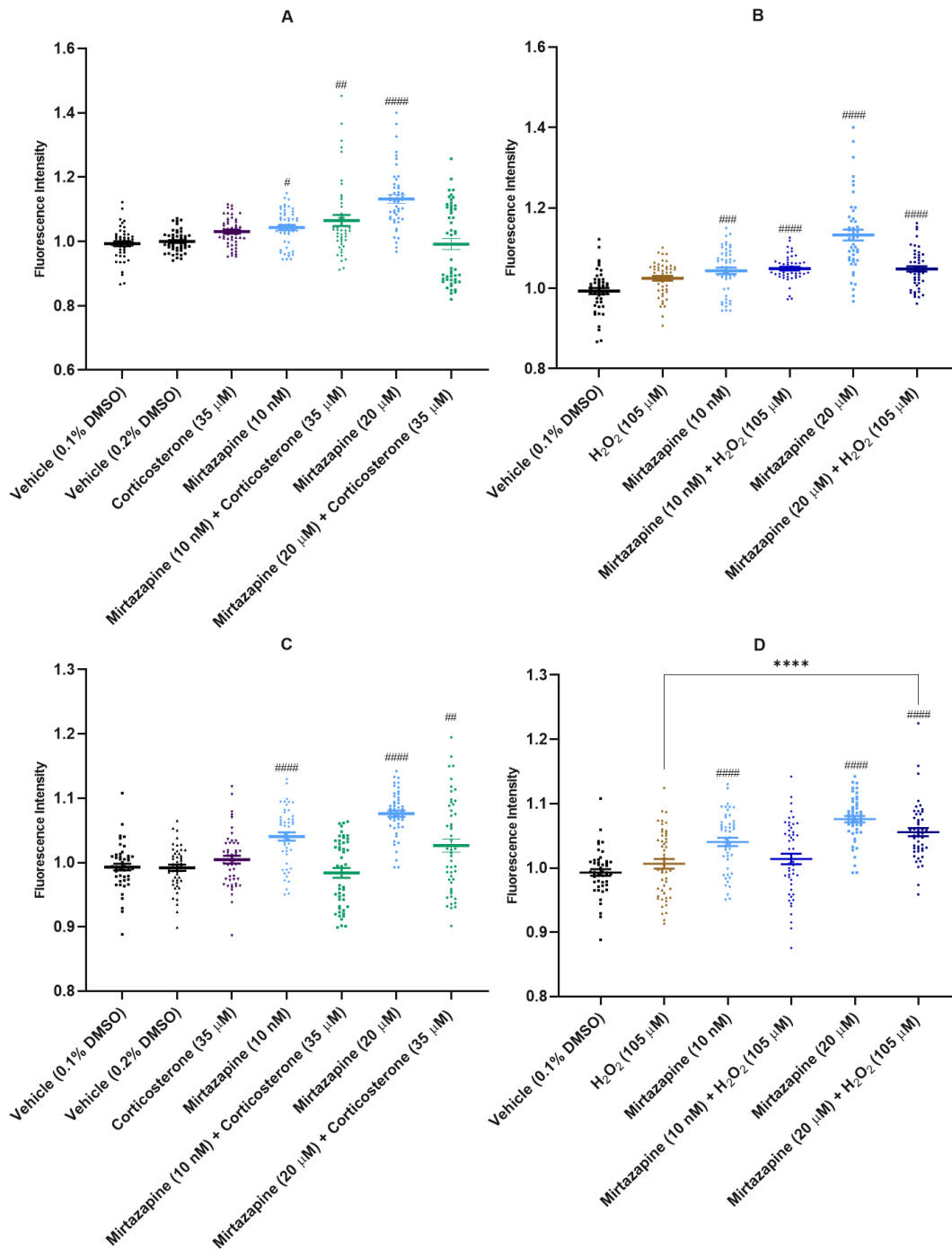


Figure 55. Fluorescence intensity of pTrkB in neuronal hippocampal cell culture incubated for 6h (A, B) or 24h (C, D) with mirtazapine 10 nM or 20 μ M combined with (A, C) corticosterone 35 μ M and (B, D) H₂O₂ 105 μ M, after immunostaining, as previously detailed in the materials and methods section. For clearer understanding and analysis, the results obtained for H₂O₂, mirtazapine, scopolamine, and corticosterone (for the same timepoint) are repeated in separate graphs. Statistically significant ## p<0.01, ### p<0.001 and #### p < 0.0001 vs. vehicle, **** p < 0.0001 vs. the aggressor (H₂O₂ 105 μ M).

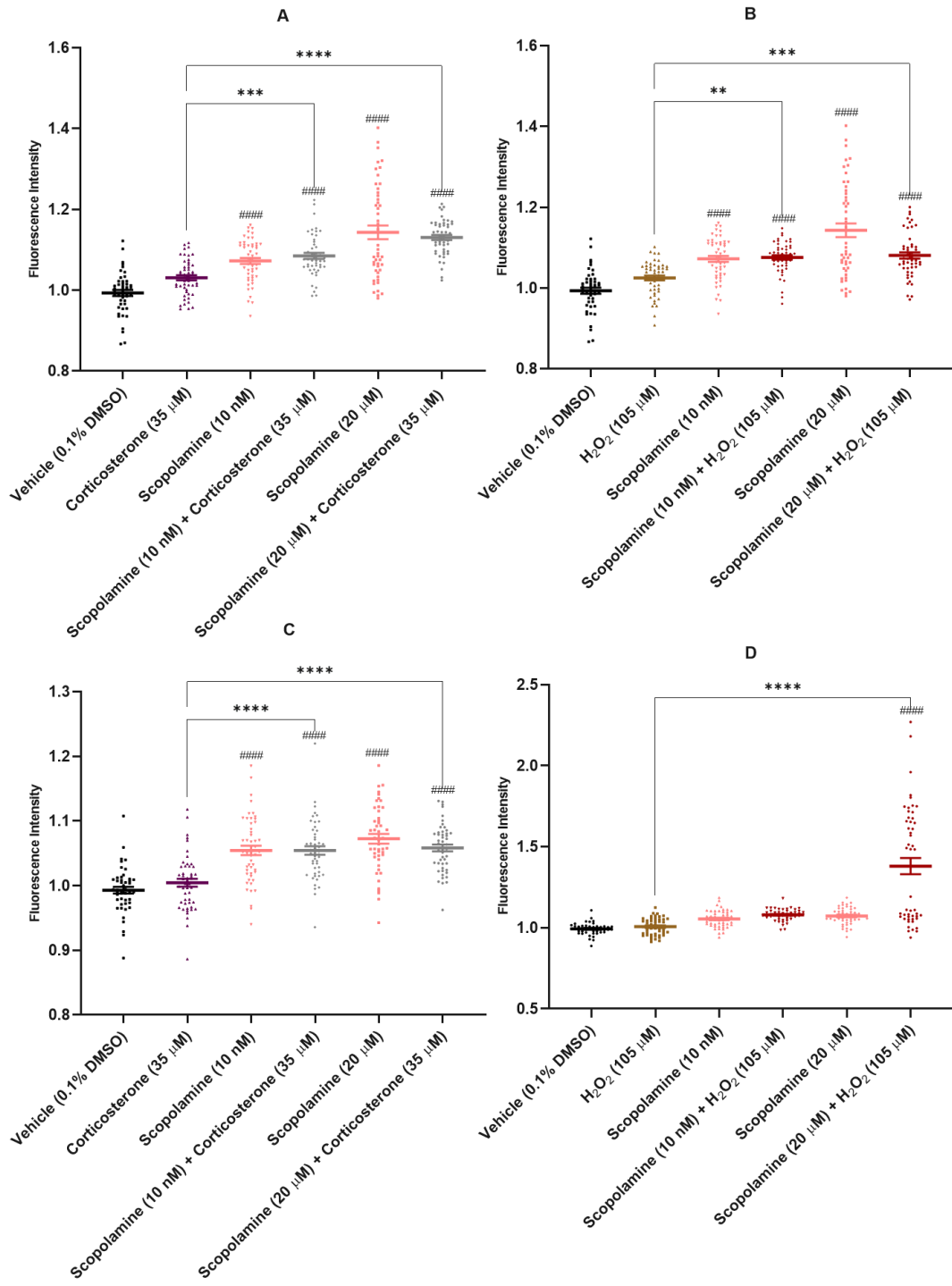


Figure 56. Fluorescence intensity of pTrkB in neuronal hippocampal cell culture incubated for 6h (A, B) or 24h (C,D) with scopolamine 10 nM or 20 μ M combined with (A, C) corticosterone 35 μ M and (B, D) H₂O₂ 105 μ M, after immunostaining, as previously detailed in the materials and methods section. For clearer understanding and analysis, the results obtained for H₂O₂, mirtazapine, scopolamine, and corticosterone (for the same timepoint) are repeated in separate graphs. Statistically significant ##### p < 0.0001 vs. vehicle, ** p < 0.01, *** p < 0.001, and **** p < 0.0001 vs. the aggressor (H₂O₂ 105 μ M or corticosterone 35 μ M).

Regarding the assessment of BDNF levels (Figures 52-54), these findings indicate that overall, mirtazapine at a concentration of 20 μ M combined with corticosterone or H₂O₂ exhibited a significant increase in BDNF expression when compared to cells with corticosterone or H₂O₂ alone. Moreover, even at a lower concentration of mirtazapine (10 nM), a notable enhancement in BDNF expression was observed when compared to the H₂O₂ treatment group, but not with corticosterone, suggesting that a higher concentration of mirtazapine is needed to counteract the effects of corticosterone (Figures 53A, C). The enhancement in BDNF expression was particularly pronounced at the 6h time point for the combination of mirtazapine with H₂O₂ (Figure 53B, D). When mirtazapine was used combined with corticosterone, it was noted that there were similar responses at both time points 6h and 24h (Figure 53A,C). In addition to mirtazapine, scopolamine also enhanced BDNF expression when compared to cells treated with corticosterone or H₂O₂ alone, at both concentrations and at both time points (Figure 54).

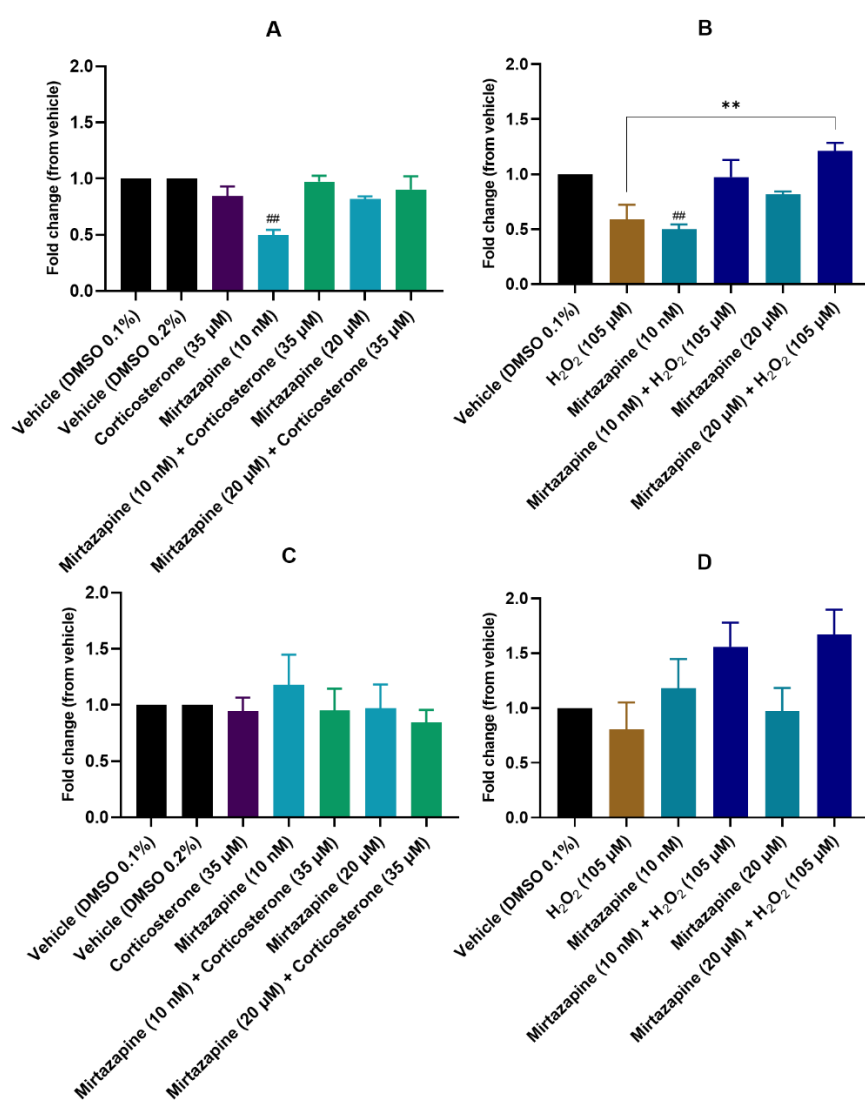
In the assessment of pTrkB levels (Figures 52, 55 and 56), these data revealed that at 6h, the combination of mirtazapine with either corticosterone or H₂O₂ did not yield a significant enhancement in pTrkB levels compared to the stimulus with corticosterone or H₂O₂ alone (Figures 55A,B). When compared to the corticosterone treatment alone, mirtazapine (20 μ M) even exhibited a tendency to decrease pTrkB levels, though it did not reach statistical significance (Figure 55A). In contrast, at 24h, mirtazapine (20 μ M) demonstrated an enhancement in pTrkB levels when compared to the H₂O₂ treatment group (Figure 55D). However, it's noteworthy that mirtazapine, when incubated independently, did indeed enhance pTrkB levels, compared to the control group. In turn, scopolamine exhibited a different profile. At both time points, scopolamine enhanced pTrkB levels when compared to corticosterone and H₂O₂ treatments (Figure 56). For the 24h time point, a higher amount of scopolamine (20 μ M instead of 10 nM) was necessary to see this effect.

The images (Figure 52) were selected from a higher number of images as representative pictures and cannot depict the whole variability commonly observed in biological systems. This variability is present in the quantitative data.

Collectively, these results suggest a complex interplay between mirtazapine, scopolamine, corticosterone, and H₂O₂ in regulating both pTrkB levels over time and BDNF expression. Nevertheless, both drugs enhance BDNF levels (especially at 6h), whereas scopolamine seems to be more effective in increasing pTrkB levels.

6.3. BDNF Levels After Mirtazapine, Scopolamine, and Cellular Stress Exposure in Neuronal Cortical Cell Culture

To further investigate the 6h and 24h impact of mirtazapine, scopolamine, H₂O₂, and corticosterone on the BDNF levels in neuronal cortical cell culture, mirtazapine and scopolamine were used, once again, at 10 nM and 20 μM, for both compounds. H₂O₂ and corticosterone were applied at concentrations of 105 μM and 35 μM, corresponding to their medium IC₅₀ values determined in HT-22 cellular viability assays. Figure 57 presents the results of the Western blot analysis.



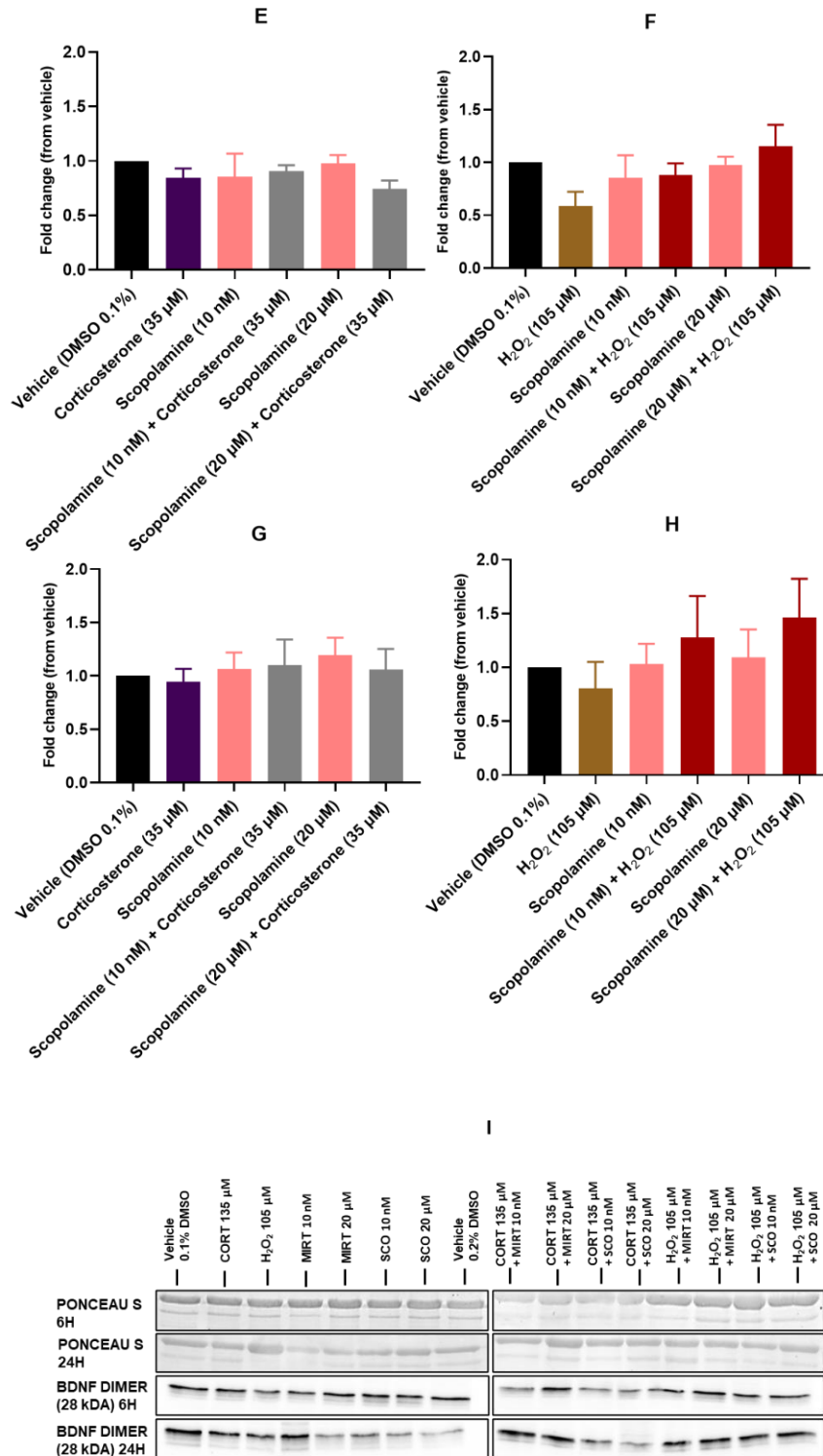


Figure 57. Western blot analysis of BDNF levels in neuronal cortical cells treated for 6h (A,B,E,F) or 24h (C,D,G,H), with mirtazapine 10 nM or 20 μ M combined with (A, C) corticosterone 35 μ M and (B, D) H₂O₂ 105 μ M, and scopolamine 10 nM or 20 μ M combined with (E,G) corticosterone 35 μ M and (F, H) H₂O₂ 105 μ M, after incubation with anti-BDNF primary antibody, previously detailed in the materials and methods section. Representative blots are presented in image I. The Ponceau lanes are representative of the bands used as the loading control for normalization. CORT: corticosterone; MIRT: mirtazapine; SCO: scopolamine. For clearer understanding and analysis, the results obtained for H₂O₂, mirtazapine, scopolamine, and

corticosterone (for the same timepoint) are repeated in separate graphs. Statistically significant ## $p < 0.01$ vs. vehicle, and ** $p < 0.01$ vs. the aggressor (H_2O_2 105 μM).

These findings highlight that only the combination of mirtazapine at 20 μM with H_2O_2 resulted in a statistically significant increase in BDNF levels at the 6h time point, (Figure 57B), when compared to H_2O_2 treatment alone. While not reaching statistical significance, there was also an observable trend at the 24h time point, where both concentrations of mirtazapine appeared to enhance BDNF levels compared to H_2O_2 treatment alone (Figure 57D). A similar trend was observed for scopolamine, incubated at both concentrations, in combination with H_2O_2 at both 6h and 24h (Figure 57F and H). Indeed, these combinations exhibited an increase in BDNF levels compared to H_2O_2 treatment alone. However, when considering the combination of both mirtazapine and scopolamine with corticosterone at both time points, no particularly notable effects were discerned (Figures 57A, C, E, G).

These studies collectively suggest that these drugs have the potential to influence BDNF expression levels when combined with H_2O_2 , while their interaction with corticosterone does not appear to produce significant effects.

7. Exploring the Role of Drug Repurposing in Bridging the Hypoxia–Depression Connection

Some evidence has established a potential relationship between hypoxia and depression (further explored in discussion). Consequently, and as a consequence of previous works within our research group [36], the present study aimed to elucidate the impact of hypoxia on the cellular response to pharmacological agents with potential to be used in depression. Thus, by the induction of hypoxia in SH-SY5Y cells through a hypoxia incubator chamber or CoCl_2 treatment, the effect of mirtazapine and other drugs with potential to be repurposed on depression (TCB-2, dextromethorphan, ketamine, quetiapine, scopolamine, celecoxib, and lamotrigine) on SH-SY5Y cellular viability and morphology was explored. Furthermore, we assessed the impact of these drugs under hypoxic conditions while inhibiting hypoxia-inducible factor 1 (HIF-1) using echinomycin.

This preliminary study seeks to understand how these compounds interact with hypoxia-induced cellular responses, with potential implications for depression management by targeting hypoxia-affected cellular mechanisms.

7.1. The Effect of the Hypoxia Incubator Chamber on SH-SY5Y Cellular Viability and Morphology

To evaluate the effect of a hypoxic environment (2% O₂, 10% CO₂, and 88% N₂ atmosphere) on the SH-SY5Y cells, first, it was compared both vehicle-treated cells under hypoxia or normoxia conditions (21% O₂). For these experiments, one plate was placed in the hypoxia incubator and the other plate was placed under normoxia conditions. After 48h, cellular viability was evaluated with MTT assay (Figure 58A). Cellular morphology assessment was also carried out (Figure 58B,C). After that, mirtazapine (Figures 59A,B and 60A), TCB-2 (Figures 59C,D and 60B), dextromethorphan (Figures 59E,F and 60C), ketamine (Figures 59G,H and 60D), quetiapine (Figures 59I, J and 60E), scopolamine (Figures 59K,L and 60F), celecoxib (Figures 59M,N and 60G), and lamotrigine (Figures 59O,P and 60H) were added to these cells in concentrations of 10 nM and 20 μM, for 48h, aiming to understand the effect of these drugs under a hypoxic environment induced by the hypoxia incubator. Cell viability was assessed using MTT (Figure 59), and morphological changes in the cells were also evaluated (Figure 60). Figure 61 demonstrates the effect of every single drug under normoxic conditions.

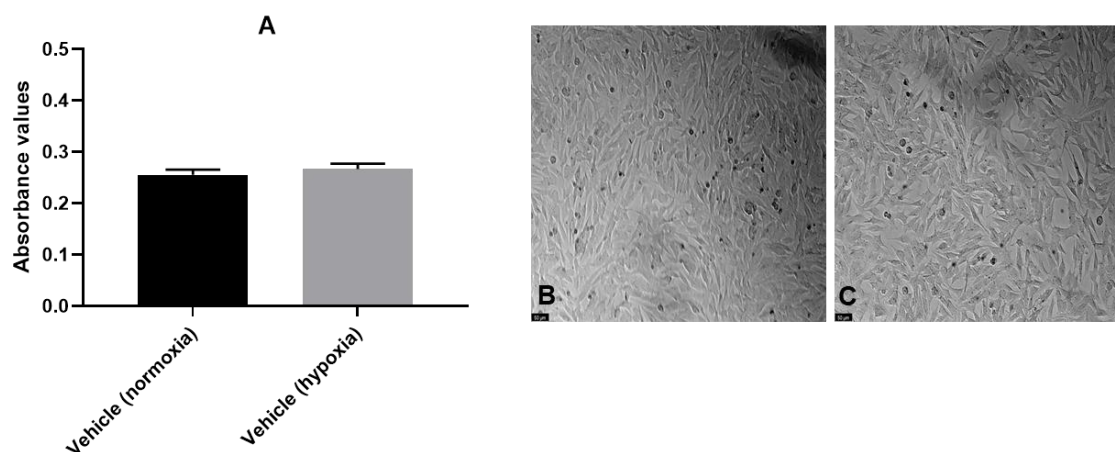


Figure 58. (A) Comparative effect of induced hypoxia (with the hypoxia incubator) vs. normoxia on SH-SY5Y cell lines, 48h. The results represent the mean ± SEM of three independent experiments, and representative images (100 × total magnification) of SH-SY5Y cells under (B) hypoxia and (C) normoxia. Scale bar: 50 μm.

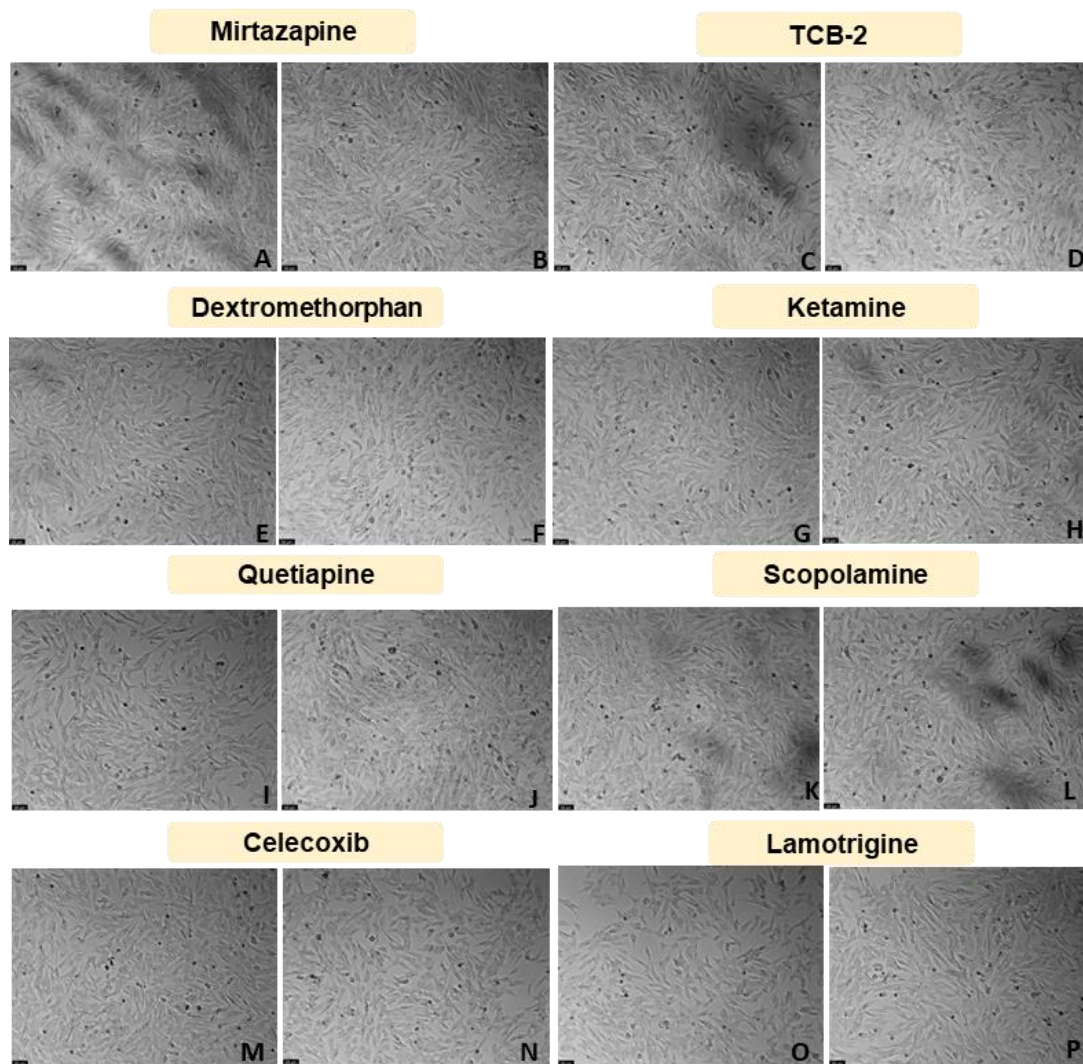


Figure 59. Representative images (100 × total magnification) of SH-SY5Y cells under hypoxia conditions, induced by the hypoxia incubator chamber. Cells were treated with (A) mirtazapine 10 nM, (B) mirtazapine 20 μM, (C) TCB-2 10 nM, (D) TCB-2 20 μM, (E) dextromethorphan 10 nM, (F) dextromethorphan 20 μM, (G) ketamine 10 nM, (H) ketamine 20 μM, (I) quetiapine 10 nM (J) quetiapine 20 μM, (K) scopolamine 10 nM, (L) scopolamine 20 μM, (M) celecoxib 10 nM, (N) celecoxib 20 μM, (O) lamotrigine 10 nM, and (P) lamotrigine 20 μM. Scale bar: 50 μm.

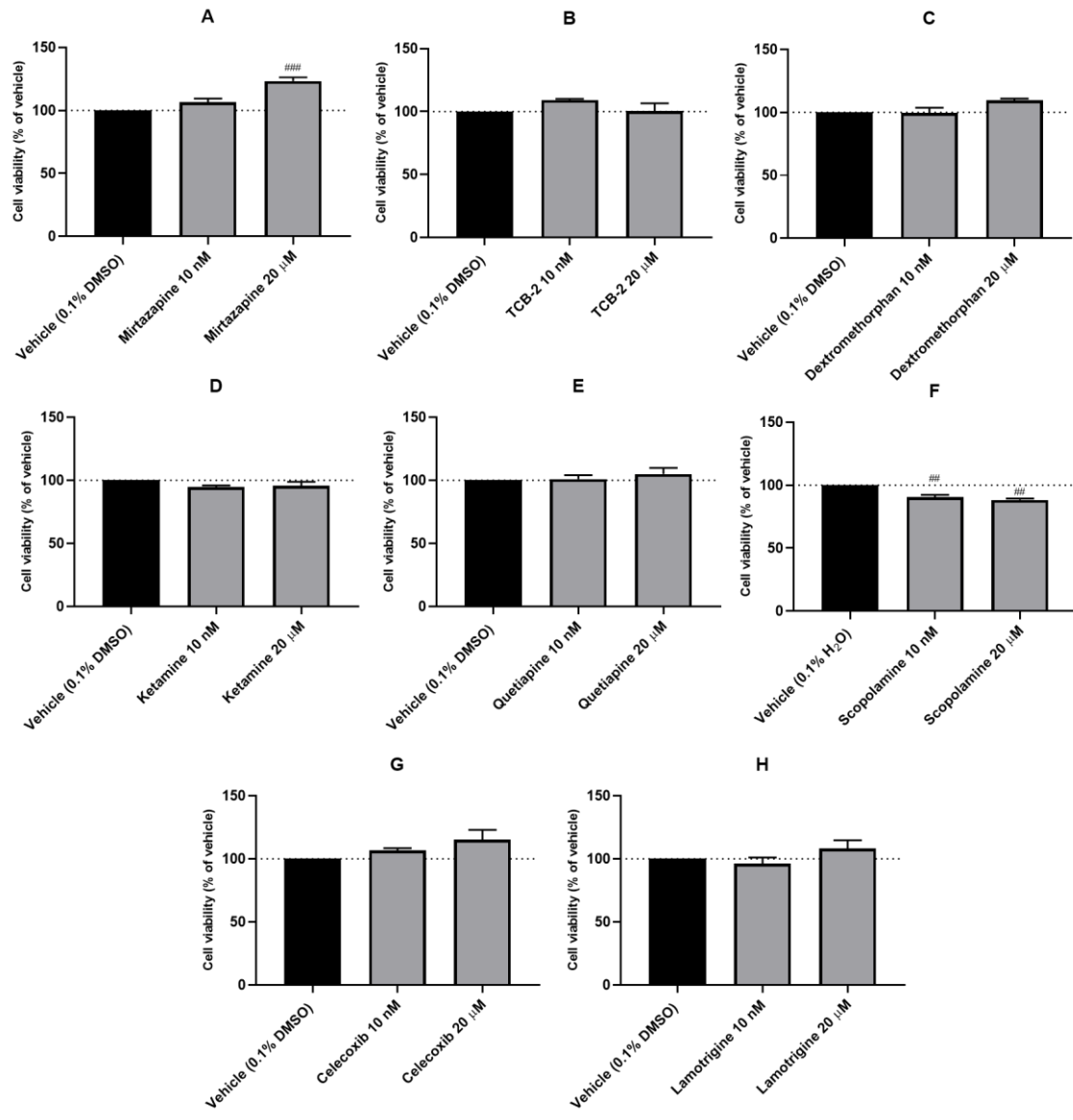


Figure 60. Effect of the incubation of 10 nM and 20 μM of (A) mirtazapine, (B) TCB-2, (C) dextromethorphan, (D) ketamine, (E) quetiapine, (F) scopolamine, (G) celecoxib, and (H) lamotrigine on the viability of SH-SY5Y cells, under hypoxia conditions induced by the hypoxia incubator chamber, determined by MTT assay. The results represent the mean ± SEM of three independent experiments, expressed as the percentage of the hypoxia vehicle (100%). Statistically significant ## $p < 0.01$ and ### $p < 0.001$ vs. vehicle.

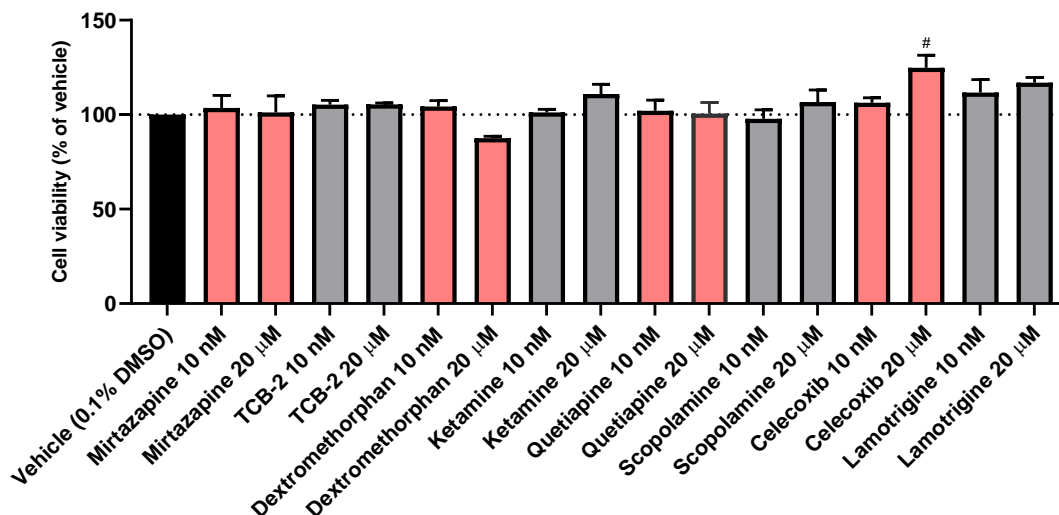


Figure 61. Effect of the incubation of 10 nM and 20 μM of mirtazapine, TCB-2, dextromethorphan, ketamine, quetiapine, scopolamine, celecoxib, and lamotrigine on the viability of SH-SY5Y cells, determined by MTT assay. The results represent the mean ± SEM of three independent experiments, expressed as the percentage of the normoxia vehicle (100%). Statistically significant # $p < 0.05$ vs. vehicle.

These findings indicate that 48h hypoxic exposure with the hypoxia chamber did not significantly alter cellular viability compared to normoxic conditions. Absorbance measurements, indicative of cell viability, were equivalent: 0.26 ± 0.01 under normoxia and 0.27 ± 0.01 under hypoxia (Figure 58A). Indeed, the morphological assessment confirmed no discernible differences between the two conditions, with cells maintaining a normal phenotype (Figure 58B,C).

Following cell treatment with the various pharmacological agents, analysis revealed that cellular morphology remained similar between treatment groups and vehicle controls (Figure 59). Moreover, cell viability assays indicated no significant deviation from control values (Figure 60). However, mirtazapine (20 μM) increased cell viability to $123.4\% \pm 2.9\%$ under hypoxia (Figure 60A). It is important to note that, as illustrated in Figure 61, none of these drugs had a significant impact on SH-SY5Y cells when compared to the cells treated with the vehicle, except celecoxib (20 μM).

7.2. The Effect of Chemically Induced Hypoxia with Cobalt Chloride on SH-SY5Y Cellular Viability and Morphology

To identify the optimal CoCl_2 concentration for chemically induce hypoxia, SHSY5Y cells were exposed to different concentrations of this compound (ranging from 0.1 to 1 mM) over a period of 48h, based on previous studies [417,418]. Cellular morphology is represented in Figure 62, while Figure 63 presents the data obtained from the MTT assay, which represents cell viability.

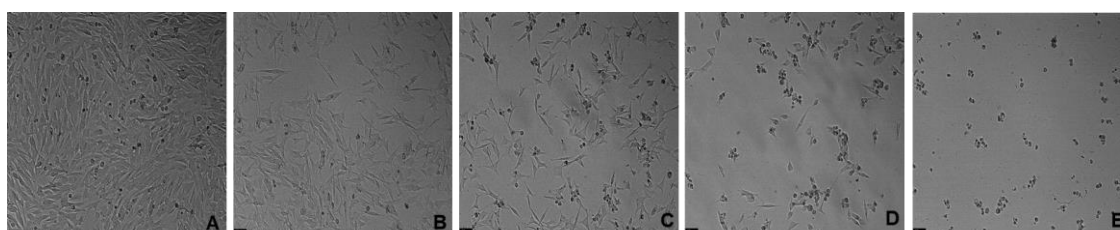


Figure 62. Representative images ($100\times$ total magnification) of SH-SY5Y cells after exposure to (A) 0.1% H_2O (vehicle), (B) CoCl_2 0.1 mM, (C) CoCl_2 0.25 mM, (D) CoCl_2 0.5 mM, and (E) CoCl_2 1 mM. Scale bar: 50 μm .

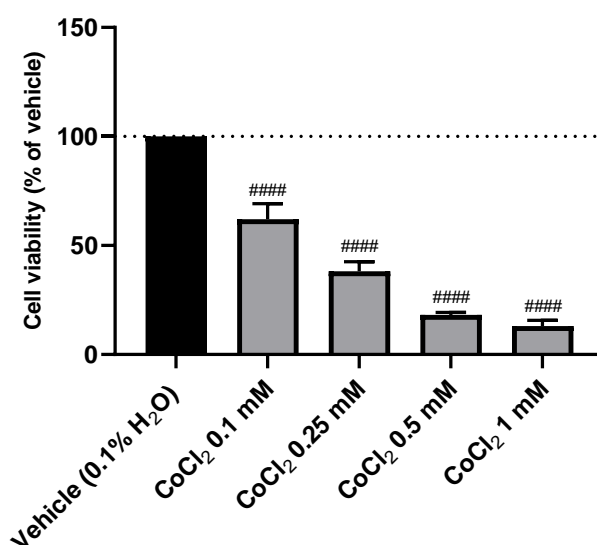


Figure 63. Effect of the incubation of 0.1–1 mM of CoCl_2 , on the viability of SH-SY5Y cells, determined by MTT assay. The results represent the mean \pm SEM of three independent experiments, expressed as the percentage of the vehicle (100%). Statistically significant #### $p < 0.0001$ vs. vehicle.

These findings demonstrate that the viability of cells decreases in response to increasing concentrations of CoCl_2 . This is clearly depicted in Figure 62, where it can be observed that higher concentrations of CoCl_2 result in a reduced number of cells, which

also exhibit more damage and a smaller, more rounded morphology. In line with previous studies [417,418], it was selected a concentration of CoCl_2 that would cause approximately half of the cells to be damaged. This approach allowed the observation of the cellular response to hypoxia-induced damage without causing harm to all cells. Consequently, a concentration of 0.1 mM CoCl_2 to induce chemical hypoxia in the cells was selected, which led to a cell viability of $62.1\% \pm 3.1\%$ (Figure 63).

7.3. The Effect of Echinomycin and the Combination of Echinomycin with Cobalt Chloride on SH-SY5Y Cellular Viability and Morphology

After determining the optimal concentration of CoCl_2 to chemically induce cellular hypoxia, the identification of the ideal concentration of echinomycin for inhibiting HIF-1 DNA-binding and transcriptional activity was carried out. Echinomycin was introduced to the cells for a 48h incubation period, using a range of concentrations from 0.1 to 5 nM, based on previous studies [419,420]. Figure 64 illustrates the analysis of cellular morphology, while cell viability was assessed through the MTT assay, as shown in Figure 65.

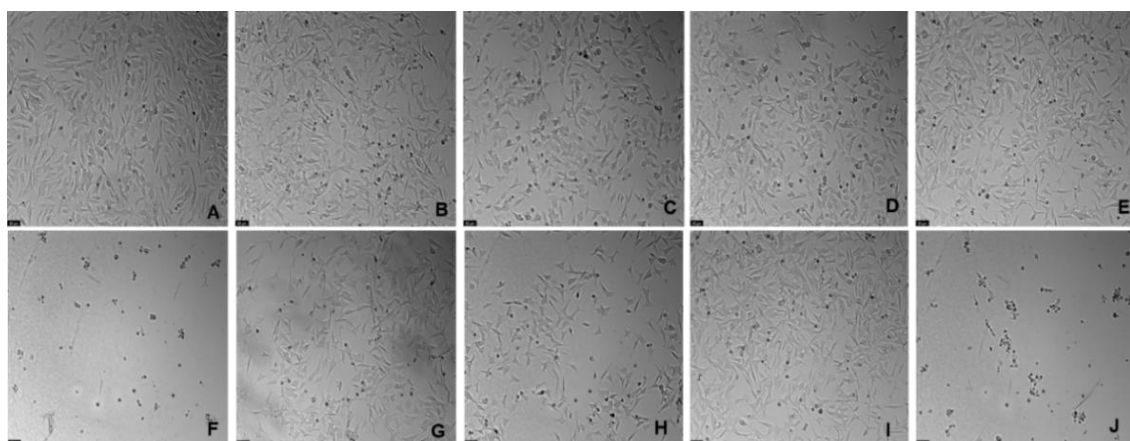


Figure 64. Representative images ($100 \times$ total magnification) of SH-SY5Y cells treated with (A) vehicle (0.1% DMSO), (B) CoCl_2 0.1 mM, (C) echinomycin 0.1 nM, (D) echinomycin 0.5 nM, (E) echinomycin 1 nM, (F) echinomycin 5 nM, (G) CoCl_2 0.1 mM + echinomycin 0.1 nM, (H) CoCl_2 0.1 mM + echinomycin 0.5 nM (I) CoCl_2 0.1 mM + echinomycin 1 nM, and (J) CoCl_2 0.1 mM + echinomycin 5 nM. Scale bar: 50 μm .

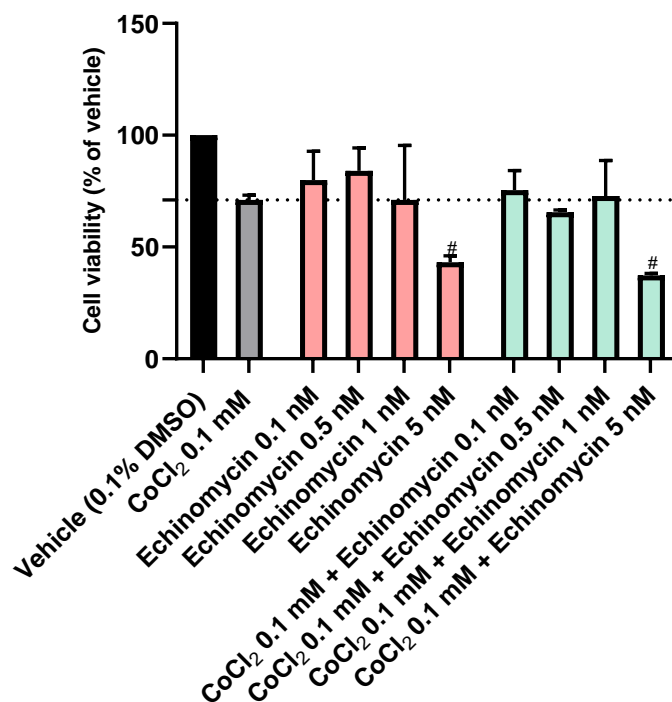


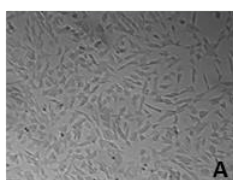
Figure 65. Effect of the incubation of CoCl₂ 0.1 mM, echinomycin 0.1 nM-5 nM, and the combination of CoCl₂ 0.1 mM with echinomycin 0.1 nM-5 nM on the viability of SH-SY5Y cells, determined by MTT assay. The results represent the mean \pm SEM of three independent experiments, expressed as the percentage of the vehicle (100%). Statistically significant # $p < 0.05$ vs. vehicle.

Following data analysis, it was apparent that echinomycin exerted a concentration-dependent influence on cellular viability (Figures 64 and 65). Furthermore, as depicted in Figure 64, higher concentrations of echinomycin resulted in a notable decrease in the cell number and an increase in cellular damage, characterized by a more pronounced round morphology and a reduction in cell size. As a result of these observations, the concentration of 0.5 nM echinomycin to proceed with the study was selected. Notably, this selected concentration did not elicit significant cell death under normoxic conditions. Moreover, when combined with CoCl₂ at a concentration of 0.1 mM, this compound did not significantly induce a reduction in cell viability compared to cells treated solely with CoCl₂.

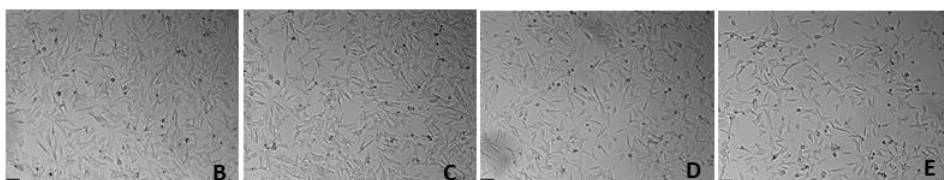
7.4. The Effect of Echinomycin and Cobalt Chloride on SH-SY5Y Cellular Viability and Morphology After Drug Application

Then, to investigate the impact of the tested drugs on SH-SY5Y cells under conditions involving both CoCl₂ treatment and CoCl₂ treatment with HIF-1 inhibition using echinomycin, CoCl₂ at 0.1 mM was combined with 10 nM and 20 μM of mirtazapine (Figures 66B-E and 67A), dextromethorphan (Figures 66F-G and 67B), quetiapine (Figures 66J-K and 67C), celecoxib (Figures 66N-O and 67D), TCB-2 (Figures 66R-U and 67E), ketamine (Figures 66V-Y and 67F), scopolamine (Figures 66Z-AC and 67G), and lamotrigine (Figures 66AD-AG and 67H). Additionally, CoCl₂ was combined with the same compounds along with echinomycin at a concentration of 0.5 nM, and this incubation was maintained for 48h. Morphological analysis was conducted (Figure 66), followed by the assessment of cellular viability through the MTT assay (Figure 67).

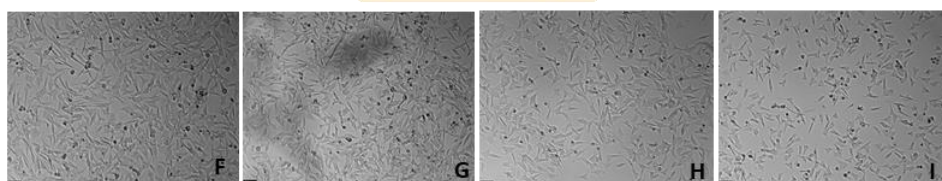
Vehicle (0.2% DMSO)



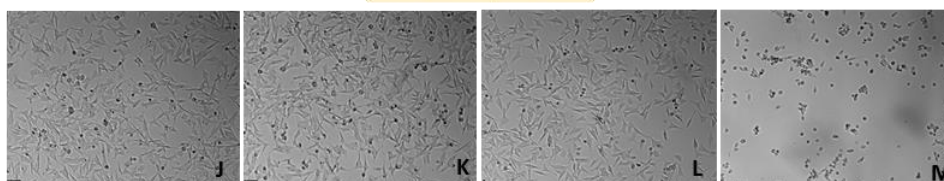
Mirtazapine



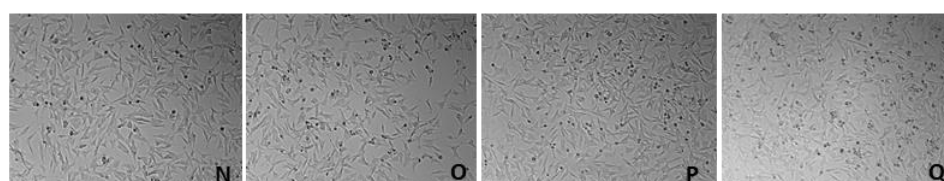
Dextromethorphan



Quetiapine



Celecoxib



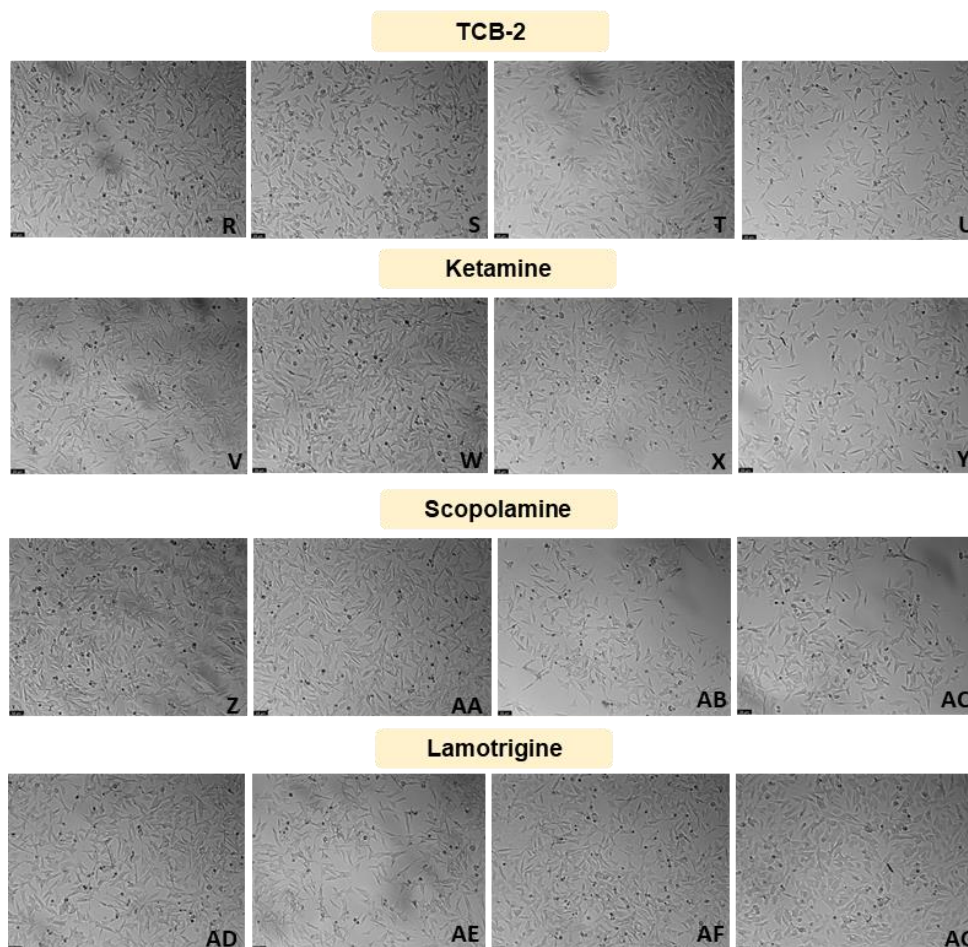


Figure 66. Representative images (100 × total magnification) of SH-SY5Y cells treated with (A) vehicle (0.2% DMSO), (B) CoCl_2 0.1 mM + mirtazapine 10 nM, (C) CoCl_2 0.1 mM + mirtazapine 20 μM , (D) echinomycin 0.5 nM + CoCl_2 0.1 mM + mirtazapine 10 nM, (E) echinomycin 0.5 nM + CoCl_2 0.1 mM + mirtazapine 20 μM , (F) CoCl_2 0.1 mM + dextromethorphan 10 nM, (G) CoCl_2 0.1 mM + dextromethorphan 20 μM , (H) echinomycin 0.5 nM + CoCl_2 0.1 mM + dextromethorphan 10 nM, (I) echinomycin 0.5 nM + CoCl_2 0.1 mM + dextromethorphan 20 μM , (J) CoCl_2 0.1 mM + quetiapine 10 nM, (K) CoCl_2 0.1 mM + quetiapine 20 μM , (L) echinomycin 0.5 nM + CoCl_2 0.1 mM + quetiapine 10 nM, (M) Echinomycin 0.5 nM + CoCl_2 0.1 mM + quetiapine 20 μM , (N) CoCl_2 0.1 mM + celecoxib 10 nM, (O) CoCl_2 0.1 mM + celecoxib 20 μM , (P) echinomycin 0.5 nM + CoCl_2 0.1 mM + celecoxib 10 nM, (Q) echinomycin 0.5 nM + CoCl_2 0.1 mM + celecoxib 20 μM , (R) CoCl_2 0.1 mM + TCB-2 10 nM, (S) CoCl_2 0.1 mM + TCB-2 20 μM , (T) echinomycin 0.5 nM + CoCl_2 0.1 mM + TCB-2 10 nM, (U) echinomycin 0.5 nM + CoCl_2 0.1 mM + TCB-2 20 μM , (V) CoCl_2 0.1 mM + ketamine 10 nM (W) CoCl_2 0.1 mM + ketamine 20 μM , (X) echinomycin 0.5 nM + CoCl_2 0.1 mM + ketamine 10 nM, (Y) echinomycin 0.5 nM + CoCl_2 0.1 mM + ketamine 20 μM , (Z) CoCl_2 0.1 mM + scopolamine 10 nM, (AA) CoCl_2 0.1 mM + scopolamine 20 μM , (AB) echinomycin 0.5 nM + CoCl_2 0.1 mM + scopolamine 10 nM, (AC) echinomycin 0.5 nM + CoCl_2 0.1 mM + scopolamine 20 μM , (AD) CoCl_2 0.1 mM + lamotrigine 10 nM, and (AE) CoCl_2 0.1 mM + lamotrigine 20 μM , (AF) echinomycin 0.5 nM + CoCl_2 0.1 mM + lamotrigine 10 nM, and (AG) echinomycin 0.5 nM + CoCl_2 0.1 mM + lamotrigine 20 μM . Scale bar: 50 μm .

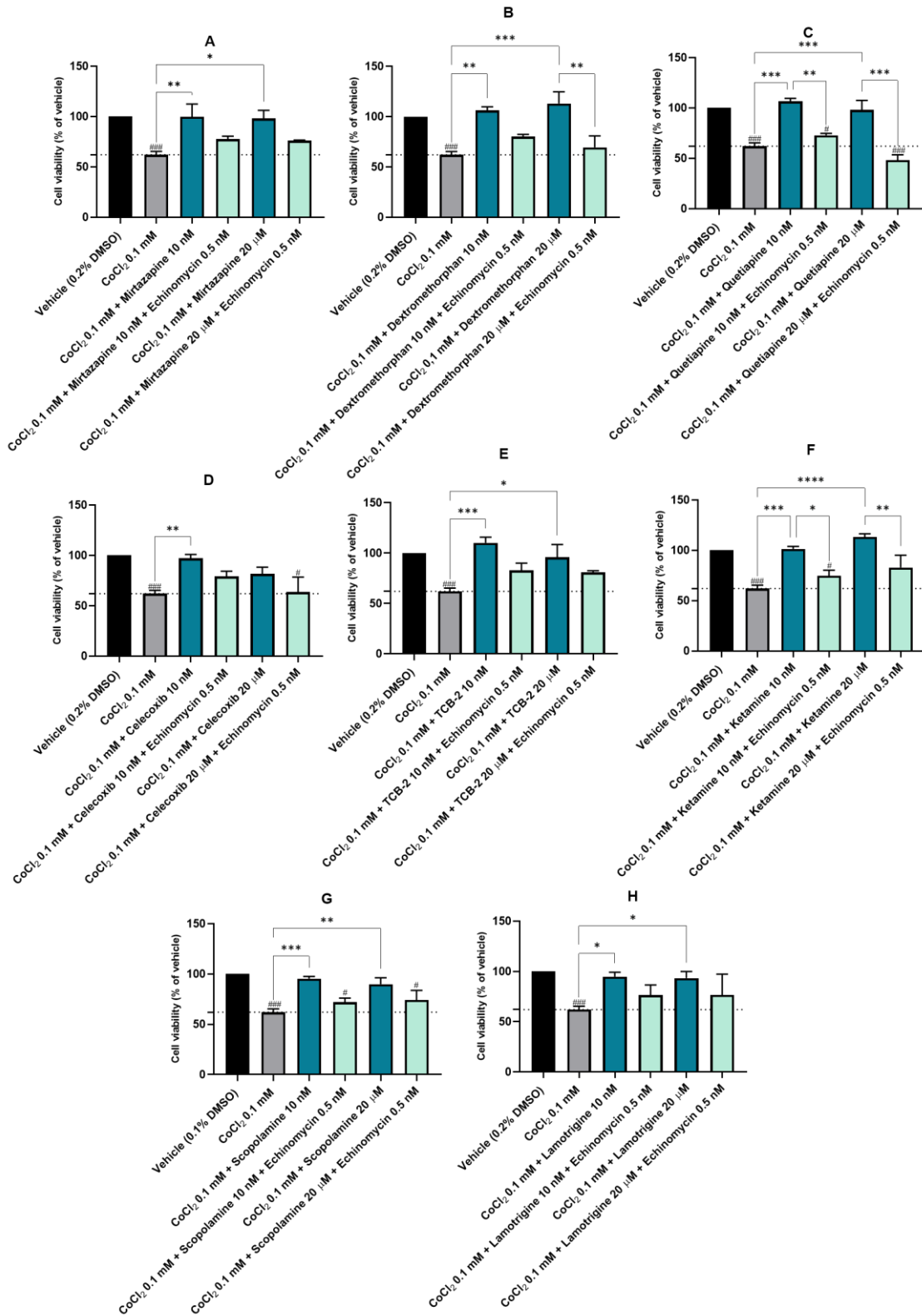


Figure 67. Effect of the incubation of SH-SY5Y cells with CoCl₂ 0.1 mM in combination with either 10 nM or 20 μM of (A) mirtazapine, (B) dextromethorphan, (C) quetiapine, (D) celecoxib, (E) TCB-2, (F) ketamine, (G) scopolamine, and (H) lamotrigine on cell viability, and effect of incubating these cells with a combination of CoCl₂ 0.1 mM, echinomycin 0.5 nM, and either 10 nM or 20 μM of the same compounds (A-H) on cell viability, using the MTT assay. The results represent the mean ± SEM of three independent experiments, expressed

as the percentage of the vehicle (100%). Statistically significant # $p < 0.05$, ### $p < 0.001$, vs. vehicle, and * $p < 0.05$, ** $p < 0.01$, *** $p < 0.001$, and **** $p < 0.0001$ vs. CoCl_2 0.1 mM or CoCl_2 0.1 mM combined with the different drugs.

These findings demonstrate that all the drugs, except celecoxib (20 μM), at both concentrations, significantly enhanced cell viability in comparison to the cells treated with CoCl_2 alone. When comparing the cellular viability values obtained from combinations of CoCl_2 and the tested drugs with those obtained from the introduction of echinomycin into these combinations, our findings indicate that all drugs, across all tested concentrations, exhibited a reduction in cell viability when combined with echinomycin under CoCl_2 -induced hypoxia conditions. Notably, statistically significant reductions were observed with dextromethorphan at 20 μM ($69.5\% \pm 11.4\%$ vs. $113.1\% \pm 11.7\%$), quetiapine at 10 nM ($72.9\% \pm 1.93\%$ vs. $106.5\% \pm 3.1\%$) and 20 μM ($48.2\% \pm 5.3\%$ vs. $98.1\% \pm 0.5\%$), ketamine at 10 nM ($74.7\% \pm 5.4\%$ vs. $101.4\% \pm 2.6\%$) and 20 μM ($82.8\% \pm 12.4\%$ vs. $113.3\% \pm 3.1\%$). It is worth highlighting the consistent agreement between the MTT assay results and the morphological evaluation of the cells. These results will be further discussed.

8. Supplementary Results

8.1. Assessing the Impact of 24-Hour Exposure to Mirtazapine and Its Combination with Hydrogen Peroxide on the Viability of SH-SY5Y Cells

To explore the impact of a shorter incubation period with mirtazapine alone, and in combination with H₂O₂ on the viability and morphology of SH-SY5Y cells, mirtazapine was applied to the cell cultures in a range of concentrations from 0.01 to 20 μM. Additionally, it was combined with H₂O₂ at a concentration of 132 μM, correlating to the IC₅₀ value for SH-SY5Y cell viability, as detailed in Table 8. The cellular morphology was evaluated immediately after 24 hours of treatment (Figure S1). Subsequently, the cellular viability was measured using the MTT assay (Figure S2).

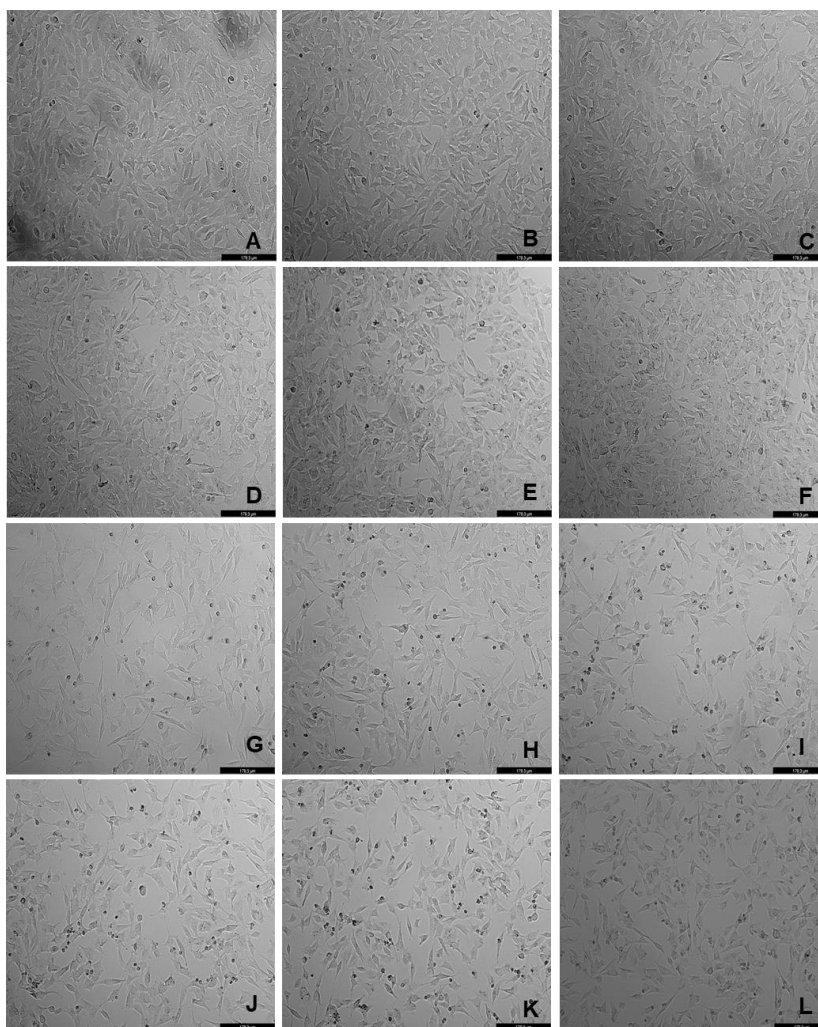


Figure S1. Representative images (total magnification 100x) of SH-SY5Y cells morphology after exposure to mirtazapine, H₂O₂, and to the combination of mirtazapine with H₂O₂. Cells were incubated with (A) vehicle (0.1% methanol), (B) mirtazapine 0.01 μM, (C) mirtazapine 0.1 μM, (D) mirtazapine 1 μM, (E) mirtazapine 10 μM, (F) mirtazapine 20 μM, (G) H₂O₂ 132 μM, (H) H₂O₂ 132 μM + mirtazapine 0.01 μM, (I) H₂O₂ 132 μM + mirtazapine 0.1 μM, (J) H₂O₂ 132 μM + mirtazapine 1 μM, (K) H₂O₂ 132 μM + mirtazapine 10 μM, (L) H₂O₂ 132 μM + mirtazapine 20 μM. Scale bar: 179.3 μm.

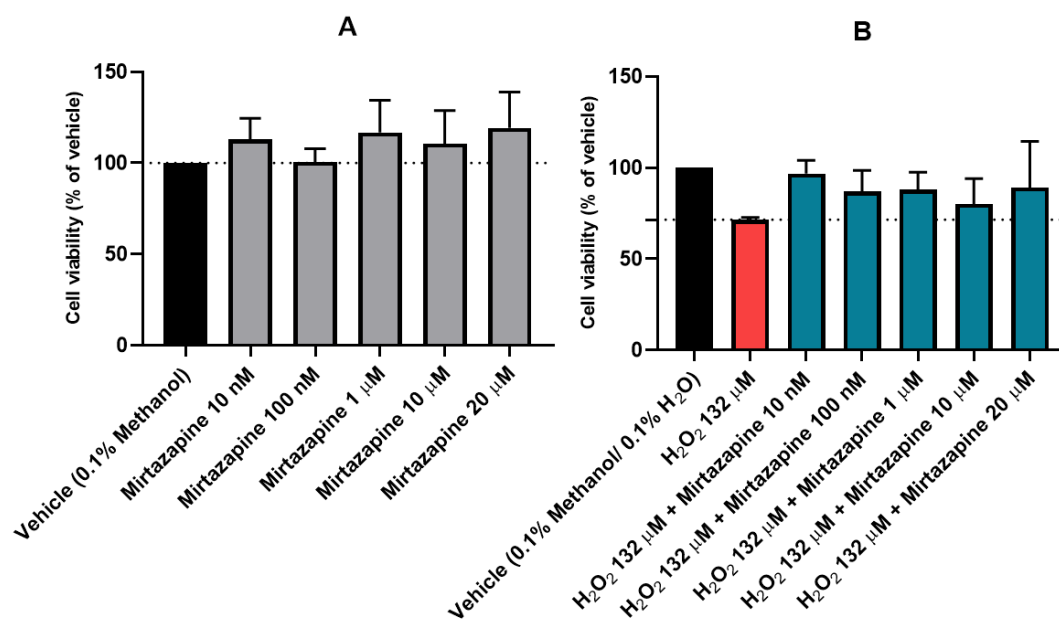


Figure S2. Effect of increasing concentrations of (A) mirtazapine, and (B) mirtazapine in combination with H₂O₂, on the viability of SH-SY5Y cells, obtained by the MTT assay. The results are expressed as the percentage of the respective vehicles and represent the mean \pm SEM of three independent experiments.

These results indicate that mirtazapine showed no toxicity across various concentrations tested (Figure S1A-F and Figure S2A). While it appeared to mitigate H₂O₂-induced cell viability reduction, these effects lacked statistical significance, compared to the 48h results (Figure 20A).

8.2. Effect of Serotonin Exposure on SH-SY5Y and HT-22 Cellular Viability

After exploring mirtazapine and L-TRP in more detail, it was interesting to further explore the role of 5-HT to attenuate H₂O₂ or corticosterone-induced stress on SH-SY5Y and HT-22 cells. For that, 5-HT (alone) was first added to the cells in concentrations ranging from 0.1 nM to 100 μ M for 48h. Following this, cell morphology was analyzed (Figure S3), and cellular viability was assessed using the MTT assay (Figure S4).

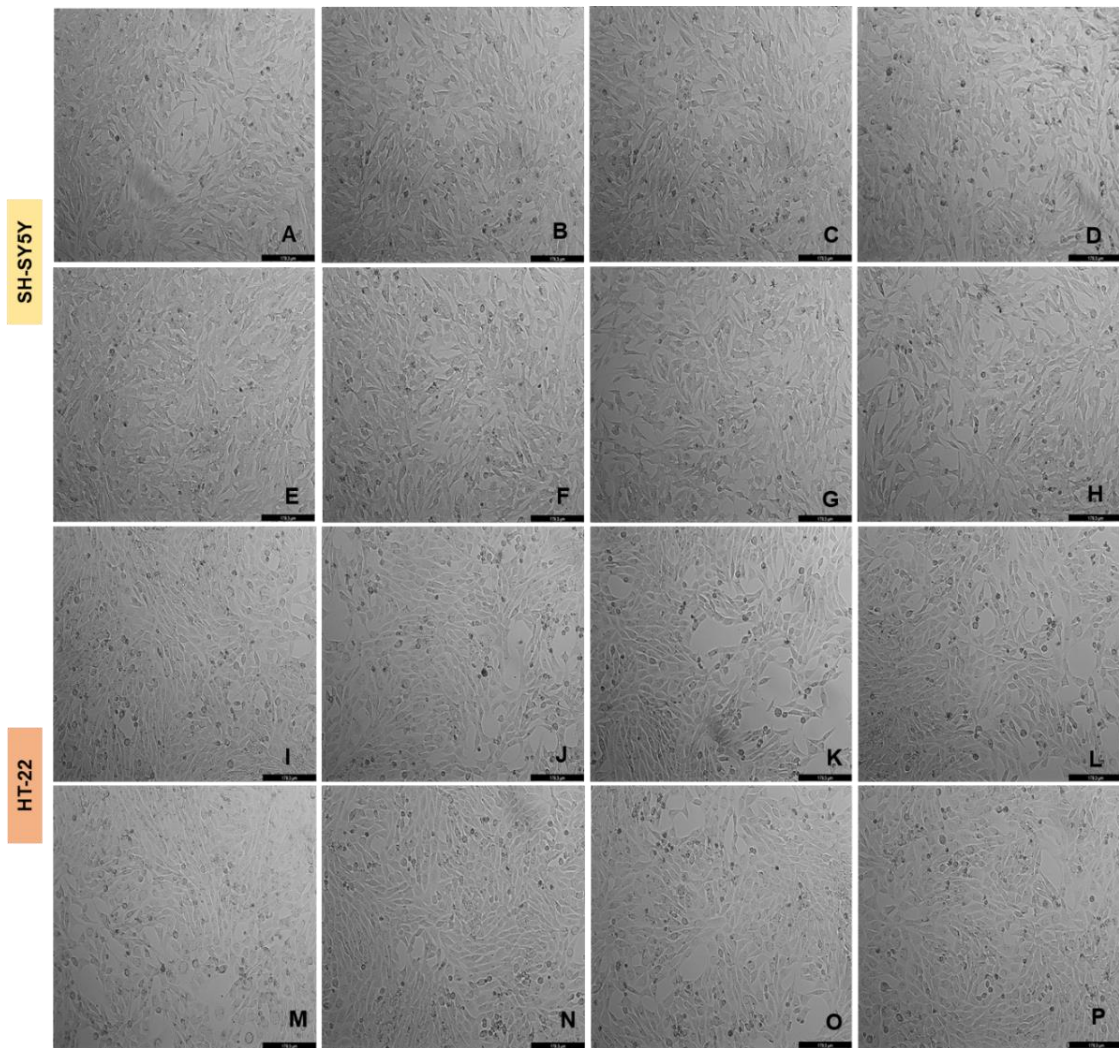


Figure S3. Representative images (100 × total magnification) of SH-SY5Y and HT-22 cells after incubation of increasing concentrations of L-TRP. Cells were treated with (A,I) vehicle (0.1% H₂O) (B,J) 5-HT 0.1 nM, (C,K) 5-HT 1 nM, (D,L) 5-HT 10 nM, (E,M) 5-HT 100 nM, (F,N) 5-HT 1 μM, (G,O) 5-HT 10 μM, (H,P) 5-HT 100 μM. Scale bar: 179.3 μm.

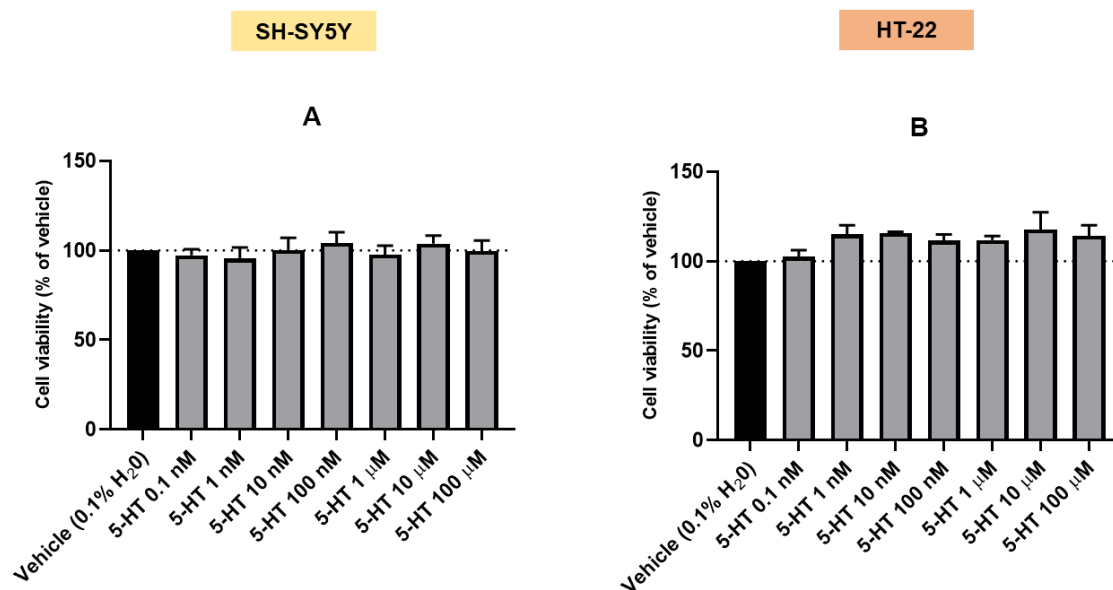


Figure S4. Effect of the incubation of 0.1 nM-100 μM of 5-HT on the viability of (A) SH-SY5Y cells and (B) HT-22 cells, determined by MTT methodology. The results represent the mean ± SEM of three independent experiments, expressed as the percentage of the vehicle (100%).

Analyzing these results, it can be inferred that, much like mirtazapine (Figure 10) and L-TRP (Figure 24), 5-HT demonstrated no signs of toxicity towards the cells across all tested concentrations.

8.3. Effect of the Combination of Serotonin with Hydrogen Peroxide and Corticosterone on SH-SY5Y and HT-22 Cellular Viability

To determine the impact of 5-HT combined with H₂O₂ (Figures S5 and S6) or corticosterone (Figures S7 and S8) on SH-SY5Y and HT-22 cell viability, 5-HT was introduced at concentrations ranging from 0.1 nM to 100 μM, H₂O₂ was added at 132 μM for SH-SY5Y cells and 105 μM for HT-22 cells, and corticosterone was added at 322 μM and 35 μM for SH-SY5Y cells and HT-22 cells, respectively, for a period of incubation of 48h. Cell morphology was then analyzed (Figures S5 and S7), followed by a cellular viability evaluation using the MTT assay (Figure S6 and S8).

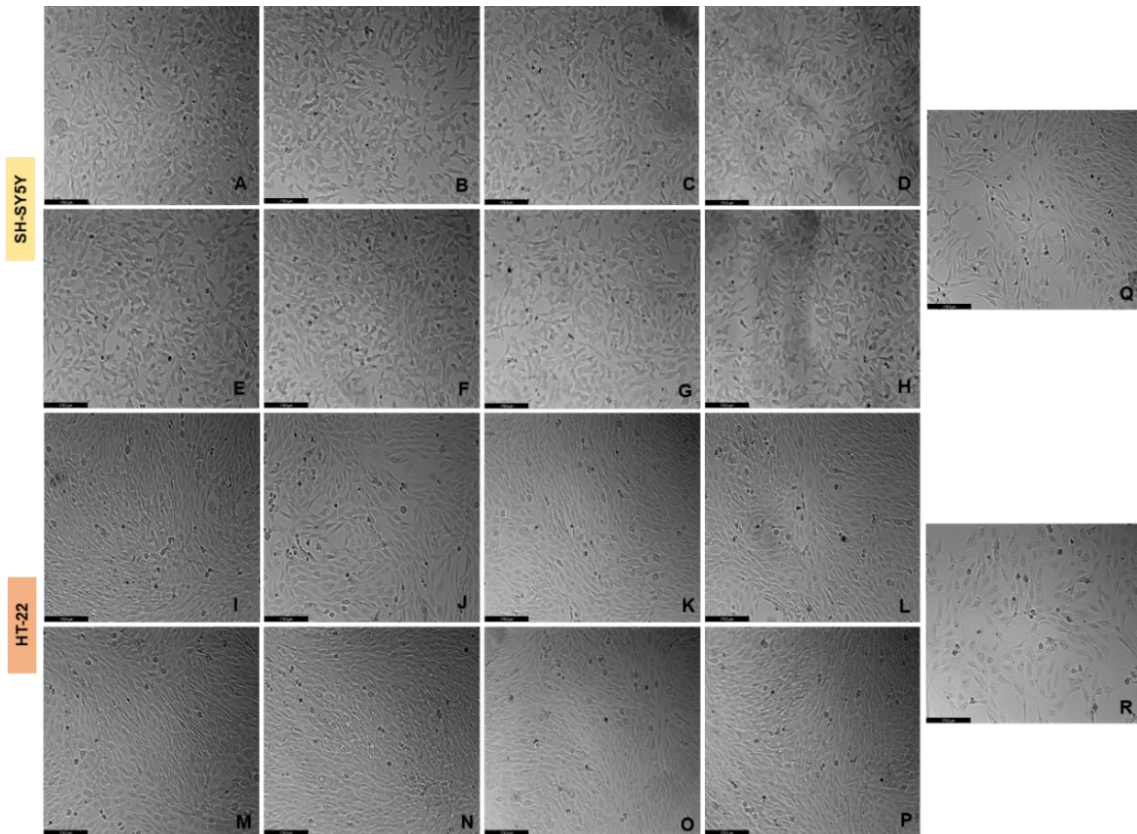


Figure S5. Representative images (100 × total magnification) of SH-SY5Y and HT-22 cells after incubation of H₂O₂ in combination with 5-HT. Cells were treated with (A,I) vehicle (0.1% H₂O), (B,J) 5-HT 0.1 nM + H₂O₂ 132 μM/ 105 μM, (C,K) 5-HT 1 nM + H₂O₂ 132 μM/ 105 μM, (D,L) 5-HT 10 nM + H₂O₂ 132 μM/ 105 μM, (E,M) 5-HT 100 nM + H₂O₂ 132 μM/ 105 μM, (F,N) 5-HT 1 μM + H₂O₂ 132 μM/ 105 μM, (G,O) 5-HT 10 μM + H₂O₂ 132 μM/ 105 μM, (H,P) 5-HT 100 μM + H₂O₂ 132 μM/ 105 μM, (Q) H₂O₂ 132 μM, (R) H₂O₂ 105 μM. Scale bar: 179.3 μm.

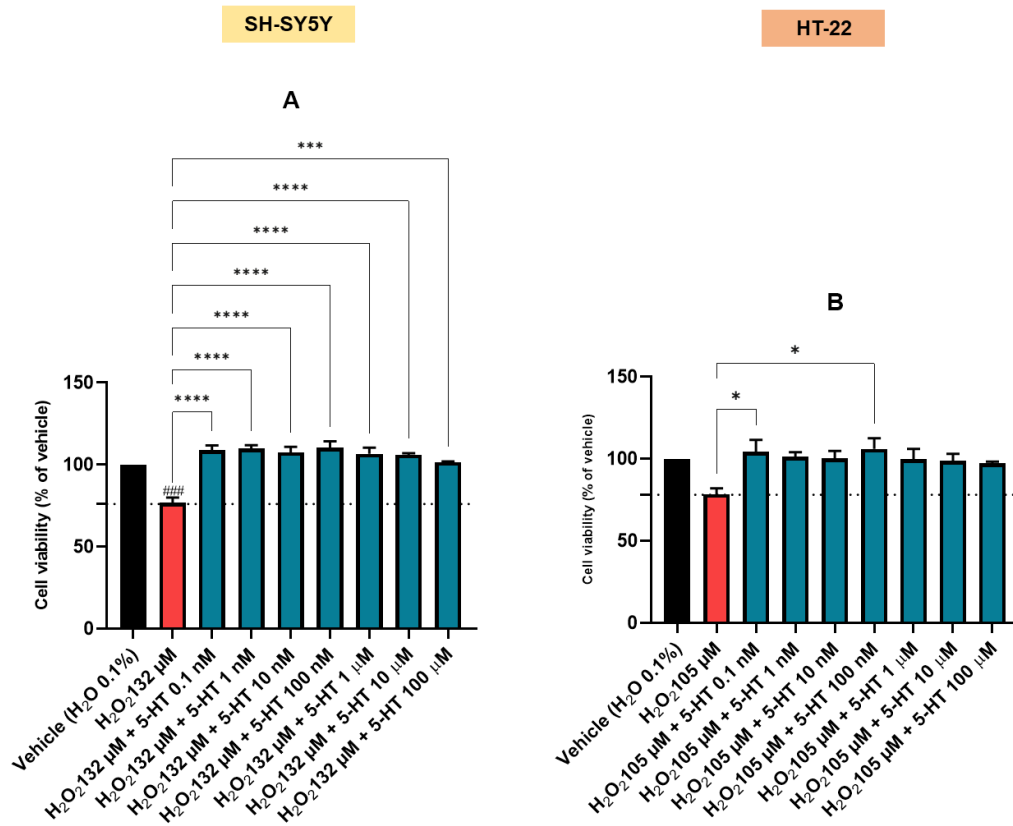


Figure S6. Effect of the incubation of (A) 132 μM of H₂O₂ and (B) 105 μM of H₂O₂, in combination with 0.1 nM–100 μM of 5-HT, determined by MTT methodology. The results represent the mean ± SEM of three independent experiments, expressed as the percentage of the vehicle (100%). Statistically significant ### p < 0.001 vs. vehicle, * p < 0.05 vs. H₂O₂ 105 μM, and *** p < 0.001, **** p < 0.0001 vs. H₂O₂ 132 μM.

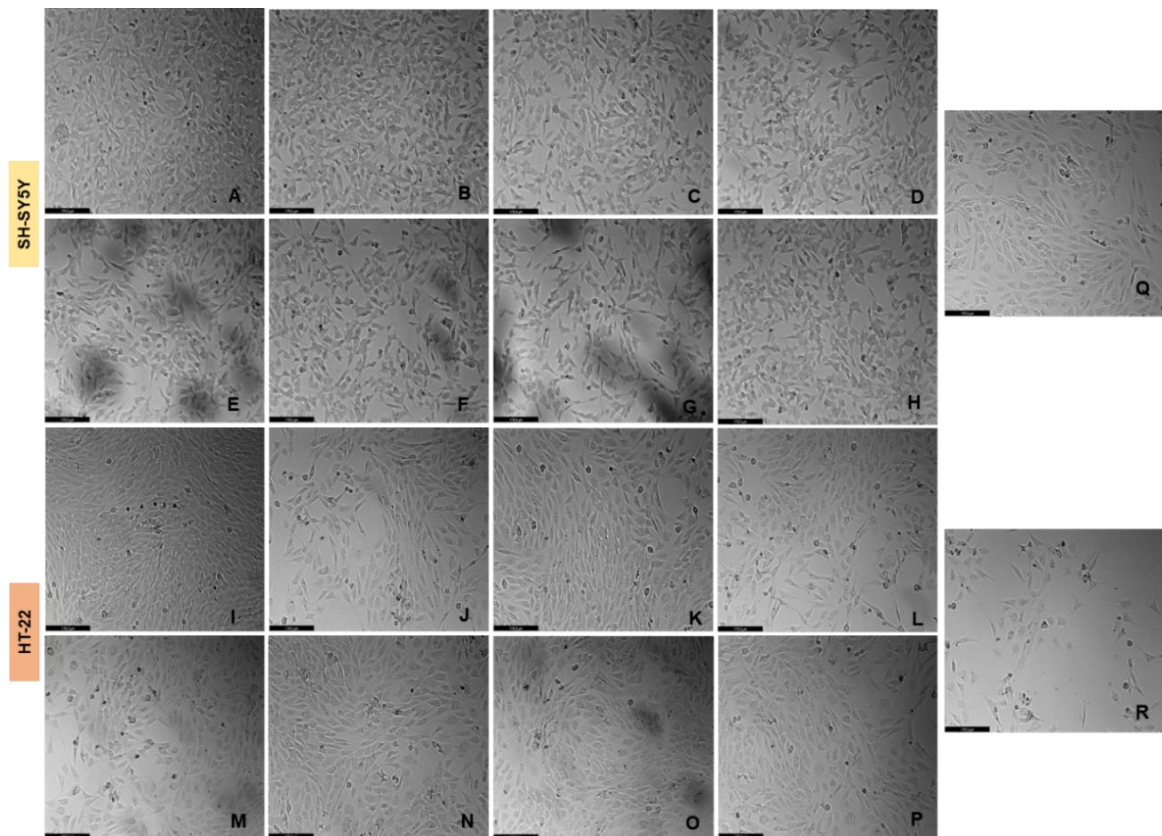


Figure S7. Representative images (100 × total magnification) of SH-SY5Y and HT-22 cells after incubation of corticosterone in combination with 5-HT. Cells were treated with (A,I) vehicle (0.1% methanol), (B,J) 5-HT 0.1 nM + corticosterone 322 μM/ 35 μM, (C,K) 5-HT 1 nM + corticosterone 322 μM/ 35 μM, (D,L) 5-HT 10 nM + corticosterone 322 μM/ 35 μM, (E,M) 5-HT 100 nM + corticosterone 322 μM/ 35 μM, (F,N) 5-HT 1 μM + corticosterone 322 μM/ 35 μM, (G,O) 5-HT 10 μM + corticosterone 322 μM/ 35 μM, (H,P) 5-HT 100 μM + corticosterone 322 μM/ 35 μM, (Q) corticosterone 322 μM, (R) corticosterone 35 μM. Scale bar: 179.3 μm.

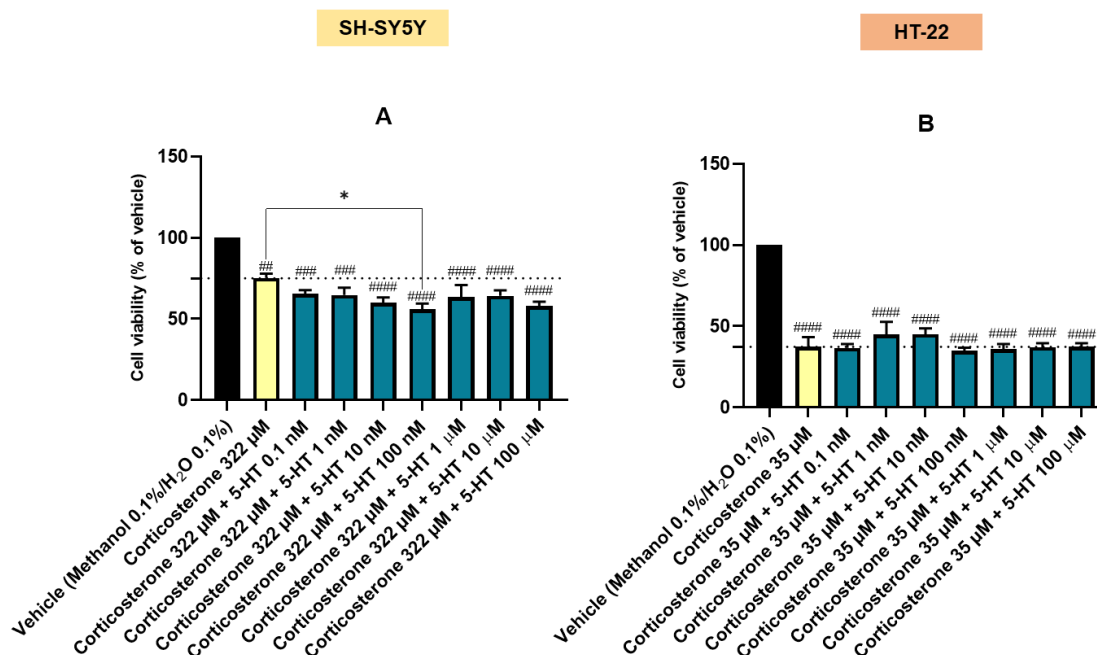


Figure S8. Effect of the incubation of (A) 322 μM of corticosterone and (B) 35 μM of corticosterone, in combination with 0.1 nM–100 μM of 5-HT, determined by MTT methodology. The results represent the mean ± SEM of three independent experiments, expressed as the percentage of the vehicle (100%). Statistically significant ## p < 0.01, ### p < 0.001, #### p < 0.0001 vs. vehicle, and * p < 0.05 vs. corticosterone 322 μM.

Analysis of these results highlighted that 5-HT effectively improved cellular viability in response to H₂O₂ exposure, particularly in SH-SY5Y cells, with a discernible trend in HT-22 cells (Figures S5 and S6). This suggests that, similar to L-TRP and mirtazapine, 5-HT has potential as a stress mitigation agent (Figures 20 and 26). However, it did not exhibit efficacy in countering the effects of corticosterone exposure (Figures S7 and S8), consistent with the findings for L-TRP and mirtazapine (Figures 22 and 28).

8.4. Effect of Quetiapine, Ketamine, Dextromethorphan, Celecoxib and TCB-2 in Combination with Hydrogen Peroxide and Corticosterone on SH-SY5Y Cell Viability

Consistent with the study conducted in subsection 7.4, the effects of combining quetiapine, ketamine, dextromethorphan, celecoxib, and TCB-2 with H₂O₂ and corticosterone on the viability of SH-SY5Y cells were explored. For this experiment, each drug was applied at a fixed concentration of 20 μM, in combination with 132 μM of H₂O₂ and 322 μM of corticosterone. Morphological analysis was conducted (Figures S9 and

10), followed by the assessment of cellular viability through the MTT assay (Figure S11 and S12), after 48h.

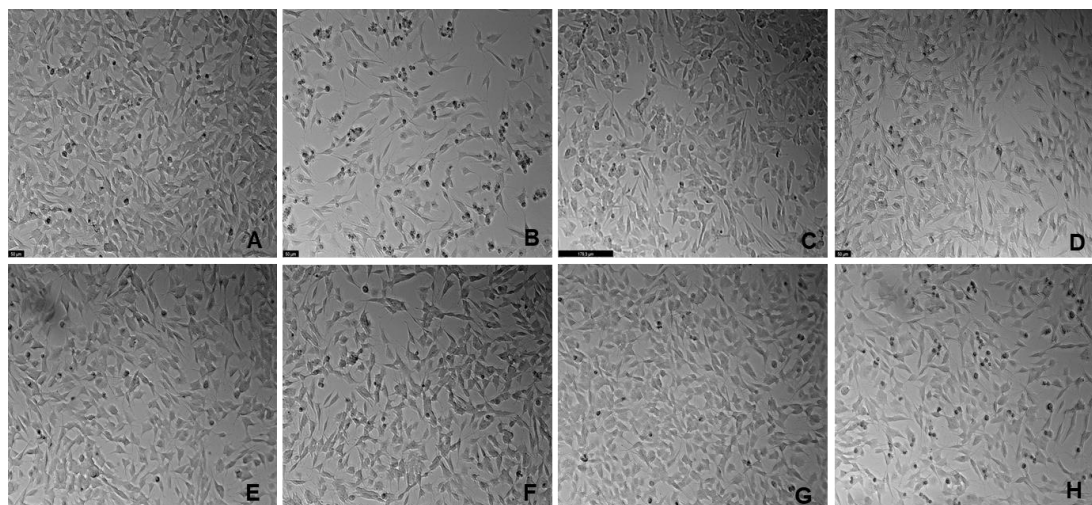


Figure S9. Representative images (100 × total magnification) of SH-SY5Y after incubation of (A) vehicle (0.1% DMSO), (B) H₂O₂ 132 μM, (C) corticosterone 322 μM, (D) quetiapine 20 μM, (E) ketamine 20 μM, (F) dextromethorphan 20 μM, (G) celecoxib 20 μM, (H) TCB-2 20 μM. Scale bars: 50 and 179.3 μm.

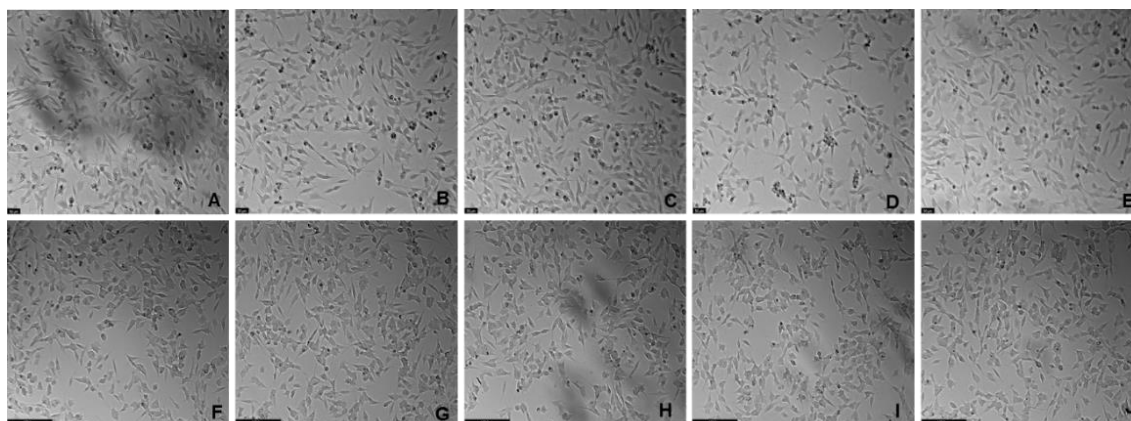


Figure S10. Representative images (100 × total magnification) of SH-SY5Y after incubation of (A) quetiapine 20 μM + H₂O₂ 132 μM, (B) ketamine 20 μM + H₂O₂ 132 μM, (C) dextromethorphan 20 μM + H₂O₂ 132 μM, (D) celecoxib 20 μM + H₂O₂ 132 μM, (E) TCB-2 20 μM + H₂O₂ 132 μM, (F) quetiapine 20 μM + corticosterone 332 μM, (G) ketamine 20 μM + corticosterone 332 μM, (H) dextromethorphan 20 μM + corticosterone 332 μM, (I) celecoxib 20 μM + corticosterone 332 μM, (J) TCB-2 20 μM + corticosterone 332 μM. Scale bars: 50 and 179.3 μm.

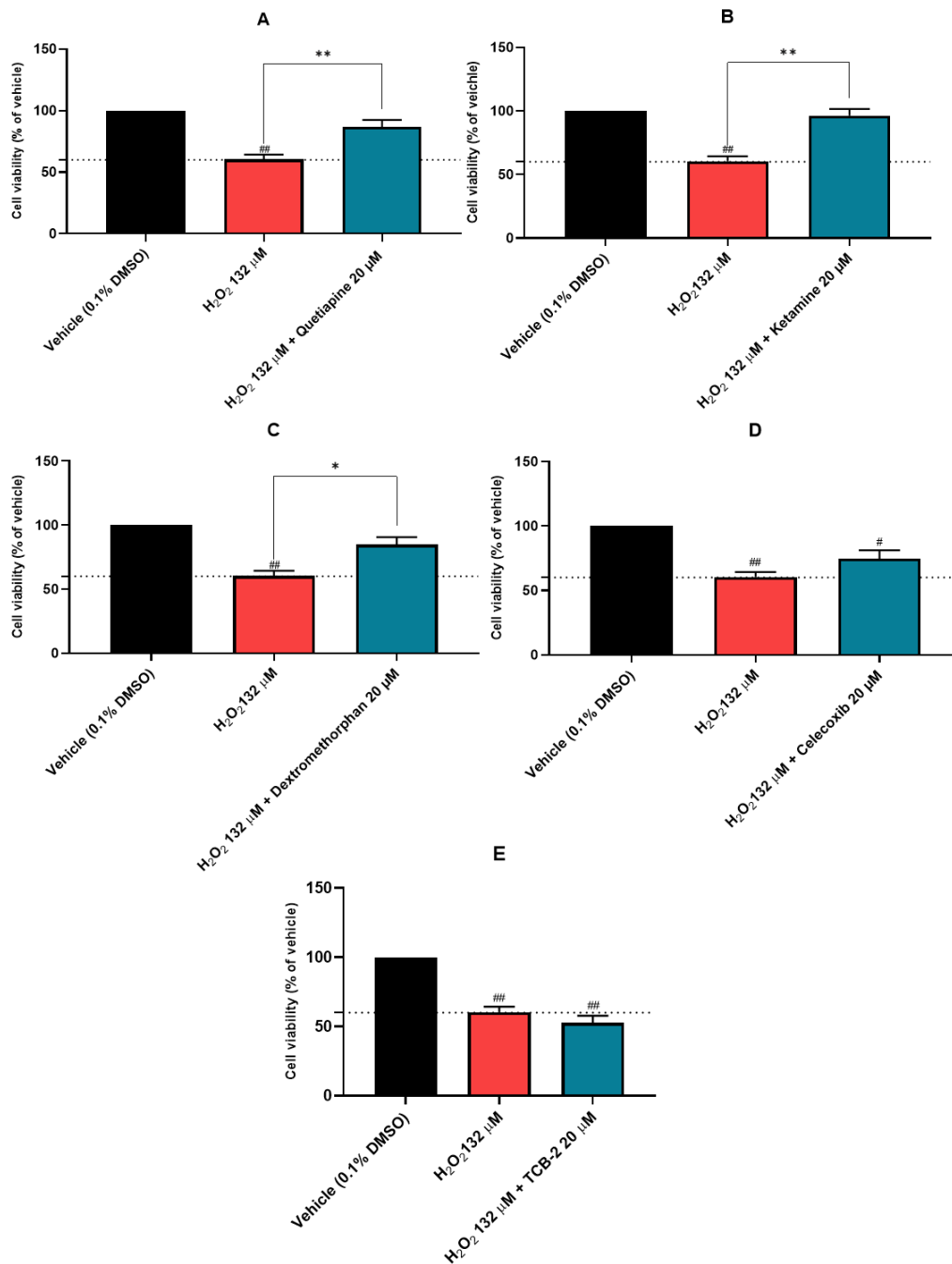


Figure S11. Effect of the incubation of 132 μM of H₂O₂ in combination with (A) quetiapine 20 μM, (B) ketamine 20 μM, (C) dextromethorphan 20 μM, (D) celecoxib 20 μM, and (E) TCB-2 20 μM, determined by MTT methodology. The results represent the mean ± SEM of three independent experiments, expressed as the percentage of the vehicle (100%). Statistically significant # $p < 0.05$, ## $p < 0.01$ vs. vehicle, and * $p < 0.05$, ** $p < 0.01$ vs. H₂O₂ 132 μM.

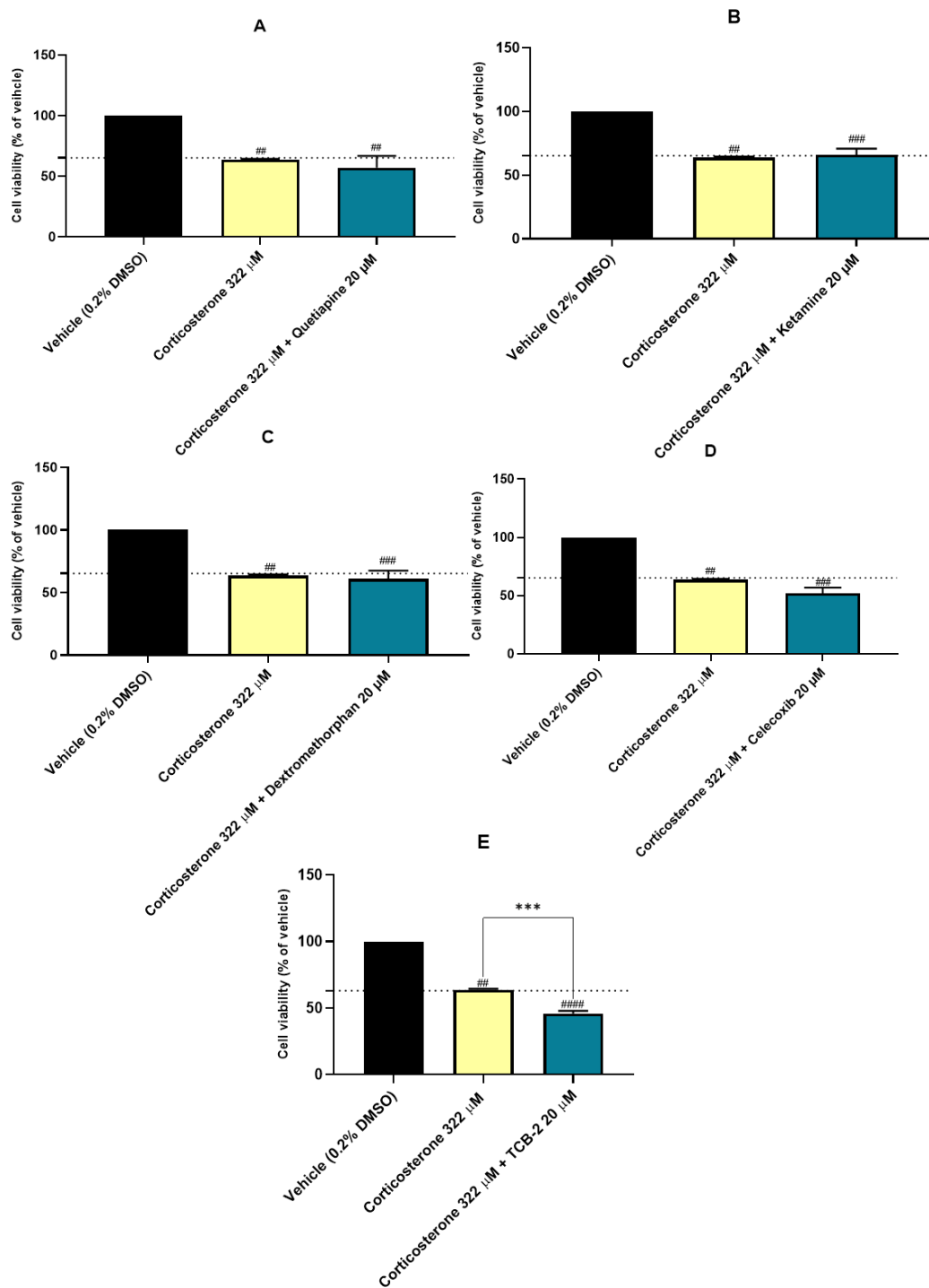


Figure S12. Effect of the incubation of 322 μM of corticosterone in combination with (A) quetiapine 20 μM, (B) ketamine 20 μM, (C) dextromethorphan 20 μM, (D) celecoxib 20 μM, and (E) TCB-2 20 μM, determined by MTT methodology. The results represent the mean ± SEM of three independent experiments, expressed as the percentage of the vehicle (100%). Statistically significant # $p < 0.05$, ## $p < 0.01$, ### $p < 0.01$ vs. vehicle, and *** $p < 0.001$ vs. corticosterone 322 μM.

These findings demonstrate the potential of quetiapine, ketamine, and dextromethorphan to effectively mitigate H₂O₂-induced stress in SH-SY5Y cells (Figures S11A, B, C and S10A, B, C). Celecoxib showed a trend in this direction but did not significantly counteract the effects (Figures S11D and S10D). TCB-2, however, had no mitigating effect and yielded results similar to H₂O₂ alone (Figures S11E and S10E).

In the case of corticosterone-induced stress, none of the drugs were able to alleviate its impact (Figure S12 and S10). Instead, they led to cellular viability values similar to those seen with corticosterone alone, with TCB-2 even exacerbating the nocive effects (Figure S12E and S10E).

Collectively, these results highlight the varying effects of these drugs on cellular stress responses, particularly in the context of H₂O₂ and corticosterone-induced stress.

V. Discussion

This discussion includes all the outcomes presented in this thesis. To enhance readability of the content, it is important to highlight that this discussion follows a structured path: it begins with a brief explanation of the research context and objectives. Next, it discusses the biological models used in the study. Then, the different treatments used were explored, emphasizing the results derived from their application and, whenever possible, a link between the various results obtained was attempted. However, it is important to note that the studies on hypoxia and BDNF, regarding their specificity, were primarily focused on the end of this part of the discussion. Additionally, a brief overview of the methodologies used throughout the research process was also presented. Finally, a concise conclusion was also added to this discussion.

Depression is a worldwide concern of outstanding significance, representing a major healthcare challenge. This mental health condition is complex and heterogeneous, involving an interplay of multiple biological systems and molecular pathways. Resistance to existing treatments and a high rate of relapse support the need for intensive research into therapeutic modalities. Thus, the development of new therapeutic approaches, innovative research strategies, and insights into this complex disease is needed [6,421].

In the context of this thesis, the primary goal was to research into the pharmacological effects of serotonergic compounds, specifically an established antidepressant (mirtazapine), L-TRP, and explore the potential repurposing of pharmaceutical agents for the management of depression, particularly scopolamine and lamotrigine. This research was conducted across different cellular models, with the objective of understanding the capacity of these compounds to mitigate the consequences of exposure to glucocorticoids and oxidative stress. Furthermore, the goal was also to uncover how these compounds impact TRP/5-HT metabolic pathways and influence BDNF levels. Additionally, an exploratory study focusing on hypoxia stimuli was also conducted to complement these studies. Studying hypoxia stimuli in depression can offer valuable insights into the complex nature of this mental health condition, as further explained below. By performing these studies, it aims to improve the understanding of biomolecular features of depression by focusing on cellular models, thereby reducing the reliance on animal testing, mainly in preliminary stages of research.

Animal studies continue to play an important role in the research of depression, primarily because they address some of its behavioral and cognitive aspects, such as anhedonia, weight or appetite changes, and other comorbid conditions, such as social isolation. However, inherent differences between animals and humans can introduce variability into research findings. Furthermore, ethical concerns are raised regarding the necessity and ethical implications of using animals in experiments [422]. Thus, the

adherence to the principles of the 3Rs policy in research (replacement, reduction, and refinement) becomes increasingly important [423].

Cellular studies are an essential approach in the early study of depression. Neuronal and glial cell lines such as rat clonal PC12 pheochromocytoma, human SH-SY5Y neuroblastoma cells, mouse HT-22 hippocampal cells, rat glioma C6, and murine BV2 microglial cell lines are commonly used in this context. These cell models offer a controlled environment for the investigation of biomarkers associated with depression, enabling the exploration of molecular mechanisms at the cellular level [424,425]. Despite the important lack of the behavioral component, there are several advantages to using cell models in understanding and treating this disease. Indeed, cell models enable the manipulation and observation of the effects of various factors, including genetic mutations or exposure to stress hormones, on cellular mechanisms. Moreover, cell models are instrumental in drug discovery and testing, enabling the rapid screening of potential antidepressant compounds, enhancing our understanding of drugs act at the cellular level [425–427]. Furthermore, cells can be personalized by deriving them from patients with depression, using techniques like induced pluripotent stem cells. This approach helps in understanding the specific cellular dysfunctions in individual patients, being important for personalized medicine in psychiatry. It also contributes to the identification of biomarkers for depression [427]. Finally, cellular models play a crucial role in studying the long-term effects of depression and its treatments on cells, including changes in gene expression and neural connectivity. This kind of research contributes significantly to our understanding of the chronic nature of depression and the development of more effective treatments [425,428].

This project extensively used both SH-SY5Y, and HT-22 cell lines. Despite the disadvantages of studying in cell lines (such as lack of complexity), these cells, capable of readily expanding in culture, offer a standardized and potentially limitless avenue for studying the cellular mechanisms associated with depression [425,429].

The SH-SY5Y cell line is a derivative subline of the SK-N-SH neuroblastoma cell line, originally isolated in 1970 from a metastatic bone tumor [430]. These cells represent one of the most frequently used human neuronal cell lines for investigating neuropsychiatric diseases. Indeed, they play a significant role in the study of depression, primarily through their use in modeling the effects of antidepressants and stressors at the cellular level, being used to understand the cellular and molecular mechanisms of depression and to preliminary test potential treatments [424,425,431,432]. This cell line exhibits distinct neuronal characteristics, such as neurite outgrowth [430], neurotransmitter modulation [430,433], and the expression of relevant receptors, such as 5-HT₂ [434], 5-HT₁ [433], and 5-HT₃ (demonstrated in this work), having capability

to differentiate into more mature neuronal-like cells. However, in this work, only undifferentiated SH-SY5Y cells were used mainly because there is a high variability in the differentiation protocols used in different studies. Indeed, protocols may vary in the use of growth factors, duration of differentiation, and other conditions, affecting the process of differentiation. Moreover, differentiation can be extremely time-consuming, costly and challenging [435].

HT-22 cells were also used in this work to complement some studies with SH-SY5Y cells. Nonetheless, most studies were conducted using SH-SY5Y cells instead of HT-22 cells, mainly due to their human origin. HT-22 is an immortalized cell line originating from the hippocampus region of a mouse's brain, being used as a model for hippocampal neurons in numerous research, including depression research [318,425,436,437]. As previously mentioned in the introduction, the hippocampus is critically linked to depression, with conditions like reduced hippocampal volume observed in MDD, providing an opportunity to study the pathophysiology of depression and mechanisms of action of antidepressants in a hippocampal context [438]. These cells also present key serotonergic features, being ideal for studying this aspect of depression [438]. Indeed, they express receptors such as 5-HT_{2A} [439], 5-HT_{1A} [440], and 5-HT₃ (demonstrated in this work).

In the final stages of the work, to broaden our study from cell lines, we examined the impact of mirtazapine and scopolamine on BDNF levels, after H₂O₂ or corticosterone insults, initially using hippocampal slices and later with hippocampal and cortical neuronal cultures. Both cortical and hippocampal neurons play significant roles in depression, each contributing in different ways to the complex pathophysiology of this disorder.

Hippocampal slice cultures offer advantages in experimental research compared to other hippocampal preparations, as they preserve the intact hippocampal structure and synaptic circuits, with the main distinction being the lack of afferent input [441]. Two commonly used types are acute hippocampal slices and organotypic slice cultures. Acute slices are suited for short studies, as once removed from the brain, their viability declines rapidly, as it is challenging to provide them with the same level of oxygen / nutrients that they would receive in a living brain. On the other hand, organotypic slice cultures can be maintained *in vitro* for extended periods (weeks to months). Acute slices require less preparation and maintenance effort, preserving synaptic connections close to their *in vivo* state at the time of harvest, making them a preferred choice for these experiments [441]. Thus, for studying BDNF expression, acute slices were selected and for a period of 6h.

Primary neuronal cell culture is also widely used to study the structure and function of neurons in a controlled environment, offering insights into neuronal function and neurological diseases. However, culturing neuronal cells presents several challenges due to their non-dividing nature, which is hard to establish and maintain. Also, primary cultures have limited cell numbers and require careful separation from other cell types, such as astrocytes, to ensure purity [442]. Nevertheless, in contrast to acute hippocampal slices, these cultures allowed us to explore the effect of the drugs towards only neurons and to expand the drug exposure duration to an extended 24h timepoint. Additionally, we also tried a period of 48h drug exposure, but cells began to decline their viability, making us maintain the 24h timepoint for a more robust experimental approach.

To conduct this work, diverse compounds and methodologies were selected to advance our research goals. Some important aspects regarding the methodologies will be explored later in this discussion.

Corticosterone and hydrocortisone were used to study the effect of glucocorticoid-mediated stress in the different cells used. Corticosterone is the main glucocorticoid in rodents, controlling the metabolism and stress response. In humans, the activity of corticosterone is weak, being also converted to aldosterone in a series of chemical reaction catalyzed by aldosterone synthase, found only in glomerulosa cells, that are present in the adrenal cortex [443,444]. In humans, the main glucocorticoid is cortisol, produced in the adrenal cortex and predominantly regulated by the neuroendocrine HPA axis [445]. Hydrocortisone is a synthetic form of cortisol, being often stable in a laboratory setting [446]. In the research of depression, corticosterone is widely used. In fact, research involving corticosterone helps in understanding how stress might lead to /exacerbate depressive symptoms, frequently used to create models of depression in animals [447]. When using human cells such as SH-SY5Y, cortisol/hydrocortisone is also frequently used [407,448]. It is worth noting that both cortisol and corticosterone can exert similar effects on cellular processes due to their shared glucocorticoid properties. However, corticosterone may be preferred over cortisol in SH-SY5Y cells in certain experimental contexts, being also widely used in these cells [449,450]. If the research involves comparing findings between rodents and humans/human cells, using corticosterone in SH-SY5Y cells may provide a relevant model for studying the effects of glucocorticoids, being one of the reasons why corticosterone was mainly used in this work, in addition to the lack of response observed by the exposure of cells to hydrocortisone.

The experiments involving hydrocortisone led to intriguing results. This compound exhibited a positive impact on the viability of SH-SY5Y cells, while showing a tendency towards decreasing viability in HT-22 cells. It was also observed that this

glucocorticoid had no considerable impact on the DNA of SH-SY5Y cells, which aligns with the findings from the viability studies. The different responses of SH-SY5Y and HT-22 cells to hydrocortisone might be due to differences in glucocorticoid receptor signaling, cell type-specific gene expression profiles, and the different characteristics of each cell line. Indeed, one hypothesis could be the induction of survival pathways in SH-SY5Y cells, that are cancer cells. These pathways may not be triggered to the same extent in the non-tumoral HT-22 cells. A study supporting this provided interesting findings into the impact of P-glycoprotein on hormone penetration in both mouse and human brain. Specifically, this study revealed that while P-glycoprotein impedes the entry of cortisol, it is not a similar barrier to corticosterone. In other words, the study's data suggest that in both mice and human brains, corticosterone exhibits greater accessibility compared to cortisol due to the influence of P-glycoprotein [451]. This observation highlights the differential transport mechanisms of these hormones in the presence of P-glycoprotein. Additionally, it is worth mentioning that P-glycoprotein is frequently found to be overexpressed in cancer cells, contributing to the development of resistance mechanisms during cancer treatment [452]. This phenomenon is observed in various cancer cell types, including SH-SY5Y cells [453,454]. Another interesting study of Parkinson's disease using SH-SY5Y cells, demonstrated that hydrocortisone (10 μ M) enhanced cellular stress resistance primarily by upregulating parkin expression [455]. This protein is a neuroprotective protein, important in the mitochondrial quality control pathway [456]. Collectively, these studies and hypothesis may explain the differences in hydrocortisone effect on both cell types.

Regarding corticosterone, this glucocorticoid reduced cell viability in both cell lines, with different IC_{50} values, being more potent in HT-22 cells. Corticosterone and cortisol bind to the same types of receptors, that are the high-affinity MRs and lower-affinity GRs [457]. However, once again, the variation in response intensity may be attributed to the cancer characteristic of SH-SY5Y cells, that generally exhibit an enhanced resistance to apoptosis [458]. This resistance might result in a reduced sensitivity to the pro-apoptotic effects of corticosterone. It is also important to note that these pro-apoptotic effects of corticosterone depend on factors such as the concentration of this compound. In fact, a recent study highlighted a protective role of corticosterone (0.03 μ M, 72h) against H_2O_2 -induced cell death in SH-SY5Y cells, being a situation of eustress: a stress that helps the body and becomes a positive signal to have strong adaptability [459]. Thus, the specific effects of corticosterone on these cells can vary depending on experimental conditions like concentration, duration of exposure, and the presence of other biological factors. Besides inducing cell death, corticosterone did not lead to significant high levels of ROS production, contrasting with previous studies in

these cells [460,461]. In fact, prolonged glucocorticoid exposure is known to lead to overproduction of ROS [462]. These findings support the importance of more research into the relationship between corticosterone and the production of ROS. Additionally, this glucocorticoid did not lead to significant modulation of BDNF levels (explored in deeper detail later in this discussion).

H₂O₂ was used to study the effect of oxidative stress in cells, as well as the modulation of this effect by several compounds. In fact, the addition of H₂O₂ is a method frequently used to trigger oxidative stress in the cells. This compound is generally used in particularly high concentrations due to the catalase action, the enzyme that decomposes H₂O₂ into water and oxygen [412]. The Fenton reaction, which occurs when H₂O₂ reacts with ferrous ions (Fe²⁺), is recognized as the primary pathway to produce highly reactive hydroxyl radicals (OH•), playing a central role in oxidative damage [412]. In depression research, H₂O₂ is used in several ways: to induce oxidative stress in biological models, to test the effectiveness of various antioxidants and drugs in protecting neurons from oxidative damage, to study the molecular and genetic changes that occur in response to oxidative stress and to study cell death and survival pathways in neuronal cells [263,463,464]. The obtained results demonstrate that this agent led to similar effects on both SH-SY5Y and HT-22 cells, leading to cell viability decline and high levels of ROS levels, as expected. This agent also affected the expression of BDNF, enhancing its levels in hippocampal cells (at 24h of exposure), explored in deeper detail further in this discussion. H₂O₂ also led to significant levels of DNA damage in SH-SY5Y cells. Indeed, the connection between high levels of oxidative stress and DNA damage is widely reported. ROS can oxidize the nitrogenous bases in DNA, and these modifications can lead to mismatches during DNA replication. ROS can also attack the deoxyribose of DNA, leading to strand breaks that can lead to genomic instability and thus interfere with DNA function [465].

The effectiveness of a clinically established antidepressant and other drugs with potential applications in the treatment of depression was also explored. This approach allowed us to determine if the repurposed drugs could induce antidepressant responses like those of the established antidepressant. Mirtazapine was selected as a reference antidepressant. As previously reported in the introduction, mirtazapine is an atypical antidepressant that targets distinct neuronal pathways, including different 5-HT receptors [390]. Exploring the impact of mirtazapine on several aspects related to the biochemistry of depression, such as oxidative stress, BDNF modulation and glucocorticoid mediated stress can offer valuable insights into the complex interaction of various neurotransmitters and receptors, opening doors to future studies. Furthermore, mirtazapine is also known for its characteristic side effect profile, that includes sedation

and weight gain, among other effects [390]. More exploration of these side effects has the potential to enhance the ability to manage them effectively, improving the overall treatment for individuals undergoing depression treatment with mirtazapine. Moreover, through a Pubmed search, it was found that in a year, 128 studies were conducted involving this drug, in contrast to 522 studies with fluoxetine, for example. This emphasizes the need for mirtazapine to be further explored.

In this study, the concentrations of mirtazapine tested did not induce loss of cell viability to the cells, as expected from literature research [263,404,405,466]. Additionally, when applied in combination with H₂O₂, this drug could mitigate the loss of cell viability. Moreover, during a 24h exposure period, mirtazapine exhibited a tendency towards enhancing cell viability compared to H₂O₂ alone. It is important to emphasize that, as an example, when examining the effects of mirtazapine, this antidepressant usually starts demonstrating its therapeutic benefits in individuals over a span of 4 to 6 weeks. This delay may be attributed to the drug's complex interactions within the human brain, processes that typically need time for adaptation [467]. For the study of mirtazapine in cell lines over a 48h period, the objectives and outcomes are different from those in human clinical use. In cell culture studies, the focus is often on understanding the immediate/ early cellular and molecular responses to the drug, as explained early in this discussion. Indeed, the 48h incubation period is used in many types of cell culture experiments, as it allows enough time for the cells to respond to many treatments, as shown in this work.

Beside the effects on cell viability, when applied in combination with H₂O₂, mirtazapine, overall, decreased ROS production, the DNA damage, increased the concentration of 5-HT in the extracellular medium, and increased BDNF levels in hippocampal and cortical primary cultures, compared with H₂O₂ alone. However, glucocorticoid-mediated stress was not modulated by this antidepressant, except regarding 5-HT levels, where the combination of mirtazapine with corticosterone seemed to increase 5-HT levels in the extracellular medium compared with corticosterone alone in SH-SY5Y cells. Collectively, these effects induced by mirtazapine in combination with H₂O₂ might be explained by its previously reported antioxidant capabilities, protecting cells against oxidative stress and DNA damage [263,466,468]. Possibly by acting on 5-HT related pathways, mirtazapine induces neuroprotection mechanisms that oppose the harmful effects of H₂O₂. Indeed, several studies demonstrate that serotonergic pathways are involved in antioxidant mechanisms in depression. For example, attenuating hippocampal oxidative damage induced by 5-HT depletion in mice [469]. This topic was explored in the introduction. Moreover, mirtazapine downregulates pro-apoptotic pathways, protecting cells from oxidative stress-induced apoptosis [470]. In fact, it is

known that this antidepressant acts on the gene expressions of pro-apoptotic (Bax and p53) proteins, reducing their expressions [263]. Additionally, this drug can enhance neurotrophic factors like BDNF, as shown in this work, which are vital for neuron survival and can counteract the toxic effects of oxidative stress [261,470]. Moreover, this antidepressant can mitigate the increased ROS production and elevated expression level of NADPH oxidase 4 (NOX4) in cells exposed to stressors [466]. NOX4 is expressed in SH-SY5Y cells and HT-22 cells, as well as in several brain regions such as the hippocampus and the cortex [471–473].

On the other hand, the lack of efficacy of mirtazapine in counteract corticosterone-induced stress to the cells is intriguing, because, for example, by inducing survival pathways, it would be expected that mirtazapine could counteract the glucocorticoid toxic effect. However, the effect of mirtazapine in corticosterone/ cortisol levels is complex and not totally understood. Indeed, literature reports that in a study with mice, mirtazapine reversed corticosterone-induced depressive-like behaviors probably via its antioxidant effects [474]. Also, this drug decreased corticosterone levels in serum plasma of rats, demonstrating anti-anxiety activity [475]. On the other hand, studies in mice also revealed that mirtazapine can increase basal corticosterone levels after one single oral treatment, having no effect on these levels in subchronic treatment [476]. Interestingly, other study found that mirtazapine inhibited GR function, which in turn decreased corticosterone-induced gene transcription. However, this effect was observed only at the highest concentration (30 μ M), for a period of 5 days, in mouse fibroblasts [477]. These discrepancies could be due to differences in the experimental conditions, such as the duration of treatment and the dose of mirtazapine used. In fact, the interactions between the neuroendocrine system and the neurological system are extremely complex. It is also interesting to note that this drug seemed to decrease even more the cell viability when combined with corticosterone (compared to corticosterone alone), in SH-SY5Y cells, suggesting a synergistic effect between mirtazapine and corticosterone in this experimental context. A possible hypothesis might be a chemical interaction between both drugs in these cells, possibly modifying its active forms, increasing toxicity. Also, the combination might induce genetic or epigenetic changes in the cells, affecting their viability. However, the exact mechanism of this apparent synergy in SH-SY5Y cells is not known and would require more studies to be confirmed. Moreover, it was interesting that mirtazapine increased 5-HT levels in the extracellular medium after being combined with corticosterone (compared with corticosterone alone) in SH-SY5Y cells. So, the combination of mirtazapine with corticosterone decreased cellular viability, but seemed to increase 5-HT extracellular levels to levels similar to the untreated control. One possible explanation for the apparent independence of decreased

cellular viability from 5-HT extracellular levels is the presence of multiple signaling pathways within cells: while 5-HT play an important role in cell function, other factors also influence cellular viability. Nevertheless, alterations in extracellular 5-HT levels are linked to depression, and this relationship is complex and associated with several contradictions, as mentioned in the introduction. Low extracellular levels of 5-HT have traditionally been associated with depression and related psychiatric disorders [478]. It's crucial for 5-HT to be in this extracellular space to bind to its receptors on neurons and exert its effects. Indeed, studies demonstrate that mirtazapine enhances 5-HT release from serotonergic neurons by inhibiting adrenergic α_2 receptors, leading to increased synaptic availability of 5-HT. Thus, blocking these receptors causes enhanced release of 5-HT [479]. Nevertheless, another study also demonstrated that when mirtazapine (at concentrations ranging from 0.1 to 100 μ M) was applied to rat raphe slice cultures, it failed to induce a significant alteration in 5-HT extracellular concentration, during acute treatment or prolonged exposure [480].

Scopolamine and lamotrigine were also included in this research due to their documented potential in the treatment of depression, as mentioned in the introduction. Briefly, some points to highlight in scopolamine's potential effect in depression are the rapid antidepressant effects and potential to target treatment-resistant depression, despite has not been officially approved for the treatment of depression [362]. There is also evidence suggesting that lamotrigine can be beneficial in cases of treatment-resistant depression, as well as used in adjunctive treatment. However, there is still a lot explore regarding the effects of these drugs in depression [362,481].

These drugs were also studied due to their poorly explored role with 5-HT₃ receptor. Notably, numerous studies have explored the significance of these receptors as promising targets for antidepressants, despite being an area that is still expanding [141,482–484]. In the case of scopolamine, this drug has been documented as an antagonist of 5-HT₃ receptors [358]. Similarly, reports on lamotrigine suggest its inhibitory effect on the 5-HT₃ receptor. Specifically, lamotrigine hinders receptor activity by binding to the open state of the channels, resulting in the blockage of channel activation or acceleration of desensitization [485,486]. The exact nature and implications of these interactions are still being researched.

Collectively, our findings indicated that like mirtazapine, these drugs did not exhibit any toxicity in both cell lines in the tested concentrations. These observations are aligned with the literature, which supports the potential use of these drugs in depression therapy [481,487]. It is crucial to highlight that when testing the impact of drugs on various stressors within the context of depression, these pharmaceutical agents must not induce any toxicity but rather should demonstrate neuroprotective properties. The HPLC

analysis of these drugs revealed that they generally have minimal impact on extracellular 5-HT levels when compared to the untreated cells, in both cell lines. However, an exception was observed with the apparent slight decrease in extracellular 5-HT levels following the addition of lamotrigine, particularly in SH-SY5Y cells. Interestingly, an old study revealed that this drug inhibited 5-HT reuptake in rat brain synaptosomes [488]. Also, in another study, it was found that lamotrigine decreased the basal extracellular 5-HT level in the hippocampus of rats [489]. The apparent contradiction between these two studies can be explained by considering different aspects of the experimental conditions. Indeed, the first study focuses on 5-HT uptake inhibition in rat brain synaptosomes, which are isolated nerve terminals. In contrast, the second study investigates the drug's impact on the hippocampus, a broader system. However, more studies should be considered regarding the role of lamotrigine in the modulation of 5-HT levels. For scopolamine, its exact impact on 5-HT levels remains poorly documented. No direct studies or evidence linking scopolamine to extracellular 5-HT levels have been identified, emphasizing the necessity for further research in this area. Moreover, similar to what was observed with mirtazapine, the combinations of H₂O₂ with scopolamine and lamotrigine, also revealed that these drugs could increase the levels of extracellular 5-HT, compared with H₂O₂ alone, in both cell lines. Additionally, the cellular damage caused by H₂O₂ was attenuated by the presence of these drugs. Conversely, these drugs did not mitigate the stress induced by corticosterone or elevated 5-HT levels. The findings from this study suggest that these drugs play a key role in combating oxidative stress, although they may not have a significant impact on glucocorticoid stress, as previously discussed regarding mirtazapine. This leads to the speculation that the 5-HT₃ receptor could be important in understanding and addressing these stress responses. Indeed, a study demonstrated that 5-HT₃ receptor antagonists substantially reduced apoptosis and ROS generation. These observed neuroprotective properties were all mediated through 5-HT₃ receptor antagonism since they were completely blocked by concurrent treatment with a 5-HT₃ receptor agonist, suggesting that 5-HT₃ receptors might play a role in managing oxidative stress in the cells [490]. Other study revealed that an experimental 5-HT₃ receptor antagonist (6z) attenuated brain oxidative damage, demonstrating antidepressant-like activity [141]. However, in another study, an experimental 5-HT₃ receptor antagonist (4i) reversed corticosterone induced depressive-like deficits in mice [491]. Thus, more investigation is important to clarify the interplay between corticosterone / oxidative stress / 5-HT₃ receptors and discover how this interplay may have a role in depression. Because this is a preliminary, exploratory study, future studies to verify the exact involvement of 5-HT₃ receptor in this context are needed. For example, 5-HT₃ knockdown/knockout studies in these cells would be necessary. Further

investigation into the role of the 5-HT₃ receptor in this context might provide deeper insights into how these drugs function.

Considering the impact of the drugs studied in this work on serotonergic pathways, the inclusion of L-TRP as a potential stress-modulator compound in this research was due to being the precursor for 5-HT synthesis, and could potentially modulate the functioning of serotonergic pathways [492]. In fact, L-TRP mitigated the damage on cellular viability caused by H₂O₂, especially notorious on SH-SY5Y cells. In HT-22, this effect was not observed to the same extent, but a notorious trend for stress alleviation by TRP was especially highlighted by morphological analysis. These differences between both cells were similarly observed with the combination of mirtazapine with H₂O₂. On the other hand, L-TRP did not attenuate cell damage caused by corticosterone in both cells, once again having a similar response to mirtazapine. Future studies to explore mirtazapine and L-TRP's lack of efficiency in reverting corticosterone-induced cellular stress may be important and relevant. Nevertheless, an analysis of the combined results on cellular viability and ROS production suggests that both mirtazapine and L-TRP responses may involve serotonergic pathways in addressing oxidative stress in depression. This hypothesis is highlighted by the fact that both compounds did not significantly attenuate cell damage caused by corticosterone in both cells, but only attenuated the damage caused by H₂O₂. Indeed, studies demonstrated that dietary TRP can attenuate the oxidative stress in the liver, reflecting antioxidant capability [493]. Also, a study found out that TRP supplementation improved gut health by boosting antioxidant status and reducing inflammation in piglet intestines after a lipopolysaccharide challenge [494]. Moreover, another research demonstrated that L-TRP effectively mitigated oxidative damage in bovine intestinal epithelial cells exposed to H₂O₂ by enhancing the cells' antioxidant defenses and inhibiting apoptotic processes [495]. However, other study highlighted that free TRP does not have significant antioxidant properties, and the observed antioxidant capabilities may be attributed to its metabolites [496]. Moreover, to corroborate this hypothesis, it was observed a similar response pattern to mirtazapine and L-TRP when 5-HT was applied to the cells in combination H₂O₂ and corticosterone. Thus, the modulation of 5-HT pathways might modulate different cellular signaling pathways in response to oxidative stress, compared to glucocorticoid-induced stress. For example, 5-HT might upregulate antioxidant defenses or repair mechanisms in the case of oxidative stress, which are not effective against the changes induced by corticosterone, in the context of this experiment.

Regarding this, we also aimed to study the impairment of L-TRP/5-HT pathway with the major focus on HPLC analysis of the extracellular levels of L-TRP, 5-HTP, 5-HT,

and 5-HIAA, after induction of oxidative or glucocorticoid stress on SH-SY5Y cells. It is also important to note that future studies on L-TRP/KYN pathways would also be valuable. Similar to findings in existing literature, this study reports on the disturbances of L-TRP/5-HT pathways, coupled with oxidative stress and glucocorticoid effects [246,247,273]. Despite the antioxidant character of L-TRP described above, high levels of oxidative stress can generate neurotoxic compounds by the oxidation of the L-TRP. It is also known that L-TRP may be metabolized to KYN directly by high levels of ROS. Then, KYN may be metabolized to the oxidant compounds 3-HK and QA, associated with diseases, such as depressive disorders [242,243], as mentioned in the introduction. High levels of glucocorticoids are also reported to increase the KYN production, decreasing the activity of the 5-HT branch of L-TRP metabolism [273]. Moreover, several studies demonstrate the importance of compounds that act on L-TRP /5-HT pathway in the modulation of glucocorticoid and oxidative stress [244,246,497].

Based on the obtained data, very high concentrations of H₂O₂ and corticosterone were selected to proceed with the HPLC analysis. As previously mentioned, higher concentrations can produce more pronounced effects, making it easier to observe and measure cellular responses, particularly useful in experiments where subtle changes might be difficult to detect, allowing a better interpretation and examination of the results. Collectively, the combination of L-TRP, 5-HTP, 5-HT, and 5-HIAA with H₂O₂ / corticosterone did not mitigate the effect of both stressors, demonstrating that these high concentrations of corticosterone and H₂O₂ influenced the cellular viability inducer effect of the isolated L-TRP metabolites. On the other side, the extracellular concentrations of each introduced metabolite exhibited significant fluctuations, regardless of cellular viability values. Notably, the assessments of cellular viability and morphology yielded consistent results in all tested metabolites. However, the same level of uniformity was not observed in the extracellular concentration data, suggesting that distinct chemical transformations occurred during the study period, which did not have a discernible impact on cell morphology or viability, at least in the exposure time chosen.

The results show that combining each metabolite with corticosterone caused more cell damage than their combination with H₂O₂, especially concerning cellular viability and morphology. However, when looking at extracellular medium concentrations, there was more variation observed in the combinations of metabolites with H₂O₂ compared to corticosterone. It is also highlighted how H₂O₂ concentration-dependently reduces extracellular 5-HT levels, while corticosterone results in minimal fluctuations. This difference can be due to the high oxidative nature of H₂O₂, possibly being more reactive with the extracellular metabolites [498]. Generally, the oxidative environment induced by H₂O₂ can cause degradation or structural changes in metabolites, such as

protein oxidation [499]. In contrast, corticosterone may not chemically directly react with these compounds. This might explain why metabolites combined with corticosterone remain less altered, unlike those exposed to H_2O_2 . An exception to this is observed with 5-HIAA, as detailed below. These findings support the importance of exploring various stress induction methods due to their diverse cellular responses, needing further research.

L-TRP, 5-HTP, and 5-HIAA exhibited a consistent pattern of either decreasing or increasing extracellular concentration when applied in combination with both corticosterone and H_2O_2 . In another words, when L-TRP and 5-HIAA were applied in combination with both stressors, they led to an increase in extracellular concentration, while 5-HTP resulted in a decrease. For 5-HT, there was a contrasting response depending on the stimuli. When combined with corticosterone, it led to an increase in the extracellular concentration of this neurotransmitter, but in combination with H_2O_2 , it caused a decrease. Again, the electrochemical detection results illustrate this trend in relation to the extracellular levels of 5-HT, in response to the addition of corticosterone or H_2O_2 (without external addition of 5-HT). These findings suggest that various methods of inducing stress can have distinct effects on 5-HT levels. Notably, 5-HT is known for its protective role in preventing the oxidation of membrane lipids [500]. It's possible that 5-HT is more actively used to counteract the oxidative effects of H_2O_2 , leading to its depletion. Indeed, when an antioxidant comes into contact with H_2O_2 , it can react with it and decrease in concentration. Antioxidants work by donating a hydrogen atom to H_2O_2 , which can quench the H_2O_2 [501]. This process can lead to a decrease in the concentration of the antioxidant, a process that can explain why 5-HT levels decrease after being combined with H_2O_2 . The antioxidant properties of 5-HT make this pathway important for the potential development of drugs that target serotonergic receptors in the context of stress management [502].

Considering both L-TRP and 5-HIAA, it was observed an increase in their extracellular levels when they were combined with corticosterone and particularly with H_2O_2 . This phenomenon may be attributed to chemical characteristics of these compounds. For L-TRP, it is documented that it is susceptible to oxidation by free radicals, resulting in the formation of products like tryptophanyl (indolyl) radical [503]. These oxidation products are easily masked with L-TRP in its non-oxidized form, which may explain the observed increase in extracellular levels. As for 5-HIAA, an explanation may involve the transport of these metabolites. Essentially, this compound cannot be metabolized within cells. Subsequently, based on their initial concentration, they may exit the cells, leading to an increased presence in the extracellular space. In contrast, 5-HTP exhibited a decrease in its levels when combined with H_2O_2 , being practically unaltered

when applied alone or combined with corticosterone. This may be attributed to its hydroxyl group, which makes it highly vulnerable to oxidation, particularly when exposed to H₂O₂ [504]. In fact, 5-HTP is also known for its antioxidant properties [502]. The presence of hydroxyl groups in molecules is often associated with antioxidant activity. These hydroxyl groups can help eliminate free radicals [505].

It's important to study the extracellular levels of L-TRP, 5-HTP, 5-HT, and 5-HIAA in response to various stress stimuli to maintain the balance between these metabolites and their homeostatic levels. This equilibrium is important because deviations from normal levels can have significant implications for health. For example, low levels of 5-HT are linked to various disorders, including depression, while high levels can lead to conditions like 5-HT syndrome, which can be life-threatening [506]. These findings support that different methods of inducing stress produce distinct responses in the extracellular concentration of L-TRP, 5-HTP, 5-HT, and 5-HIAA within the SH-SY5Y cells. Importantly, the various chemical transformations that occurred during the study did not result in differences in cell morphology or viability among the different metabolites. Indeed, the lack of change in cell morphology and viability in response to different chemical transformations may demonstrate resilience and adaptability of the cells. Based on the contrasting responses in the extracellular medium concentration of 5-HT following exposure to both corticosterone and H₂O₂, it appears that the 5-HT pathway is particularly sensitive to environmental modulation.

In the final stages of this work, we also aimed to understand the impact of the studied compounds on mature BDNF levels, by using Western blot and immunofluorescence assays. These techniques are commonly used in molecular biology, offering insights into protein localization (for immunofluorescence) and quantification. Briefly, and as mentioned in the introduction, BDNF is involved in various brain functions including neuronal survival and synaptic plasticity [176]. Different regions of the cerebral cortex, particularly the PFC, show significant BDNF activity, and, also, the hippocampus is one of the primary sites of BDNF expression in the brain [165]. This protein is linked to numerous psychiatric and neurological disorders, notably MDD, as reduced BDNF levels are often associated with a higher risk of depression and its symptoms [192]. Once bound to its canonical receptor, TrkB-FL, BDNF initiates intracellular signaling pathways, a process that occurs through two-steps: (1) BDNF binds to TrkB, causing receptor dimerization, and (2) BDNF induces TrkB autophosphorylation at specific tyrosine residues, enabling protein binding and subsequent activation of intracellular signaling cascades [507]. Thus, given these roles, studying the BDNF/TrkB signaling pathway is highly relevant in the context of depression,

aiming to contribute to the advance of the understanding of the biological basis of depression and for developing more effective treatments.

Both antibodies used in Western blot and immunofluorescence to detect BDNF, can detect monomeric (~14 kDa) and dimeric (~28 kDa) forms of this protein [508,509]. However, in this study, only in the hippocampal slices was possible to detect the BDNF monomer by Western blot. A possible explanation might be that hippocampal slices contain a more diverse array and amount of cell types, including neurons, glia, and possibly other supporting cells in their native arrangement [510], possibly leading to the different pattern of BDNF monomer found in the Western blot. In immunofluorescence, as the antibody recognizes both forms, the results can be interpreted as the overall BDNF levels. It is also important to mention that detecting BDNF may be very challenging because this is a protein that is also present in the extracellular space. Indeed, it has been reported that many BDNF studies lack reproducibility [511]. Furthermore, it would be important to test antibodies recognizing only the BDNF prodomain (anti-proBDNF), as this isoform can also be detected by immunofluorescence with the antibody used [512].

Numerous studies have consistently reported high levels of oxidative stress with diminished BDNF levels, underscoring the potential protective function of BDNF against oxidative harm within neuronal tissues [513]. Interestingly, a study reported that H₂O₂ applied in a range of 100-250 μM initiate PC12 cell death, but also significantly promoted BDNF signaling, contributing to neuroprotection of these cells [514]. Indeed, the obtained immunofluorescence results demonstrated that this compound after 24h of exposure, enhanced BDNF and pTrkB levels, compared to the untreated condition though this did not occur at 6h. This suggests a time-dependent response. The cells may initially counteract the oxidative stress, with the effects only becoming apparent after more prolonged exposure. In fact, these patterns of responses were also observed by the performed cellular viability assays, where the lower levels of cellular viability were observed on more prolonged exposure time. Thus, this suggests that more prolonged time of exposure of H₂O₂ leads to more cytotoxicity, and the enhancement in BDNF levels at 24h is probably a mechanism of neuroprotection, consistent with literature reports [514].

High levels of corticosterone are also connected to BDNF/TrkB impairments. However, a study in mice suggested that corticosterone has different effects on proBDNF processing: proBDNF increased in the hippocampus and cerebellum but remained unchanged in the PFC and hypothalamus. Both proBDNF and mBDNF increased significantly in the pituitary gland, while proBDNF decreased significantly in the adrenal gland [320]. Moreover, the effect of corticosterone on BDNF might follow an inverted U-

shaped curve. Indeed, a study suggested that as cortisol levels increase from low to moderate levels, it may enhance neuroplasticity. However, as cortisol levels continue to rise beyond a certain point, they may start to have a detrimental effect on neuroplasticity. So, the relationship between cortisol and neuroplasticity is not linear, as there is an optimal range where cortisol may have a positive influence on plasticity, but excessive levels could be nocive [515]. The obtained data revealed the complexity of BDNF/TrkB assessment after exposure to corticosterone. Immunofluorescence results, for both time points, demonstrated that corticosterone alone had no significant effect on BDNF levels nor pTrkB, compared to the untreated condition. This effect on BDNF levels was also observed in cortical cells by Western blot analysis. However, Western blot analysis of hippocampal slices demonstrated a trend to corticosterone upregulation of BDNF levels after corticosterone addition, particularly the BDNF monomer. Possibly, hippocampal slices as a whole, might initially respond to corticosterone adverse stimulus by increasing BDNF production as a protective or adaptive response, being a feedback mechanism. Supporting this, a recent study explored the effect of acute and chronic stress in BDNF levels, in humans, revealing that acute psychosocial stress increases serum BDNF and cortisol, whereas chronic stress was linked to lower basal serum BDNF levels [516].

Mirtazapine is known to promote the activation of TrkB receptor [517] and to induce BDNF levels in the serum of depressed patients [261]. Indeed, a study demonstrated that repeated mirtazapine administration (10 mg/kg) increased BDNF mRNA levels in rat hippocampus and cerebral cortex. In the same study, a lower dose of mirtazapine (5 mg/kg) did not have effects on BDNF mRNA levels in these rats [518]. Other study also highlighted that chronic mirtazapine administration in a chronic unpredictable mild stress rat model, enhanced hippocampal and PFC BDNF levels, inhibiting also the increase of plasma corticosterone level [519]. Our findings demonstrated the impact of mirtazapine on the regulation of mature BDNF and pTrkB levels, both in isolation and in combination with the different stimuli. Notably, our results highlight the dynamic nature of this modulation, with variations in response observed across different time-points and concentrations, consistent with previously reported findings in the literature. Indeed, our previous findings indicated that mirtazapine (particularly 20 μ M) exhibited a greater capacity to mitigate the adverse effects of oxidative stress, suggesting that the higher concentration may induce more robust neuroprotective effects. This effect was also demonstrated in the BDNF levels of hippocampal cells, where it becomes apparent that only the highest concentration of mirtazapine was effective in mitigating the effects of corticosterone, and the effects of H₂O₂ in cortical cells. Regarding pTrkB levels, only 20 μ M mirtazapine was also capable of enhance these levels, after H₂O₂ stimulus. These results align with the previously

obtained results, supporting that the combination of mirtazapine 20 μM with H_2O_2 seems to exert neuroprotective effects. At 6h, mirtazapine (10 nM) decreased significantly BDNF levels in cortical cells, returning to values similar to the control group at 24h, suggesting that the initial decrease may have been a transient effect, and the cells eventually adapted to the presence of mirtazapine. In fact, supporting this idea is a study that highlights this variability investigated the impact of various antidepressants (such as reboxetine and desipramine) on BDNF expression in SH-SY5Y cells at different time intervals (6h, 24h, 48h). This study demonstrated that a short-term exposure (6h) to reboxetine or desipramine resulted in a reduction of total BDNF. In contrast, a longer-term treatment (48h) led to a significant increase in total BDNF levels [520]. In the case of hippocampal slices, mirtazapine (20 μM) exerted a significant influence on BDNF dimer levels, leading to a reduction in these levels compared to the control group. In these slices, the combination of mirtazapine with H_2O_2 did not affect BDNF levels compared to H_2O_2 alone. In this biological model and in cortical cells, the combination of the antidepressant with corticosterone did not result in statistically significant effects on BDNF levels when compared to corticosterone alone. However, it did suggest a trend toward decreased BDNF levels, not reaching statistical significance. Interestingly, the previously obtained results with this combination on cellular viability and ROS production also revealed that overall, mirtazapine did not attenuate damages induced by corticosterone, but only attenuated damages induced by H_2O_2 . Once more, it becomes evident that, despite fluctuations between neuronal systems, this consistent pattern of response supports the neuroprotective action of mirtazapine when confronted with oxidative stress stimulation.

Scopolamine was selected to study BDNF levels based on the potential of this drug as an antidepressant, as well as the results presented in this work. This drug is also reported to modulate BDNF expression and release, which is essential for its rapid antidepressant effects [521]. The antidepressant effects of scopolamine, mediated through the muscarinic acetylcholine receptors in the medial PFC, involves increasing the expression of BDNF [522]. As previously mentioned, a study demonstrated that scopolamine attenuated reserpine-induced depression in mice partially by regulating BDNF in the hippocampus and PFC of mice [307]. However, there are also reports that refer that scopolamine damage mouse memory by downregulating the BDNF/TrkB/Akt pathway [523], highlighting the importance of studies. Our research findings confirm that scopolamine indeed exerted varying effects on mature BDNF and pTrkB levels. Notably, either alone or when applied in combination with the stimuli, scopolamine overall enhanced BDNF and pTrkB levels in mouse hippocampal cells. However, it conversely reduced BDNF levels in rat hippocampal slices. These apparent divergent outcomes

support the necessity for additional research to fully elucidate the underlying mechanisms. In cortical cells, scopolamine demonstrated no effect on BDNF levels. However, when combined with H₂O₂, showed a tendency to increase BDNF levels, particularly at a 20 μM concentration, and at both time points. However, when scopolamine was combined with corticosterone, it didn't significantly impact BDNF levels compared to corticosterone alone. Collectively, these observations suggest that scopolamine's effect on BDNF and pTrkB is complex and context dependent. Indeed, it highlights the importance of considering the specific type of brain cells and the presence of other stimuli (corticosterone and H₂O₂). It is particularly noteworthy that similar to mirtazapine, in cortical and hippocampal cells, scopolamine combined with H₂O₂ also enhanced BDNF levels, compared to H₂O₂ alone. This is consistent with the previous obtained results exploring cell viability in these conditions, highlighting that oxidative stress attenuation might involve upregulation of BDNF levels, according with the previous mentioned literature reports.

In conclusion, these experiments revealed complex and context-dependent responses to these compounds, demonstrating a complicated dynamics of BDNF signaling in different neuronal systems. The findings support the importance of considering various cellular contexts when evaluating the responses of neurons to different treatments and stimulus. Thus, globally, this research aims to contribute with valuable insights into the biological basis of depression and open avenues for developing targeted therapies that modulate BDNF/TrkB signaling pathways.

Hypoxia-inducing stimuli were also explored according to previous experiments within the research group [36]. Decreased levels of oxygen (hypoxia) lead to high levels of stress, resulting in processes such as inflammation, brain injury, mitochondrial oxidative stress, and apoptosis, disturbing homeostasis [13,524–526]. Hypoxia is also implicated in anxiety and depressive disorders. In fact, studies indicate that hypoxia can disrupt the normal neurohormonal balance in the brain, increasing the potential for depressive features [527]. In people that live at high altitudes and are chronically exposed to hypoxia, increased suicide rates are observed, possibly connected to hypoxic exposure. Indeed, increased altitude leads to the reduced partial pressure of arterial oxygen (PaO₂) and limiting the brain's access to oxygen is a risk factor for mood disorders [527–529]. It is also suggested that in hypoxia, TPH may not function normally due to lack of oxygen saturation, decreasing 5-HT synthesis. Moreover, studies suggest that increases in blood oxygen can elevate brain 5-HT synthesis by enhancing TPH functioning [528,530]. A study that focused on the effects of hypoxia on 5-HT_{1A} receptor revealed that after the exposure of cells to hypoxia, a significant reduction in ligand

binding was observed, along with the disruption of downstream signaling of the 5-HT1A receptor, particularly cAMP-mediated signaling [531].

In response to hypoxia, there are adaptive responses. One of the most important regulators of this response is the major transcription factor denominated HIF-1. This dimeric complex presents an alpha subunit (HIF-1 α), highly sensitive to oxygen and degraded by the proteasome in normoxic cells [532]. Under hypoxic conditions, HIF-1 targets genes related to angiogenesis, cell proliferation/survival, and glucose/iron metabolism, which are essential to cell survival in hypoxic environments [533]. Some studies hypothesize that increasing the levels of HIF-1 may be a new therapeutic target to depression [534]. Additionally, the administration of the potent HIF-1 inhibitor topotecan worsened the severity of the depressive-like symptoms in an experimental model of depression in rats [535]. Another study also revealed that FG-4592 (an inhibitor of prolyl hydroxylase) improved depressive-like symptoms by mediating neurogenesis and synaptic plasticity through HIF-1 [536]. Other study demonstrated that in rodent models of depression, the administration of ginsenoside has shown positive effects, significantly reversing depression-like behavior and positively impacting the mRNA and protein expression of the HIF-1 α signaling pathway and regulators associated with synaptic plasticity. Additionally, inhibiting HIF-1 α expression abolished the compound's antidepressant-like effect [537]. The exact role of HIF-1 in the treatment of depression is still an active area of research. While there have been advancements, many aspects of this topic are still being explored.

The molecular and cellular characterization of the hypoxia response and pathways involved in this mechanism is greatly possible due to hypoxia models in cell culture [524]. To induce hypoxia in cells, as previously mentioned, the cells were exposed to a hypoxia incubator chamber enriched with a 2% O₂, 10% CO₂, and 88% N₂ atmosphere, contrasting with the 21% O₂ present in normoxic conditions [538]. Additionally, the cells were exposed to CoCl₂, which is widely used to artificially induce hypoxia in the cells, defined as chemical hypoxia. CoCl₂ is known to stabilize HIF-1, mimicking one of the central pathways activated during hypoxia [539]. This methodology of hypoxia induction is widely used because CoCl₂ is a straightforward and accessible method for inducing hypoxia-like conditions, and uniformly affects all cells in the culture, ensuring consistent exposure to hypoxia-like conditions. Additionally, by controlling the concentration of CoCl₂ added to the cells, there is the possibility of manipulating the response of the cells in the desirable period of study [540]. However, while CoCl₂ stabilizes HIF-1, it may not activate all the pathways that are involved in the cellular response to hypoxia, limiting the research findings [524]. Thus, CoCl₂-induced hypoxia is generally suitable for studies where the focus is on specific pathways like HIF-1 activation and when resources are

limited, not replicating the complete range of physiological responses to hypoxia, that may be obtained using chamber-Induced hypoxia.

In this study, using the SH-SY5Y cells, the induction of hypoxia with the hypoxia incubator chamber showed practically no differences compared to normoxia conditions, contrary to what we can observe through the induction of hypoxia with CoCl_2 , where lower cellular viability values were observed, comparing to a normoxic environment. This finding wasn't entirely unexpected, as prior studies had already linked hypoxia to the survival and proliferation of neuroblastoma cell lines [36,541,542], likely due to increased HIF expression. In cancer cells, HIF expression often lead to increased expression of specific genes, facilitating adaptive responses [543]. On the other hand, the use of CoCl_2 allowed us to observe a cellular response to the hypoxia stimulus for 48h, which was the main reason we continued this study with this model of chemical induction of hypoxia, adding to the importance of this model in studying HIF-1 effects, as discussed above. Indeed, some explanations might be possible to explain these differences between the two models. As mentioned above, while CoCl_2 chemically stabilizes HIF-1 and can induce other stress responses, the hypoxia chamber reduces the oxygen concentration, more closely mimicking physiological hypoxia. The cells might be more sensitive or responsive to the biochemical changes induced by CoCl_2 than to the physical reduction of oxygen. SH-SY5Y cells might have some capacity to adapt to low oxygen conditions, which could make them more resilient to low oxygen levels, as explained above [544]. In fact, mitochondria can trigger cell death or activate survival genes in low oxygen conditions. The BCL-2 proteins regulate cell death in anoxia (0–0.5% O_2), while in hypoxia (0.5–3% O_2), mitochondrial oxidative stress activates HIFs to promote cell survival [545]. A study in this regard revealed that hypoxic preconditioning with the hypoxia chamber (3% O_2 for 4 - 24h followed with normoxic recovery for 24h) protected SH-SY5Y cell against oxidative stress, highlighting the role of adaptive mechanisms [546]. A hypothesis is that this adaptation might not be triggered in the same extent in the case of CoCl_2 exposure because pathways that promote cell survival might be overwhelmed by the chemical stress imposed by CoCl_2 .

After testing the drugs within a hypoxic environment induced by CoCl_2 , all these drugs demonstrated a marked increase in cellular viability when compared to the cells only treated with CoCl_2 . However, in this context, the connection between the tested drugs and hypoxia is not straightforwardly established in the available literature. Nevertheless, these results can be attributed to several potential mechanisms. One important connection is the well-established link between hypoxia and elevated levels of oxidative stress [35]. In this research, the impact of mirtazapine on the ROS levels was explored, revealing its capacity to attenuate oxidative stress induced by H_2O_2 . This

mechanism could underline the observed responses to mirtazapine within the context of hypoxia. Additionally, TPH1 is inhibited by acute hypoxia, leading to reduced 5-HT levels [547]. Also, a systematic review explored the effects of hypoxia or anoxia during the perinatal period on the serotonergic network in rodents. The findings showed that hypoxia led to a disturbance in the serotonergic system, including reduced 5-HT fibers, and decreased brain levels of 5-HT [548]. All these studies highlight that the serotonergic system and hypoxia response are connected. Thus, these drugs might protect cells from hypoxia adverse stimulus by modulating 5-HT signaling.

Another possible mechanism contributing to these observed responses may involve the modulation of HIF-1 expression, which plays an important role in facilitating cell survival within hypoxic environments [532]. Thus, to explore whether the tested drugs were inducing this factor, echinomycin, a potent HIF-1 inhibitor that works by inhibiting its DNA-binding and transcriptional activity [549], was used in SH-SY5Y cells in combination with the tested drugs under hypoxic environment, to understand the impact in the cellular viability. Previously, echinomycin blocked the CoCl₂ effects on bone-marrow-derived mesenchymal stem cells [550]. So, in theory, the hypothesis was that if the observed increase in cell viability (when the drugs were combined with CoCl₂) was a consequence of the modulation of HIF-1-related pathways, then the introduction of a non-toxic concentration of echinomycin should counteract this increase in cell viability by inhibiting the HIF-1 response, despite the need for additional studies to confirm this hypothesis. The data obtained from these experiments demonstrated that when echinomycin was combined with all the tested drugs, it overall led to a reduction in cell viability within a hypoxic environment, which aligned with our initial hypothesis.

The existing body of knowledge concerning the effects of these drugs under hypoxic conditions remains limited, and the role of HIF-1 in the context of depression remains a subject of limited exploration and controversy within the scientific community [535,551]. Nevertheless, it is essential to highlight that some studies have suggested that celecoxib has the potential to down-regulate HIF-1 expression [552,553]. However, the observed responses may be related to specific cellular, or animal models used, as well as the dosages/ concentrations of the drugs used. Nonetheless, all the tested drugs have previously demonstrated potential antidepressant properties in several studies [367,390,554], attributed to their interactions with various biological factors, including inflammatory responses, oxidative stress levels, neurotransmitter levels and associated pathways, and potentially the modulation of HIF-1 expression, as supported by these experiments. In contrast, TCB-2 is a drug with an absence of studies exploring its potential in depression. However, TCB-2 is a high-affinity 5-HT_{2A} receptor agonist and exploring the effects of TCB-2 can provide valuable insights into how 5-HT modulation

influences depressive features [555]. Furthermore, like other psychedelic compounds, TCB-2 may have therapeutic promise in treating depression, particularly in cases resistant to conventional treatments. Indeed, investigating how psychedelics can deliver rapid and sustained antidepressant effects is an expanding area of research [556].

This preliminary research aims for further research into the involvement of hypoxia and HIF-1 in the pathophysiology of depression, holding promise for the advancement of therapeutic approaches in the field of depression. More steps should include the application of advanced molecular biology techniques. Specifically, Western blot analyses to quantify HIF-1 α protein levels would be important for validating our initial hypothesis and understanding the relationship between different degrees of hypoxia and depressive conditions.

Based on these results, we also explored the effect of quetiapine, ketamine, dextromethorphan, celecoxib, and TCB-2 in combination with H₂O₂ and corticosterone on SH-SY5Y cellular viability. Interestingly, quetiapine, ketamine, and dextromethorphan displayed significant efficacy in mitigating H₂O₂-induced cellular damage, while exhibiting no impact on corticosterone-induced stress. Once again, this supports the potential of these drugs to provide protection against oxidative stress, mirroring the actions of mirtazapine, L-TRP, and 5-HT. In contrast, TCB-2 and celecoxib exhibited minimal influence on H₂O₂-induced cell damage. When it came to corticosterone-induced cellular damage, TCB-2 demonstrated exacerbation, whereas celecoxib showed no discernible effects. In fact, between these drugs, quetiapine, ketamine, and dextromethorphan are the reported ones with more evidence regarding antidepressive effects. Ketamine and dextromethorphan have been widely studied in recent years (as described in the introduction), both having reported protective effects over oxidative stress [557,558]. On the other hand, TCB-2 lacks studies exploring its potential in depression, as explained above. Interestingly, this drug is an agonist of 5-HT_{2A} receptors, whereas mirtazapine and quetiapine are antagonists of this receptor. Hence, it becomes intriguing to understand the specific functions of this receptor in this context. Interestingly, research revealed that direct stimulation of the 5-HT_{2A} receptors by 3,4-methylenedioxymethamphetamine (MDMA) induced intracellular oxidative stress, resulting in neuronal apoptosis [559]. On the other hand, other study with TCB-2 in the context of Alzheimer's disease revealed that this compound could reduce oxidative stress and neuronal loss in a rat model of this disease [560]. Thus, as mentioned earlier, the precise impact of 5-HT_{2A} receptor modulators on depression is a subject of incomplete comprehension. The exact nature of this relationship can be complex and context-dependent, varying across different cell types and pathological states. Celecoxib, despite having evidence of positive effects on depression (detailed in the

introduction), as a COX-2 inhibitor, potentially acts in depression treatment by reducing the production of pro-inflammatory cytokines, which are linked to the hyperactivity of immune inflammatory responses in depression [561], a condition that was not present in this cellular study.

In addition to different cell models and compounds already discussed, in this study, different methodologies were also used, each complementing the others, to provide diverse insights into different aspects of the research questions. Thus, it is important to discuss some specific aspects of these methods, to elucidate their rationale and potential limitations that could impact the interpretation of our findings.

MTT and NR were both used to assess the effect of the different compounds on mitochondrial activity and lysosomal activity, respectively. They are used for cytotoxicity testing, being compatible with different cell types, as well as simple and cost-effective. Regarding sensitivity, it's important to highlight that the sensitivity of the NR and MTT assays can vary based on the specific compounds and cell lines being tested [562–564]. We chose to incorporate a higher number of MTT assays in our study because in studies involving SH-SY5Y cells, the MTT assay is generally more frequently used compared to the NR assay, because neuronal cells are highly energy-demanding, and their function, including the propagation of action potentials and the release of neurotransmitters, requires a constant supply of ATP, produced by the mitochondria [565]. Nevertheless, it is important to note that lysosomal functions are also important in neurons, and both assays can be used complementarily to a more complete approach. In the context of depression research, the evaluation of cellular viability is important in for aspects such as neurotoxicity/ neuroprotection, and the influence of antidepressants/ other compounds on general cell viability. Indeed, numerous studies use these methodologies to conduct initial screenings of compounds with potential antidepressant properties, investigate the impact of specific stressors on cell viability, and explore the protective effects of certain compounds against cellular toxicity [566–570], as performed in this work.

DCFDA assay, used as a fluorescent indicator of ROS formation is highly sensitive to ROS, making it suitable for detecting low levels of oxidative stress, allowing real-time monitoring of ROS in live cells without the need for cell lysis or extraction [571]. However, this probe can react with various ROS and reactive nitrogen species (RNS), making it hard to distinguish between different types of reactive species, being important to note that DCFDA is a non-specific probe [572]. Several studies use this technique in the research of depression. In fact, as depression is connected with high levels of oxidative stress, it can be used to measure oxidative stress levels, evaluate if drugs can reduce oxidative stress in neuronal cells, understanding how oxidative stress impacts

the neurons [246,437,573]. In this study, the assay provided valuable insights into the varying levels of ROS induced by H₂O₂ and corticosterone in two different types of cell lines, exploring also how mirtazapine and L-TRP can modulate these responses.

Comet assay is a highly sensitive methodology for detecting DNA, providing quantitative data on the extent of DNA damage in individual cells [415,574]. In the context of depression research, this methodology is not frequently used. However, there are some applications of the comet assay in the research of this disease. Since oxidative stress can cause DNA damage [575], the comet assay could be used to investigate the levels of DNA damage in certain cell types as a result of increased oxidative stress. In fact, in this study, this experiment was performed mainly with this purpose. Additionally, given the role of inflammation in depression, and the fact that inflammation can lead to oxidative stress (as explored in the introduction) and thus DNA damage, the comet assay could potentially be used to study these processes. The effect of various environmental toxins and lifestyle factors (such as smoking and dietary habits), as risk factors for developing depression may also be detected at a DNA level in the context of depression [576–580]. In fact, this study clearly demonstrated that exposure to high oxidative stress resulted in DNA damage, which was effectively modulated by the application of the antidepressant mirtazapine. In the future, it would be interesting to perform this study with lamotrigine and scopolamine.

In this research, it was also used two HPLC methodologies: with ECD and regular HPLC, both analytical techniques used for separating, identifying, and quantifying compounds in a mixture, differing in their detection mechanisms and applications [416,581]. ECD involves measuring the current resulting from the oxidation or reduction of analytes at an electrode surface, being highly sensitive and selective for compounds that can be oxidized or reduced (in this case, 5-HT) [416]. On the other side, regular HPLC is versatile and can be used for a wide range of analytes, being less sensitive than ECD-HPLC and, in this case, using UV/Vis absorption for detection [416]. In the context of these studies using HPLC, we used a single sample (N=1), derived from the pooling of cell supernatants from three distinct experiments (N=3). By combining samples from three separate experiments, we aimed to create a representative average sample. Also, given the constraints of HPLC in terms of sample volume and the costs associated with reagents and maintenance, it was beneficial to analyze a single, pooled sample. However, it also comes with limitations, particularly in terms of the ability to assess inter-sample variability, being a gap that we intend to overcome in the future.

Because of its sensitivity, ECD-HPLC was used to detect the levels of 5-HT in the extracellular medium of the cells without enrichment with this neurotransmitter. Using this methodology, it was evident that both SH-SY5Y cells and HT-22 cells displayed the

synthesis of 5-HT, and this production was modulated by the various applied compounds. In fact, a study demonstrated that proteins required for serotonergic neurotransmission, such as TPH2, 5HT1A receptor, and SERT were significantly upregulated in differentiated HT-22 cells, that also enhanced the functional serotonergic properties of HT-22 cells, as evidenced by an increase in intracellular 5-HT levels, indicating that these cells can produce 5-HT, especially when they are differentiated [438]. In the case of SH-SY5Y cells, it is well-established that their differentiation can also result in an upregulation of proteins essential for serotonergic neurotransmission, thereby influencing the expression of 5-HT properties [582]. Nonetheless, the knowledge about the specific functions of undifferentiated SH-SY5Y and HT-22 cells regarding their capacity for 5-HT production, remains limited. This gap supports the significance of this study, especially considering the challenges associated with the cell differentiation process, as outlined above.

Taking together, this research explores various cellular models, drugs, and methodologies to enhance the current understanding of the depression disorder. The study significantly contributes to the field by examining the effects of serotonergic compounds, particularly mirtazapine, and other pharmaceuticals such as scopolamine, on cellular responses to stressors like glucocorticoids and oxidative stress. Also, the work underscores the importance of considering various cellular contexts in evaluating neuroprotective and adaptive responses, paving the way for more effective treatments for depression.

VI. Concluding Remarks and Future Perspectives

This thesis focused on MDD cellular mechanisms, mainly exploring the effectiveness of compounds like mirtazapine, L-TRP and scopolamine in reducing oxidative stress and glucocorticoid-induced stress in different cellular models that included cell lines, primary cell cultures and hippocampal slices. In a summarized way, a key achievement was demonstrating these drugs' ability to protect cells from oxidative stress, but not glucocorticoid induced stress, highlighted by the different methodologies used. Also, the research demonstrated complex, context-dependent responses of BDNF to these treatments. Additionally, it examined the role of hypoxia in drug responses, revealing increased cell viability under chemical hypoxia, after treatment with the different drugs.

This study contributes to our understanding of depression at a cellular level. It not only elucidates the effects of compounds exhibiting antidepressant properties on cellular stress responses, but also highlights the complex interaction of factors like BDNF and hypoxic conditions in the efficacy of these treatments, aiming to pave the way for more targeted and effective therapeutic strategies in the management of major depressive disorder.

As outlined in the discussion, the use of cell lines presents a valuable method for studying the molecular and cellular mechanisms associated with diseases like depression. However, given their constraints, it is crucial to expand these studies to include more advanced cell models in the future steps of the research. Advanced cell models encompass techniques such as using induced pluripotent stem cells for creating personalized models from patient cells, such as mentioned in the discussion. Brain organoids also address the limitations of two-dimensional cultures by replicating the complex neuronal and glial architecture found in specific brain regions, essential for functional understanding. These organoids, grown in matrix substrates, self-organize to accurately mimic the functional and structural development of adult organs, such as brain [583]. Additionally, CRISPR-Cas9 gene editing enables precise genomic modifications in cell models, such as creating or correcting mutations associated with depression [584]. Furthermore, microfluidic systems, or lab-on-a-chip technologies, facilitate the study of cells in controlled microenvironments. They enable the modeling of neural circuits involved in depression and allow for precise measurements and manipulations of the extracellular environment [585].

Reducing waste in scientific research is also very important. Platforms that repurpose animal tissues not used in other studies can minimize the number of animals sacrificed. This approach is already being implemented on i3S. In future research, using clinical and biological patient samples, such as blood, saliva, or brain imaging, can provide insights into molecular features like cortisol levels. Clinical settings offer access

to these samples, along with brain imaging data, allowing for the study of hormonal imbalances, genetic factors, and brain structure/ function differences. Exploring other drugs with potential to be repurposed for the depression therapy is also an approach that must be increasingly implemented, as it allows reduction in time and cost associated with bringing a drug to market. Since repurposed drugs have already passed through several stages of clinical testing, particularly for safety and dosage, the process of approval for a new use is often much quicker and cheaper than developing a new drug, being a more sustainable approach to pharmaceutical development. It uses existing resources and minimizes waste, contributing to a more environmentally friendly and economically sustainable healthcare system [586].

A deeper exploration of molecular mechanisms, especially concerning serotonergic pathways and BDNF levels in oxidative and glucocorticoid-induced stress, is crucial for the next steps of this work. Particularly, further investigation into why these drugs did not mitigate corticosterone-induced stress in cells would also be highly valuable. Additionally, a deeper examination of the roles of HIF-1 and the 5-HT₃ receptor using molecular biology techniques could clarify the data presented and may be important in developing new therapeutic approaches for depression.

Despite the already discussed complexity in studying depression, it is extremely important to act about this disease. The importance of studying depression lies in its impact and prevalence, and as a mental health condition affecting millions globally, depression profoundly influences individuals' everyday lives, including their work, relationships, and overall well-being. Gaining a deeper understanding of depression is crucial for creating effective treatments and supportive environments. Indeed, research into depression is a key driver in promoting mental health awareness. This awareness is critical for early intervention, which can significantly improve the outcomes of treatment. Furthermore, understanding depression's risk factors and early signs is essential for developing preventative strategies. This knowledge is particularly valuable in reducing the onset of depression, especially among vulnerable populations. A focus on mental health can result in a healthier and more productive society and decreases the burden on healthcare systems.

In conclusion, the study of depression and related drugs are important for enhancing the quality of life and promoting the well-being of society. Every effort dedicated to the study of this disease is a valuable contribution to confronting this mental health challenge, aiming to alleviate the burden of depression and improve the lives of those who suffer from it.

VII. References

1. Six common depression types - Harvard Health Available online: <https://www.health.harvard.edu/mind-and-mood/six-common-depression-types> (accessed on Sep 18, 2023).
2. WHO. Depressive disorder (depression) Available online: <https://www.who.int/news-room/fact-sheets/detail/depression> (accessed on Jun 28, 2023).
3. Depressão | SNS24 Available online: <https://www.sns24.gov.pt/tema/saude-mental/depressao/#sec-16> (accessed on Sep 13, 2022).
4. Otte, C.; Gold, S.M.; Penninx, B.W.; Pariante, C.M.; Etkin, A.; Fava, M.; Mohr, D.C.; Schatzberg, A.F. Major depressive disorder. *Nat. Rev. Dis. Prim.* **2016**, *2*, 16065, doi:10.1038/nrdp.2016.65.
5. Kennedy, S.H. Core symptoms of major depressive disorder: relevance to diagnosis and treatment. *Dialogues Clin. Neurosci.* **2008**, *10*, 271–277, doi:10.31887/DCNS.2008.10.3/shkennedy.
6. Major depressive disorder. *Nat. Rev. Dis. Prim.* **2023**, *9*, 45, doi:10.1038/s41572-023-00460-3.
7. Rasic, D.; Hajek, T.; Alda, M.; Uher, R. Risk of Mental Illness in Offspring of Parents With Schizophrenia, Bipolar Disorder, and Major Depressive Disorder: A Meta-Analysis of Family High-Risk Studies. *Schizophr. Bull.* **2014**, *40*, 28–38, doi:10.1093/schbul/sbt114.
8. Cuijpers, P. The Challenges of Improving Treatments for Depression. *JAMA* **2018**, *320*, 2529, doi:10.1001/jama.2018.17824.
9. Maj, M.; Stein, D.J.; Parker, G.; Zimmerman, M.; Fava, G.A.; De Hert, M.; Demyttenaere, K.; McIntyre, R.S.; Widiger, T.; Wittchen, H. The clinical characterization of the adult patient with depression aimed at personalization of management. *World Psychiatry* **2020**, *19*, 269–293, doi:10.1002/wps.20771.
10. El-Hage, W.; Leman, S.; Camus, V.; Belzung, C. Mechanisms of antidepressant resistance. *Front. Pharmacol.* **2013**, *4*, doi:10.3389/fphar.2013.00146.
11. Barroca, N.C.B.; Della Santa, G.; Suchecki, D.; García-Cairasco, N.; Umeoka, E.H. de L. Challenges in the use of animal models and perspectives for a translational view of stress and psychopathologies. *Neurosci. Biobehav. Rev.* **2022**, *140*, 104771, doi:10.1016/j.neubiorev.2022.104771.
12. Jesulola, E.; Micalos, P.; Baguley, I.J. Understanding the pathophysiology of depression: From monoamines to the neurogenesis hypothesis model - are we there yet? *Behav. Brain Res.* **2018**, *341*, 79–90, doi:10.1016/j.bbr.2017.12.025.
13. Burtscher, J.; Niedermeier, M.; Hüfner, K.; van den Burg, E.; Kopp, M.; Stoop, R.; Burtscher, M.; Gatterer, H.; Millet, G.P. The interplay of hypoxic and mental stress: Implications for anxiety and depressive disorders. *Neurosci. Biobehav. Rev.* **2022**, *138*, 104718, doi:10.1016/j.neubiorev.2022.104718.
14. Zhang, F.; Peng, W.; Sweeney, J.A.; Jia, Z.; Gong, Q. Brain structure alterations in depression: Psychoradiological evidence. *CNS Neurosci. Ther.* **2018**, *24*, 994–1003, doi:10.1111/cns.12835.
15. Gradin, V.B.; Pomi, A. The Role of Hippocampal Atrophy in Depression: A Neurocomputational Approach. *J. Biol. Phys.* **2008**, *34*, 107–120,

doi:10.1007/s10867-008-9099-7.

16. Videbech, P. Hippocampal Volume and Depression: A Meta-Analysis of MRI Studies. *Am. J. Psychiatry* **2004**, *161*, 1957–1966, doi:10.1176/appi.ajp.161.11.1957.
17. BioRender Available online: <https://biorender.com/> (accessed on Jan 20, 2022).
18. Pizzino, G.; Irrera, N.; Cucinotta, M.; Pallio, G.; Mannino, F.; Arcoraci, V.; Squadrito, F.; Altavilla, D.; Bitto, A. Oxidative Stress: Harms and Benefits for Human Health. *Oxid. Med. Cell. Longev.* **2017**, *2017*, doi:10.1155/2017/8416763.
19. Carraro, E.; Schilirò, T.; Biorci, F.; Romanazzi, V.; Degan, R.; Buonocore, D.; Verri, M.; Dossena, M.; Bonetta, S.; Gilli, G. Physical Activity, Lifestyle Factors and Oxidative Stress in Middle Age Healthy Subjects. *Int. J. Environ. Res. Public Health* **2018**, *15*, 1152, doi:10.3390/ijerph15061152.
20. Perillo, B.; Di Donato, M.; Pezone, A.; Di Zazzo, E.; Giovannelli, P.; Galasso, G.; Castoria, G.; Migliaccio, A. ROS in cancer therapy: the bright side of the moon. *Exp. Mol. Med.* **2020**, *52*, 192–203, doi:10.1038/s12276-020-0384-2.
21. Sharifi-Rad, M.; Anil Kumar, N. V.; Zucca, P.; Varoni, E.M.; Dini, L.; Panzarini, E.; Rajkovic, J.; Tsouh Fokou, P.V.; Azzini, E.; Peluso, I.; et al. Lifestyle, Oxidative Stress, and Antioxidants: Back and Forth in the Pathophysiology of Chronic Diseases. *Front. Physiol.* **2020**, *11*, 694, doi:10.3389/fphys.2020.00694.
22. Finkel, T.; Holbrook, N.J. Oxidants, oxidative stress and the biology of ageing. *Nature* **2000**, *408*, 239–247, doi:10.1038/35041687.
23. Yang, S.; Lian, G. ROS and diseases: role in metabolism and energy supply. *Mol. Cell. Biochem.* **2020**, *467*, 1–12, doi:10.1007/s11010-019-03667-9.
24. Kurutas, E.B. The importance of antioxidants which play the role in cellular response against oxidative/nitrosative stress: current state. *Nutr. J.* **2016**, *15*, 1–22, doi:10.1186/S12937-016-0186-5.
25. Sies, H. Oxidative Stress: Concept and Some Practical Aspects. *Antioxidants* **2020**, *9*, 852, doi:10.3390/antiox9090852.
26. Deponte, M. Glutathione catalysis and the reaction mechanisms of glutathione-dependent enzymes. *Biochim. Biophys. Acta - Gen. Subj.* **2013**, *1830*, 3217–3266, doi:10.1016/j.bbagen.2012.09.018.
27. Sindhu, R.K.; Kaur, P.; Kaur, P.; Singh, H.; Batiha, G.E.S.; Verma, I. Exploring multifunctional antioxidants as potential agents for management of neurological disorders. *Environ. Sci. Pollut. Res. Int.* **2022**, *29*, 24458–24477, doi:10.1007/S11356-021-17667-0.
28. Lobo, V.; Patil, A.; Phatak, A.; Chandra, N. Free radicals, antioxidants and functional foods: Impact on human health. *Pharmacogn. Rev.* **2010**, *4*, 118, doi:10.4103/0973-7847.70902.
29. Liu, N.; Wang, Z.-Z.; Zhao, M.; Zhang, Y.; Chen, N.-H. Role of non-coding RNA in the pathogenesis of depression. *Gene* **2020**, *735*, 144276, doi:10.1016/j.gene.2019.144276.
30. Bhatt, S.; Nagappa, A.N.; Patil, C.R. Role of oxidative stress in depression. *Drug Discov. Today* **2020**, *25*, 1270–1276, doi:10.1016/j.drudis.2020.05.001.
31. Bajpai, A.; Verma, A.K.; Srivastava, M.; Srivastava, R. Oxidative stress and major depression. *J. Clin. Diagn. Res.* **2014**, *8*, CC04-7,

doi:10.7860/jdcr/2014/10258.5292.

32. Ji, N.; Lei, M.; Chen, Y.; Tian, S.; Li, C.; Zhang, B. How Oxidative Stress Induces Depression? *ASN Neuro* **2023**, *15*, doi:10.1177/17590914231181037.
33. Ferriani, L.O.; Silva, D.A.; Molina, M. del C.B.; Mill, J.G.; Brunoni, A.R.; da Fonseca, M. de J.M.; Moreno, A.B.; Benseñor, I.M.; de Aguiar, O.B.; Barreto, S.M.; et al. Associations of depression and intake of antioxidants and vitamin B complex: Results of the Brazilian Longitudinal Study of Adult Health (ELSA-Brasil). *J. Affect. Disord.* **2022**, *297*, 259–268, doi:https://doi.org/10.1016/j.jad.2021.10.027.
34. Lanctot, K.L.; Mazereeuw, G.; Herrmann, N.; Andreazza, A.; Khan, M. A meta-analysis of lipid peroxidation markers in major depression. *Neuropsychiatr. Dis. Treat.* **2015**, *2479*, doi:10.2147/NDT.S89922.
35. McGarry, T.; Biniecka, M.; Veale, D.J.; Fearon, U. Hypoxia, oxidative stress and inflammation. *Free Radic. Biol. Med.* **2018**, *125*, 15–24, doi:10.1016/j.freeradbiomed.2018.03.042.
36. Silva, D.; Rocha, R.; Correia, A.S.; Mota, B.; Madeira, M.D.; Vale, N.; Cardoso, A. Repurposed Edaravone, Metformin, and Perampanel as a Potential Treatment for Hypoxia–Ischemia Encephalopathy: An In Vitro Study. *Biomedicines* **2022**, *10*, 3043, doi:10.3390/biomedicines10123043.
37. Liu, T.; Zhong, S.; Liao, X.; Chen, J.; He, T.; Lai, S.; Jia, Y. A Meta-Analysis of Oxidative Stress Markers in Depression. *PLoS One* **2015**, *10*, e0138904, doi:10.1371/journal.pone.0138904.
38. Yager, S.; Forlenza, M.J.; Miller, G.E. Depression and oxidative damage to lipids. *Psychoneuroendocrinology* **2010**, *35*, 1356–1362, doi:10.1016/j.psyneuen.2010.03.010.
39. Camkurt, M.A.; Findıklı, E.; İzci, F.; Kurutaş, E.B.; Tuman, T.C. Evaluation of malondialdehyde, superoxide dismutase and catalase activity and their diagnostic value in drug naïve, first episode, non-smoker major depression patients and healthy controls. *Psychiatry Res.* **2016**, *238*, 81–85, doi:10.1016/j.psychres.2016.01.075.
40. Parul; Mishra, A.; Singh, S.; Singh, S.; Tiwari, V.; Chaturvedi, S.; Wahajuddin, M.; Palit, G.; Shukla, S. Chronic unpredictable stress negatively regulates hippocampal neurogenesis and promote anxious depression-like behavior via upregulating apoptosis and inflammatory signals in adult rats. *Brain Res. Bull.* **2021**, *172*, 164–179, doi:10.1016/j.brainresbull.2021.04.017.
41. Zlatković, J.; Todorović, N.; Bošković, M.; Pajović, S.B.; Demajo, M.; Filipović, D. Different susceptibility of prefrontal cortex and hippocampus to oxidative stress following chronic social isolation stress. *Mol. Cell. Biochem.* **2014**, *393*, 43–57, doi:10.1007/s11010-014-2045-z.
42. Khanzode, S.D.; Dakhale, G.N.; Khanzode, S.S.; Saoji, A.; Palasodkar, R. Oxidative damage and major depression: the potential antioxidant action of selective serotonin re-uptake inhibitors. *Redox Rep.* **2003**, *8*, 365–370, doi:10.1179/135100003225003393.
43. Wei, X.; Ma, Y.; Li, F.; He, H.; Huang, H.; Huang, C.; Chen, Z.; Chen, D.; Chen, J.; Yuan, X. Acute Diallyl Disulfide Administration Prevents and Reverses Lipopolysaccharide-Induced Depression-Like Behaviors in Mice via Regulating Neuroinflammation and Oxido-Nitrosative Stress. *Inflammation* **2021**, *44*, 1381–

1395, doi:10.1007/s10753-021-01423-0.

44. DeMorrow, S. Role of the Hypothalamic–Pituitary–Adrenal Axis in Health and Disease. *Int. J. Mol. Sci.* **2018**, *19*, 986, doi:10.3390/ijms19040986.
45. Frigerio, F. The HPA Axis and the Regulation of Energy Balance. In *Cellular Physiology and Metabolism of Physical Exercise*; Luzi, L., Ed.; Springer Milan: Milano, 2012; pp. 109–121 ISBN 978-88-470-2418-2.
46. Smith, S.M.; Vale, W.W. The role of the hypothalamic-pituitary-adrenal axis in neuroendocrine responses to stress. *Dialogues Clin. Neurosci.* **2006**, *8*, 383–395, doi:10.31887/dcns.2006.8.4/ssmith.
47. Hemmerle, A.M.; Herman, J.P.; Seroogy, K.B. Stress, depression and Parkinson's disease. *Exp. Neurol.* **2012**, *233*, 79–86, doi:10.1016/j.expneurol.2011.09.035.
48. Su, Y.A.; Lin, J.Y.; Liu, Q.; Lv, X.Z.; Wang, G.; Wei, J.; Zhu, G.; Chen, Q.L.; Tian, H.J.; Zhang, K.R.; et al. Associations among serum markers of inflammation, life stress and suicide risk in patients with major depressive disorder. *J. Psychiatr. Res.* **2020**, *129*, 53–60, doi:10.1016/j.jpsychires.2020.06.008.
49. Dziurkowska, E.; Wesolowski, M. Cortisol as a Biomarker of Mental Disorder Severity. *J. Clin. Med.* **2021**, *10*, 5204, doi:10.3390/jcm10215204.
50. Russell, G.; Lightman, S. The human stress response. *Nat. Rev. Endocrinol.* **2019**, *15*, 525–534, doi:10.1038/s41574-019-0228-0.
51. Vaz, R.P.; Cardoso, A.; Serrão, P.; Pereira, P.A.; Madeira, M.D. Chronic stress leads to long-lasting deficits in olfactory-guided behaviors, and to neuroplastic changes in the nucleus of the lateral olfactory tract. *Horm. Behav.* **2018**, *98*, 130–144, doi:10.1016/j.yhbeh.2017.12.006.
52. Law, R.; Clow, A. Stress, the cortisol awakening response and cognitive function. In *International Review of Neurobiology*; Academic Press, 2020; Vol. 150, pp. 187–217 ISBN 9780128167526.
53. McEwen, B.S. Physiology and Neurobiology of Stress and Adaptation: Central Role of the Brain. *Physiol. Rev.* **2007**, *87*, 873–904, doi:10.1152/physrev.00041.2006.
54. de Kloet, E.R.; Vreugdenhil, E.; Oitzl, M.S.; Joëls, M. Brain Corticosteroid Receptor Balance in Health and Disease*. *Endocr. Rev.* **1998**, *19*, 269–301, doi:10.1210/edrv.19.3.0331.
55. Dallman, M.F. Fast glucocorticoid actions on brain: Back to the future. *Front. Neuroendocrinol.* **2005**, *26*, 103–108, doi:10.1016/j.yfrne.2005.08.001.
56. Groeneweg, F.L.; Karst, H.; de Kloet, E.R.; Joëls, M. Rapid non-genomic effects of corticosteroids and their role in the central stress response. *J. Endocrinol.* **2011**, *209*, 153–167, doi:10.1530/JOE-10-0472.
57. Binder, E.B. The role of FKBP5, a co-chaperone of the glucocorticoid receptor in the pathogenesis and therapy of affective and anxiety disorders. *Psychoneuroendocrinology* **2009**, *34*, S186–S195.
58. Gardill, B.R.; Vogl, M.R.; Lin, H.-Y.; Hammond, G.L.; Muller, Y.A. Corticosteroid-Binding Globulin: Structure-Function Implications from Species Differences. *PLoS One* **2012**, *7*, 52759, doi:10.1371/journal.pone.0052759.
59. Chapman, K.; Holmes, M.; Seckl, J. 11 β -Hydroxysteroid Dehydrogenases: Intracellular Gate-Keepers of Tissue Glucocorticoid Action. *Physiol. Rev.* **2013**,

- 93, 1139–1206, doi:10.1152/physrev.00020.2012.
60. Pariante, C.M.; Lightman, S.L. The HPA axis in major depression: classical theories and new developments. *Trends Neurosci.* **2008**, *31*, 464–468, doi:10.1016/j.tins.2008.06.006.
 61. Pariante, C.M. Why are depressed patients inflamed? A reflection on 20 years of research on depression, glucocorticoid resistance and inflammation. *Eur. Neuropsychopharmacol.* **2017**, *27*, 554–559, doi:10.1016/j.euroneuro.2017.04.001.
 62. Menke, A. Is the HPA axis as target for depression outdated, or is there a new hope? *Front. psychiatry* **2019**, *10*, 101, doi:10.3389/fpsyt.2019.00101.
 63. Anacker, C.; Zunszain, P.A.; Carvalho, L.A.; Pariante, C.M. The glucocorticoid receptor: Pivot of depression and of antidepressant treatment? *Psychoneuroendocrinology* **2011**, *36*, 415–425, doi:10.1016/j.psyneuen.2010.03.007.
 64. Wong, M.L.; Lewis, M.; Licinio, J. 2.2 Translational Research in Endocrinology and Neuroimmunology Applied to Depression. In *Biomedical Chemistry*; De Gruyter Open Poland, 2015; pp. 119–131 ISBN 9783110468755.
 65. Wróbel, A.; Serefko, A.; Szopa, A.; Rojek, K.; Poleszak, E.; Skalicka-Woźniak, K.; Dudka, J. Inhibition of the CRF1 receptor influences the activity of antidepressant drugs in the forced swim test in rats. *Naunyn. Schmiedeberg's Arch. Pharmacol.* **2017**, *390*, 769–774, doi:10.1007/s00210-017-1377-0.
 66. Leonard, B.E. The concept of depression as a dysfunction of the immune system. In *Depression: From Psychopathology to Pharmacotherapy*; S. Karger AG, 2010; Vol. 27, pp. 53–71 ISBN 9783805596060.
 67. Belleau, E.L.; Treadway, M.T.; Pizzagalli, D.A. The Impact of Stress and Major Depressive Disorder on Hippocampal and Medial Prefrontal Cortex Morphology. *Biol. Psychiatry* **2019**, *85*, 443–453, doi:10.1016/j.biopsych.2018.09.031.
 68. Song, Y.; Miyaki, K.; Suzuki, T.; Sasaki, Y.; Tsutsumi, A.; Kawakami, N.; Shimazu, A.; Takahashi, M.; Inoue, A.; Kan, C.; et al. Altered DNA methylation status of human brain derived neurotrophin factor gene could be useful as biomarker of depression. *Am. J. Med. Genet. Part B Neuropsychiatr. Genet.* **2014**, *165*, 357–364, doi:10.1002/ajmg.b.32238.
 69. Sapolsky, R.; Krey, L.; McEwen, B. Prolonged glucocorticoid exposure reduces hippocampal neuron number: implications for aging. *J. Neurosci.* **1985**, *5*, 1222–1227, doi:10.1523/jneurosci.05-05-01222.1985.
 70. Tian, L.; Hui, C.W.; Bisht, K.; Tan, Y.; Sharma, K.; Chen, S.; Zhang, X.; Tremblay, M.-E. Microglia under psychosocial stressors along the aging trajectory: Consequences on neuronal circuits, behavior, and brain diseases. *Prog. Neuro-Psychopharmacology Biol. Psychiatry* **2017**, *79*, 27–39, doi:10.1016/j.pnpbp.2017.01.007.
 71. Banasr, M.; Dwyer, J.M.; Duman, R.S. Cell atrophy and loss in depression: reversal by antidepressant treatment. *Curr. Opin. Cell Biol.* **2011**, *23*, 730–737, doi:10.1016/j.ceb.2011.09.002.
 72. Takahashi, T.; Kimoto, T.; Tanabe, N.; Hattori, T.; Yasumatsu, N.; Kawato, S. Corticosterone acutely prolonged N-methyl-D-aspartate receptor-mediated Ca²⁺ elevation in cultured rat hippocampal neurons. *J. Neurochem.* **2002**, *83*, 1441–1451, doi:10.1046/j.1471-4159.2002.01251.x.

73. Tata, D.A.; Marciano, V.A.; Anderson, B.J. Synapse loss from chronically elevated glucocorticoids: Relationship to neuropil volume and cell number in hippocampal area CA3. *J. Comp. Neurol.* **2006**, *498*, 363–374, doi:10.1002/cne.21071.
74. Liston, C.; Gan, W.-B. Glucocorticoids are critical regulators of dendritic spine development and plasticity in vivo. *Proc. Natl. Acad. Sci.* **2011**, *108*, 16074–16079, doi:10.1073/pnas.1110444108.
75. Czéh, B.; Michaelis, T.; Watanabe, T.; Frahm, J.; De Biurrun, G.; Van Kampen, M.; Bartolomucci, A.; Fuchs, E. Stress-induced changes in cerebral metabolites, hippocampal volume, and cell proliferation are prevented by antidepressant treatment with tianeptine. *Proc. Natl. Acad. Sci. U. S. A.* **2001**, *98*, 12796–12801, doi:10.1073/pnas.211427898.
76. Bustamante, A.C.; Aiello, A.E.; Galea, S.; Ratanatharathorn, A.; Noronha, C.; Wildman, D.E.; Uddin, M. Glucocorticoid receptor DNA methylation, childhood maltreatment and major depression. *J. Affect. Disord.* **2016**, *206*, 181–188, doi:10.1016/j.jad.2016.07.038.
77. Radtke, K.M.; Schauer, M.; Gunter, H.M.; Ruf-Leuschner, M.; Sill, J.; Meyer, A.; Elbert, T. Epigenetic modifications of the glucocorticoid receptor gene are associated with the vulnerability to psychopathology in childhood maltreatment. *Transl. Psychiatry* **2015**, *5*, doi:10.1038/tp.2015.63.
78. Swartz, J.R.; Hariri, A.R.; Williamson, D.E. An epigenetic mechanism links socioeconomic status to changes in depression-related brain function in high-risk adolescents. *Mol. Psychiatry* **2017**, *22*, 209–214, doi:10.1038/mp.2016.82.
79. Booij, L.; Szyf, M.; Carballedo, A.; Frey, E.M.; Morris, D.; Dymov, S.; Vaisheva, F.; Ly, V.; Fahey, C.; Meaney, J.; et al. DNA methylation of the serotonin transporter gene in peripheral cells and stress-related changes in hippocampal volume: A study in depressed patients and healthy controls. *PLoS One* **2015**, *10*, doi:10.1371/journal.pone.0119061.
80. Weder, N.; Zhang, H.; Jensen, K.; Yang, B.Z.; Simen, A.; Jackowski, A.; Lipschitz, D.; Douglas-Palumberi, H.; Ge, M.; Perepletchikova, F.; et al. Child abuse, depression, and methylation in genes involved with stress, neural plasticity, and brain circuitry. *J. Am. Acad. Child Adolesc. Psychiatry* **2014**, *53*, doi:10.1016/j.jaac.2013.12.025.
81. Sadeh, N.; Spielberg, J.M.; Logue, M.W.; Wolf, E.J.; Smith, A.K.; Lusk, J.; Hayes, J.P.; Sperbeck, E.; Milberg, W.P.; McGlinchey, R.E.; et al. SKA2 methylation is associated with decreased prefrontal cortical thickness and greater PTSD severity among trauma-exposed veterans. *Mol. Psychiatry* **2016**, *21*, 357–363, doi:10.1038/mp.2015.134.
82. Binder, E.B.; Salyakina, D.; Lichtner, P.; Wochnik, G.M.; Ising, M.; Pütz, B.; Papiol, S.; Seaman, S.; Lucae, S.; Kohli, M.A. Polymorphisms in FKBP5 are associated with increased recurrence of depressive episodes and rapid response to antidepressant treatment. *Nat. Genet.* **2004**, *36*, 1319–1325.
83. Amasi-Hartoonian, N.; Sforzini, L.; Cattaneo, A.; Pariante, C.M. Cause or consequence? Understanding the role of cortisol in the increased inflammation observed in depression. *Curr. Opin. Endocr. Metab. Res.* **2022**, *24*, 100356, doi:10.1016/j.coemr.2022.100356.
84. Weber, M.D.; Godbout, J.P.; Sheridan, J.F. Repeated Social Defeat, Neuroinflammation, and Behavior: Monocytes Carry the Signal. *Neuropsychopharmacology* **2017**, *42*, 46–61, doi:10.1038/npp.2016.102.

85. Horowitz, M.A.; Zunszain, P.A.; Anacker, C.; Musaelyan, K.; Pariante, C.M. Glucocorticoids and Inflammation: A Double-Headed Sword in Depression? In *Inflammation in Psychiatry*; Halaris, A., Leonard, B.E., Eds.; S.Karger AG, 2013; Vol. 28, pp. 127–143 ISBN 978-3-318-02310-7.
86. Houwing, D.J.; Buwalda, B.; van der Zee, E.A.; de Boer, S.F.; Olivier, J.D.A. The Serotonin Transporter and Early Life Stress: Translational Perspectives. *Front. Cell. Neurosci.* **2017**, *11*, doi:10.3389/fncel.2017.00117.
87. Dantzer, R. Cytokine, Sickness Behavior, and Depression. *Immunol. Allergy Clin. North Am.* **2009**, *29*, 247–264, doi:10.1016/j.iac.2009.02.002.
88. Qing, H.; Desrouleaux, R.; Israni-Winger, K.; Mineur, Y.S.; Fogelman, N.; Zhang, C.; Rashed, S.; Palm, N.W.; Sinha, R.; Picciotto, M.R.; et al. Origin and Function of Stress-Induced IL-6 in Murine Models. *Cell* **2020**, *182*, 372-387.e14, doi:10.1016/j.cell.2020.05.054.
89. Goshen, I.; Yirmiya, R. Interleukin-1 (IL-1): A central regulator of stress responses. *Front. Neuroendocrinol.* **2009**, *30*, 30–45, doi:10.1016/j.yfrne.2008.10.001.
90. Alam, A.; Voronovich, Z.; Carley, J.A. A Review of Therapeutic Uses of Mirtazapine in Psychiatric and Medical Conditions. *Prim. Care Companion CNS Disord.* **2013**, *15*, doi:10.4088/PCC.13r01525.
91. Wohleb, E.S.; Hanke, M.L.; Corona, A.W.; Powell, N.D.; Stiner, L.M.; Bailey, M.T.; Nelson, R.J.; Godbout, J.P.; Sheridan, J.F. β -Adrenergic Receptor Antagonism Prevents Anxiety-Like Behavior and Microglial Reactivity Induced by Repeated Social Defeat. *J. Neurosci.* **2011**, *31*, 6277–6288, doi:10.1523/jneurosci.0450-11.2011.
92. Afridi, R.; Suk, K. Microglial Responses to Stress-Induced Depression: Causes and Consequences. *Cells* **2023**, *12*, 1521, doi:10.3390/cells12111521.
93. Jia, X.; Gao, Z.; Hu, H. Microglia in depression: current perspectives. *Sci. China Life Sci.* **2021**, *64*, 911–925, doi:10.1007/s11427-020-1815-6.
94. Mariani, N.; Everson, J.; Pariante, C.M.; Borsini, A. Modulation of microglial activation by antidepressants. *J. Psychopharmacol.* **2022**, *36*, 131–150, doi:10.1177/02698811211069110.
95. Millor, G.; Lecours, C.; Samson, L.; Bisht, K.; Poggini, S.; Pagani, F.; Deflorio, C.; Lauro, C.; Alboni, S.; Limatola, C.; et al. Fractalkine receptor deficiency impairs microglial and neuronal responsiveness to chronic stress. *Brain. Behav. Immun.* **2016**, *55*, 114–125, doi:10.1016/j.bbi.2015.07.024.
96. Wang, H.; He, Y.; Sun, Z.; Ren, S.; Liu, M.; Wang, G.; Yang, J. Microglia in depression: an overview of microglia in the pathogenesis and treatment of depression. *J. Neuroinflammation* **2022**, *19*, 132, doi:10.1186/s12974-022-02492-0.
97. Platten, M.; Nollen, E.A.A.; Röhrig, U.F.; Fallarino, F.; Opitz, C.A. Tryptophan metabolism as a common therapeutic target in cancer, neurodegeneration and beyond. *Nat. Rev. Drug Discov.* **2019**, *18*, 379–401, doi:10.1038/s41573-019-0016-5.
98. Savitz, J. The kynurenine pathway: a finger in every pie. *Mol. Psychiatry* **2020**, *25*, 131–147, doi:10.1038/s41380-019-0414-4.
99. Cervenka, I.; Agudelo, L.Z.; Ruas, J.L. Kynurenines: Tryptophan's metabolites in exercise, inflammation, and mental health. *Science* **2017**, *357*,

doi:10.1126/science.aaf9794.

100. Hsu, C.-N.; Tain, Y.-L. Developmental Programming and Reprogramming of Hypertension and Kidney Disease: Impact of Tryptophan Metabolism. *Int. J. Mol. Sci.* **2020**, *21*, 8705, doi:10.3390/ijms21228705.
101. Berger, M.; Gray, J.A.; Roth, B.L. The Expanded Biology of Serotonin. *Annu. Rev. Med.* **2009**, *60*, 355–366, doi:10.1146/annurev.med.60.042307.110802.
102. Comai, S.; Bertazzo, A.; Brughera, M.; Crotti, S. Tryptophan in health and disease. In *Advances in clinical chemistry*; Adv Clin Chem, 2020; Vol. 95, pp. 165–218 ISBN 9780128211656.
103. Höglund, E.; Øverli, Ø.; Winberg, S. Tryptophan Metabolic Pathways and Brain Serotonergic Activity: A Comparative Review. *Front. Endocrinol. (Lausanne)*. **2019**, *10*, 158, doi:10.3389/fendo.2019.00158.
104. Chen, K.; Shih, J.C. Monoamine Oxidase A and B: Structure, Function, and Behavior. In; Goldstein, D.S., Eisenhofer, G., McCarty, R.B.T.-A. in P., Eds.; Academic Press, 1997; Vol. 42, pp. 292–296 ISBN 1054-3589.
105. Cowen, P.J.; Browning, M. What has serotonin to do with depression? *World Psychiatry* **2015**, *14*, 158–160, doi:10.1002/wps.20229.
106. Chen, Y.; Xu, H.; Zhu, M.; Liu, K.; Lin, B.; Luo, R.; Chen, C.; Li, M. Stress inhibits tryptophan hydroxylase expression in a rat model of depression. *Oncotarget* **2017**, *8*, 63247–63257, doi:10.18632/oncotarget.18780.
107. Betari, N.; Sahlholm, K.; Morató, X.; Godoy-Marín, H.; Jáuregui, O.; Teigen, K.; Ciruela, F.; Haavik, J. Inhibition of Tryptophan Hydroxylases and Monoamine Oxidase-A by the Proton Pump Inhibitor, Omeprazole—In Vitro and In Vivo Investigations. *Front. Pharmacol.* **2020**, *11*, 593416, doi:10.3389/fphar.2020.593416.
108. Bach-Mizrachi, H.; Underwood, M.D.; Kassir, S.A.; Bakalian, M.J.; Sibille, E.; Tamir, H.; Mann, J.J.; Arango, V. Neuronal Tryptophan Hydroxylase mRNA Expression in the Human Dorsal and Median Raphe Nuclei: Major Depression and Suicide. *Neuropsychopharmacol.* *2006* *314* **2005**, *31*, 814–824, doi:10.1038/sj.npp.1300897.
109. Fukuda, K. Etiological classification of depression based on the enzymes of tryptophan metabolism. *BMC Psychiatry* **2014**, *14*, 372, doi:10.1186/s12888-014-0372-y.
110. Maffei, M.E. 5-Hydroxytryptophan (5-HTP): Natural Occurrence, Analysis, Biosynthesis, Biotechnology, Physiology and Toxicology. *Int. J. Mol. Sci.* **2020**, *22*, 181, doi:10.3390/ijms22010181.
111. Ryan, N.D. Neuroendocrine Response to L-5-Hydroxytryptophan Challenge in Prepubertal Major Depression. *Arch. Gen. Psychiatry* **1992**, *49*, 843, doi:10.1001/archpsyc.1992.01820110007001.
112. Lopez Ibor Alino, J.J.; Ayuso Gutierrez, J.L.; Montejo Iglesias, M.L. 5-Hydroxytryptophan (5-HTP) and a MAOI (nialamide) in the treatment of depressions. A double-blind controlled study. *Int. Pharmacopsychiatry* **1976**, *11*, 8–15, doi:10.1159/000468207.
113. Mendlewicz, J.; Youdim, M.B.H. Antidepressant potentiation of 5-hydroxytryptophan by L-deprenil in affective illness. *J. Affect. Disord.* **1980**, *2*, 137–146, doi:10.1016/0165-0327(80)90013-0.

114. Thase, M.E. The Role of Monoamine Oxidase Inhibitors in Depression Treatment Guidelines. *J. Clin. Psychiatry* **2012**, *73*, 10–16, doi:10.4088/JCP.11096su1c.02.
115. Jones, D.N.; Raghanti, M.A. The role of monoamine oxidase enzymes in the pathophysiology of neurological disorders. *J. Chem. Neuroanat.* **2021**, *114*, 101957, doi:10.1016/j.jchemneu.2021.101957.
116. Moriguchi, S.; Wilson, A.A.; Miler, L.; Rusjan, P.M.; Vasdev, N.; Kish, S.J.; Rajkowska, G.; Wang, J.; Bagby, M.; Mizrahi, R.; et al. Monoamine Oxidase B Total Distribution Volume in the Prefrontal Cortex of Major Depressive Disorder. *JAMA Psychiatry* **2019**, *76*, 634, doi:10.1001/jamapsychiatry.2019.0044.
117. Placidi, G.P.A.; Oquendo, M.A.; Malone, K.M.; Huang, Y.Y.; Ellis, S.P.; Mann, J.J. Aggressivity, suicide attempts, and depression: relationship to cerebrospinal fluid monoamine metabolite levels. *Biol. Psychiatry* **2001**, *50*, 783–791, doi:10.1016/S0006-3223(01)01170-2.
118. Tonon, A.C.; Pilz, L.K.; Markus, R.P.; Hidalgo, M.P.; Elisabetsky, E. Melatonin and Depression: A Translational Perspective From Animal Models to Clinical Studies. *Front. Psychiatry* **2021**, *12*, 452, doi:10.3389/FPSYT.2021.638981/BIBTEX.
119. Ogłodek, E.A.; Just, M.J.; Szromek, A.R.; Araszkievicz, A. Melatonin and neurotrophins NT-3, BDNF, NGF in patients with varying levels of depression severity. *Pharmacol. Reports* **2016**, *68*, 945–951, doi:10.1016/j.pharep.2016.04.003.
120. Ali, T.; Rahman, S.U.; Hao, Q.; Li, W.; Liu, Z.; Ali Shah, F.; Murtaza, I.; Zhang, Z.; Yang, X.; Liu, G.; et al. Melatonin prevents neuroinflammation and relieves depression by attenuating autophagy impairment through FOXO3a regulation. *J. Pineal Res.* **2020**, *69*, doi:10.1111/jpi.12667.
121. Qin, Y.; Wang, N.; Zhang, X.; Han, X.; Zhai, X.; Lu, Y. IDO and TDO as a potential therapeutic target in different types of depression. *Metab. Brain Dis.* **2018**, *33*, 1787–1800, doi:10.1007/S11011-018-0290-7.
122. Guillemin, G.J.; Smythe, G.; Takikawa, O.; Brew, B.J. Expression of indoleamine 2,3-dioxygenase and production of quinolinic acid by human microglia, astrocytes, and neurons. *Glia* **2005**, *49*, 15–23, doi:10.1002/glia.20090.
123. Guillemin, G.J.; Smith, D.G.; Kerr, S.J.; Smythe, G.A.; Kapoor, V.; Armati, P.J.; Brew, B.J. Characterisation of kynurenine pathway metabolism in human astrocytes and implications in neuropathogenesis. *Redox Rep.* **2000**, *5*, 108–111, doi:10.1179/135100000101535375.
124. Wigner, P.; Czarny, P.; Synowiec, E.; Bijak, M.; Białek, K.; Talarowska, M.; Galecki, P.; Szemraj, J.; Sliwinski, T. Association between single nucleotide polymorphisms of TPH1 and TPH2 genes, and depressive disorders. *J. Cell. Mol. Med.* **2018**, *22*, 1778–1791, doi:10.1111/jcmm.13459.
125. Steiner, J.; Walter, M.; Gos, T.; Guillemin, G.J.; Bernstein, H.G.; Sarnyai, Z.; Mawrin, C.; Brisch, R.; Bielau, H.; zu Schwabedissen, L.M.; et al. Severe depression is associated with increased microglial quinolinic acid in subregions of the anterior cingulate gyrus: evidence for an immune-modulated glutamatergic neurotransmission? *J. Neuroinflammation* **2011**, *8*, doi:10.1186/1742-2094-8-94.
126. Bansal, Y.; Singh, R.; Parhar, I.; Kuhad, A.; Soga, T. Quinolinic Acid and Nuclear Factor Erythroid 2-Related Factor 2 in Depression: Role in Neuroprogression. *Front. Pharmacol.* **2019**, *10*, doi:10.3389/fphar.2019.00452.
127. Miura, H.; Ozaki, N.; Sawada, M.; Isobe, K.; Ohta, T.; Nagatsu, T. A link between

- stress and depression: Shifts in the balance between the kynurenine and serotonin pathways of tryptophan metabolism and the etiology and pathophysiology of depression. <http://dx.doi.org/10.1080/10253890701754068> **2009**, *11*, 198–209, doi:10.1080/10253890701754068.
128. Wang, D.; Wu, J.; Zhu, P.; Xie, H.; Lu, L.; Bai, W.; Pan, W.; Shi, R.; Ye, J.; Xia, B.; et al. Tryptophan-rich diet ameliorates chronic unpredictable mild stress induced depression- and anxiety-like behavior in mice: The potential involvement of gut-brain axis. *Food Res. Int.* **2022**, *157*, 111289, doi:10.1016/j.foodres.2022.111289.
 129. Bastiaanssen, T.F.S.; Cusotto, S.; Claesson, M.J.; Clarke, G.; Dinan, T.G.; Cryan, J.F. Gutted! Unraveling the Role of the Microbiome in Major Depressive Disorder. *Harv. Rev. Psychiatry* **2020**, *28*, 26–39, doi:10.1097/hrp.0000000000000243.
 130. Deng, Y.; Zhou, M.; Wang, J.; Yao, J.; Yu, J.; Liu, W.; Wu, L.; Wang, J.; Gao, R. Involvement of the microbiota-gut-brain axis in chronic restraint stress: disturbances of the kynurenine metabolic pathway in both the gut and brain. *Gut Microbes* **2021**, *13*, 1–16, doi:10.1080/19490976.2020.1869501.
 131. Marin, I.A.; Goertz, J.E.; Ren, T.; Rich, S.S.; Onengut-Gumuscu, S.; Farber, E.; Wu, M.; Overall, C.C.; Kipnis, J.; Gaultier, A. Microbiota alteration is associated with the development of stress-induced despair behavior. *Sci. Rep.* **2017**, *7*, 43859, doi:10.1038/srep43859.
 132. Desbonnet, L.; Garrett, L.; Clarke, G.; Bienenstock, J.; Dinan, T.G. The probiotic *Bifidobacteria infantis*: An assessment of potential antidepressant properties in the rat. *J. Psychiatr. Res.* **2008**, *43*, 164–174, doi:10.1016/j.jpsychires.2008.03.009.
 133. Li, H.; Wang, P.; Zhou, Y.; Zhao, F.; Gao, X.; Wu, C.; Wu, T.; Jiang, L.; Zhang, D. Correlation between intestinal microbial imbalance and <sc>5-HT</sc> metabolism, immune inflammation in chronic unpredictable mild stress male rats. *Genes, Brain Behav.* **2022**, *21*, doi:10.1111/gbb.12806.
 134. Wikoff, W.R.; Anfora, A.T.; Liu, J.; Schultz, P.G.; Lesley, S.A.; Peters, E.C.; Siuzdak, G. Metabolomics analysis reveals large effects of gut microflora on mammalian blood metabolites. *Proc. Natl. Acad. Sci.* **2009**, *106*, 3698–3703, doi:10.1073/pnas.0812874106.
 135. Julius, D. Molecular Biology of Serotonin Receptors. *Annu. Rev. Neurosci.* **1991**, *14*, 335–360, doi:10.1146/annurev.ne.14.030191.002003.
 136. Raghupathi, R.; Duffield, M.D.; Zelkas, L.; Meedeniya, A.; Brookes, S.J.H.; Sia, T.C.; Wattchow, D.A.; Spencer, N.J.; Keating, D.J. Identification of unique release kinetics of serotonin from guinea-pig and human enterochromaffin cells. *J. Physiol.* **2013**, *591*, 5959–5975, doi:10.1113/jphysiol.2013.259796.
 137. Mohammad-Zadeh, L.F.; Moses, L.; Gwaltney-Brant, S.M. Serotonin: a review. *J. Vet. Pharmacol. Ther.* **2008**, *31*, 187–99, doi:10.1111/j.1365-2885.2008.00944.x.
 138. Marin, P.; Bécamel, C.; Chaumont-Dubel, S.; Vandermoere, F.; Bockaert, J.; Claeysen, S. Classification and signaling characteristics of 5-HT receptors: toward the concept of 5-HT receptosomes. In *Handbook of the Behavioral Neurobiology of Serotonin*; Müller, C.P., Cunningham, K.A.B.T.-H. of B.N., Eds.; Elsevier, 2020; Vol. 31, pp. 91–120 ISBN 1569-7339.
 139. Pytliak, M.; Vargová, V.; Mechírová, V.; Felšöci, M. Serotonin receptors - from

- molecular biology to clinical applications. *Physiol. Res.* **2011**, *60*, 15–25, doi:10.33549/physiolres.931903.
140. Overview - Antidepressants - NHS Available online: <https://www.nhs.uk/mental-health/talking-therapies-medicine-treatments/medicines-and-psychiatry/antidepressants/overview/> (accessed on Oct 11, 2023).
 141. Gupta, D.; Radhakrishnan, M.; Kurhe, Y.; Thangaraj, D.; Prabhakar, V.; Kanade, P. Antidepressant-like effects of a novel 5-HT₃ receptor antagonist 6z in acute and chronic murine models of depression. *Acta Pharmacol. Sin.* **2014**, *35*, 1493–1503, doi:10.1038/aps.2014.89.
 142. Zięba, A.; Stępnicki, P.; Matosiuk, D.; Kaczor, A.A. Overcoming Depression with 5-HT_{2A} Receptor Ligands. *Int. J. Mol. Sci.* **2021**, *23*, 10, doi:10.3390/ijms23010010.
 143. Nautiyal, K.M.; Hen, R. Serotonin receptors in depression: from A to B. *F1000Research* **2017**, *6*, 123, doi:10.12688/f1000research.9736.1.
 144. Smith, A.L.W.; Harmer, C.J.; Cowen, P.J.; Murphy, S.E. The Serotonin 1A (5-HT_{1A}) Receptor as a Pharmacological Target in Depression. *CNS Drugs* **2023**, *37*, 571–585, doi:10.1007/s40263-023-01014-7.
 145. Yohn, C.N.; Gergues, M.M.; Samuels, B.A. The role of 5-HT receptors in depression. *Mol. Brain* **2017**, *10*, 1–12, doi:10.1186/S13041-017-0306-Y.
 146. Meneses, A.; Antonietta De Luca, M.; Di Giovanni, G.; Zhang, G.; Stackman Jr, R.W. The role of serotonin 5-HT_{2A} receptors in memory and cognition. **2015**, *101*, 19, doi:10.3389/fphar.2015.00225.
 147. Bhatt, S.; Devadoss, T.; Manjula, S.N.; Rajangam, J. 5-HT₃ Receptor Antagonism: A Potential Therapeutic Approach for the Treatment of Depression and other Disorders. *Curr. Neuropharmacol.* **2021**, *19*, 1545–1559, doi:10.2174/1570159X18666201015155816.
 148. Albert, P.; Le François, B. Modifying 5-HT_{1A} Receptor Gene Expression as a New Target for Antidepressant Therapy. *Front. Neurosci.* **2010**, *4*.
 149. Kaufman, J.; DeLorenzo, C.; Choudhury, S.; Parsey, R. V The 5-HT_{1A} receptor in Major Depressive Disorder. *Eur. Neuropsychopharmacol.* **2016**, *26*, 397–410, doi:10.1016/j.euroneuro.2015.12.039.
 150. Guiard, B.P.; Giovanni, G. Di Central serotonin-2A (5-HT_{2A}) receptor dysfunction in depression and epilepsy: the missing link? *Front. Pharmacol.* **2015**, *6*, 46, doi:10.3389/fphar.2015.00046.
 151. Gööz, M.; Gööz, P.; Luttrell, L.M.; Raymond, J.R. 5-HT_{2A} Receptor Induces ERK Phosphorylation and Proliferation through ADAM-17 Tumor Necrosis Factor- α -converting Enzyme (TACE) Activation and Heparin-bound Epidermal Growth Factor-like Growth Factor (HB-EGF) Shedding in Mesangial Cells. *J. Biol. Chem.* **2006**, *281*, 21004–21012, doi:10.1074/jbc.M512096200.
 152. Wang, J.Q.; Mao, L. The ERK Pathway: Molecular Mechanisms and Treatment of Depression. *Mol. Neurobiol.* **2019**, *56*, 6197–6205, doi:10.1007/s12035-019-1524-3.
 153. Shukla, A.K.; Dwivedi-Agnihotri, H. Structure and function of β -arrestins, their emerging role in breast cancer, and potential opportunities for therapeutic manipulation. In *Advances in cancer research*; Europe PMC Funders, 2020; Vol.

145, pp. 139–156.

154. Schmid, C.L.; Raehal, K.M.; Bohn, L.M. Agonist-directed signaling of the serotonin 2A receptor depends on β -arrestin-2 interactions in vivo. *Proc. Natl. Acad. Sci.* **2008**, *105*, 1079–1084, doi:10.1073/pnas.0708862105.
155. Abbas, A.; Roth, B.L. Arresting serotonin. *Proc. Natl. Acad. Sci.* **2008**, *105*, 831–832, doi:10.1073/pnas.0711335105.
156. Felsing, D.E.; Nilson, A.; Jain, M.; Raval, S.; Inoue, A.; Allen, J. β -arrestins mediate rapid 5-HT_{2A} receptor endocytosis to regulate intensity and duration of signaling. *FASEB J.* **2019**, *33*, 502.3–502.3, doi:10.1096/fasebj.2019.33.1.
157. Peters, J.A.; Lambert, J.J. Electrophysiology of 5-HT₃ receptors in neuronal cell lines. *Trends Pharmacol. Sci.* **1989**, *10*, 172–175, doi:10.1016/0165-6147(89)90230-7.
158. Bétry, C.; Etiévant, A.; Oosterhof, C.; Ebert, B.; Sanchez, C.; Haddjeri, N. Role of 5-HT₃ Receptors in the Antidepressant Response. *Pharmaceuticals* **2011**, *4*, 603–629, doi:10.3390/ph4040603.
159. van Hooft, J. 5-HT₃ receptors and neurotransmitter release in the CNS: a nerve ending story? *Trends Neurosci.* **2000**, *23*, 605–610, doi:10.1016/S0166-2236(00)01662-3.
160. Moncrieff, J.; Cooper, R.E.; Stockmann, T.; Amendola, S.; Hengartner, M.P.; Horowitz, M.A. The serotonin theory of depression: a systematic umbrella review of the evidence. *Mol. Psychiatry* **2022**, 1–14, doi:10.1038/s41380-022-01661-0.
161. Jauhar, S.; Arnone, D.; Baldwin, D.S.; Bloomfield, M.; Browning, M.; Cleare, A.J.; Corlett, P.; Deakin, J.F.W.; Erritzoe, D.; Fu, C.; et al. A leaky umbrella has little value: evidence clearly indicates the serotonin system is implicated in depression. *Mol. Psychiatry* **2023**, doi:10.1038/s41380-023-02095-y.
162. Jauhar, S.; Cowen, P.J.; Browning, M. Fifty years on: Serotonin and depression. *J. Psychopharmacol.* **2023**, *37*, 237–241, doi:10.1177/02698811231161813.
163. Ruhé, H.G.; Mason, N.S.; Schene, A.H. Mood is indirectly related to serotonin, norepinephrine and dopamine levels in humans: a meta-analysis of monoamine depletion studies. *Mol. Psychiatry* **2007**, *124*, **2007**, *12*, 331–359, doi:10.1038/sj.mp.4001949.
164. Fusar-Poli, P.; Allen, P.; McGuire, P.; Placentino, A.; Cortesi, M.; Perez, J. Neuroimaging and electrophysiological studies of the effects of acute tryptophan depletion: a systematic review of the literature. *Psychopharmacology (Berl.)* **2006**, *188*, 131–143, doi:10.1007/s00213-006-0493-1.
165. Miranda, M.; Morici, J.F.; Zanoni, M.B.; Bekinschtein, P. Brain-Derived Neurotrophic Factor: A Key Molecule for Memory in the Healthy and the Pathological Brain. *Front. Cell. Neurosci.* **2019**, *13*, 363, doi:10.3389/fncel.2019.00363.
166. Schirò, G.; Iacono, S.; Ragonese, P.; Aridon, P.; Salemi, G.; Balistreri, C.R. A Brief Overview on BDNF-Trk Pathway in the Nervous System: A Potential Biomarker or Possible Target in Treatment of Multiple Sclerosis? *Front. Neurol.* **2022**, *13*, 917527, doi:10.3389/fneur.2022.917527.
167. Miranda-Lourenço, C.; Ribeiro-Rodrigues, L.; Fonseca-Gomes, J.; Tanqueiro, S.R.; Belo, R.F.; Ferreira, C.B.; Rei, N.; Ferreira-Manso, M.; de Almeida-Borlido, C.; Costa-Coelho, T.; et al. Challenges of BDNF-based therapies: From common

- to rare diseases. *Pharmacol. Res.* **2020**, *162*, 105281, doi:10.1016/j.phrs.2020.105281.
168. Je, H.S.; Yang, F.; Ji, Y.; Nagappan, G.; Hempstead, B.L.; Lu, B. Role of pro-brain-derived neurotrophic factor (proBDNF) to mature BDNF conversion in activity-dependent competition at developing neuromuscular synapses. *Proc. Natl. Acad. Sci.* **2012**, *109*, 15924–15929, doi:10.1073/pnas.1207767109.
 169. Brigadski, T.; Leßmann, V. BDNF: a regulator of learning and memory processes with clinical potential. *e-Neuroforum* **2014**, *5*, 1–11, doi:10.1007/s13295-014-0053-9.
 170. Wang, C.S.; Kavalali, E.T.; Monteggia, L.M. BDNF signaling in context: From synaptic regulation to psychiatric disorders. *Cell* **2022**, *185*, 62–76, doi:10.1016/j.cell.2021.12.003.
 171. Pruunsild, P.; Kazantseva, A.; Aid, T.; Palm, K.; Timmusk, T. Dissecting the human BDNF locus: Bidirectional transcription, complex splicing, and multiple promoters. *Genomics* **2007**, *90*, 397–406, doi:10.1016/j.ygeno.2007.05.004.
 172. Nair, B.; Wong-Riley, M.T.T. Transcriptional Regulation of Brain-derived Neurotrophic Factor Coding Exon IX. *J. Biol. Chem.* **2016**, *291*, 22583–22593, doi:10.1074/jbc.M116.742304.
 173. Pathak, H.; Borchert, A.; Garaali, S.; Burkert, A.; Frieling, H. BDNF exon IV promoter methylation and antidepressant action: a complex interplay. *Clin. Epigenetics* **2022**, *14*, 187, doi:10.1186/s13148-022-01415-3.
 174. Li, Y.-J.; Xu, M.; Gao, Z.-H.; Wang, Y.-Q.; Yue, Z.; Zhang, Y.-X.; Li, X.-X.; Zhang, C.; Xie, S.-Y.; Wang, P.-Y. Alterations of Serum Levels of BDNF-Related miRNAs in Patients with Depression. *PLoS One* **2013**, *8*, e63648, doi:10.1371/journal.pone.0063648.
 175. Numakawa, T.; Odaka, H. Brain-Derived Neurotrophic Factor Signaling in the Pathophysiology of Alzheimer's Disease: Beneficial Effects of Flavonoids for Neuroprotection. *Int. J. Mol. Sci.* **2021**, *22*, 5719, doi:10.3390/ijms22115719.
 176. Oh, H.; Lewis, D.A.; Sibille, E. The Role of BDNF in Age-Dependent Changes of Excitatory and Inhibitory Synaptic Markers in the Human Prefrontal Cortex. *Neuropsychopharmacology* **2016**, *41*, 3080–3091, doi:10.1038/npp.2016.126.
 177. Bathina, S.; Das, U.N. Brain-derived neurotrophic factor and its clinical implications. *Arch. Med. Sci.* **2015**, *11*, 1164–1178, doi:10.5114/aoms.2015.56342.
 178. Cohen-Cory, S.; Kidane, A.H.; Shirkey, N.J.; Marshak, S. Brain-derived neurotrophic factor and the development of structural neuronal connectivity. *Dev. Neurobiol.* **2010**, *70*, 271–288, doi:10.1002/dneu.20774.
 179. Lu, B.; Nagappan, G.; Lu, Y. BDNF and synaptic plasticity, cognitive function, and dysfunction. *Handb. Exp. Pharmacol.* **2014**, *220*, 223–250, doi:10.1007/978-3-642-45106-5_9.
 180. Mizoguchi, Y.; Yao, H.; Imamura, Y.; Hashimoto, M.; Monji, A. Lower brain-derived neurotrophic factor levels are associated with age-related memory impairment in community-dwelling older adults: the Sefuri study. *Sci. Rep.* **2020**, *10*, 16442, doi:10.1038/s41598-020-73576-1.
 181. Numakawa, T.; Odaka, H.; Adachi, N. Actions of brain-derived neurotrophin factor in the neurogenesis and neuronal function, and its involvement in the

- pathophysiology of brain diseases. *Int. J. Mol. Sci.* **2018**, *19*, 3650, doi:10.3390/ijms19113650.
182. Chen, S.-D.; Wu, C.-L.; Hwang, W.-C.; Yang, D.-I. More Insight into BDNF against Neurodegeneration: Anti-Apoptosis, Anti-Oxidation, and Suppression of Autophagy. *Int. J. Mol. Sci.* **2017**, *18*, 545, doi:10.3390/ijms18030545.
183. Citri, A.; Malenka, R.C. Synaptic Plasticity: Multiple Forms, Functions, and Mechanisms. *Neuropsychopharmacology* **2008**, *33*, 18–41, doi:10.1038/sj.npp.1301559.
184. Jewett, B.E.; Thapa, B. Physiology, NMDA receptor. In *StatPearls [Internet]*; StatPearls Publishing, 2021.
185. Horch, H.W.; Katz, L.C. BDNF release from single cells elicits local dendritic growth in nearby neurons. *Nat. Neurosci.* **2002**, *5*, 1177–1184, doi:10.1038/nn927.
186. Ming, G.; Song, H. Adult Neurogenesis in the Mammalian Brain: Significant Answers and Significant Questions. *Neuron* **2011**, *70*, 687–702, doi:10.1016/j.neuron.2011.05.001.
187. Gao, J.; Liu, J.; Yao, M.; Zhang, W.; Yang, B.; Wang, G. Panax notoginseng Saponins Stimulates Neurogenesis and Neurological Restoration After Microsphere-Induced Cerebral Embolism in Rats Partially Via mTOR Signaling. *Front. Pharmacol.* **2022**, *13*, 2213, doi:10.3389/fphar.2022.889404.
188. Yang, T.; Nie, Z.; Shu, H.; Kuang, Y.; Chen, X.; Cheng, J.; Yu, S.; Liu, H. The Role of BDNF on Neural Plasticity in Depression. *Front. Cell. Neurosci.* **2020**, *14*, 82, doi:10.3389/fncel.2020.00082.
189. Scharfman, H.; Goodman, J.; Macleod, A.; Phani, S.; Antonelli, C.; Croll, S. Increased neurogenesis and the ectopic granule cells after intrahippocampal BDNF infusion in adult rats. *Exp. Neurol.* **2005**, *192*, 348–356, doi:10.1016/j.expneurol.2004.11.016.
190. Paduchová, Z.; Katrenčíková, B.; Vaváková, M.; Laubertová, L.; Nagyová, Z.; Garaiova, I.; Zdenkařduračková, Z.Z.; Trebatická, J. The Effect of Omega-3 Fatty Acids on Thromboxane, Brain-Derived Neurotrophic Factor, Homocysteine, and Vitamin D in Depressive Children and Adolescents: Randomized Controlled Trial. *Nutrients* **2021**, *13*, 1095, doi:10.3390/nu13041095.
191. Miranda-Lourenço, C.; Duarte, S.T.; Palminha, C.; Gaspar, C.; Rodrigues, T.M.; Magalhães-Cardoso, T.; Rei, N.; Colino-Oliveira, M.; Gomes, R.; Ferreira, S.; et al. Impairment of adenosinergic system in Rett syndrome: Novel therapeutic target to boost BDNF signalling. *Neurobiol. Dis.* **2020**, *145*, 105043, doi:10.1016/j.nbd.2020.105043.
192. Martinowich, K.; Manji, H.; Lu, B. New insights into BDNF function in depression and anxiety. *Nat. Neurosci.* **2007**, *10*, 1089–1093, doi:10.1038/nn1971.
193. Eisch, A.J.; Petrik, D. Depression and Hippocampal Neurogenesis: A Road to Remission? *Science (80-.)*. **2012**, *338*, 72–75, doi:10.1126/science.1222941.
194. Berger, T.; Lee, H.; Young, A.H.; Aarsland, D.; Thuret, S. Adult Hippocampal Neurogenesis in Major Depressive Disorder and Alzheimer's Disease. *Trends Mol. Med.* **2020**, *26*, 803–818, doi:10.1016/j.molmed.2020.03.010.
195. Boldrini, M.; Santiago, A.N.; Hen, R.; Dwork, A.J.; Rosoklija, G.B.; Tamir, H.; Arango, V.; John Mann, J. Hippocampal Granule Neuron Number and Dentate

- Gyrus Volume in Antidepressant-Treated and Untreated Major Depression. *Neuropsychopharmacol.* 2013 386 **2013**, 38, 1068–1077, doi:10.1038/npp.2013.5.
196. Boldrini, M.; Hen, R.; Underwood, M.D.; Rosoklija, G.B.; Dwork, A.J.; Mann, J.J.; Arango, V. Hippocampal Angiogenesis and Progenitor Cell Proliferation Are Increased with Antidepressant Use in Major Depression. *Biol. Psychiatry* **2012**, 72, 562–571, doi:10.1016/j.biopsych.2012.04.024.
 197. Boldrini, M.; Underwood, M.D.; Hen, R.; Rosoklija, G.B.; Dwork, A.J.; John Mann, J.; Arango, V. Antidepressants increase neural progenitor cells in the human hippocampus. *Neuropsychopharmacol.* 2009 3411 **2009**, 34, 2376–2389, doi:10.1038/npp.2009.75.
 198. Azman, K.F.; Zakaria, R. Recent Advances on the Role of Brain-Derived Neurotrophic Factor (BDNF) in Neurodegenerative Diseases. *Int. J. Mol. Sci.* **2022**, 23, 6827, doi:10.3390/ijms23126827.
 199. Erickson, K.I.; Voss, M.W.; Prakash, R.S.; Basak, C.; Szabo, A.; Chaddock, L.; Kim, J.S.; Heo, S.; Alves, H.; White, S.M.; et al. Exercise training increases size of hippocampus and improves memory. *Proc. Natl. Acad. Sci.* **2011**, 108, 3017–3022, doi:10.1073/pnas.1015950108.
 200. You, H.; Lu, B. Diverse Functions of Multiple Bdnf Transcripts Driven by Distinct Bdnf Promoters. *Biomolecules* **2023**, 13, 655, doi:10.3390/biom13040655.
 201. Yoshimura, R.; Okamoto, N.; Chibaatar, E.; Natsuyama, T.; Ikenouchi, A. The Serum Brain-Derived Neurotrophic Factor Increases in Serotonin Reuptake Inhibitor Responders Patients with First-Episode, Drug-Naïve Major Depression. *Biomedicines* **2023**, 11, 584, doi:10.3390/biomedicines11020584.
 202. Chen, B.; Dowlathshahi, D.; MacQueen, G.M.; Wang, J.F.; Young, L.T. Increased hippocampal bdnf immunoreactivity in subjects treated with antidepressant medication. *Biol. Psychiatry* **2001**, 50, 260–265, doi:10.1016/S0006-3223(01)01083-6.
 203. Dwivedi, Y. Involvement of Brain-Derived Neurotrophic Factor in Late-Life Depression. *Am. J. Geriatr. Psychiatry* **2013**, 21, 433–449, doi:10.1016/j.jagp.2012.10.026.
 204. Youssef, M.M.; Underwood, M.D.; Huang, Y.-Y.; Hsiung, S.; Liu, Y.; Simpson, N.R.; Bakalian, M.J.; Rosoklija, G.B.; Dwork, A.J.; Arango, V.; et al. Association of BDNF Val66Met Polymorphism and Brain BDNF Levels with Major Depression and Suicide. *Int. J. Neuropsychopharmacol.* **2018**, 21, 528–538, doi:10.1093/ijnp/pyy008.
 205. Kubera, M.; Obuchowicz, E.; Goehler, L.; Brzeszcz, J.; Maes, M. In animal models, psychosocial stress-induced (neuro) inflammation, apoptosis and reduced neurogenesis are associated to the onset of depression. *Prog. Neuro-Psychopharmacology Biol. Psychiatry* **2011**, 35, 744–759, doi:10.1016/j.pnpbp.2010.08.026.
 206. Jesse, C.R.; Donato, F.; Giacomeli, R.; Del Fabbro, L.; da Silva Antunes, M.; De Gomes, M.G.; Goes, A.T.R.; Boeira, S.P.; Prigol, M.; Souza, L.C. Chronic unpredictable mild stress decreases BDNF and NGF levels and Na⁺, K⁺-ATPase activity in the hippocampus and prefrontal cortex of mice: Antidepressant effect of chrysin. *Neuroscience* **2015**, 289, 367–380, doi:10.1016/j.neuroscience.2014.12.048.

207. Jin, Y.; Sun, L.H.; Yang, W.; Cui, R.J.; Xu, S.B. The Role of BDNF in the Neuroimmune Axis Regulation of Mood Disorders. *Front. Neurol.* **2019**, *10*, 515, doi:10.3389/fneur.2019.00515.
208. Mohammadi, S.; Beh-Pajoo, A.; Ahmadimanesh, M.; Amini, M.; Ghazi-Khansari, M.; Moallem, S.A.; Hosseini, R.; Nourian, Y.H.; Ghahremani, M.H. Evaluation of DNA methylation in BDNF, SLC6A4, NR3C1 and FKBP5 before and after treatment with selective serotonin-reuptake inhibitor in major depressive disorder. *Epigenomics* **2022**, *14*, 1269–1280, doi:10.2217/epi-2022-0246.
209. Park, C.; Kim, J.; Namgung, E.; Lee, D.-W.; Kim, G.H.; Kim, M.; Kim, N.; Kim, T.D.; Kim, S.; Lyoo, I.K. The BDNF Val66Met polymorphism affects the vulnerability of the brain structural network. *Front. Hum. Neurosci.* **2017**, *11*, 400, doi:10.3389/fnhum.2017.00400.
210. Pathak, P.; Mehra, A.; Ram, S.; Pal, A.; Grover, S. Association of serum BDNF level and Val66Met polymorphism with response to treatment in patients of major depressive disease: A step towards personalized therapy. *Behav. Brain Res.* **2022**, *430*, 113931, doi:10.1016/j.bbr.2022.113931.
211. Jahromy, M.H.; Baghchesara, B.; Javanshir, S. Effects of Allopurinol as a xanthine oxidase inhibitor on depressive-like behavior of rats and changes in serum BDNF level. *IBRO Neurosci. Reports* **2022**, *13*, 373–377, doi:10.1016/j.ibneur.2022.10.004.
212. Wu, S.; Ning, K.; Wang, Y.; Zhang, L.; Liu, J. Up-regulation of BDNF/TrkB signaling by δ opioid receptor agonist SNC80 modulates depressive-like behaviors in chronic restraint-stressed mice. *Eur. J. Pharmacol.* **2023**, *942*, 175532, doi:https://doi.org/10.1016/j.ejphar.2023.175532.
213. Ryu, D.; Jee, H.-J.; Kim, S.-Y.; Hwang, S.-H.; Pil, G.-B.; Jung, Y.-S. Luteolin-7-O-Glucuronide Improves Depression-like and Stress Coping Behaviors in Sleep Deprivation Stress Model by Activation of the BDNF Signaling. *Nutrients* **2022**, *14*, 3314, doi:10.3390/nu14163314.
214. Cai, T.; Zheng, S.; Shi, X.; Yuan, L.; Hu, H.; Zhou, B.; Xiao, S.; Wang, F. Therapeutic effect of fecal microbiota transplantation on chronic unpredictable mild stress-induced depression. *Front. Cell. Infect. Microbiol.* **2022**, 1101, doi:10.3389/fcimb.2022.900652.
215. Sleiman, S.F.; Henry, J.; Al-Haddad, R.; El Hayek, L.; Abou Haidar, E.; Stringer, T.; Ulja, D.; Karuppagounder, S.S.; Holson, E.B.; Ratan, R.R.; et al. Exercise promotes the expression of brain derived neurotrophic factor (BDNF) through the action of the ketone body β -hydroxybutyrate. *Elife* **2016**, *5*, doi:10.7554/eLife.15092.
216. García-Suárez, P.C.; Rentería, I.; Plaisance, E.P.; Moncada-Jiménez, J.; Jiménez-Maldonado, A. The effects of interval training on peripheral brain derived neurotrophic factor (BDNF) in young adults: a systematic review and meta-analysis. *Sci. Reports* **2021**, *11*, 1–14, doi:10.1038/s41598-021-88496-x.
217. Saarelainen, T.; Hendolin, P.; Lucas, G.; Koponen, E.; Sairanen, M.; MacDonald, E.; Agerman, K.; Haapasalo, A.; Nawa, H.; Aloyz, R.; et al. Activation of the TrkB Neurotrophin Receptor Is Induced by Antidepressant Drugs and Is Required for Antidepressant-Induced Behavioral Effects. *J. Neurosci.* **2003**, *23*, 349–357, doi:10.1523/jneurosci.23-01-00349.2003.
218. Castrén, E.; Monteggia, L.M. Brain-Derived Neurotrophic Factor Signaling in

- Depression and Antidepressant Action. *Biol. Psychiatry* **2021**, *90*, 128–136, doi:10.1016/j.biopsych.2021.05.008.
219. Casarotto, P.C.; Girysh, M.; Fred, S.M.; Kovaleva, V.; Moliner, R.; Enkavi, G.; Biojone, C.; Cannarozzo, C.; Sahu, M.P.; Kaurinkoski, K.; et al. Antidepressant drugs act by directly binding to TRKB neurotrophin receptors. *Cell* **2021**, *184*, 1299–1313.e19, doi:10.1016/j.cell.2021.01.034.
 220. Arosio, B.; Guerini, F.R.; Voshaar, R.C.O.; Aprahamian, I. Blood Brain-Derived Neurotrophic Factor (BDNF) and Major Depression: Do We Have a Translational Perspective? *Front. Behav. Neurosci.* **2021**, *15*, 626906, doi:10.3389/fnbeh.2021.626906.
 221. Homberg, J.R.; Molteni, R.; Calabrese, F.; Riva, M.A. The serotonin–BDNF duo: Developmental implications for the vulnerability to psychopathology. *Neurosci. Biobehav. Rev.* **2014**, *43*, 35–47, doi:10.1016/j.neubiorev.2014.03.012.
 222. Correia, A.S.; Cardoso, A.; Vale, N. Oxidative Stress in Depression: The Link with the Stress Response, Neuroinflammation, Serotonin, Neurogenesis and Synaptic Plasticity. *Antioxidants* **2023**, *12*, 470, doi:10.3390/antiox12020470.
 223. Kunugi, H.; Hori, H.; Adachi, N.; Numakawa, T. Interface between hypothalamic-pituitary-adrenal axis and brain-derived neurotrophic factor in depression. *Psychiatry Clin. Neurosci.* **2010**, *64*, 447–459, doi:10.1111/j.1440-1819.2010.02135.x.
 224. Ait Tayeb, A.E.K.; Poinsignon, V.; Chappell, K.; Bouligand, J.; Becquemont, L.; Verstuyft, C. Major Depressive Disorder and Oxidative Stress: A Review of Peripheral and Genetic Biomarkers According to Clinical Characteristics and Disease Stages. *Antioxidants* **2023**, *12*, 942, doi:10.3390/antiox12040942.
 225. Trifunovic, S.; Stevanovic, I.; Milosevic, A.; Ristic, N.; Janjic, M.; Bjelobaba, I.; Savic, D.; Bozic, I.; Jakovljevic, M.; Tesovic, K.; et al. The Function of the Hypothalamic–Pituitary–Adrenal Axis During Experimental Autoimmune Encephalomyelitis: Involvement of Oxidative Stress Mediators. *Front. Neurosci.* **2021**, *15*, doi:10.3389/fnins.2021.649485.
 226. Du, J.; Wang, Y.; Hunter, R.; Wei, Y.; Blumenthal, R.; Falke, C.; Khairova, R.; Zhou, R.; Yuan, P.; Machado-Vieira, R.; et al. Dynamic regulation of mitochondrial function by glucocorticoids. *Proc. Natl. Acad. Sci.* **2009**, *106*, 3543–3548, doi:10.1073/pnas.0812671106.
 227. Spiers, J.G.; Chen, H.-J.C.; Sernia, C.; Lavidis, N.A. Activation of the hypothalamic-pituitary-adrenal stress axis induces cellular oxidative stress. *Front. Neurosci.* **2015**, *8*, doi:10.3389/fnins.2014.00456.
 228. Sato, H.; Takahashi, T.; Sumitani, K.; Takatsu, H.; Urano, S. Glucocorticoid Generates ROS to Induce Oxidative Injury in the Hippocampus, Leading to Impairment of Cognitive Function of Rats. *J. Clin. Biochem. Nutr.* **2010**, *47*, 224–232, doi:10.3164/jcfn.10-58.
 229. Aquino, G.A.; Sousa, C.N.S.; Medeiros, I.S.; Almeida, J.C.; Cysne Filho, F.M.S.; Santos Júnior, M.A.; Vasconcelos, S.M.M. Behavioral alterations, brain oxidative stress, and elevated levels of corticosterone associated with a pressure injury model in male mice. *J. Basic Clin. Physiol. Pharmacol.* **2022**, *33*, 789–801, doi:10.1515/jbcpp-2021-0056.
 230. Camargo, A.; Dalmagro, A.P.; Rikel, L.; da Silva, E.B.; Simão da Silva, K.A.B.; Zeni, A.L.B. Cholecalciferol counteracts depressive-like behavior and oxidative

- stress induced by repeated corticosterone treatment in mice. *Eur. J. Pharmacol.* **2018**, 833, 451–461, doi:10.1016/j.ejphar.2018.07.002.
231. Zeni, A.L.B.; Camargo, A.; Dalmagro, A.P. Lutein prevents corticosterone-induced depressive-like behavior in mice with the involvement of antioxidant and neuroprotective activities. *Pharmacol. Biochem. Behav.* **2019**, 179, 63–72, doi:10.1016/j.pbb.2019.02.004.
 232. Xiao, Q.; Xiong, Z.; Yu, C.; Zhou, J.; Shen, Q.; Wang, L.; Xie, X.; Fu, Z. Antidepressant activity of crocin-I is associated with amelioration of neuroinflammation and attenuates oxidative damage induced by corticosterone in mice. *Physiol. Behav.* **2019**, 212, 112699, doi:10.1016/j.physbeh.2019.112699.
 233. Song, L.; Wu, X.; Wang, J.; Guan, Y.; Zhang, Y.; Gong, M.; Wang, Y.; Li, B. Antidepressant effect of catalpol on corticosterone-induced depressive-like behavior involves the inhibition of HPA axis hyperactivity, central inflammation and oxidative damage probably via dual regulation of NF- κ B and Nrf2. *Brain Res. Bull.* **2021**, 177, 81–91, doi:10.1016/j.brainresbull.2021.09.002.
 234. Shuster, A.L.; Rocha, F.E.; Wayszceyk, S.; de Lima, D.D.; Barauna, S.C.; Lopes, B.G.; Alberton, M.D.; Magro, D.D.D. Protective effect of *Myrcia pubipetala* Miq. against the alterations in oxidative stress parameters in an animal model of depression induced by corticosterone. *Brain Res.* **2022**, 1774, 147725, doi:10.1016/j.brainres.2021.147725.
 235. Ozyurek, P.; Cevik, C.; Kilic, I.; Aslan, A. Effects of Day and Night Shifts on Stress, Anxiety, Quality of Life, and Oxidative Stress Parameters in Nurses. *Florence Nightingale J. Nurs.* **2021**, 29, 81–92, doi:10.5152/fjn.2021.19141.
 236. Samad, N.; Rafeeqe, M.; Imran, I. Free-L-Cysteine improves corticosterone-induced behavioral deficits, oxidative stress and neurotransmission in rats. *Metab. Brain Dis.* **2023**, 38, 983–997, doi:10.1007/s11011-022-01143-w.
 237. Lew, S.Y.; Lim, S.H.; Lim, L.W.; Wong, K.H. Neuroprotective effects of *Hericium erinaceus* (Bull.: Fr.) Pers. against high-dose corticosterone-induced oxidative stress in PC-12 cells. *BMC Complement. Med. Ther.* **2020**, 20, 340, doi:10.1186/s12906-020-03132-x.
 238. Filatova, E. V.; Shadrina, M.I.; Slominsky, P.A. Major Depression: One Brain, One Disease, One Set of Intertwined Processes. *Cells* **2021**, 10, 1283, doi:10.3390/cells10061283.
 239. Riveros, M.E.; Ávila, A.; Schruers, K.; Ezquer, F. Antioxidant Biomolecules and Their Potential for the Treatment of Difficult-to-Treat Depression and Conventional Treatment-Resistant Depression. *Antioxidants* **2022**, 11, 540, doi:10.3390/antiox11030540.
 240. Abdel-Salam, O.M.E.; Morsy, S.M.Y.; Sleem, A.A. The effect of different antidepressant drugs on oxidative stress after lipopolysaccharide administration in mice. *EXCLI J.* **2011**, 10, 290–302.
 241. Behr, G.A.; Moreira, J.C.F.; Frey, B.N. Preclinical and Clinical Evidence of Antioxidant Effects of Antidepressant Agents: Implications for the Pathophysiology of Major Depressive Disorder. *Oxid. Med. Cell. Longev.* **2012**, 2012, 1–13, doi:10.1155/2012/609421.
 242. Müller, A.; Leichert, L.I. Redox Proteomics. In *Oxidative Stress and Redox Regulation*; Springer Netherlands: Dordrecht, 2013; pp. 157–186 ISBN 9789400757875.

243. Bakunina, N.; Pariante, C.M.; Zunszain, P.A. Immune mechanisms linked to depression via oxidative stress and neuroprogression. *Immunology* **2015**, *144*, 365–373, doi:10.1111/imm.12443.
244. Ribaldo, G.; Bortoli, M.; Witt, C.E.; Parke, B.; Mena, S.; Oselladore, E.; Zagotto, G.; Hashemi, P.; Orian, L. ROS-Scavenging Selenofluoxetine Derivatives Inhibit In Vivo Serotonin Reuptake. *ACS Omega* **2022**, *7*, 8314–8322, doi:10.1021/acsomega.1c05567.
245. Correia, A.S.; Cardoso, A.; Vale, N. Significant Differences in the Reversal of Cellular Stress Induced by Hydrogen Peroxide and Corticosterone by the Application of Mirtazapine or L-Tryptophan. *Int. J. Transl. Med.* **2022**, *2*, 482–505, doi:10.3390/ijtm2030036.
246. Wauquier, F.; Boutin-Wittrant, L.; Pourtau, L.; Gaudout, D.; Moras, B.; Vignault, A.; Monchaux De Oliveira, C.; Gabaston, J.; Vaysse, C.; Bertrand, K.; et al. Circulating Human Serum Metabolites Derived from the Intake of a Saffron Extract (Safr'Inside™) Protect Neurons from Oxidative Stress: Consideration for Depressive Disorders. *Nutrients* **2022**, *14*, 1511, doi:10.3390/nu14071511.
247. Omachi, T.; Matsuyama, N.; Hasegawa, Y. Nacre extract from pearl oyster suppresses LPS-induced depression and anxiety. *J. Funct. Foods* **2023**, *100*, 105373, doi:10.1016/j.jff.2022.105373.
248. Yu, H.; Shao, S.; Xu, J.; Guo, H.; Zhong, Z.; Xu, J. Persimmon leaf extract alleviates chronic social defeat stress-induced depressive-like behaviors by preventing dendritic spine loss via inhibition of serotonin reuptake in mice. *Chin. Med.* **2022**, *17*, 65, doi:10.1186/s13020-022-00609-4.
249. Vašíček, O.; Lojek, A.; Číž, M. Serotonin and its metabolites reduce oxidative stress in murine RAW264.7 macrophages and prevent inflammation. *J. Physiol. Biochem.* **2020**, *76*, 49–60, doi:10.1007/s13105-019-00714-3.
250. Yang, Y.; Zhao, S.; Yang, X.; Li, W.; Si, J.; Yang, X. The antidepressant potential of lactobacillus casei in the postpartum depression rat model mediated by the microbiota-gut-brain axis. *Neurosci. Lett.* **2022**, *774*, 136474, doi:https://doi.org/10.1016/j.neulet.2022.136474.
251. Jorgensen, A.; Köhler-Forsberg, K.; Henriksen, T.; Weimann, A.; Brandslund, I.; Ellervik, C.; Poulsen, H.E.; Knudsen, G.M.; Frokjaer, V.G.; Jorgensen, M.B. Systemic DNA and RNA damage from oxidation after serotonergic treatment of unipolar depression. *Transl. Psychiatry* **2022**, *12*, 204, doi:10.1038/s41398-022-01969-z.
252. Wang, D.; Li, H.; Du, X.; Zhou, J.; Yuan, L.; Ren, H.; Yang, X.; Zhang, G.; Chen, X.; Cuellar-Barboza, A.B.; et al. Circulating Brain-Derived Neurotrophic Factor, Antioxidant Enzymes Activities, and Mitochondrial DNA in Bipolar Disorder: An Exploratory Report. *Psychiatry* **2020**, *11*, 514658, doi:10.3389/fpsy.2020.514658.
253. Santos, S.S.; Moreira, J.B.; Costa, M.; Rodrigues, R.S.; Sebastião, A.M.; Xapelli, S.; Solá, S. The Mitochondrial Antioxidant Sirtuin3 Cooperates with Lipid Metabolism to Safeguard Neurogenesis in Aging and Depression. *Cells* **2021**, *11*, 90, doi:10.3390/cells11010090.
254. Zhao, Y.-T.; Yin, H.; Hu, C.; Zeng, J.; Zhang, S.; Chen, S.; Zheng, W.; Li, M.; Jin, L.; Liu, Y.; et al. Tilapia Skin Peptides Ameliorate Cyclophosphamide-Induced Anxiety- and Depression-Like Behavior via Improving Oxidative Stress, Neuroinflammation, Neuron Apoptosis, and Neurogenesis in Mice. *Front. Nutr.* **2022**, *9*, doi:10.3389/fnut.2022.882175.

255. Birmann, P.T.; Casaril, A.M.; Zugno, G.P.; Acosta, G.G.; Severo Sabedra Sousa, F.; Collares, T.; Seixas, F.K.; Jacob, R.G.; Brüning, C.A.; Savegnago, L.; et al. Flower essential oil of *Tagetes minuta* mitigates oxidative stress and restores BDNF-Akt/ERK2 signaling attenuating inflammation- and stress-induced depressive-like behavior in mice. *Brain Res.* **2022**, *1784*, 147845, doi:10.1016/j.brainres.2022.147845.
256. Suwannakot, K.; Sritawan, N.; Naewla, S.; Aranarochana, A.; Sirichoat, A.; Pannangrong, W.; Wigmore, P.; Welbat, J.U. Melatonin Attenuates Methotrexate-Induced Reduction of Antioxidant Activity Related to Decreases of Neurogenesis in Adult Rat Hippocampus and Prefrontal Cortex. *Oxid. Med. Cell. Longev.* **2022**, *2022*, 1–13, doi:10.1155/2022/1596362.
257. de Sousa, C.N.S.; Medeiros, I. da S.; Vasconcelos, G.S.; de Aquino, G.A.; Cysne Filho, F.M.S.; de Almeida Cysne, J.C.; Macêdo, D.S.; Vasconcelos, S.M.M. Involvement of oxidative pathways and BDNF in the antidepressant effect of carvedilol in a depression model induced by chronic unpredictable stress. *Psychopharmacology (Berl.)* **2022**, *239*, 297–311, doi:10.1007/s00213-021-05994-6.
258. Yu, Y.; Li, Y.; Qi, K.; Xu, W.; Wei, Y. Rosmarinic acid relieves LPS-induced sickness and depressive-like behaviors in mice by activating the BDNF/Nrf2 signaling and autophagy pathway. *Behav. Brain Res.* **2022**, *433*, 114006, doi:https://doi.org/10.1016/j.bbr.2022.114006.
259. Abbas, F.; Eladl, M.A.; El-Sherbiny, M.; Abozied, N.; Nabil, A.; Mahmoud, S.M.; Mokhtar, H.I.; Zaitone, S.A.; Ibrahim, D. Celastrol and thymoquinone alleviate aluminum chloride-induced neurotoxicity: Behavioral psychomotor performance, neurotransmitter level, oxidative-inflammatory markers, and BDNF expression in rat brain. *Biomed. Pharmacother.* **2022**, *151*, 113072, doi:10.1016/j.biopha.2022.113072.
260. An, L.; Li, M.; Zou, C.; Wang, K.; Zhang, W.; Huang, X.; Wang, Y. Walnut polyphenols and the active metabolite urolithin A improve oxidative damage in SH-SY5Y cells by up-regulating PKA/CREB/BDNF signaling. *Food Funct.* **2023**, *14*, 2698–2709, doi:10.1039/D2FO03310K.
261. Gupta, R.; Gupta, K.; Tripathi, A.K.; Bhatia, M.S.; Gupta, L.K. Effect of Mirtazapine Treatment on Serum Levels of Brain-Derived Neurotrophic Factor and Tumor Necrosis Factor- α in Patients of Major Depressive Disorder with Severe Depression. *Pharmacology* **2016**, *97*, 184–188, doi:10.1159/000444220.
262. Correia, A.S.; Fraga, S.; Teixeira, J.P.; Vale, N. Cell Model of Depression: Reduction of Cell Stress with Mirtazapine. *Int. J. Mol. Sci.* **2022**, *23*, 4942, doi:10.3390/ijms23094942.
263. Lieberknecht, V.; Engel, D.; Rodrigues, A.L.S.; Gabilan, N.H. Neuroprotective effects of mirtazapine and imipramine and their effect in pro- and anti-apoptotic gene expression in human neuroblastoma cells. *Pharmacol. Reports* **2020**, *72*, 563–570, doi:10.1007/s43440-019-00009-w.
264. Dionisie, V.; Ciobanu, A.M.; Toma, V.A.; Manea, M.C.; Baldea, I.; Olteanu, D.; Sevastre-Berghian, A.; Clichici, S.; Manea, M.; Riga, S.; et al. Escitalopram Targets Oxidative Stress, Caspase-3, BDNF and MeCP2 in the Hippocampus and Frontal Cortex of a Rat Model of Depression Induced by Chronic Unpredictable Mild Stress. *Int. J. Mol. Sci.* **2021**, *22*, 7483, doi:10.3390/ijms22147483.
265. Zhou, C.; Zhong, J.; Zou, B.; Fang, L.; Chen, J.; Deng, X.; Zhang, L.; Zhao, X.; Qu, Z.; Lei, Y.; et al. Meta-analyses of comparative efficacy of antidepressant

- medications on peripheral BDNF concentration in patients with depression. *PLoS One* **2017**, *12*, e0172270, doi:10.1371/journal.pone.0172270.
266. Hacıoglu, G.; Senturk, A.; Ince, I.; Alver, A. Assessment of oxidative stress parameters of brain-derived neurotrophic factor heterozygous mice in acute stress model. *Iran. J. Basic Med. Sci.* **2016**, *19*, 388, doi:10.22038/ijmbs.2016.6810.
 267. Wu, Q.; Lin, M.; Wu, P.; Zhao, C.; Yang, S.; Yu, H.; Xian, W.; Song, J. TPPU Downregulates Oxidative Stress Damage and Induces BDNF Expression in PC-12 Cells. **2022**, doi:10.1155/2022/7083022.
 268. Amiry, G.Y.; Haidary, M.; Azhdari-Zarmehri, H.; Beheshti, F.; Ahmadi-Soleimani, S.M. Omega-3 fatty acids prevent nicotine withdrawal-induced exacerbation of anxiety and depression by affecting oxidative stress balance, inflammatory response, BDNF and serotonin metabolism in rats. *Eur. J. Pharmacol.* **2023**, *947*, 175634, doi:10.1016/j.ejphar.2023.175634.
 269. Alizadeh Makvandi, A.; Khalili, M.; Roghani, M.; Amiri Moghaddam, S. Hesperetin ameliorates electroconvulsive therapy-induced memory impairment through regulation of hippocampal BDNF and oxidative stress in a rat model of depression. *J. Chem. Neuroanat.* **2021**, *117*, 102001, doi:10.1016/j.jchemneu.2021.102001.
 270. Chen, Y.; Yang, X.; Li, H.; Fang, J. Red Raspberry Extract Decreases Depression-Like Behavior in Rats by Modulating Neuroinflammation and Oxidative Stress. *Biomed Res. Int.* **2022**, *2022*, doi:10.1155/2022/9943598.
 271. Sorgdrager, F.J.H.; Doornbos, B.; Penninx, B.W.J.H.; de Jonge, P.; Kema, I.P. The association between the hypothalamic pituitary adrenal axis and tryptophan metabolism in persons with recurrent major depressive disorder and healthy controls. *J. Affect. Disord.* **2017**, *222*, 32–39, doi:10.1016/j.jad.2017.06.052.
 272. Messaoud, A.; Mensi, R.; Douki, W.; Neffati, F.; Najjar, M.F.; Gobbi, G.; Valtorta, F.; Gaha, L.; Comai, S. Reduced peripheral availability of tryptophan and increased activation of the kynurenine pathway and cortisol correlate with major depression and suicide. *World J. Biol. Psychiatry* **2019**, *20*, 703–711, doi:10.1080/15622975.2018.1468031.
 273. Oxenkrug, G.F. Tryptophan kynurenine metabolism as a common mediator of genetic and environmental impacts in major depressive disorder: the serotonin hypothesis revisited 40 years later. *Isr. J. Psychiatry Relat. Sci.* **2010**, *47*, 56–63.
 274. La Torre, D.; Dalile, B.; de Loor, H.; Van Oudenhove, L.; Verbeke, K. Changes in kynurenine pathway metabolites after acute psychosocial stress in healthy males: a single-arm pilot study. *Stress* **2021**, *24*, 920–930, doi:10.1080/10253890.2021.1959546.
 275. O'Farrell, K.; Harkin, A. Stress-related regulation of the kynurenine pathway: Relevance to neuropsychiatric and degenerative disorders. *Neuropharmacology* **2017**, *112*, 307–323, doi:10.1016/j.neuropharm.2015.12.004.
 276. Gibney, S.M.; Fagan, E.M.; Waldron, A.M.; O'Byrne, J.; Connor, T.J.; Harkin, A. Inhibition of stress-induced hepatic tryptophan 2,3-dioxygenase exhibits antidepressant activity in an animal model of depressive behaviour. *Int. J. Neuropsychopharmacol.* **2014**, *17*, 917–928, doi:10.1017/S1461145713001673.
 277. Lawson, M.A.; Parrott, J.M.; McCusker, R.H.; Dantzer, R.; Kelley, K.W.; O'Connor, J.C. Intracerebroventricular administration of lipopolysaccharide induces indoleamine-2,3-dioxygenase-dependent depression-like behaviors. *J. Neuroinflammation* **2013**, *10*, 875, doi:10.1186/1742-2094-10-87.

278. O'Connor, J.C.; Lawson, M.A.; André, C.; Moreau, M.; Lestage, J.; Castanon, N.; Kelley, K.W.; Dantzer, R. Lipopolysaccharide-induced depressive-like behavior is mediated by indoleamine 2,3-dioxygenase activation in mice. *Mol. Psychiatry* **2009**, *14*, 511–522, doi:10.1038/sj.mp.4002148.
279. Agudelo, L.Z.; Femenía, T.; Orhan, F.; Porsmyr-Palmertz, M.; Goiny, M.; Martinez-Redondo, V.; Correia, J.C.; Izadi, M.; Bhat, M.; Schuppe-Koistinen, I.; et al. Skeletal Muscle PGC-1 α 1 Modulates Kynurenine Metabolism and Mediates Resilience to Stress-Induced Depression. *Cell* **2014**, *159*, 33–45, doi:10.1016/j.cell.2014.07.051.
280. Den Buuse, M.; Hale, M.W. Serotonin in stress. In *Stress: Physiology, Biochemistry, and Pathology Handbook of Stress Series, Volume 3*; Elsevier, 2019; pp. 115–123 ISBN 9780128131466.
281. Bethea, C.L.; Centeno, M.L.; Cameron, J.L. *Neurobiology of stress-induced reproductive dysfunction in female macaques*; 2008; Vol. 38, pp. 199–230;.
282. Zhang, F.; Zhu, X.; Yu, P.; Sheng, T.; Wang, Y.; Ye, Y. Crocin ameliorates depressive-like behaviors induced by chronic restraint stress via the NAMPT-NAD⁺-SIRT1 pathway in mice. *Neurochem. Int.* **2022**, *157*, 105343, doi:10.1016/j.neuint.2022.105343.
283. Samant, N.P.; Gupta, G.L. Gossypetin- based therapeutics for cognitive dysfunction in chronic unpredictable stress- exposed mice. *Metab. Brain Dis.* **2022**, *37*, 1527–1539, doi:10.1007/S11011-022-00971-0.
284. Youssef, B.; Ramadan, K.S.; ElShebiney, S.; Ibrahim, E.A. Antidepressant-like effects of aqueous extracts of miswak (*Salvadora persica*) and date palm (*Phoenix dactylifera*) on depression-like behaviors using CUMS model in male rats. *J. Food Biochem.* **2022**, doi:10.1111/jfbc.14164.
285. Zhu, X.; Sun-Waterhouse, D.; Tao, Q.; Li, W.; Shu, D.; Cui, C. The enhanced serotonin (5-HT) synthesis and anti-oxidative roles of Trp oligopeptide in combating anxious depression C57BL/6 mice. *J. Funct. Foods* **2020**, *67*, 103859, doi:10.1016/j.jff.2020.103859.
286. Raap, D.; Van de Kar, L.D. Selective serotonin reuptake inhibitors and neuroendocrine function. *Life Sci.* **1999**, *65*, 1217–1235, doi:10.1016/S0024-3205(99)00169-1.
287. To, C.T.; Anheuer, Z.E.; Bagdy, G. Effects of acute and chronic fluoxetine treatment on CRH-induced anxiety. *Neuroreport* **1999**, *10*, 553–555, doi:10.1097/00001756-199902250-00020.
288. Young, E.A.; Altemus, M.; Lopez, J.F.; Kocsis, J.H.; Schatzberg, A.F.; DeBattista, C.; Zubieta, J.-K. HPA axis activation in major depression and response to fluoxetine: a pilot study. *Psychoneuroendocrinology* **2004**, *29*, 1198–1204, doi:10.1016/j.psyneuen.2004.02.002.
289. MIKKELSEN, J.D.; HAY-SCHMIDT, A.; KISS, A. Serotonergic Stimulation of the Rat Hypothalamo-Pituitary-Adrenal Axis: Interaction between 5-HT 1A and 5-HT 2A Receptors. *Ann. N. Y. Acad. Sci.* **2004**, *1018*, 65–70, doi:10.1196/annals.1296.007.
290. Jensen; Jessop; Harbuz; Mørk; Sánchez; Mikkelsen Acute and Long-Term Treatments with the Selective Serotonin Reuptake Inhibitor Citalopram Modulate the HPA Axis Activity at Different Levels in Male Rats. *J. Neuroendocrinol.* **1999**, *11*, 465–471, doi:10.1046/j.1365-2826.1999.00362.x.

291. Neumeister, A.; Yuan, P.; Young, T.A.; Bonne, O.; Luckenbaugh, D.A.; Charney, D.S.; Manji, H. Effects of Tryptophan Depletion on Serum Levels of Brain-Derived Neurotrophic Factor in Unmedicated Patients With Remitted Depression and Healthy Subjects. *Am. J. Psychiatry* **2005**, *162*, 805–807, doi:10.1176/appi.ajp.162.4.805.
292. Kopra, E.; Mondelli, V.; Pariante, C.; Nikkheslat, N. Ketamine's effect on inflammation and kynurenine pathway in depression: A systematic review. *J. Psychopharmacol.* **2021**, *35*, 934–945, doi:10.1177/02698811211026426.
293. Dugan, A.M.; Parrott, J.M.; Redus, L.; Hensler, J.G.; O'Connor, J.C. Low-Level Stress Induces Production of Neuroprotective Factors in Wild-Type but Not BDNF +/- Mice: Interleukin-10 and Kynurenic Acid. *Int. J. Neuropsychopharmacol.* **2016**, *19*, pyv089, doi:10.1093/ijnp/pyv089.
294. Ieraci, A.; Beggiano, S.; Ferraro, L.; Barbieri, S.S.; Popoli, M. Kynurenine pathway is altered in BDNF Val66Met knock-in mice: Effect of physical exercise. *Brain. Behav. Immun.* **2020**, *89*, 440–450, doi:10.1016/j.bbi.2020.07.031.
295. Gao, L.; Gao, T.; Zeng, T.; Huang, P.; Wong, N.-K.; Dong, Z.; Li, Y.; Deng, G.; Wu, Z.; Lv, Z. Blockade of Indoleamine 2, 3-dioxygenase 1 ameliorates hippocampal neurogenesis and BOLD-fMRI signals in chronic stress precipitated depression. *Aging (Albany, NY).* **2021**, *13*, 5875–5891, doi:10.18632/aging.202511.
296. Eadie, B.D.; Redila, V.A.; Christie, B.R. Voluntary exercise alters the cytoarchitecture of the adult dentate gyrus by increasing cellular proliferation, dendritic complexity, and spine density. *J. Comp. Neurol.* **2005**, *486*, 39–47, doi:10.1002/cne.20493.
297. Leschik, J.; Gentile, A.; Cicek, C.; Péron, S.; Tevosian, M.; Beer, A.; Radyushkin, K.; Bludau, A.; Ebner, K.; Neumann, I.; et al. Brain-derived neurotrophic factor expression in serotonergic neurons improves stress resilience and promotes adult hippocampal neurogenesis. *Prog. Neurobiol.* **2022**, *217*, 102333, doi:10.1016/j.pneurobio.2022.102333.
298. Rumajogee, P.; Vergé, D.; Hanoun, N.; Brisorgueil, M.; Hen, R.; Lesch, K.; Hamon, M.; Miquel, M. Adaption of the serotonergic neuronal phenotype in the absence of 5-HT autoreceptors or the 5-HT transporter: involvement of BDNF and cAMP. *Eur. J. Neurosci.* **2004**, *19*, 937–944, doi:10.1111/j.0953-816X.2004.03194.x.
299. Murawska-Ciałowicz, E.; Wiatr, M.; Ciałowicz, M.; Gomes de Assis, G.; Borowicz, W.; Rocha-Rodrigues, S.; Paprocka-Borowicz, M.; Marques, A. BDNF Impact on Biological Markers of Depression-Role of Physical Exercise and Training. *Int. J. Environ. Res. Public Health* **2021**, *18*, doi:10.3390/ijerph18147553.
300. Martinowich, K.; Lu, B. Interaction between BDNF and Serotonin: Role in Mood Disorders. *Neuropsychopharmacology* **2008**, *33*, 73–83, doi:10.1038/sj.npp.1301571.
301. Rios, M.; Lambe, E.K.; Liu, R.; Teillon, S.; Liu, J.; Akbarian, S.; Roffler-Tarlov, S.; Jaenisch, R.; Aghajanian, G.K. Severe deficits in 5-HT 2A -mediated neurotransmission in BDNF conditional mutant mice. *J. Neurobiol.* **2006**, *66*, 408–420, doi:10.1002/neu.20233.
302. Hensler, J.G.; Advani, T.; Monteggia, L.M. Regulation of Serotonin-1A Receptor Function in Inducible Brain-Derived Neurotrophic Factor Knockout Mice After Administration of Corticosterone. *Biol. Psychiatry* **2007**, *62*, 521–529,

doi:10.1016/j.biopsych.2006.10.015.

303. Moliner, R.; Giry, M.; Brunello, C.A.; Kovaleva, V.; Biojone, C.; Enkavi, G.; Antenucci, L.; Kot, E.F.; Goncharuk, S.A.; Kaurinkoski, K.; et al. Psychedelics promote plasticity by directly binding to BDNF receptor TrkB. *Nat. Neurosci.* **2023**, *26*, 1032–1041, doi:10.1038/s41593-023-01316-5.
304. Fukumoto, K.; Fogaça, M. V.; Liu, R.-J.; Duman, C.H.; Li, X.-Y.; Chaki, S.; Duman, R.S. Medial PFC AMPA receptor and BDNF signaling are required for the rapid and sustained antidepressant-like effects of 5-HT_{1A} receptor stimulation. *Neuropsychopharmacology* **2020**, *45*, 1725–1734, doi:10.1038/s41386-020-0705-0.
305. Quintero-Villegas, A.; Valdés-Ferrer, S.I. Central nervous system effects of 5-HT₇ receptors: a potential target for neurodegenerative diseases. *Mol. Med.* **2022**, *28*, 70, doi:10.1186/s10020-022-00497-2.
306. Benmansour, S.; Deltheil, T.; Piotrowski, J.; Nicolas, L.; Reperant, C.; Gardier, A.M.; Frazer, A.; David, D.J. Influence of brain-derived neurotrophic factor (BDNF) on serotonin neurotransmission in the hippocampus of adult rodents. *Eur. J. Pharmacol.* **2008**, *587*, 90–98, doi:10.1016/j.ejphar.2008.03.048.
307. Yu, H.; Lv, D.; Shen, M.; Zhang, Y.; Zhou, D.; Chen, Z.; Wang, C. BDNF mediates the protective effects of scopolamine in reserpine-induced depression-like behaviors via up-regulation of 5-HTT and TPH1. *Psychiatry Res.* **2019**, *271*, 328–334, doi:10.1016/j.psychres.2018.12.015.
308. Park, S.-A.; Son, S.Y.; Lee, A.-Y.; Park, H.-G.; Lee, W.-L.; Lee, C.H. Metabolite Profiling Revealed That a Gardening Activity Program Improves Cognitive Ability Correlated with BDNF Levels and Serotonin Metabolism in the Elderly. *Int. J. Environ. Res. Public Health* **2020**, *17*, 541, doi:10.3390/ijerph17020541.
309. Evisukova, V.S.; Bazovkina, D.; Bazhenova, E.; Kulikova, E.A.; Kulikov, A. V. Tryptophan Hydroxylase 2 Deficiency Modifies the Effects of Fluoxetine and Pargyline on the Behavior, 5-HT- and BDNF-Systems in the Brain of Zebrafish (*Danio rerio*). *Int. J. Mol. Sci.* **2021**, *22*, 12851, doi:10.3390/ijms222312851.
310. Musumeci, G.; Castrogiovanni, P.; Castorina, S.; Imbesi, R.; Szychlinska, M.A.; Scuderi, S.; Loreto, C.; Giunta, S. Changes in serotonin (5-HT) and brain-derived neurotrophic factor (BDNF) expression in frontal cortex and hippocampus of aged rat treated with high tryptophan diet. *Brain Res. Bull.* **2015**, *119*, 12–18, doi:10.1016/j.brainresbull.2015.09.010.
311. Pietrelli, A.; Matković, L.; Vacotto, M.; Lopez-Costa, J.J.; Basso, N.; Brusco, A. Aerobic exercise upregulates the BDNF-Serotonin systems and improves the cognitive function in rats. *Neurobiol. Learn. Mem.* **2018**, *155*, 528–542, doi:10.1016/j.nlm.2018.05.007.
312. Bazzari, A.H.; Bazzari, F.H. BDNF Therapeutic Mechanisms in Neuropsychiatric Disorders. *Int. J. Mol. Sci.* **2022**, *23*, 8417, doi:10.3390/ijms23158417.
313. Naert, G.; Zussy, C.; Tran Van Ba, C.; Chevallier, N.; Tang, Y.-P.; Maurice, T.; Givalois, L. Involvement of Endogenous Brain-Derived Neurotrophic Factor in Hypothalamic-Pituitary-Adrenal Axis Activity. *J. Neuroendocrinol.* **2015**, *27*, 850–860, doi:10.1111/jne.12324.
314. Barfield, E.T.; Gourley, S.L. Prefrontal cortical trkB, glucocorticoids, and their interactions in stress and developmental contexts. **2018**, doi:10.1016/j.neubiorev.2018.10.015.

315. Hennings, J.M.; Kohli, M.A.; Uhr, M.; Holsboer, F.; Ising, M.; Lucae, S. Polymorphisms in the BDNF and BDNFOS genes are associated with hypothalamus-pituitary axis regulation in major depression. *Prog. Neuro-Psycho pharmacology Biol. Psychiatry* **2019**, *95*, 109686, doi:10.1016/j.pnpbp.2019.109686.
316. Zhang, K.; Wang, F.; Zhai, M.; He, M.; Hu, Y.; Feng, L.; Li, Y.; Yang, J.; Wu, C. Hyperactive neuronal autophagy depletes BDNF and impairs adult hippocampal neurogenesis in a corticosterone-induced mouse model of depression. *Theranostics* **2023**, *13*, 1059–1075, doi:10.7150/thno.81067.
317. Mori, M.; Shizunaga, H.; Harada, H.; Tajiri, Y.; Murata, Y.; Terada, K.; Ohe, K.; Enjoji, M. Oxytocin treatment improves dexamethasone-induced depression-like symptoms associated with enhancement of hippocampal CREB-BDNF signaling in female mice. *Neuropsychopharmacol. Reports* **2022**, *42*, 356–361, doi:10.1002/npr2.12271.
318. He, Z.; Yu, H.; Wu, H.; Su, L.; Shi, K.; Zhao, Y.; Zong, Y.; Chen, W.; Du, R. Antidepressant effects of total alkaloids of *Fibraurea recisa* on improving corticosterone-induced apoptosis of HT-22 cells and chronic unpredictable mild stress-induced depressive-like behaviour in mice. *Pharm. Biol.* **2022**, *60*, 1436–1448, doi:10.1080/13880209.2022.2099429.
319. Ishola, I.O.; Olubodun-Obadun, T.G.; Bakre, O.A.; Ojo, E.S.; Adeyemi, O.O. Kolaviron ameliorates chronic unpredictable mild stress-induced anxiety and depression: involvement of the HPA axis, antioxidant defense system, cholinergic, and BDNF signaling. *Drug Metab. Pers. Ther.* **2022**, *37*, 277–287, doi:10.1515/dmpt-2021-0125.
320. Lin, L.; Herselman, M.F.; Zhou, X.-F.; Bobrovskaya, L. Effects of corticosterone on BDNF expression and mood behaviours in mice. *Physiol. Behav.* **2022**, *247*, 113721, doi:10.1016/j.physbeh.2022.113721.
321. Li, Z.; Ruan, M.; Chen, J.; Fang, Y. Major Depressive Disorder: Advances in Neuroscience Research and Translational Applications. *Neurosci. Bull.* **2021**, *37*, 863–880, doi:10.1007/s12264-021-00638-3.
322. Lopez-Munoz, F.; Alamo, C. Monoaminergic Neurotransmission: The History of the Discovery of Antidepressants from 1950s Until Today. *Curr. Pharm. Des.* **2009**, *15*, 1563–1586, doi:10.2174/138161209788168001.
323. Hillhouse, T.M.; Porter, J.H.; Clin, E.; Author, P. A brief history of the development of antidepressant drugs: From monoamines to glutamate HHS Public Access Author manuscript. *Exp Clin Psychopharmacol* **2015**, *23*, 1–21, doi:10.1037/a0038550.
324. Stahl, S.M. Mechanism of action of serotonin selective reuptake inhibitors. *J. Affect. Disord.* **1998**, *51*, 215–235, doi:10.1016/S0165-0327(98)00221-3.
325. Sheffler, Z.M.; Patel, P.; Abdijadid, S. Antidepressants. *StatPearls*.
326. Kolovos, S.; Kleiboer, A.; Cuijpers, P. Effect of psychotherapy for depression on quality of life: meta-analysis. *Br. J. Psychiatry* **2016**, *209*, 460–468, doi:10.1192/bjp.bp.115.175059.
327. Stachowicz, K.; Sowa-Kućma, M. The treatment of depression — searching for new ideas. *Front. Pharmacol.* **2022**, *13*, 988648, doi:10.3389/fphar.2022.988648.
328. Search for: Depression | Card Results | ClinicalTrials.gov Available online: <https://clinicaltrials.gov/search?cond=Depression> (accessed on Oct 17, 2023).

329. Thase, M.E. Have Effective Antidepressants Finally Arrived? Developments in Major Depressive Disorder Therapy. *J. Clin. Psychiatry* **2023**, *84*, 48388, doi:10.4088/JCP.mulmdd3048sho.
330. Khodoruth, M.A.S.; Estudillo-Guerra, M.A.; Pacheco-Barrios, K.; Nyundo, A.; Chapa-Koloffon, G.; Ouanes, S. Glutamatergic System in Depression and Its Role in Neuromodulatory Techniques Optimization. *Front. Psychiatry* **2022**, *13*, 886918, doi:10.3389/fpsy.2022.886918.
331. Sarawagi, A.; Soni, N.D.; Patel, A.B. Glutamate and GABA Homeostasis and Neurometabolism in Major Depressive Disorder. *Front. Psychiatry* **2021**, *12*, 637863, doi:10.3389/fpsy.2021.637863.
332. Ghosal, S.; Hare, B.D.; Duman, R.S. Prefrontal cortex GABAergic deficits and circuit dysfunction in the pathophysiology and treatment of chronic stress and depression. *Curr. Opin. Behav. Sci.* **2017**, *14*, 1–8, doi:10.1016/j.cobeha.2016.09.012.
333. Lin, J.; Ling, F.; Huang, P.; Chen, M.; Song, M.; Lu, K.; Wang, W. The Development of GABAergic Network in Depression in Recent 17 Years: A Visual Analysis Based on CiteSpace and VOSviewer. *Front. Psychiatry* **2022**, *13*, 874137, doi:10.3389/fpsy.2022.874137.
334. Aleksandrova, L.R.; Phillips, A.G.; Wang, Y.T. Antidepressant effects of ketamine and the roles of AMPA glutamate receptors and other mechanisms beyond NMDA receptor antagonism. *J. Psychiatry Neurosci.* **2017**, *42*, 222–229, doi:10.1503/jpn.160175.
335. Berman, R.M.; Cappiello, A.; Anand, A.; Oren, D.A.; Heninger, G.R.; Charney, D.S.; Krystal, J.H. Antidepressant effects of ketamine in depressed patients. *Biol. Psychiatry* **2000**, *47*, 351–354, doi:10.1016/S0006-3223(99)00230-9.
336. Popova, V.; Daly, E.J.; Trivedi, M.; Cooper, K.; Lane, R.; Lim, P.; Mazzucco, C.; Hough, D.; Thase, M.E.; Shelton, R.C.; et al. Efficacy and Safety of Flexibly Dosed Esketamine Nasal Spray Combined With a Newly Initiated Oral Antidepressant in Treatment-Resistant Depression: A Randomized Double-Blind Active-Controlled Study. *Am J Psychiatry* **2019**, *176*, 428–438, doi:10.1176/appi.ajp.2019.19020172.
337. Kavakbasi, E.; Hassan, A.; Baune, B.T. Combination of Electroconvulsive Therapy Alternating With Intravenous Esketamine Can Lead to Rapid Remission of Treatment Resistant Depression. *J. ECT* **2021**, *37*, e20–e21, doi:10.1097/YCT.0000000000000733.
338. Ryskamp, D.A.; Korban, S.; Zhemkov, V.; Kraskovskaya, N.; Bezprozvanny, I. Neuronal Sigma-1 Receptors: Signaling Functions and Protective Roles in Neurodegenerative Diseases. *Front. Neurosci.* **2019**, *13*, doi:10.3389/fnins.2019.00862.
339. Pedraz-Petrozzi, B.; Deuschle, M.; Gilles, M. Improvement of depressive symptoms, after a suicide attempt, with dextromethorphan/bupropion combination treatment in a patient with treatment-resistant depression and psychiatric comorbidities. *Clin. Case Reports* **2023**, *11*, doi:10.1002/ccr3.7045.
340. Blair, H.A. Dextromethorphan/bupropion in major depressive disorder: a profile of its use. *Drugs Ther. Perspect.* **2023**, *39*, 270–278, doi:10.1007/s40267-023-01009-w.
341. Fava, M.; Stahl, S.M.; De Martin, S.; Mattarei, A.; Bettini, E.; Comai, S.; Alimonti,

- A.; Bifari, F.; Pani, L.; Folli, F.; et al. Esmethadone-HCl (REL-1017): a promising rapid antidepressant. *Eur. Arch. Psychiatry Clin. Neurosci.* **2023**, *273*, 1463–1476, doi:10.1007/s00406-023-01571-4.
342. Fava, M.; Stahl, S.; Pani, L.; De Martin, S.; Pappagallo, M.; Guidetti, C.; Alimonti, A.; Bettini, E.; Mangano, R.M.; Wessel, T.; et al. REL-1017 (Esmethadone) as Adjunctive Treatment in Patients With Major Depressive Disorder: A Phase 2a Randomized Double-Blind Trial. *Am. J. Psychiatry* **2022**, *179*, 122–131, doi:10.1176/APPI.AJP.2021.21020197.
 343. Cornett, E.M.; Rando, L.; Labbé, A.M.; Perkins, W.; Kaye, A.M.; Kaye, A.D.; Viswanath, O.; Urits, I. Brexanolone to Treat Postpartum Depression in Adult Women. *Psychopharmacol. Bull.* **51**, 115.
 344. Clayton, A.H.; Lasser, R.; Parikh, S. V.; Iosifescu, D. V.; Jung, J.; Kotecha, M.; Forrestal, F.; Jonas, J.; Kaner, S.J.; Doherty, J. Zuranolone for the Treatment of Adults With Major Depressive Disorder: A Randomized, Placebo-Controlled Phase 3 Trial. *Am. J. Psychiatry* **2023**, *180*, 676–684, doi:10.1176/appi.ajp.20220459.
 345. Fagan, H.; Jones, E.; Baldwin, D.S. Orexin Receptor Antagonists in the Treatment of Depression: A Leading Article Summarising Pre-clinical and Clinical Studies. *CNS Drugs* **2023**, *37*, 1–12, doi:10.1007/s40263-022-00974-6.
 346. Mi, W.; Di, X.; Wang, Y.; Li, H.; Xu, X.; Li, L.; Wang, H.; Wang, G.; Zhang, K.; Tian, F.; et al. A phase 3, multicenter, double-blind, randomized, placebo-controlled clinical trial to verify the efficacy and safety of ansofaxine (LY03005) for major depressive disorder. *Transl. Psychiatry* **2023**, *13*, 163, doi:10.1038/s41398-023-02435-0.
 347. Bansal, Y.; Bhandari, R.; Kaur, S.; Kaur, J.; Singh, R.; Kuhad, A. Gepirone hydrochloride: a novel antidepressant with 5-HT_{1A} agonistic properties. *Drugs of Today* **2019**, *55*, 423–437, doi:10.1358/dot.2019.55.7.2958474.
 348. Goodwin, G.M.; Croal, M.; Feifel, D.; Kelly, J.R.; Marwood, L.; Mistry, S.; O’Keane, V.; Peck, S.K.; Simmons, H.; Sisa, C.; et al. Psilocybin for treatment resistant depression in patients taking a concomitant SSRI medication. *Neuropsychopharmacol.* **2023**, *48*, 1492–1499, doi:10.1038/s41386-023-01648-7.
 349. Von Rotz, R.; Schindowski, E.M.; Jungwirth, J.; Schuldt, A.; Rieser, N.M.; Zahoranszky, K.; Seifritz, E.; Nowak, A.; Nowak, P.; Jäncke, L.; et al. Single-dose psilocybin-assisted therapy in major depressive disorder: a placebo-controlled, double-blind, randomised clinical trial. **2022**, doi:10.1016/j.eclinm.2022.101809.
 350. Dulawa, S.C.; Janowsky, D.S. Cholinergic regulation of mood: from basic and clinical studies to emerging therapeutics. *Mol. Psychiatry* **2019**, *24*, 694–709, doi:10.1038/s41380-018-0219-x.
 351. Fitzgerald, P.J.; Hale, P.J.; Ghimire, A.; Watson, B.O. Repurposing Cholinesterase Inhibitors as Antidepressants? Dose and Stress-Sensitivity May Be Critical to Opening Possibilities. *Front. Behav. Neurosci.* **2021**, *14*, 620119, doi:10.3389/fnbeh.2020.620119.
 352. Sun, J.; Qiu, L.; Zhang, H.; Zhou, Z.; Ju, L.; Yang, J. CRHR1 antagonist alleviates LPS-induced depression-like behaviour in mice. *BMC Psychiatry* **2023**, *23*, 17, doi:10.1186/s12888-023-04519-z.
 353. Brown, S.J.; Huang, X.-F.; Newell, K.A. The kynurenine pathway in major

- depression: What we know and where to next. *Neurosci. Biobehav. Rev.* **2021**, *127*, 917–927, doi:10.1016/j.neubiorev.2021.05.018.
354. Mohammad Sadeghi, H.; Adeli, I.; Mousavi, T.; Daniali, M.; Nikfar, S.; Abdollahi, M. Drug Repurposing for the Management of Depression: Where Do We Stand Currently? *Life* **2021**, *11*, 774, doi:10.3390/life11080774.
 355. Sizar, O.; Khare, S.; Jamil, R.T.; Talati, R. Statin Medications. *StatPearls* **2023**.
 356. Gutlapalli, S.D.; Farhat, H.; Irfan, H.; Muthiah, K.; Pallipamu, N.; Taheri, S.; Thiagaraj, S.S.; Shukla, T.S.; Giva, S.; Penumetcha, S.S. The Anti-Depressant Effects of Statins in Patients With Major Depression Post-Myocardial Infarction: An Updated Review 2022. *Cureus* **2022**, *14*, doi:10.7759/cureus.32323.
 357. De Giorgi, R.; Pesci, N.R.; Rosso, G.; Maina, G.; Cowen, P.J.; Harmer, C.J. The pharmacological bases for repurposing statins in depression: a review of mechanistic studies. *Transl. Psychiatry* **2023**, *13*, 253, doi:10.1038/s41398-023-02533-z.
 358. Lochner, M.; Thompson, A.J. The muscarinic antagonists scopolamine and atropine are competitive antagonists at 5-HT₃ receptors. *Neuropharmacology* **2016**, *108*, 220–228, doi:10.1016/j.neuropharm.2016.04.027.
 359. Fang, Y.; Guo, P.; Lv, L.; Feng, M.; Wang, H.; Sun, G.; Wang, S.; Qian, M.; Chen, H. Scopolamine augmentation for depressive symptoms and cognitive functions in treatment-resistant depression: A case series. *Asian J. Psychiatr.* **2023**, *82*, 103484, doi:10.1016/J.AJP.2023.103484.
 360. Wang, X.; Zhu, X.; Ji, X.; Yang, J.; Zhou, J. Group-Based Symptom Trajectory of Intramuscular Administration of Scopolamine Augmentation in Moderate to Severe Major Depressive Disorder: A Post-Hoc Analysis. *Neuropsychiatr. Dis. Treat.* **2023**, *Volume 19*, 1043–1053, doi:10.2147/NDT.S408794.
 361. Home | ClinicalTrials.gov Available online: <https://clinicaltrials.gov/> (accessed on Oct 18, 2023).
 362. Moćko, P.; Śladowska, K.; Kawalec, P.; Babii, Y.; Pilc, A. The Potential of Scopolamine as an Antidepressant in Major Depressive Disorder: A Systematic Review of Randomized Controlled Trials. *Biomedicines* **2023**, *11*, 2636, doi:10.3390/biomedicines11102636.
 363. Chateauvieux, S.; Morceau, F.; Diederich, M. Valproic Acid. *Encycl. Toxicol. Third Ed.* **2023**, 905–908, doi:10.1016/B978-0-12-386454-3.00073-7.
 364. Brian Chen, Y.-C.; Liang, C.-S.; Wang, L.-J.; Hung, K.-C.; Carvalho, A.F.; Solmi, M.; Vieta, E.; Tseng, P.-T.; Lin, P.-Y.; Tu, Y.-K.; et al. Comparative effectiveness of valproic acid in different serum concentrations for maintenance treatment of bipolar disorder: A retrospective cohort study using target trial emulation framework. *eClinicalMedicine* **2022**, *54*, 101678, doi:10.1016/j.
 365. Ghabrash, M.F.; Comai, S.; Tabaka, J.; Saint-Laurent, M.; Booij, L.; Gobbi, G. Valproate augmentation in a subgroup of patients with treatment-resistant unipolar depression. *World J. Biol. Psychiatry* **2016**, *17*, 165–170, doi:10.3109/15622975.2015.1073856.
 366. Yonemoto, L. Lamotrigine. In *The Essence of Analgesia and Analgesics*; Cambridge University Press, 2010; pp. 306–309 ISBN 9780511841378.
 367. Matsuzaka, Y.; Urashima, K.; Sakai, S.; Morimoto, Y.; Kanegae, S.; Kinoshita, H.; Imamura, A.; Ozawa, H. The effectiveness of lamotrigine for persistent depressive

- disorder: A case report. *Neuropsychopharmacol. Reports* **2022**, *42*, 120–123, doi:10.1002/npr2.12228.
368. Singh, G.; Can, A.S.; Correa, R. *Pioglitazone*; StatPearls Publishing, 2024;
369. Colle, R.; de Larminat, D.; Rotenberg, S.; Hozer, F.; Hardy, P.; Verstuyft, C.; Fève, B.; Corruble, E. Pioglitazone could induce remission in major depression: a meta-analysis. *Neuropsychiatr. Dis. Treat.* **2016**, *Volume 13*, 9–16, doi:10.2147/NDT.S121149.
370. Watson, K.; Akil, H.; Rasgon, N. Toward a Precision Treatment Approach for Metabolic Depression: Integrating Epidemiology, Neuroscience, and Psychiatry. *Biol. Psychiatry Glob. Open Sci.* **2023**, *3*, 623–631, doi:10.1016/j.bpsgos.2023.08.008.
371. Zhao, Q.; Wu, X.; Yan, S.; Xie, X.; Fan, Y.; Zhang, J.; Peng, C.; You, Z. The antidepressant-like effects of pioglitazone in a chronic mild stress mouse model are associated with PPAR γ -mediated alteration of microglial activation phenotypes. *J. Neuroinflammation* **2016**, *13*, 259, doi:10.1186/s12974-016-0728-y.
372. Beheshti, F.; Hosseini, M.; Hashemzahi, M.; Soukhtanloo, M.; Asghari, A. The effects of PPAR- γ agonist pioglitazone on anxiety and depression-like behaviors in lipopolysaccharide injected rats. *Toxin Rev.* **2021**, *40*, 1223–1232, doi:10.1080/15569543.2019.1673425.
373. Rague, J. N-Acetylcysteine. In *History of Modern Clinical Toxicology*; Elsevier, 2022; pp. 201–212 ISBN 9780128222188.
374. Hans, D.; Rengel, A.; Hans, J.; Bassett, D.; Hood, S. N-Acetylcysteine as a novel rapidly acting anti-suicidal agent: A pilot naturalistic study in the emergency setting. *PLoS One* **2022**, *17*, e0263149, doi:10.1371/journal.pone.0263149.
375. Brivio, P.; Gallo, M.T.; Gruca, P.; Lason, M.; Litwa, E.; Fumagalli, F.; Papp, M.; Calabrese, F. Chronic N-Acetyl-Cysteine Treatment Enhances the Expression of the Immediate Early Gene Nr4a1 in Response to an Acute Challenge in Male Rats: Comparison with the Antidepressant Venlafaxine. *Int. J. Mol. Sci.* **2023**, *24*, 7321, doi:10.3390/ijms24087321.
376. Nazarian, S.; Akhondi, H. Minocycline. *StatPearls* **2022**.
377. Nettis, M.A. Minocycline in Major Depressive Disorder: An overview with considerations on treatment-resistance and comparisons with other psychiatric disorders. *Brain, Behav. Immun. - Heal.* **2021**, *17*, 100335, doi:10.1016/j.bbih.2021.100335.
378. Qiu, Y.; Duan, A.; Yin, Z.; Xie, M.; Chen, Z.; Sun, X.; Wang, Z.; Zhang, X. Efficacy and tolerability of minocycline in depressive patients with or without treatment-resistant: a meta-analysis of randomized controlled trials. *Front. Psychiatry* **2023**, *14*, 1139273, doi:10.3389/fpsy.2023.1139273.
379. Rojewska, E.; Ciapała, K.; Piotrowska, A.; Makuch, W.; Mika, J. Pharmacological Inhibition of Indoleamine 2,3-Dioxygenase-2 and Kynurenine 3-Monooxygenase, Enzymes of the Kynurenine Pathway, Significantly Diminishes Neuropathic Pain in a Rat Model. *Front. Pharmacol.* **2018**, *9*, doi:10.3389/fphar.2018.00724.
380. Tippens, A.S. Nimodipine. In *xPharm: The Comprehensive Pharmacology Reference*; Elsevier, 2007; pp. 1–7 ISBN 9780080552323.
381. Zink, C.F.; Giegerich, M.; Prettyman, G.E.; Carta, K.E.; van Ginkel, M.; O'Rourke,

- M.P.; Singh, E.; Fuchs, E.J.; Hendrix, C.W.; Zimmerman, E.; et al. Nimodipine improves cortical efficiency during working memory in healthy subjects. *Transl. Psychiatry* **2020**, *10*, 372, doi:10.1038/s41398-020-01066-z.
382. Taragano, F.E.; Allegri, R.; Vicario, A.; Bagnatti, P.; Lyketsos, C.G. A double blind, randomized clinical trial assessing the efficacy and safety of augmenting standard antidepressant therapy with nimodipine in the treatment of 'vascular depression.' *Int. J. Geriatr. Psychiatry* **2001**, *16*, 254–260, doi:10.1002/GPS.340.
 383. Maan, J.S.; Ershadi, M.; Khan, I.; Saadabadi, A. Quetiapine. *StatPearls* **2023**.
 384. Tran, K.; Argáez, C. Quetiapine for Major Depressive Disorder: A Review of Clinical Effectiveness, Cost-Effectiveness, and Guidelines. *Quetiapine Major Depress. Disord. A Rev. Clin. Eff. Cost-Effectiveness, Guidel.* **2020**.
 385. Ravindran, N.; McKay, M.; Paric, A.; Johnson, S.; Chandrasena, R.; Abraham, G.; Ravindran, A. V. Randomized, Placebo-Controlled Effectiveness Study of Quetiapine XR in Comorbid Depressive and Anxiety Disorders. *J. Clin. Psychiatry* **2022**, *83*, 40248, doi:10.4088/JCP.21m14096.
 386. Bauer, M.; Pretorius, H.W.; Constant, E.L.; Earley, W.R.; Szamosi, J.; Brecher, M. Extended-Release Quetiapine as Adjunct to an Antidepressant in Patients With Major Depressive Disorder: Results of a Randomized, Placebo-Controlled, Double-Blind Study. *J. Clin. Psychiatry* **2009**, *70*, 7032, doi:10.4088/JCP.08M04629.
 387. Marino, J. Celecoxib. In *The Essence of Analgesia and Analgesics*; Cambridge University Press, 2010; pp. 238–242 ISBN 9780511841378.
 388. Wang, Z.; Wu, Q.; Wang, Q. Effect of celecoxib on improving depression: A systematic review and meta-analysis. *World J. Clin. Cases* **2022**, *10*, 7872–7882, doi:10.12998/wjcc.v10.i22.7872.
 389. Gędek, A.; Szular, Z.; Antosik, A.Z.; Mierzejewski, P.; Dominiak, M. Celecoxib for Mood Disorders: A Systematic Review and Meta-Analysis of Randomized Controlled Trials. *J. Clin. Med.* **2023**, *12*, 3497, doi:10.3390/jcm12103497.
 390. Jilani, T.N.; Gibbons, J.R.; Faizy, R.M.; Saadabadi, A. Mirtazapine. *StatPearls* **2021**.
 391. Watanabe, N.; Omori, I.M.; Nakagawa, A.; Cipriani, A.; Barbui, C.; Churchill, R.; Furukawa, T.A. Mirtazapine versus other antidepressive agents for depression. *Cochrane Database Syst. Rev.* **2011**, doi:10.1002/14651858.CD006528.pub2.
 392. Matthews, M.; Basil, B.; Evcimen, H.; Adetunji, B.; Joseph, S. Mirtazapine-Induced Nightmares. *Prim. Care Companion J. Clin. Psychiatry* **2006**, *08*, 311, doi:10.4088/PCC.v08n0510b.
 393. Barkin, R.L.; Schwer, W.A.; Barkin, S.J. Recognition and Management of Depression in Primary Care. *Am. J. Ther.* **2000**, *7*, 205–228, doi:10.1097/00045391-200007030-00008.
 394. Blier, P.; Gobbi, G.; Turcotte, J.E.; de Montigny, C.; Boucher, N.; Hébert, C.; Debonnel, G. Mirtazapine and paroxetine in major depression: A comparison of monotherapy versus their combination from treatment initiation. *Eur. Neuropsychopharmacol.* **2009**, *19*, 457–465, doi:10.1016/j.euroneuro.2009.01.015.
 395. Blier, P.; Ward, H.E.; Tremblay, P.; Laberge, L.; Hébert, C.; Bergeron, R. Combination of Antidepressant Medications From Treatment Initiation for Major

- Depressive Disorder: A Double-Blind Randomized Study. *Am. J. Psychiatry* **2010**, *167*, 281–288, doi:10.1176/appi.ajp.2009.09020186.
396. Thase, M.E.; Nierenberg, A.A.; Vrijland, P.; van Oers, H.J.J.; Schutte, A.-J.; Simmons, J.H. Remission with mirtazapine and selective serotonin reuptake inhibitors: a meta-analysis of individual patient data from 15 controlled trials of acute phase treatment of major depression. *Int. Clin. Psychopharmacol.* **2010**, *25*, 189–198, doi:10.1097/YIC.0b013e328330adb2.
 397. Wang, S.-M.; Han, C.; Bahk, W.-M.; Lee, S.-J.; Patkar, A.A.; Masand, P.S.; Pae, C.-U. Addressing the Side Effects of Contemporary Antidepressant Drugs: A Comprehensive Review. *Chonnam Med. J.* **2018**, *54*, 101, doi:10.4068/CMJ.2018.54.2.101.
 398. Furukawa, T.A.; Cipriani, A.; Cowen, P.J.; Leucht, S.; Egger, M.; Salanti, G. Optimal dose of selective serotonin reuptake inhibitors, venlafaxine, and mirtazapine in major depression: a systematic review and dose-response meta-analysis. *The Lancet Psychiatry* **2019**, *6*, 601–609, doi:10.1016/S2215-0366(19)30217-2.
 399. Al-Majed, A.; Bakheit, A.H.; Alharbi, R.M.; Abdel Aziz, H.A. Mirtazapine. In *Profiles of Drug Substances, Excipients and Related Methodology*; Academic Press, 2018; Vol. 43, pp. 209–254.
 400. Bengtsson, H.J.; Kele, J.; Johansson, J.; Hjorth, S. Interaction of the antidepressant mirtazapine with α 2-adrenoceptors modulating the release of 5-HT in different rat brain regions in vivo. *Naunyn. Schmiedeberg's Arch. Pharmacol.* **2000**, *362*, 406–412, doi:10.1007/s002100000294.
 401. Sato, H.; Ito, C.; Tashiro, M.; Hiraoka, K.; Shibuya, K.; Funaki, Y.; Iwata, R.; Matsuoka, H.; Yanai, K. Histamine H1 receptor occupancy by the new-generation antidepressants fluvoxamine and mirtazapine: a positron emission tomography study in healthy volunteers. *Psychopharmacology (Berl)*. **2013**, *230*, 227–234, doi:10.1007/s00213-013-3146-1.
 402. Bessa, M.J.; Brandão, F.; Fokkens, P.H.B.; Leseman, D.L.A.C.; Boere, A.J.F.; Cassee, F.R.; Salmatouidis, A.; Viana, M.; Vulpoi, A.; Simon, S.; et al. In vitro toxicity of industrially relevant engineered nanoparticles in human alveolar epithelial cells: Air–liquid interface versus submerged cultures. *Nanomaterials* **2021**, *11*, 3225, doi:10.3390/nano11123225.
 403. Correia, A.S.; Duarte, D.; Silva, I.; Reguengo, H.; Oliveira, J.C.; Vale, N. Serotonin after β -Adrenoreceptors' Exposition: New Approaches for Personalized Data in Breast Cancer Cells. *J. Pers. Med.* **2021**, *11*, 954, doi:10.3390/jpm11100954.
 404. Olanas, M.C.; Dedoni, S.; Onali, P. LPA_1 is a key mediator of intracellular signalling and neuroprotection triggered by tetracyclic antidepressants in hippocampal neurons. *J. Neurochem.* **2017**, *143*, 183–197, doi:10.1111/jnc.14150.
 405. Hisaoka-Nakashima, K.; Taki, S.; Watanabe, S.; Nakamura, Y.; Nakata, Y.; Morioka, N. Mirtazapine increases glial cell line-derived neurotrophic factor production through lysophosphatidic acid 1 receptor-mediated extracellular signal-regulated kinase signaling in astrocytes. *Eur. J. Pharmacol.* **2019**, *860*, 172539, doi:10.1016/j.ejphar.2019.172539.
 406. Zhao, X.; Fang, J.; Li, S.; Gaur, U.; Xing, X.; Wang, H.; Zheng, W. Artemisinin Attenuated Hydrogen Peroxide (H₂O₂)-Induced Oxidative Injury in SH-SY5Y and Hippocampal Neurons via the Activation of AMPK Pathway. *Int. J. Mol. Sci.* **2019**,

20, 2680, doi:10.3390/ijms20112680.

407. Rossato, R.C.; Granato, A.E.C.; Moraes, C.D.G. de O.; Salles, G.N.; Soares, C.P.; de Oliveira Moraes, C.D.G.; Salles, G.N.; Soares, C.P. Neuroprotective effects of taurine on SH-SY5Y cells under hydrocortisone induced stress. *Res. Soc. Dev.* **2021**, *10*, e55510918426–e55510918426, doi:10.33448/rsd-v10i9.18426.
408. Gite, S.; Ross, R.P.; Kirke, D.; Guihéneuf, F.; Aussant, J.; Stengel, D.B.; Dinan, T.G.; Cryan, J.F.; Stanton, C. Nutraceuticals to promote neuronal plasticity in response to corticosterone-induced stress in human neuroblastoma cells. *Nutr. Neurosci.* **2019**, *22*, 551–568, doi:10.1080/1028415X.2017.1418728.
409. Tian, J.; Liu, S.; He, X.; Xiang, H.; Chen, J.; Gao, Y.; Zhou, Y.; Qin, X. Metabolomics studies on corticosterone-induced PC12 cells: A strategy for evaluating an in vitro depression model and revealing the metabolic regulation mechanism. *Neurotoxicol. Teratol.* **2018**, *69*, 27–38, doi:10.1016/j.ntt.2018.07.002.
410. Zhang, Y.; He, Y.; Deng, N.; Chen, Y.; Huang, J.; Xie, W. Protective effect of resveratrol against corticosterone-induced neurotoxicity in PC12 cells. *Transl. Neurosci.* **2019**, *10*, 235–240, doi:10.1515/tnsci-2019-0038.
411. Ramos-Hryb, A.B.; Platt, N.; Freitas, A.E.; Heinrich, I.A.; López, M.G.; Leal, R.B.; Kaster, M.P.; Rodrigues, A.L.S. Protective Effects of Ursolic Acid Against Cytotoxicity Induced by Corticosterone: Role of Protein Kinases. *Neurochem. Res.* **2019**, *44*, 2843–2855, doi:10.1007/s11064-019-02906-1.
412. Ransy, C.; Vaz, C.; Lombès, A.; Bouillaud, F. Use of H₂O₂ to Cause Oxidative Stress, the Catalase Issue. *Int. J. Mol. Sci.* **2020**, *21*, 9149, doi:10.3390/ijms21239149.
413. Galluzzi, L.; Vitale, I.; Aaronson, S.A.; Abrams, J.M.; Adam, D.; Agostinis, P.; Alnemri, E.S.; Altucci, L.; Amelio, I.; Andrews, D.W.; et al. Molecular mechanisms of cell death: recommendations of the Nomenclature Committee on Cell Death 2018. *Cell Death Differ.* **2018**, *25*, 486–541, doi:10.1038/s41418-017-0012-4.
414. Ng, N.; Ooi, L. Correction Notice: A Simple Microplate Assay for Reactive Oxygen Species Generation and Rapid Cellular Protein Normalization. *Bio-Protocol* **2023**, *13*, e3877–e3877, doi:10.21769/BioProtoc.4877.
415. Olive, P.L.; Banáth, J.P. The comet assay: a method to measure DNA damage in individual cells. *Nat. Protoc.* **2006**, *1*, 23–29, doi:10.1038/nprot.2006.5.
416. Wang, C.; Xu, J.; Zhou, G.; Qu, Q.; Yang, G.; Hu, X. Electrochemical Detection Coupled with High-Performance Liquid Chromatography in Pharmaceutical and Biomedical Analysis: A Mini Review. *Comb. Chem. High Throughput Screen.* **2007**, *10*, 547–554, doi:10.2174/138620707782152362.
417. Lee, H.-S.; Jeong, G.-S. Protective Effects of 6,7,4'-Trihydroxyflavanone on Hypoxia-Induced Neurotoxicity by Enhancement of HO-1 through Nrf2 Signaling Pathway. *Antioxidants* **2021**, *10*, 341, doi:10.3390/antiox10030341.
418. Yoo, S.-Y.; Yoo, J.-Y.; Kim, H.-B.; Baik, T.-K.; Lee, J.-H.; Woo, R.-S. Neuregulin-1 Protects Neuronal Cells Against Damage due to CoCl₂-Induced Hypoxia by Suppressing Hypoxia-Inducible Factor-1 α and P53 in SH-SY5Y Cells. *Int. Neurorol. J.* **2019**, *23*, S111-118, doi:10.5213/inj.1938190.095.
419. Wang, Y.; Yang, J.; Li, H.; Wang, X.; Zhu, L.; Fan, M.; Wang, X. Hypoxia Promotes Dopaminergic Differentiation of Mesenchymal Stem Cells and Shows Benefits for Transplantation in a Rat Model of Parkinson's Disease. *PLoS One* **2013**, *8*,

e54296, doi:10.1371/journal.pone.0054296.

420. Vlaminck, B.; Toffoli, S.; Ghislain, B.; Demazy, C.; Raes, M.; Michiels, C. Dual effect of echinomycin on hypoxia-inducible factor-1 activity under normoxic and hypoxic conditions. *FEBS J.* **2007**, *274*, 5533–5542, doi:10.1111/j.1742-4658.2007.06072.x.
421. Blackburn, T.P. Depressive disorders: Treatment failures and poor prognosis over the last 50 years. *Pharmacol. Res. Perspect.* **2019**, *7*, e00472, doi:10.1002/prp2.472.
422. Becker, M.; Pinhasov, A.; Ornoy, A. Animal Models of Depression: What Can They Teach Us about the Human Disease? *Diagnostics* **2021**, *11*, 123, doi:10.3390/diagnostics11010123.
423. Fenwick, N.; Griffin, G.; Gauthier, C. The welfare of animals used in science: How the “Three Rs” ethic guides improvements. *Can. Vet. J.* **2009**, *50*, 523.
424. Borsini, A.; Zunszain, P.A. Advances in stem cells biology: New approaches to understand depression. *Stem Cells Neuroendocrinol.* **2016**, 123–133.
425. Jantas, D. Cell-Based Systems of Depression: An Overview. In *Herbal Medicine in Depression*; Springer International Publishing: Cham, 2016; pp. 75–117 ISBN 9783319140216.
426. Avior, Y.; Ron, S.; Kroitorou, D.; Albeldas, C.; Lerner, V.; Corneo, B.; Nitzan, E.; Laifenfeld, D.; Cohen Solal, T. Depression patient-derived cortical neurons reveal potential biomarkers for antidepressant response. *Transl. Psychiatry* **2021**, *11*, 201, doi:10.1038/s41398-021-01319-5.
427. Lago, S.G.; Tomasik, J.; Bahn, S. Functional patient-derived cellular models for neuropsychiatric drug discovery. *Transl. Psychiatry* **2021**, *11*, 128, doi:10.1038/s41398-021-01243-8.
428. Talishinsky, A.; Downar, J.; Vértés, P.E.; Seidlitz, J.; Dunlop, K.; Lynch, C.J.; Whalley, H.; McIntosh, A.; Vila-Rodriguez, F.; Daskalakis, Z.J.; et al. Regional gene expression signatures are associated with sex-specific functional connectivity changes in depression. *Nat. Commun.* **2022**, *13*, 5692, doi:10.1038/s41467-022-32617-1.
429. Segeritz, C.-P.; Vallier, L. Cell Culture. In *Basic Science Methods for Clinical Researchers*; Jalali, M., Saldanha, F.Y.L., Jalali, M.B.T.-B.S.M. for C.R., Eds.; Elsevier: Boston, 2017; pp. 151–172 ISBN 978-0-12-803077-6.
430. Kovalevich, J.; Langford, D. Considerations for the Use of SH-SY5Y Neuroblastoma Cells in Neurobiology. In *Methods in molecular biology (Clifton, N.J.)*; NIH Public Access, 2013; Vol. 1078, pp. 9–21 ISBN 9781627036399.
431. Yu, Z.; Kong, D.; Liang, Y.; Zhao, X.; Du, G. Protective effects of VMY-2-95 on corticosterone-induced injuries in mice and cellular models. *Acta Pharm. Sin. B* **2021**, *11*, 1903–1913, doi:10.1016/j.apsb.2021.03.002.
432. Li, D.; Li, W.; Shi, W.; Wu, X.; Liu, X.; Gao, P. Exploring the Active Components of *Ziziphus jujuba* Mill. in Treatment of Depression by Network Pharmacology Combined with Neuroprotective Effects in SH-SY5Y Cells. *Pharm. Chem. J.* **2023**, *57*, 712–724, doi:10.1007/s11094-023-02942-w.
433. Adeosun, S.O.; Albert, P.R.; Austin, M.C.; Iyo, A.H. 17 β -Estradiol-Induced Regulation of the Novel 5-HT1A-Related Transcription Factors NUDR and Freud-1 in SH SY5Y Cells. *Cell. Mol. Neurobiol.* **2012**, *32*, 517–521, doi:10.1007/s10571-

012-9809-3.

434. Jerman, J.C.; Brough, S.J.; Gager, T.; Wood, M.; Coldwell, M.C.; Smart, D.; Middlemiss, D.N. Pharmacological characterisation of human 5-HT₂ receptor subtypes. *Eur. J. Pharmacol.* **2001**, *414*, 23–30, doi:10.1016/S0014-2999(01)00775-0.
435. Shipley, M.M.; Mangold, C.A.; Szpara, M.L. Differentiation of the SH-SY5Y Human Neuroblastoma Cell Line. *J. Vis. Exp.* **2016**, 53193, doi:10.3791/53193.
436. Liu, J.; Li, L.; Suo, W.Z. HT22 hippocampal neuronal cell line possesses functional cholinergic properties. *Life Sci.* **2009**, *84*, 267–271, doi:10.1016/j.lfs.2008.12.008.
437. Pei, H.; Zeng, J.; He, Z.; Zong, Y.; Zhao, Y.; Li, J.; Chen, W.; Du, R. Palmatine ameliorates LPS-induced HT-22 cells and mouse models of depression by regulating apoptosis and oxidative stress. *J. Biochem. Mol. Toxicol.* **2023**, *37*, e23225, doi:10.1002/jbt.23225.
438. Lim, J.; Bang, Y.; Kim, K.-M.; Choi, H.J. Differentiated HT22 cells as a novel model for in vitro screening of serotonin reuptake inhibitors. *Front. Pharmacol.* **2023**, *13*, 1062650, doi:10.3389/fphar.2022.1062650.
439. Plach, M.; Schäfer, T.; Borroto-Escuela, D.O.; Weikert, D.; Gmeiner, P.; Fuxe, K.; Friedland, K. Differential allosteric modulation within dopamine D₂R - neurotensin NTS1R and D₂R - serotonin 5-HT_{2A}R receptor complexes gives bias to intracellular calcium signalling. *Sci. Rep.* **2019**, *9*, 16312, doi:10.1038/s41598-019-52540-8.
440. Lim, J.; Bang, Y.; Choi, J.-H.; Han, A.; Kwon, M.-S.; Liu, K.H.; Choi, H.J. LRRK2 G2019S Induces Anxiety/Depression-like Behavior before the Onset of Motor Dysfunction with 5-HT_{1A} Receptor Upregulation in Mice. *J. Neurosci.* **2018**, *38*, 1611–1621, doi:10.1523/jneurosci.4051-15.2017.
441. Lein, P.J.; Barnhart, C.D.; Pessah, I.N. Acute Hippocampal Slice Preparation and Hippocampal Slice Cultures., doi:10.1007/978-1-61779-170-3_8.
442. Gordon, J.; Amini, S.; White, M.K. General Overview of Neuronal Cell Culture. In; 2013; pp. 1–8.
443. Katsu, Y.; Baker, M.E. Corticosterone. In *Handbook of Hormones*; Ando, H., Ukena, K., Nagata, S.B.T.-H. of H. (Second E., Eds.; Elsevier: San Diego, 2021; pp. 935–937 ISBN 978-0-12-820649-2.
444. Katsu, Y.; Iguchi, T. 18-Hydroxycorticosterone. In *Handbook of Hormones*; Takei, Y., Ando, H., Tsutsui, K.B.T.-H. of H., Eds.; Elsevier: San Diego, 2016; pp. 529-e95B-3 ISBN 978-0-12-801028-0.
445. Stalder, T.; Kirschbaum, C. Cortisol. In *Encyclopedia of Behavioral Medicine*; Gellman, M.D., Ed.; Springer International Publishing: Cham, 2020; pp. 561–567 ISBN 978-3-030-39903-0.
446. Hindmarsh, P.C.; Geertsma, K. Hydrocortisone. In *Congenital Adrenal Hyperplasia*; Hindmarsh, P.C., Geertsma, K.B.T.-C.A.H., Eds.; Elsevier, 2017; pp. 231–249 ISBN 978-0-12-811483-4.
447. Planchez, B.; Surget, A.; Belzung, C. Animal models of major depression: drawbacks and challenges. *J. Neural Transm.* **2019**, *126*, 1383–1408, doi:10.1007/s00702-019-02084-y.
448. Motta, J.R.; Jung, I.E. da C.; Azzolin, V.F.; Teixeira, C.F.; Braun, L.E.; De Oliveira

- Nerys, D.A.; Motano, M.A.E.; Duarte, M.M.M.F.; Maia-Ribeiro, E.A.; da Cruz, I.B.M.; et al. Avocado oil (*Persea americana*) protects SH-SY5Y cells against cytotoxicity triggered by cortisol by the modulation of BDNF, oxidative stress, and apoptosis molecules. *J. Food Biochem.* **2021**, *45*, e13596, doi:10.1111/jfbc.13596.
449. Oh, D.-R.R.; Kim, M.-J.J.; Choi, E.-J.J.; Kim, Y.; Lee, H.-S.S.; Bae, D.; Choi, C. Protective Effects of p-Coumaric Acid Isolated from *Vaccinium bracteatum* Thunb. Leaf Extract on Corticosterone-Induced Neurotoxicity in SH-SY5Y Cells and Primary Rat Cortical Neurons. *Processes* **2021**, *9*, 869, doi:10.3390/pr9050869.
450. Yang, G.; Li, J.; Cai, Y.; Yang, Z.; Li, R.; Fu, W. Glycyrrhizic Acid Alleviates 6-Hydroxydopamine and Corticosterone-Induced Neurotoxicity in SH-SY5Y Cells Through Modulating Autophagy. *Neurochem. Res.* **2018**, *43*, 1914–1926, doi:10.1007/s11064-018-2609-5.
451. Karszen, A.M.; Meijer, O.C.; van der Sandt, I.C.J.; Lucassen, P.J.; de Lange, E.C.M.; de Boer, A.G.; de Kloet, E.R. Multidrug Resistance P-Glycoprotein Hampers the Access of Cortisol But Not of Corticosterone to Mouse and Human Brain. *Endocrinology* **2001**, *142*, 2686–2694, doi:10.1210/endo.142.6.8213.
452. Nanayakkara, A.K.; Follit, C.A.; Chen, G.; Williams, N.S.; Vogel, P.D.; Wise, J.G. Targeted inhibitors of P-glycoprotein increase chemotherapeutic-induced mortality of multidrug resistant tumor cells. *Sci. Rep.* **2018**, *8*, 967, doi:10.1038/s41598-018-19325-x.
453. Sieczkowski, E.; Lehner, C.; Ambros, P.F.; Hohenegger, M. Double impact on p-glycoprotein by statins enhances doxorubicin cytotoxicity in human neuroblastoma cells. *Int. J. Cancer* **2010**, *126*, 2025–2035, doi:10.1002/ijc.24885.
454. Liu, J.; Geng, T.; Duan, K.; Gao, X.; Huang, C.; Wang, J.; Huang, W.; Huang, L.; Wang, Z.; Xiao, W. Cellular pharmacokinetics and pharmacodynamics mechanisms of ginkgo diterpene lactone and its modulation of P-glycoprotein expression in human SH-SY5Y cells. *Biomed. Chromatogr.* **2019**, *33*, e4692, doi:10.1002/bmc.4692.
455. Ham, S.; Lee, Y.-I.; Jo, M.; Kim, H.; Kang, H.; Jo, A.; Lee, G.H.; Mo, Y.J.; Park, S.C.; Lee, Y.S.; et al. Hydrocortisone-induced parkin prevents dopaminergic cell death via CREB pathway in Parkinson's disease model. *Sci. Rep.* **2017**, *7*, 525, doi:10.1038/s41598-017-00614-w.
456. Seirafi, M.; Kozlov, G.; Gehring, K. Parkin structure and function. *FEBS J.* **2015**, *282*, 2076–2088, doi:10.1111/febs.13249.
457. Meijer, O.C.; Buurstede, J.C.; Schaaf, M.J.M. Corticosteroid Receptors in the Brain: Transcriptional Mechanisms for Specificity and Context-Dependent Effects. *Cell. Mol. Neurobiol.* **2019**, *39*, 539–549, doi:10.1007/s10571-018-0625-2.
458. Kalyanaraman, B. Teaching the basics of cancer metabolism: Developing antitumor strategies by exploiting the differences between normal and cancer cell metabolism. *Redox Biol.* **2017**, *12*, 833–842, doi:10.1016/j.redox.2017.04.018.
459. Lee, C.; Jang, J.-H.; Park, G.H. Protective Role of Corticosterone against Hydrogen Peroxide-Induced Neuronal Cell Death in SH-SY5Y Cells. *Biomol. Ther. (Seoul)*. **2022**, *30*, 570–575, doi:10.4062/biomolther.2022.126.
460. Wang, Y.; Liu, Z.; Wei, J.; Di, L.; Wang, S.; Wu, T.; Li, N. Norlignans and phenolics from genus *Curculigo* protect corticosterone-injured neuroblastoma cells SH-SY5Y by inhibiting endoplasmic reticulum stress-mitochondria pathway. *J.*

Ethnopharmacol. **2022**, 296, 115430, doi:10.1016/j.jep.2022.115430.

461. Zheng, Y.; Huang, J.; Tao, L.; Shen, Z.; Li, H.; Mo, F.; Wang, X.; Wang, S.; Shen, H. Corticosterone increases intracellular Zn²⁺ release in hippocampal HT-22 cells. *Neurosci. Lett.* **2015**, 588, 172–177, doi:10.1016/j.neulet.2015.01.016.
462. Costantini, D.; Marasco, V.; Møller, A.P. A meta-analysis of glucocorticoids as modulators of oxidative stress in vertebrates. *J. Comp. Physiol. B* **2011**, 181, 447–456, doi:10.1007/s00360-011-0566-2.
463. Huang, S.; Galaj, E.; Wang, J.; Guo, Y.; Wang, S.; Shi, M.; Yin, X.; Liu, K.; Luo, Y.; Meng, L.; et al. Repurposing antimalarial artesunate for the prophylactic treatment of depression: Evidence from preclinical research. *Brain Behav.* **2023**, 13, e2833, doi:10.1002/brb3.2833.
464. Wang, C.-M.; Yang, C.-Q.; Cheng, B.-H.; Chen, J.; Bai, B. Orexin-A protects SH-SY5Y cells against H₂O₂-induced oxidative damage via the PI3K/MEK 1/2/ERK 1/2 signaling pathway. *Int. J. Immunopathol. Pharmacol.* **2018**, 32, 205873841878573, doi:10.1177/2058738418785739.
465. Juan, C.A.; Pérez de la Lastra, J.M.; Plou, F.J.; Pérez-Lebeña, E. The Chemistry of Reactive Oxygen Species (ROS) Revisited: Outlining Their Role in Biological Macromolecules (DNA, Lipids and Proteins) and Induced Pathologies. *Int. J. Mol. Sci.* **2021**, 22, 4642, doi:10.3390/ijms22094642.
466. Wang, Q.; Ma, M.; Yu, H.; Yu, H.; Zhang, S.; Li, R. Mirtazapine prevents cell activation, inflammation, and oxidative stress against isoflurane exposure in microglia. *Bioengineered* **2022**, 13, 521–530, doi:10.1080/21655979.2021.2009971.
467. Lavergne, F.; Berlin, I.; Gamma, A.; Stassen, H.; Angst, J. Onset of improvement and response to mirtazapine in depression: a multicenter naturalistic study of 4771 patients. *Neuropsychiatr. Dis. Treat.* **2005**, 1, 59–68, doi:10.2147/ndt.1.1.59.52296.
468. Gulec, M.; Oral, E.; Dursun, O.B.; Yucel, A.; Hacimuftuoglu, A.; Akcay, F.; Suleyman, H. Mirtazapine protects against cisplatin-induced oxidative stress and DNA damage in the rat brain. *Psychiatry Clin. Neurosci.* **2013**, 67, 50–58, doi:10.1111/j.1440-1819.2012.02395.x.
469. Gall, J.I.; Gonçalves Alves, A.; Carraro Júnior, L.R.; da Silva Teixeira Rech, T.; dos Santos Neto, J.S.; Alves, D.; Pereira Soares, M.S.; Spohr, L.; Spanevello, R.M.; Brüning, C.A.; et al. Insights into serotonergic and antioxidant mechanisms involved in antidepressant-like action of 2-phenyl-3-(phenylselanyl)benzofuran in mice. *Prog. Neuro-Psychopharmacology Biol. Psychiatry* **2020**, 102, 109956, doi:10.1016/j.pnpbp.2020.109956.
470. Engel, D.; Zomkowski, A.D.E.; Lieberknecht, V.; Rodrigues, A.L.; Gabilan, N.H. Chronic administration of duloxetine and mirtazapine downregulates proapoptotic proteins and upregulates neurotrophin gene expression in the hippocampus and cerebral cortex of mice. *J. Psychiatr. Res.* **2013**, 47, 802–808, doi:10.1016/j.jpsychires.2013.02.013.
471. Auer, S.; Rinnerthaler, M.; Bischof, J.; Streubel, M.K.; Breitenbach-Koller, H.; Geisberger, R.; Aigner, E.; Cadamuro, J.; Richter, K.; Sopjani, M.; et al. The Human NADPH Oxidase, Nox4, Regulates Cytoskeletal Organization in Two Cancer Cell Lines, HepG2 and SH-SY5Y. *Front. Oncol.* **2017**, 7, 111, doi:10.3389/fonc.2017.00111.

472. Choi, D.-H.; Choi, I.-A.; Lee, C.; Yun, J.; Lee, J. The Role of NOX4 in Parkinson's Disease with Dementia. *Int. J. Mol. Sci.* **2019**, *20*, 696, doi:10.3390/ijms20030696.
473. Luengo, E.; Trigo-Alonso, P.; Fernández-Mendivil, C.; Nuñez, Á.; Campo, M. del; Porrero, C.; García-Magro, N.; Negrodo, P.; Senar, S.; Sánchez-Ramos, C.; et al. Implication of type 4 NADPH oxidase (NOX4) in tauopathy. *Redox Biol.* **2022**, *49*, 102210, doi:10.1016/j.redox.2021.102210.
474. Oliveira, T. de Q.; Sousa, C.N.S. de; Vasconcelos, G.S.; de Sousa, L.C.; de Oliveira, A.A.; Patrocínio, C.F.V.; Medeiros, I. da S.; Honório Júnior, J.E.R.; Maes, M.; Macedo, D.; et al. Brain antioxidant effect of mirtazapine and reversal of sedation by its combination with alpha-lipoic acid in a model of depression induced by corticosterone. *J. Affect. Disord.* **2017**, *219*, 49–57, doi:10.1016/j.jad.2017.05.022.
475. Barbar Shemirani, S.; Nasiri Khalili, M.A.; Mahdavi, S.M.; Modarresi Chahardehi, A. The effect of mirtazapine on reducing chronic stress in male rats. *Int Clin Neurosci J* **2022**, *9*, e21.
476. Weber, C.-C.; Eckert, G.P.; Müller, W.E. Effects of Antidepressants on the Brain/Plasma Distribution of Corticosterone. *Neuropsychopharmacology* **2006**, *31*, 2443–2448, doi:10.1038/sj.npp.1301076.
477. Augustyn, M.; Otczyk, M.; Budziszewska, B.; Jagła, G.; Nowak, W.; Basta-Kaim, A.; Jaworska-Feil, L.; Kubera, M.; Tetich, M.; Leśkiewicz, M.; et al. Effects of some new antidepressant drugs on the glucocorticoid receptor-mediated gene transcription in fibroblast cells. *Pharmacol. Rep.* **2005**, *57*, 766–73.
478. Jacobsen, J.P.R.; Medvedev, I.O.; Caron, M.G. The 5-HT deficiency theory of depression: perspectives from a naturalistic 5-HT deficiency model, the tryptophan hydroxylase 2 Arg 439 His knockin mouse. *Philos. Trans. R. Soc. B Biol. Sci.* **2012**, *367*, 2444–2459, doi:10.1098/rstb.2012.0109.
479. Kikuoka, R.; Miyazaki, I.; Kubota, N.; Maeda, M.; Kagawa, D.; Moriyama, M.; Sato, A.; Murakami, S.; Kitamura, Y.; Sendo, T.; et al. Mirtazapine exerts astrocyte-mediated dopaminergic neuroprotection. *Sci. Rep.* **2020**, *10*, 20698, doi:10.1038/s41598-020-77652-4.
480. Nagayasu, K.; Kitaichi, M.; Nishitani, N.; Asaoka, N.; Shirakawa, H.; Nakagawa, T.; Kaneko, S. Chronic effects of antidepressants on serotonin release in rat raphe slice cultures: high potency of milnacipran in the augmentation of serotonin release. *Int. J. Neuropsychopharmacol.* **2013**, *16*, 2295–2306, doi:10.1017/S1461145713000771.
481. Goh, K.K.; Chen, C.H.; Chiu, Y.H.; Lu, M.L. Lamotrigine augmentation in treatment-resistant unipolar depression: A comprehensive meta-analysis of efficacy and safety. *J. Psychopharmacol.* **2019**, *33*, 700–713, doi:10.1177/0269881119844199.
482. Rajkumar, R.; Mahesh, R. The auspicious role of the 5-HT₃ receptor in depression: A probable neuronal target? *J. Psychopharmacol.* **2010**, *24*, 455–469, doi:10.1177/0269881109348161.
483. Bétry, C.; Etiévant, A.; Oosterhof, C.; Ebert, B.; Sanchez, C.; Haddjeri, N. Role of 5-HT₃ Receptors in the Antidepressant Response. *Pharmaceuticals* **2011**, *4*, 603, doi:10.3390/PH4040603.
484. Ramamoorthy, R.; Radhakrishnan, M.; Borah, M. Antidepressant-like effects of serotonin type-3 antagonist, ondansetron: an investigation in behaviour-based

- rodent models. *Behav. Pharmacol.* **2008**, *19*, 29–40, doi:10.1097/FBP.0b013e3282f3cfd4.
485. Kim, K.J.; Jeun, S.H.; Sung, K.-W. Lamotrigine, an antiepileptic drug, inhibits 5-HT 3 receptor currents in NCB-20 neuroblastoma cells. *Korean J. Physiol. Pharmacol.* **2017**, *21*, 169, doi:10.4196/kjpp.2017.21.2.169.
486. Abelaira, H.M.; Réus, G.Z.; Ribeiro, K.F.; Zappellini, G.; Ferreira, G.K.; Gomes, L.M.; Carvalho-Silva, M.; Luciano, T.F.; Marques, S.O.; Streck, E.L.; et al. Effects of acute and chronic treatment elicited by lamotrigine on behavior, energy metabolism, neurotrophins and signaling cascades in rats. *Neurochem. Int.* **2011**, *59*, 1163–1174, doi:10.1016/j.neuint.2011.10.007.
487. Martin, A.E.; Schober, D.A.; Nikolayev, A.; Tolstikov, V. V.; Anderson, W.H.; Higgs, R.E.; Kuo, M.-S.; Laksmanan, A.; Catlow, J.T.; Li, X.; et al. Further Evaluation of Mechanisms Associated with the Antidepressantlike Signature of Scopolamine in Mice. *CNS Neurol. Disord. - Drug Targets* **2017**, *16*, doi:10.2174/1871527316666170309142646.
488. Southam, E.; Kirkby, D.; Higgins, G.A.; Hagan, R.M. Lamotrigine inhibits monoamine uptake in vitro and modulates 5-hydroxytryptamine uptake in rats. *Eur. J. Pharmacol.* **1998**, *358*, 19–24, doi:https://doi.org/10.1016/S0014-2999(98)00580-9.
489. Ahmad, S.; Fowler, L.J.; Whitton, P.S. Effects of combined lamotrigine and valproate on basal and stimulated extracellular amino acids and monoamines in the hippocampus of freely moving rats. *Naunyn. Schmiedebergs. Arch. Pharmacol.* **2005**, *371*, 1–8, doi:10.1007/s00210-004-1008-4.
490. Ju Yeon Ban; Yeon Hee Seong Blockade of 5-HT3 receptor with MDL72222 and Y25130 reduces β -amyloid protein (25–35)-induced neurotoxicity in cultured rat cortical neurons. *Eur. J. Pharmacol.* **2005**, *520*, 12–21, doi:10.1016/j.ejphar.2005.07.021.
491. Gupta, D.; Radhakrishnan, M.; Kurhe, Y. Effect of a novel 5-HT3 receptor antagonist 4i, in corticosterone-induced depression-like behavior and oxidative stress in mice. *Steroids* **2015**, *96*, 95–102, doi:10.1016/j.steroids.2015.01.021.
492. Modoux, M.; Rolhion, N.; Mani, S.; Sokol, H. Tryptophan Metabolism as a Pharmacological Target. *Trends Pharmacol. Sci.* **2021**, *42*, 60–73, doi:10.1016/j.tips.2020.11.006.
493. Mao, X.; Lv, M.; Yu, B.; He, J.; Zheng, P.; Yu, J.; Wang, Q.; Chen, D. The effect of dietary tryptophan levels on oxidative stress of liver induced by diquat in weaned piglets. *J. Anim. Sci. Biotechnol.* **2014**, *5*, 49, doi:10.1186/2049-1891-5-49.
494. Liu, G.; Tao, J.; Lu, J.; Jia, G.; Zhao, H.; Chen, X.; Tian, G.; Cai, J.; Zhang, R.; Wang, J. Dietary Tryptophan Supplementation Improves Antioxidant Status and Alleviates Inflammation, Endoplasmic Reticulum Stress, Apoptosis, and Pyroptosis in the Intestine of Piglets after Lipopolysaccharide Challenge. *Antioxidants* **2022**, *11*, 872, doi:10.3390/antiox11050872.
495. Wei, X.; Li, D.; Feng, C.; Mao, H.; Zhu, J.; Cui, Y.; Yang, J.; Gao, H.; Wang, C. Effects of hydrogen peroxide and l-tryptophan on antioxidative potential, apoptosis, and mammalian target of rapamycin signaling in bovine intestinal epithelial cells. *J. Dairy Sci.* **2022**, *105*, 10007–10019, doi:10.3168/jds.2022-21869.

496. Perez-Gonzalez, A.; Muñoz-Rugeles, L.; Alvarez-Idaboy, J.R. Tryptophan: antioxidant or target of oxidative stress? A quantum chemistry elucidation. *RSC Adv.* **2014**, *4*, 56128–56131, doi:10.1039/C4RA11635F.
497. Wang, H.; Zhou, X.; Huang, J.; Mu, N.; Guo, Z.; Wen, Q.; Wang, R.; Chen, S.; Feng, Z.-P.; Zheng, W. The role of Akt/FoxO3a in the protective effect of venlafaxine against corticosterone-induced cell death in PC12 cells. *Psychopharmacology (Berl)*. **2013**, *228*, 129–141, doi:10.1007/s00213-013-3017-9.
498. Abdollahi, M.; Hosseini, A. Hydrogen Peroxide. In *Encyclopedia of Toxicology*; Elsevier, 2014; pp. 967–970 ISBN 9780123864543.
499. García-Caparrós, P.; De Filippis, L.; Gul, A.; Hasanuzzaman, M.; Ozturk, M.; Altay, V.; Lao, M.T. Oxidative Stress and Antioxidant Metabolism under Adverse Environmental Conditions: a Review. *Bot. Rev.* **2021**, *87*, 421–466, doi:10.1007/s12229-020-09231-1.
500. Azouzi, S.; Santuz, H.; Morandat, S.; Pereira, C.; Côté, F.; Hermine, O.; El Kirat, K.; Colin, Y.; Le Van Kim, C.; Etchebest, C.; et al. Antioxidant and Membrane Binding Properties of Serotonin Protect Lipids from Oxidation. *Biophys. J.* **2017**, *112*, 1863–1873, doi:10.1016/j.bpj.2017.03.037.
501. Gulcin, İ. Antioxidants and antioxidant methods: an updated overview. *Arch. Toxicol.* **2020**, *94*, 651–715, doi:10.1007/s00204-020-02689-3.
502. Munoz-Castaneda, J.; Montilla, P.; Padillo, F.; Bujalance, I.; Munoz, M.; Muntane, J.; Tunez, A. Role of serotonin in cerebral oxidative stress in rat. *Acta Neurobiol. Exp. (Wars)*. **2006**, *66*, 1–6, doi:10.55782/ane-2006-1581.
503. Fuentes-Lemus, E.; Dorta, E.; Escobar, E.; Aspée, A.; Pino, E.; Abasq, M.L.; Speisky, H.; Silva, E.; Lissi, E.; Davies, M.J.; et al. Oxidation of free, peptide and protein tryptophan residues mediated by AAPH-derived free radicals: role of alkoxyl and peroxy radicals. *RSC Adv.* **2016**, *6*, 57948–57955, doi:10.1039/C6RA12859A.
504. Wang, X.; Zhang, L. Kinetic study of hydroxyl radical formation in a continuous hydroxyl generation system. *RSC Adv.* **2018**, *8*, 40632–40638, doi:10.1039/C8RA08511K.
505. Al-Mamary, M.A.; Moussa, Z. Antioxidant Activity: The Presence and Impact of Hydroxyl Groups in Small Molecules of Natural and Synthetic Origin. In; Waisundara, V., Ed.; IntechOpen: Rijeka, 2021; p. Ch. 13 ISBN 978-1-83968-865-2.
506. Scotton, W.J.; Hill, L.J.; Williams, A.C.; Barnes, N.M. Serotonin Syndrome: Pathophysiology, Clinical Features, Management, and Potential Future Directions. *Int. J. Tryptophan Res.* **2019**, *12*, 117864691987392, doi:10.1177/1178646919873925.
507. Wang, C.S.; Kavalali, E.T.; Monteggia, L.M. BDNF signaling in context: From synaptic regulation to psychiatric disorders. *Cell* **2022**, *185*, 62–76, doi:10.1016/j.cell.2021.12.003.
508. Kolbeck, R.; Bartke, I.; Eberle, W.; Barde, Y. Brain-derived neurotrophic factor levels in the nervous system of wild-type and neurotrophin gene mutant mice. *J. Neurochem.* **1999**, *72*, 1930–1938.
509. Recombinant Anti-BDNF antibody [EPR1292] (ab108319) | Abcam Available online: <https://www.abcam.com/products/primary-antibodies/bdnf-antibody->

epr1292-ab108319.html#lb (accessed on Dec 8, 2023).

510. Ballanyi, K.; Ruangkittisakul, A. Brain Slices. In *Encyclopedia of Neuroscience*; Binder, M.D., Hirokawa, N., Windhorst, U., Eds.; Springer Berlin Heidelberg: Berlin, Heidelberg, 2009; pp. 483–490 ISBN 978-3-540-29678-2.
511. Castillo-Navarrete, J.-L.; Guzmán-Castillo, A.; Bustos, C.; Rojas, R. Peripheral brain-derived neurotrophic factor (BDNF) and salivary cortisol levels in college students with different levels of academic stress. Study protocol. *PLoS One* **2023**, *18*, e0282007.
512. BDNF Antibody (BDNF-#9) - DSHB Available online: <https://dshb.biology.uiowa.edu/BDNF-9> (accessed on Dec 8, 2023).
513. Wang, D.; Li, H.; Du, X.; Zhou, J.; Yuan, L.; Ren, H.; Yang, X.; Zhang, G.; Chen, X.; Cuellar-Barboza, A.B.; et al. Circulating Brain-Derived Neurotrophic Factor, Antioxidant Enzymes Activities, and Mitochondrial DNA in Bipolar Disorder: An Exploratory Report. *Psychiatry* **2020**, *11*, 514658, doi:10.3389/fpsyt.2020.514658.
514. Ogura, Y.; Sato, K.; Kawashima, K.I.; Kobayashi, N.; Imura, S.; Fujino, K.; Kawaguchi, H.; Nedachi, T. Subtoxic levels of hydrogen peroxide induce brain-derived neurotrophic factor expression to protect PC12 cells. *BMC Res. Notes* **2014**, *7*, 1–8, doi:10.1186/1756-0500-7-840/FIGURES/5.
515. Ekblom, M.M.; Bojsen-Møller, E.; Blom, V.; Tarassova, O.; Moberg, M.; Pontén, M.; Wang, R.; Ekblom, O. Acute effects of physical activity patterns on plasma cortisol and brain-derived neurotrophic factor in relation to corticospinal excitability. *Behav. Brain Res.* **2022**, *430*, 113926, doi:10.1016/J.BBR.2022.113926.
516. Herhaus, B.; Heni, M.; Bloch, W.; Petrowski, K. Acute and chronic psychosocial stress by the brain-derived neurotrophic factor in male humans: a highly standardized and controlled study. *medRxiv* **2023**, 2009–2023.
517. Alitalo, O.; González-Hernández, G.; Rosenholm, M.; Kohtala, P.; Matsui, N.; Müller, H.K.; Theilmann, W.; Klein, A.; Kärkkäinen, O.; Rozov, S. Linking Hypothermia and Altered Metabolism with TrkB Activation. *ACS Chem. Neurosci.* **2023**, *14*, 3212–3225.
518. Rogoz, Z.; Skuza, G.; Legutko, B. Repeated treatment with mirtazapine induces brain-derived neurotrophic factor gene expression in rats. *J. Physiol. Pharmacol.* **2005**, *56*, 661.
519. Zhang, Y.; Gu, F.; Chen, J.; Dong, W. Chronic antidepressant administration alleviates frontal and hippocampal BDNF deficits in CUMS rat. *Brain Res.* **2010**, *1366*, 141–148, doi:https://doi.org/10.1016/j.brainres.2010.09.095.
520. Donnici, L.; Tiraboschi, E.; Tardito, D.; Musazzi, L.; Racagni, G.; Popoli, M. Time-dependent biphasic modulation of human BDNF by antidepressants in neuroblastoma cells. *BMC Neurosci.* **2008**, *9*, 61, doi:10.1186/1471-2202-9-61.
521. Ghosal, S.; Bang, E.; Yue, W.; Hare, B.D.; Lepack, A.E.; Girgenti, M.J.; Duman, R.S. Activity-dependent brain-derived neurotrophic factor release is required for the rapid antidepressant actions of scopolamine. *Biol. Psychiatry* **2018**, *83*, 29–37.
522. Liu, S.; Shi, D.; Sun, Z.; He, Y.; Yang, J.; Wang, G. M2-AChR Mediates Rapid Antidepressant Effects of Scopolamine Through Activating the mTORC1-BDNF Signaling Pathway in the Medial Prefrontal Cortex. *Front. Psychiatry* **2021**, *12*, 601985, doi:10.3389/FPSYT.2021.601985/BIBTEX.

523. Baek, S.Y.; Li, F.Y.; Kim, D.H.; Kim, S.J.; Kim, M.R. Enteromorpha prolifera Extract Improves Memory in Scopolamine-Treated Mice via Downregulating Amyloid- β Expression and Upregulating BDNF/TrkB Pathway. *Antioxidants* **2020**, *9*, 620, doi:10.3390/antiox9070620.
524. Muñoz-Sánchez, J.; Chánez-Cárdenas, M.E. The use of cobalt chloride as a chemical hypoxia model. *J. Appl. Toxicol.* **2019**, *39*, 556–570, doi:10.1002/jat.3749.
525. Lee, P.; Chandel, N.S.; Simon, M.C. Cellular adaptation to hypoxia through hypoxia inducible factors and beyond. *Nat. Rev. Mol. Cell Biol.* **2020**, *21*, 268–283, doi:10.1038/S41580-020-0227-Y.
526. Bhutta, B.S.; Alghoula, F.; Berim, I. Hypoxia. *StatPearls* **2022**.
527. Kanekar, S.; Bogdanova, O. V.; Olson, P.R.; Sung, Y.-H.; D'Anci, K.E.; Renshaw, P.F. Hypobaric Hypoxia Induces Depression-like Behavior in Female Sprague-Dawley Rats, but not in Males. *High Alt. Med. Biol.* **2015**, *16*, 52–60, doi:10.1089/ham.2014.1070.
528. Young, S. Elevated incidence of suicide in people living at altitude, smokers and patients with chronic obstructive pulmonary disease and asthma: possible role of hypoxia causing decreased serotonin synthesis. *J. Psychiatry Neurosci.* **2013**, *38*, 423–426, doi:10.1503/jpn.130002.
529. Kious, B.M.; Kondo, D.G.; Renshaw, P.F. Living High and Feeling Low: Altitude, Suicide, and Depression. *Harv. Rev. Psychiatry* **2018**, *26*, 43–56, doi:10.1097/HRP.000000000000158.
530. Nishikawa, M.; Kumakura, Y.; Young, S.N.; Fiset, P.; Vogelzangs, N.; Leyton, M.; Benkelfat, C.; Diksic, M. Increasing blood oxygen increases an index of 5-HT synthesis in human brain as measured using α -[11C]methyl-I-tryptophan and positron emission tomography. *Neurochem. Int.* **2005**, *47*, 556–564, doi:10.1016/j.neuint.2005.07.006.
531. Dutta, A.; Sarkar, P.; Shrivastava, S.; Chattopadhyay, A. Effect of Hypoxia on the Function of the Human Serotonin 1A Receptor. *ACS Chem. Neurosci.* **2022**, *13*, 1456–1466, doi:10.1021/acscchemneuro.2c00181.
532. Hellwig-Bürgel, T.; Stiehl, D.P.; Wagner, A.E.; Metzen, E.; Jelkmann, W. Review: Hypoxia-Inducible Factor-1 (HIF-1): A Novel Transcription Factor in Immune Reactions. *J. Interf. Cytokine Res.* **2005**, *25*, 297–310, doi:10.1089/jir.2005.25.297.
533. Lee, J.-W.; Bae, S.-H.; Jeong, J.-W.; Kim, S.-H.; Kim, K.-W. Hypoxia-inducible factor (HIF-1) α : its protein stability and biological functions. *Exp. Mol. Med.* **2004**, *36*, 1–12, doi:10.1038/emm.2004.1.
534. Kang, I.; Kondo, D.; Kim, J.; Lyoo, I.K.; Yurgelun-Todd, D.; Hwang, J.; Renshaw, P.F. Elevating the level of hypoxia inducible factor may be a new potential target for the treatment of depression. *Med. Hypotheses* **2021**, *146*, 110398, doi:10.1016/j.mehy.2020.110398.
535. Zenko, M.Y.; Rybnikova, E.A. Antidepressant-like action of hypoxic postconditioning is accompanied by the up-regulation of hippocampal HIF-1 α and erythropoietin. *Med. Acad. J.* **2020**, *19*, 41–46, doi:10.17816/MAJ19075.
536. Li, G.; Zhao, M.; Cheng, X.; Zhao, T.; Feng, Z.; Zhao, Y.; Fan, M.; Zhu, L. FG-4592 Improves Depressive-Like Behaviors through HIF-1-Mediated Neurogenesis and Synapse Plasticity in Rats. *Neurotherapeutics* **2020**, *17*, 664–675,

doi:10.1007/s13311-019-00807-3.

537. Li, Y.; Wang, M.-L.; Zhang, B.; Fan, X.-X.; Tang, Q.; Yu, X.; Li, L.-N.; Fan, A.-R.; Chang, H.-S.; Zhang, L.-Z. Antidepressant-Like Effect and Mechanism of Ginsenoside R_d on Rodent Models of Depression. *Drug Des. Devel. Ther.* **2022**, Volume 16, 843–861, doi:10.2147/DDDT.S351421.
538. McKeown, S.R. Defining normoxia, physoxia and hypoxia in tumours—implications for treatment response. *Br. J. Radiol.* **2014**, 87, 20130676, doi:10.1259/bjr.20130676.
539. Wagatsuma, A.; Arakawa, M.; Matsumoto, H.; Matsuda, R.; Hoshino, T.; Mabuchi, K. Cobalt chloride, a chemical hypoxia-mimicking agent, suppresses myoblast differentiation by downregulating myogenin expression. *Mol. Cell. Biochem.* **2020**, 470, 199–214, doi:10.1007/s11010-020-03762-2.
540. Rinderknecht, H.; Ehnert, S.; Braun, B.; Histing, T.; Nussler, A.K.; Linnemann, C. The Art of Inducing Hypoxia. *Oxygen* **2021**, 1, 46–61, doi:10.3390/oxygen1010006.
541. Jögi, A.; Øra, I.; Nilsson, H.; Lindeheim, Å.; Makino, Y.; Poellinger, L.; Axelson, H.; Pålman, S. Hypoxia alters gene expression in human neuroblastoma cells toward an immature and neural crest-like phenotype. *Proc. Natl. Acad. Sci.* **2002**, 99, 7021–7026, doi:10.1073/pnas.102660199.
542. Pålman, S.; Mohlin, S. Hypoxia and hypoxia-inducible factors in neuroblastoma. *Cell Tissue Res.* **2018**, 372, 269–275, doi:10.1007/s00441-017-2701-1.
543. Al Tameemi, W.; Dale, T.P.; Al-Jumaily, R.M.K.; Forsyth, N.R. Hypoxia-Modified Cancer Cell Metabolism. *Front. Cell Dev. Biol.* **2019**, 7, 4, doi:10.3389/fcell.2019.00004.
544. Infantino, V.; Santarsiero, A.; Convertini, P.; Todisco, S.; Iacobazzi, V. Cancer Cell Metabolism in Hypoxia: Role of HIF-1 as Key Regulator and Therapeutic Target. *Int. J. Mol. Sci.* **2021**, 22, 5703, doi:10.3390/ijms22115703.
545. Snyder, C.M.; Chandel, N.S. Mitochondrial Regulation of Cell Survival and Death During Low-Oxygen Conditions. *Antioxid. Redox Signal.* **2009**, 11, 2673–2683, doi:10.1089/ars.2009.2730.
546. Tan, X.; Azad, S.; Ji, X. Hypoxic Preconditioning Protects SH-SY5Y Cell against Oxidative Stress through Activation of Autophagy. *Cell Transplant.* **2018**, 27, 1753–1762, doi:10.1177/0963689718760486.
547. Hilaire, G.; Voituron, N.; Menuet, C.; Ichiyama, R.M.; Subramanian, H.H.; Dutschmann, M. The role of serotonin in respiratory function and dysfunction. *Respir. Physiol. Neurobiol.* **2010**, 174, 76–88, doi:10.1016/j.resp.2010.08.017.
548. Carneiro, I.B.C.; Toscano, A.E.; da Cunha, M. de S.B.; Lacerda, D.C.; Pontes, P.B.; de Castro, R.M.; de Jesus Deiró, T.C.B.; Medeiros, J.M.B. Serotonergic mechanisms associated with experimental models of hypoxia: A systematic review. *Int. J. Dev. Neurosci.* **2022**, 82, 667–679, doi:10.1002/jdn.10226.
549. Kong, D.; Park, E.J.; Stephen, A.G.; Calvani, M.; Cardellina, J.H.; Monks, A.; Fisher, R.J.; Shoemaker, R.H.; Melillo, G. Echinomycin, a Small-Molecule Inhibitor of Hypoxia-Inducible Factor-1 DNA-Binding Activity. *Cancer Res.* **2005**, 65, 9047–9055, doi:10.1158/0008-5472.CAN-05-1235.
550. Pacary, E.; Legros, H.; Valable, S.; Duchatelle, P.; Lecocq, M.; Petit, E.; Nicole, O.; Bernaudin, M. Synergistic effects of CoCl₂ and ROCK inhibition on

- mesenchymal stem cell differentiation into neuron-like cells. *J. Cell Sci.* **2006**, *119*, 2667–2678, doi:10.1242/jcs.03004.
551. Shibata, T.; Yamagata, H.; Uchida, S.; Otsuki, K.; Hobara, T.; Higuchi, F.; Abe, N.; Watanabe, Y. The alteration of hypoxia inducible factor-1 (HIF-1) and its target genes in mood disorder patients. *Prog. Neuro-Psychopharmacology Biol. Psychiatry* **2013**, *43*, 222–229, doi:10.1016/j.pnpbp.2013.01.003.
552. Sun, Y.; Cai, N.; Liu, N. Celecoxib Down-Regulates the Hypoxia-Induced Expression of HIF-1 α and VEGF Through the PI3K/AKT Pathway in Retinal Pigment Epithelial Cells. *Cell. Physiol. Biochem.* **2017**, *44*, 1640–1650, doi:10.1159/000485764.
553. Liu, N.; Chen, L.; Cai, N. Celecoxib attenuates retinal angiogenesis in a mouse model of oxygen-induced retinopathy. *Int. J. Clin. Exp. Pathol.* **2015**, *8*, 4990.
554. Ebada, M.E. Drug repurposing may generate novel approaches to treating depression. *J. Pharm. Pharmacol.* **2017**, *69*, 1428–1436, doi:10.1111/jphp.12815.
555. Di Giovanni, G.; De Deurwaerdère, P. TCB-2 [(7R)-3-bromo-2, 5-dimethoxy-bicyclo[4.2.0]octa-1,3,5-trien-7-yl]methanamine]: A hallucinogenic drug, a selective 5-HT_{2A} receptor pharmacological tool, or none of the above? *Neuropharmacology* **2018**, *142*, 20–29, doi:10.1016/j.neuropharm.2017.10.004.
556. Husain, M.I.; Ledwos, N.; Fellows, E.; Baer, J.; Rosenblat, J.D.; Blumberger, D.M.; Mulsant, B.H.; Castle, D.J. Serotonergic psychedelics for depression: What do we know about neurobiological mechanisms of action? *Front. Psychiatry* **2023**, *13*, doi:10.3389/fpsy.2022.1076459.
557. Liu, S.-L.; Li, Y.-H.; Shi, G.-Y.; Tang, S.-H.; Jiang, S.-J.; Huang, C.-W.; Liu, P.-Y.; Hong, J.-S.; Wu, H.-L. Dextromethorphan reduces oxidative stress and inhibits atherosclerosis and neointima formation in mice. *Cardiovasc. Res.* **2009**, *82*, 161–169, doi:10.1093/cvr/cvp043.
558. Demirdaş, A.; Nazıroğlu, M.; Övey, I.S. Short-Term Ketamine Treatment Decreases Oxidative Stress Without Influencing TRPM2 and TRPV1 Channel Gating in the Hippocampus and Dorsal Root Ganglion of Rats. *Cell. Mol. Neurobiol.* **2017**, *37*, 133–144, doi:10.1007/s10571-016-0353-4.
559. Capela, J.P.; Fernandes, E.; Remião, F.; Bastos, M.L.; Meisel, A.; Carvalho, F. Ecstasy induces apoptosis via 5-HT_{2A}-receptor stimulation in cortical neurons. *Neurotoxicology* **2007**, *28*, 868–875, doi:10.1016/j.neuro.2007.04.005.
560. Afshar, S.; Shahidi, S.; Rohani, A.H.; Soleimani Asl, S.; Komaki, A. Protective effects of 5-HT_{1A} receptor antagonist and 5-HT_{2A} receptor agonist on the biochemical and histological features in a rat model of Alzheimer's disease. *J. Chem. Neuroanat.* **2019**, *96*, 140–147, doi:10.1016/j.jchemneu.2019.01.008.
561. Akhondzadeh, S.; Jafari, S.; Raisi, F.; Nasehi, A.A.; Ghoreishi, A.; Salehi, B.; Mohebbi-Rasa, S.; Raznahan, M.; Kamalipour, A. Clinical trial of adjunctive celecoxib treatment in patients with major depression: a double blind and placebo controlled trial. *Depress. Anxiety* **2009**, *26*, 607–611, doi:10.1002/da.20589.
562. van Tonder, A.; Joubert, A.M.; Cromarty, A.D. Limitations of the 3-(4,5-dimethylthiazol-2-yl)-2,5-diphenyl-2H-tetrazolium bromide (MTT) assay when compared to three commonly used cell enumeration assays. *BMC Res. Notes* **2015**, *8*, 47, doi:10.1186/s13104-015-1000-8.
563. Fotakis, G.; Timbrell, J.A. In vitro cytotoxicity assays: Comparison of LDH, neutral red, MTT and protein assay in hepatoma cell lines following exposure to cadmium

- chloride. *Toxicol. Lett.* **2006**, *160*, 171–177, doi:10.1016/j.toxlet.2005.07.001.
564. Gomez Perez, M.; Fourcade, L.; Mateescu, M.A.; Paquin, J. Neutral Red versus MTT assay of cell viability in the presence of copper compounds. *Anal. Biochem.* **2017**, *535*, 43–46, doi:10.1016/j.ab.2017.07.027.
565. Mandal, A.; Drerup, C.M. Axonal Transport and Mitochondrial Function in Neurons. *Front. Cell. Neurosci.* **2019**, *13*, 373, doi:10.3389/fncel.2019.00373.
566. Lee, W.J.; Lee, G.H.; Hur, J.; Lee, H.G.; Kim, E.; Won, J.P.; Cho, Y.; Choi, M.-J.J.; Seo, H.G. Taurine and Ginsenoside Rf Induce BDNF Expression in SH-SY5Y Cells: A Potential Role of BDNF in Corticosterone-Trigged Cellular Damage. *Molecules* **2020**, *25*, 2819, doi:10.3390/molecules25122819.
567. Wang, R.; Ren, Q.; Gao, D.; Paudel, Y.N.; Li, X.; Wang, L.; Zhang, P.; Wang, B.; Shang, X.; Jin, M. Ameliorative effect of *Gastrodia elata* Blume extracts on depression in zebrafish and cellular models through modulating reticulin 4 receptors and apoptosis. *J. Ethnopharmacol.* **2022**, *289*, 115018, doi:10.1016/j.jep.2022.115018.
568. Zhang, L.; Lu, R.-R.; Xu, R.-H.; Wang, H.-H.; Feng, W.-S.; Zheng, X.-K. Naringenin and apigenin ameliorates corticosterone-induced depressive behaviors. *Heliyon* **2023**, *9*, e15618, doi:10.1016/j.heliyon.2023.e15618.
569. Xu, L.; Su, J.; Guo, L.; Wang, S.; Deng, X.; Ma, S. Modulation of LPA1 receptor-mediated neuronal apoptosis by Saikosaponin-d: A target involved in depression. *Neuropharmacology* **2019**, *155*, 150–161, doi:10.1016/j.neuropharm.2019.05.027.
570. Wang, G.; Luo, P.; Zhang, S.; Huang, Q.; Zhang, S.; Zeng, Q.; Mao, J. Screening and Identification of Antidepressant Active Ingredients from *Puerariae Radix* Extract and Study on Its Mechanism. *Oxid. Med. Cell. Longev.* **2021**, *2021*, 1–18, doi:10.1155/2021/2230195.
571. Eruslanov, E.; Kusmartsev, S. Identification of ROS Using Oxidized DCFDA and Flow-Cytometry. In *Advanced protocols in oxidative stress II*; Springer, 2010; pp. 57–72.
572. Gardiner, B.; Dougherty, J.A.; Ponnalagu, D.; Singh, H.; Angelos, M.; Chen, C.-A.; Khan, M. Measurement of Oxidative Stress Markers In Vitro Using Commercially Available Kits. In *Measuring Oxidants and Oxidative Stress in Biological Systems*; Springer, 2020; pp. 39–60.
573. Somani, A.; Singh, A.K.; Gupta, B.; Nagarkoti, S.; Dalal, P.K.; Dikshit, M. Oxidative and Nitrosative Stress in Major Depressive Disorder: A Case Control Study. *Brain Sci.* **2022**, *12*, 144, doi:10.3390/brainsci12020144.
574. Collins, A.R.; El Yamani, N.; Lorenzo, Y.; Shaposhnikov, S.; Brunborg, G.; Azqueta, A. Controlling variation in the comet assay. *Front. Genet.* **2014**, *5*, 359, doi:10.3389/fgene.2014.00359.
575. Barzilai, A.; Yamamoto, K.-I. DNA damage responses to oxidative stress. *DNA Repair (Amst)*. **2004**, *3*, 1109–1115.
576. Panwar, R.; Sivakumar, M.; Menon, V.; Vairappan, B. Changes in the levels of comet parameters before and after fluoxetine therapy in major depression patients. *Anat. Cell Biol.* **2020**, *53*, 194–200, doi:10.5115/acb.19.217.
577. Ahmadimanesh, M.; Abbaszadegan, M.R.; Morshedi Rad, D.; Moallem, S.A.; Mohammadpour, A.H.; Ghahremani, M.H.; Farid Hosseini, F.; Behdani, F.;

- Akhondpour Manteghi, A.; Jowsey, P.; et al. Effects of selective serotonin reuptake inhibitors on DNA damage in patients with depression. *J. Psychopharmacol.* **2019**, *33*, 1364–1376, doi:10.1177/0269881119874461.
578. Winker, M.; Chauveau, A.; Smieško, M.; Potterat, O.; Areesanan, A.; Zimmermann-Klemd, A.; Gründemann, C. Immunological evaluation of herbal extracts commonly used for treatment of mental diseases during pregnancy. *Sci. Rep.* **2023**, *13*, 9630, doi:10.1038/s41598-023-35952-5.
579. Panwar, R.; Sivakumar, M. Comet parameters and plasma 8-Iso-prostaglandins F2 α : Common markers of etiopathogenesis in major depression and indicators of antioxidant action of fluoxetine. *Natl. J. Clin. Anat.* **2021**, *10*, 118–125, doi:10.4103/njca.njca_44_21.
580. Wojtas, A.; Bysiek, A.; Wawrzczak-Bargiela, A.; Szych, Z.; Majcher-Maślanka, I.; Herian, M.; Maćkowiak, M.; Gołombiowska, K. Effect of Psilocybin and Ketamine on Brain Neurotransmitters, Glutamate Receptors, DNA and Rat Behavior. *Int. J. Mol. Sci.* **2022**, *23*, 6713, doi:10.3390/ijms23126713.
581. Ali, A.H. High-Performance Liquid Chromatography (HPLC): A review. *Ann Adv Chem* **2022**, *6*, 10–20.
582. Dwane, S.; Durack, E.; Kiely, P.A. Optimising parameters for the differentiation of SH-SY5Y cells to study cell adhesion and cell migration. *BMC Res. Notes* **2013**, *6*, 366, doi:10.1186/1756-0500-6-366.
583. Villanueva, R. Advances in the knowledge and therapeutics of schizophrenia, major depression disorder, and bipolar disorder from human brain organoid research. *Front. Psychiatry* **2023**, *14*, doi:10.3389/fpsy.2023.1178494.
584. Powell, S.K.; Gregory, J.; Akbarian, S.; Brennand, K.J. Application of CRISPR/Cas9 to the study of brain development and neuropsychiatric disease. *Mol. Cell. Neurosci.* **2017**, *82*, 157–166, doi:10.1016/j.mcn.2017.05.007.
585. Croushore, C.A.; Sweedler, J. V Microfluidic systems for studying neurotransmitters and neurotransmission. *Lab Chip* **2013**, *13*, 1666, doi:10.1039/c3lc41334a.
586. Pushpakom, S.; Iorio, F.; Eyers, P.A.; Escott, K.J.; Hopper, S.; Wells, A.; Doig, A.; Guilliams, T.; Latimer, J.; McNamee, C.; et al. Drug repurposing: progress, challenges and recommendations. *Nat. Rev. Drug Discov.* **2019**, *18*, 41–58, doi:10.1038/nrd.2018.168.